Development of nondestructive inspection tools for cultural heritage artefacts with 3D THz imaging

Dandolo, Corinna Ludovica Koch

Publication date:
2015

Document Version
Publisher's PDF, also known as Version of record

Technical University of Denmark

Development of nondestructive inspection tools for cultural heritage artefacts with 3D THz imaging

by
Corinna Ludovica Koch Dandolo

A dissertation submitted in partial fulfillment of the requirements for the degree of Doctor of Philosophy

2015

DTU Fotonik
Department of Photonics Engineering

To my mum and her δαίμων

Abstract

The ability of terahertz time-domain imaging (THz-TDI) to visualize surface and subsurface features of artworks has recently been established.

A limitation in imaging subsurface features by THz-TDI in reflection mode is the difficulty to handle THz signal separation when the surface of the layer to be imaged, wherever located within the dielectric stratigraphy of the object, is uneven, especially when dealing with inhomogeneous layers as regards to the composition, thickness and morphology. Those conditions often occur when dealing with artefacts inspection, in which case the conditions are also worsened by the fact that often a large portion of an artwork needs to be scanned for extracting relevant information. An effective method that handles these problems allowing a clear representation of each subsurface layer in the artwork is presented.

Thus, insights about the artistic technique and preservation state of real valuable artefacts were obtained non-invasively, where the 3D rendering of the imaged structures was also improved and THz frequency analysis as well as false color rendering (FC) allowed to better performing surface and subsurface materials areal mapping and discrimination by enhancing contrast.

The THz-TD system was carried inside museum collections for examining inestimable visible and hidden paintings painted by famous artists, such as Fra Angelico, Nicolai Abilgaard and David Teniers The Younger. To the best of our knowledge, for the first time lacquerwares have been examined by THz-TDI. It follows that this research work has broadened the comprehension of the capabilities of THz-TDI applied to artifacts inspection, also comparing the information it provides with that obtained by other standard imaging techniques.

Resume

Terahertz tidsdomæne-imaging (THz-TDI) er I de seneste år blevet etableret som en teknik til visualisering af strukturer på og under overfladen af kunstværker.

En begrænsning i forhold til afbildning af skjulte strukturer ved hjælp af refleksionsmålinger er håndteringen af signaladskillelse når lag, placeret vilkårlige steder i stratigrafien af objektet som skal afbildes, er ujævne. Sådanne ujævnheder kan være i form af sammensætning, tykkelse og morfologi. Sådanne omstændigheder findes ofte under inspektion af kulturgenstande (artefakter). En yderligere komplikation i forhold til sådanne genstande er, at man ofte skal scanne et stort område for at kunne ekstrahere den relevante og komplette information om den lagdelte, indre struktur.

Her præsenteres en effektiv metode, der tillader en klar repræsentation af de enkelte lag under overfladen af kunstværker. Dermed muliggøres ny indsigt i den benyttede kunstneriske teknik samt den bevaringsmæssige tilstand af værdifulde kunstgenstande. Vi har udviklet 3D afbildning af lagdelingen i artefakterne, udviklet terahertz-frekvens false-color gengivelse og optimeret kontrastforhold, hvilket giver bedre og mere detaljeret visualisering og diskriminering af overflader og indre strukturer over store flader.

THz-TDI systemet er blevet anvendt direkte i museumssamlinger, hvorved det har været muligt at undersøge uvurderlige malerier fra berømte kunstnere som Fra Angelico, Nicolai Abildgaard og David Teniers den Yngre. Efter vores bedste overbevisning har vi for første gang undersøgt lakerede artefakter med THz-TDI. Det har derfor været muligt at udvide bredden af indsatsområder, hvor THz-TDI kan anvendes til inspektion af genstande fra kunst og kulturarven i samspil med andre og mere standardiserede afbildende teknikker.

Preface

"Principles for the Development of a Complete Mind:
Study the science of art. Study the art of science.
Develop your senses- especially learn how to see.
Realize that everything connects to everything else."

Leonardo da Vinci (1452 – 1519)

"All religions, arts and sciences are branches of the same tree.
All these aspirations are directed toward ennobling man's life,
lifting it from the sphere of mere physical existence
and leading the individual towards freedom."

Albert Einstein (1879 –1955)

There is a widespread perception that art and technology are notions opposite to each other. Generally, today's cultural horizon follows the stereotypical dichotomy between art and science: they are two distinct forms of knowledge, two cognitive acts respectively based on irrationality and intuition (art) and rationality and logic (science), which correspond to different perspectives, to different ways of experiencing the real.

However, they were closely linked in the Classical world. The ancient Greek word for "art" is *τέχνη* (*tékhnē*), and "technology" comes from the Greek term *τεχνολογία* (*tékhnologhìa)*, combination of the words *τέχνη* and *λογος* (*logos*, or "reasoning"), meaning the rationalization and understanding of art [1]. Likewise, *τέχνη* is the equivalent of the Latin word *ars*, which means "art", but also "technique". Broadening to humanities in general, stern rules were governing Aristotle's poetics, while the world of Nature, mathematics and music were intimately interconnected in Pythagoras´s doctrines.

The first censorship between the two worlds actually took over only in modern times, from Descartes onward, with the scientific revolution of the seventeenth century. Less than a century before, Leonardo da Vinci was

celebrating the maximum coincidence between art and science with his ingenious and polyhedral work [2].

It is again the Classical world which teaches us that history is cyclical and so are its concepts. In support of this it is possible to observe how the need of filling the gap between the two domains recurred in our century and took shape less than sixty years ago with *The Two Cultures and the Scientific Revolution* by the scientist Charles Percy Snow (1905-1980), essay based on his influential Rede Lecture (1959). According to his thesis, a major hindrance to solving the world's problems was the splitting of the intellectual life into two separated cultures, namely the sciences and the humanities. The separation of cultures must have been an issue widely felt during the following years if, in 1995, *The Times Literary Supplement* included *The Two Cultures and the Scientific Revolution* in its list of the 100 books that most influenced Western public discourse since the Second World War.

Cultural heritage seems exactly the elective field for making *one* out of the *two cultures*. This is particularly true for tangible heritage, where there is a straight connection between the esthetic and historical aspects of an object and the material one. In fact, the highly complex and diverse nature of cultural objects creates the need for an interdisciplinary approach, combining the expertise of chemists, physicists, and engineers with the knowledge and experience of art conservators, art historians, archaeologists. To this effect, interdisciplinary research is needed for a better understanding of the fundamental aspects involved, and a high level of scientific training and cultural heritage awareness, to overcome these obstacles and expand the scientific and technological tools available for the preservation of cultural artifacts [1].

As early on as the close of the 1950s, during that same period in which Snow was writing his complaint against the *two cultures*, experimental science started to be systematically interested in ancient artefacts. Experimental science opened new sceneries about the material aspects of cultural heritage, bringing to the designation of the new disciplines of *archaeometry* and *conservation science*.

Archaeology was the first humanistic field to involve scientific competencies for archaeological findings dating and provenance understanding. Those scientific applications, at first episodically, have converged into the new *archaeometry* discipline. At the same time,

experimental science started to be applied to the study of historical artefacts as well as in the conservation-restoration sector.

Over the past 40 years, scientific research activities in support of the knowledge, conservation and restoration of objects and monuments belonging to the world's cultural heritage, have grown in number and quality. This lead to the definition of a separate discipline known as conservation science (or heritage science) [3]. Conservation science is the application of science and technology to the knowledge and conservation of cultural heritage [4]. It is a broad developing field which uses the applied disciplines of science and engineering for contributing to [5]:

- the understanding of the composition of the world's cultural heritage, including the original technologies used to create works of art, which contributes to the scholarly interpretation of art and artifacts (technical art history);
- the understanding of deterioration mechanisms and the principal factors influencing damage mechanisms of objects of art;
- the evaluation and the development of conservation materials and approaches.

A large portion of the applications of experimental sciences to cultural heritage deals with the application of analytical techniques and instrumentations for artefacts inspection. Many institutes specifically dedicated to the study and conservation of cultural heritage have emerged. Small dedicated laboratories have been installed in museums, libraries, and archives, and, more recently, university laboratories are showing increased interest in this field [3].

In principle, it would seem that the unicity and convergence of purposes should produce a natural synergy between the two broad areas of historical and experimental sciences. In truth, considerable difficulties can occur in mutual understanding and cooperation at the interfacing spaces when the operators do not face the problem with a common approach but slip back toward disciplinary/sectoral legacies, following a very common psychic imprisonments [6]. Even though nowadays it is well established that modern science and technologies are crucial for a better insight into art and cultural heritage, one of the reasons for the limited adoption of new technologies is related to the need to establish common communication codes between professionals who have different educational backgrounds and perspectives on the preservation of our cultural heritage [1]. In fact, it happens very often

that interdisciplinary collaborations take place more by coming near than by compenetration. Each one does its part and exposes it separately, but there is a lack in reciprocal and convinced comprehension of one another´s cognitive methods.

Different specializations and sectorial skills should feed each other on common issues and problems, making efforts for a reciprocal methodological understanding and "contamination". It can be easily understood how difficult it is to make effective and operative such a synergy: different educational trainings (the *two cultures*) easily produce difficulties in mutual understanding and problems of identity and hierarchy within the common undertaken actions [6].

I have a background in conservation science and, during my PhD research at DTU Fotonik (Technical University of Denmark, Department of Photonics engineering), I have applied a new powerful laser-based technique, terahertz time-domain imaging (THz-TDI), to image and determine the surface and internal structure of objects of cultural heritage.

In consideration of what I have written before, I do consider the former goal of my executing PhD research project the promotion of the synergy between the cultural heritage field, natural sciences and engineering for developing new analytical approaches through multidisciplinary research, with the aim of broadening the information provided by technologies to the cultural heritage sector. Specifically, to meet this objective, I carried on interdisciplinary collaborations bridging museums/art institutes and DTU Photonics for achieving a progress in the use of THz-TDI technology applied to artefacts inspection. It is obvious that this goal could not be accomplished without the support of dedicated fundamental research and high-level interactivity with professionals and academics from different disciplines. It furthermore required me a deep technical and methodological understanding, which first relied on the transfer of THz-TDI know-how and then to its adaptation to the specific needs associated with the preservation of cultural heritage objects. This adaptation included the development of common knowledge and communication code, which I now wish to use for a further promotion of this powerful technology within the cultural heritage field.

Lastly, I like to look at my PhD project as an attempt to make one out of the *two cultures*, and a small stage in realizing "*…that everything connects to everything else"* (*Mitakuye Oyasin*).

Acknowledgments

I would like to express my full appreciation and affection to my supervisor, **Peter Uhd Jepsen**, for his open-minded curiosity and inquiring spirit, which lead him wishing to connect terahertz science and technology to the cultural heritage sector and planning the PhD project about the "development of nondestructive inspection tools for cultural heritage artefacts with 3D THz imaging". I feel extremely grateful for his trust in me to carrying out this exciting research. I want to thank him for having shared with me his great expertise, experience, knowledge and brilliant nous, thus adding considerably to my post-graduate experience.

I wish to thank my co-supervisor **Mads Christian Christiansen** (National Museum of Denmark), for his interest in the development of new technologies for artefacts inspection, for having accepted to join what was a research project proposal, thus making it become the research PhD project I just completed. I sincerely appreciate his kind and receptive character and his efforts in providing me access to the materials, samples (e.g. the European lacquerware replica) and art-pieces (e.g. the lacquered screen of the Danish Royal Family collection) belonging to the National Museum of Denmark, as well as the heritage subjected to the museum´s vigilance (e.g. the absidial wall painting of Nebbelunde Church).

It has been a great honor and privilege to work at **DTU Fotonik**, and I thank this Institute for all the opportunities it always gave me to work at best. I am thankful to its people, especially the Director **Lars-Ulrik A. Andersen**, for their interest in broadening the application fields of the science of light toward art, their interest about my PhD project and evolution and for the trust they gave me.

I sincerely wish to thank all those **researchers and academics** who decided to use their terahertz science expertise as an aid for the study and the preservation of our cultural patrimony, for having contributed in the development of terahertz technology applied to cultural heritage and for

having divulgated their valuable results to the conservation field and, through their publications, to me: I consider them my teachers. I also wish to thank them for having shown to love this sector as much as I do, overpassing the limits of the *two cultures*.

Among them, special thanks go to **Kaori Fukunaga** (National Institute of Information and Communications Technology, NICT - Tokyo), widely considered the godmother of the terahertz science applied to cultural heritage. I am glad to have collaborated with her for the joint research we carried on in Nara (Japan) and I am grateful for the unique experience and opportunity she provided me. I have particularly appreciated her kindness, her collaborative way of working with others and her exceptional polyhedral mind: a combination of engineering *ingenium* and artistic sensitivity for the beauty.

Other special thanks go to **Marcello Picollo** ("Nello Carrara" Institute of Applied Physics CNR-IFAC), well known leading figure in the field of science applied to cultural heritage, who I already knew by reputation, but I had the opportunity to meet in person thank to his research interests in terahertz technology. I am grateful to him for the interest he showed about my research, and for the opportunities he gave me to conduct joint researches with his research group, within the networking activities of COSCH (Color and space in cultural heritage, part of the intergovernmental framework for European Cooperation in Science and Technology, COST), and at the San Marco museum (Florence), where we scanned panel paintings of inestimable value by Fra Angelico painter. I got particularly impressed by his bright and brilliant mind and initiative, his effective and useful way of working, his multitask and leading temperament and his friendly character.

I would like to express my gratitude to all the people I have collaborate with, without whom this research would never have been accomplished.

In **Denmark**, I wish to thank all the people of the Conservation Department and CATS (Centre for Art Technological Studies and Conservation) of the Statens Museum for Kunst, particularly the keeper of conservation **Jørgen Wadum**, for the interest he has shown in my research and for having given me the possibility to undertake collaborations with the Department and the Center which he is leading. All the other people who

have been involved to arrange this collaboration, especially **Mette Bech Kokkenborg**. I am thankful to **Troels Filtenborg** and **Jakob Skou-Hansen**, with whom I have realized the extremely effective and fruitful investigation campaign on two unique paintings belonging to the museum collection, for their indispensable help and participation in the research, for their memorable kindness and for always having found time for me and enthusiasm for my research activity. **Aoife Daly** for having showed a great interest in the technology I was proposing her for dendrochronological applications and for having provided me her samples, but also for her nice way of having always made me feel welcomed and the for time she spent in enthusing me about her amusing research field. All the other CATS members (**Anna Villa, David Buti** and **Johanne Marie Nielsen**) and the conservation department´s team for the great hospitality they always showed me, for always having taken into consideration the research I was carried on and for the fruitful discussions we had together, including those we had at the "hyggeligt" Friday breakfasts at the Department.

I am very thankful to the National Museum of Denmark, especially **Johanne Bornemann Mogensen** for her help to make real the joint investigation on the precious Chinese lacquered screen they were restoring, and **Rikke Bjarnhof**, head of Buildings and Artefacts Conservation, who accepted and sustained with enthusiasm the THz investigation mission we had. The conservator **Anne Lisbeth Schmidt**, for the time, consideration and acceptance she gave me for testing the THz device on organic remains; **Isabelle Brajer**, for having provided me the wall paintings replicas which have been my first samples for testing and learning about THz device and signals processing.

I furthermore wish to thank the people for different reasons involved, in the on-site investigation campaign on the absidial wall painting in Nebbelunde: **Birgitte Flensburg**, Vicar, **Birthe Måhr**, head of Church Council and **Michael Viid Thage**, Churchwarden at Nebbelunde. Special thanks go to **Kirsten Trampedach**, for her essential role in finding the study case and in the organization; I would furthermore like to affectionately thank her and her husband **Puccio Speroni**, for having been my reference point at the beginning of my stay in Denmark, due to their great generosity and friendly characters. I keep warm memories of the lovely Danish/Italian dinners and conversations we had at their place and their hospitality.

Mikkel Scharff, from the Royal Academy of Fine Art of Copenhagen, for having provided us the lacquerware and the panel painting replicas and for his interest in our research activity.

In **Italy**, I wish to thank the CNR-IFAC researchers who have welcomed me in Florence and collaborated with me for the THz investigation on the panel paintings by Fra Angelico at San Marco museum, **Andrea Casini**, **Lorenzo Stefani** and especially **Costanza Cucci** for all her time and full involvement in our joint collaboration. I sincerely wish to thank **Magnolia Scudieri**, **Elena Prandi** and **Marina Ginanni** (*Ufficio e Laboratorio Restauri* of the former Soprintendenza Speciale per il Patrimonio Storico, Artistico ed Etnoantropologico e per il Polo Museale della città di Firenze – now affiliated to the Polo Museale Regionale della Toscana), for having allowed us to THz scan to the invaluable paintings by Fra Angelico from the collections of the San Marco museum, in Florence; for the prolific collaboration and discussions we had together; for having provided us the access to the relevant past diagnostic reports made by SMAArt, CNR-ISTM, CNR-ICVBC, M2ADL, the Chemistry Department of Pisa University and the PanArt sas private company, and for having provided us the test panel paintings they made. Furthermore I wish to thank the ISCR (Istituto Superiore per la Conservazione ed il Restauro) for the images and data we have accessed thanks to their online archival resource.

Antonino Cosentino (cultural heritage science open source - CHSOP) is thanked for having kindly invited me and for having arranged my research stay in Sicily, where we have conducted a very stimulating and interesting investigation campaign on several Sicilian art-pieces, together with the conservators **Angelo Cristaudo**, who allowed us to perform the THz scanning of the medieval icon belonging to the public library of Taormina, **Giovanni Calvagna**, **Giuseppe Calvagna** and **Carmelo Calvagna**. A warm thanks to all the Aci Sant'Antonio community, especially **Antonino´s family**, for their kindness and generosity.

In **Belgium**, a warm thank is for **Vincent Cattersel** (Antwerp University), for the wonderful collaboration we had together for the investigation of the lacquered cabinet from the 17th century (Barbara Piert-Borgers private collection of Far-East and European lacquerware) as part of the ELINC - European lacquer in Context project (the Royal Institute for

Cultural Heritage IRPA, the University of Antwerp and the Royal Museums of Art and Histor), and for the passion and enthusiasm he always showed when working together, and for always working at best.

In **Japan**, I´m grateful to **Yosei Kozuma** (head of the conservation science section at the Nara National Research Institute for Cultural Properties), for having accepted me in his Institute, allowed me to be part of his extremely nice work team for three months, and arranged my research stay with them about Asian lacquerwares investigation by means of THz-TDI. I have very good memories of my stay and I will keep them as a treasure for my future. A special thanks to **Akiko Tashiro**, for having been my guide while in Japan and for always having been so nice and kind with me, paying attentions to all my needs with genuine friendship and for the amazing trip we had together.

I wish to thanks the entire **Terahertz science and technology group** at DTU Fotonik: **Pernille Klarskov Pedersen**, **Krzysztof Iwaszczuk**, **Maksim Zalkovskij**, **Jonas Christian Due Buron**, **Andrew Strikwerda**, **Abebe Tilahun Tarekegne** and particularly **Tianwu Wang**, for having always shown empathy and sympathy for my successes and failures, and for the pleasant time we had together.

I´m grateful for all the nice people I met at DTU Fotonik and surrounding, including those of the Thursday-club, the Friday-bar, the Italian "lunch group", all the nice friends I gained in Denmark and all the friends I gained somewhere else in the world, which have followed my movements and my life despite the time and the space.

It is a pleasure to acknowledge with gratitude the financial support of **Otto Mønsteds Fond** and **Torben og Alice Frimodts Fond** for Lacona X conference attendance and for my external research stay in Japan.

Table of contents

Abstract ..... **v**

Resume ..... **vi**

Preface ..... **vii**

Acknowledgments ..... **xi**

Table of contents ..... **xvii**

Chapter I Introduction **1**

I.1 Science and technology for artefacts inspection 1

I.1.A Macroscopic subsurface imaging techniques for artworks inspection: an overview 1

I.2 Research context, aims and objectives 11

I.3 Overview of the dissertation 13

Chapter II Terahertz time-domain imaging (THz-TDI): fundamentals **15**

II.1 Terahertz waves 15

II.1.A Broadband terahertz generation and detection 15

II.1.B Photoconductive antennas (PCAs) for terahertz generation and detection 17

II.2 Terahertz time-domain reflectometric imaging 20

II.2.A Resolutions and signal-to-noise ratio in THz images 23

II.2.B Terahertz signals separation, deconvolution and padding 24

II.2.C Terahertz time and frequency parametric images 26

II.3 Analytical instrumentation 28

Chapter III THz-TDI applied to easel painting investigation **31**

III.1 Reflection Terahertz Time Domain-Imaging for Analysis of an 18th Century Neoclassical Easel Painting 31

III.1.A Potential of THz-TDI scans as a complementary tool to X-ray radiograms 32

III.1.B Materials and methods 33

III.1.C Results and Discussion 34

III.1.D Chapter conclusion 43

Chapter IV THz-TDI applied to panel painting investigation 45

IV.1 Analysis of a 17th Century Panel Painting by Reflection Terahertz Time Domain-Imaging (THz-TDI): contribution of ultrafast optics to museum collections inspection 47

IV.1.A The investigated panel painting 47

IV.1.B Analytical instrumentation 48

IV.1.C Results and Discussion 48

IV.1.D Final considerations 54

IV.2 Florentine Renaissance Panel Painting structures revealed by using non-invasive Terahertz Time-Domain Imaging (THz-TDI) technique 56

IV.2.A Potentials of THz-TDI to the study of panel paintings in central Italy dating to between the 12th and 16th centuries 56

IV.2.B Instrumentation and Analytical methods 58

IV.2.C Artworks investigated 58

IV.2.D Results and Discussion 61

IV.2.E Final considerations 70

IV.3 Insights on the side panels of the *Franciscan Triptych* by means of Terahertz time-domain imaging (THz-TDI) 72

IV.3.A Panel paintings description 72

IV.3.B Instrumentation and analytical methodology 74

IV.3.C Results and Discussion 75

IV.3.D Final considerations 82

IV.4 Inspection of Panel Paintings behind Gilded Finishes with Terahertz Time-Domain Imaging (THz-TDI) 85

IV.4.A Panel paintings and gilded finishes in Europe: an overview 85

IV.4.B THz-TDI as investigation tool for gilded panel paintings 86
IV.4.C Analytical Instrumentation and Methodologies 87
IV.4.D The investigated panel paintings..... 87
IV.4.E Results and discussion 89
IV.4.F Final considerations 95
IV.5 Diagnostics pre and post conservation on a 14th century gilded icon from Taormina, Sicily 97
IV.5.A The 14th century icon: preservation state 98
IV.5.B Analytical Instrumentation and Methodologies 98
IV.5.C Results and discussion 99
IV.5.D Final considerations..... 107
IV.6 Chapter conclusion..... 109
Chapter V THz-TDI applied to wall painting investigation..... 113
V.1 Inspection of Subsurface Structures Buried in Historical Plasters: the Medieval wall painting of Nebbelunde Church 114
V.1.A Subsurface imaging of wall paintings: the conservation issue 114
V.1.B Instrumentation and analytical methods..... 115
V.1.C Results and discussion 116
V.1.D Chapter conclusion 120
Chapter VI THz-TDI applied to lacquerware investigation 123
VI.1 Analysis of Asian lacquer Substructures by Terahertz Time-Domain Imaging (THz-TDI)..... 123
VI.1.A The production of Asian Lacquer-wares..... 124
VI.1.B Substructure of Asian Lacquers 124
VI.1.C X-ray radiography and THz-TDI for imaging analysis of Asian Lacquers substructures 127
VI.1.D The investigated lacquer-wares 128
VI.1.E Analytical instrumentations 130
VI.1.F Results and discussion..... 130
VI.1.G Final considerations..... 137

VI.2 Characterization of European Lacquers by Terahertz (THz) Reflectometric Imaging 139
VI.2.A Analytical Instrumentation and Methodologies 139
VI.2.B The Lacquerware Replica 139
VI.2.C Results and discussion 141
VI.2.D Final considerations 145
VI.3 Terahertz time-domain imaging of a 17th century lacquered cabinet: a contribution to European lacquerwares characterization 146
VI.3.A Materials and methods 146
VI.3.B Results and discussion 147
VI.3.C Final considerations 151
VI.4 Chapter conclusion 152
Chapter VII Conclusions, future work and outlooks 155
References 163
Appendix A Publications, lectures and oral contributions 179

Chapter I
Introduction

I.1 Science and technology for artefacts inspection

The analytical methods used for artifacts inspection are primary divided according to degree to which they are invasive, where the first partition is made among those that requires sampling (invasive) and those that do not require sampling (non-invasive). The sample taken for invasive measurements can be analyzed and used for later investigation (non-destructive methods) or it may require a preparation which do not allow it to endure in its original form after the measurement (destructive or micro-destructive methods). A further division is made among those techniques that do require a contact with the artefacts and the contactless ones, while a special attention is directed to mobile devices, which are able to investigate unmovable artifacts or artifacts whose transport should be avoided because of preservation or logistic reasons. On the other hand, non-invasive methods are divided into the imaging and the spot analyses.

The next paragraph will focus on imaging techniques, with a special attention to those capable of providing subsurface information at macroscopic level.

I.1.A Macroscopic subsurface imaging techniques for artworks inspection: an overview

According to the contrast mechanism on which they rely, imaging techniques may provide information on materials location and distribution within the whole artefact or large portions of it; consequently they are considered the first aid for locating promising sites for further spot analyses or material sampling.

Non-invasive imaging techniques include optical, atomic and nuclear techniques. Imaging techniques in artwork diagnostics can be distinguished

according to the light source they use (coherent or not), the portion of the electromagnetic range they exploit (Fig.I.1), or the type of information they provide. Depending on the light source used, it is possible to distinguish between coherent techniques, which involve the use of laser sources, and "enhanced" visual techniques, involving broadband imaging [7].

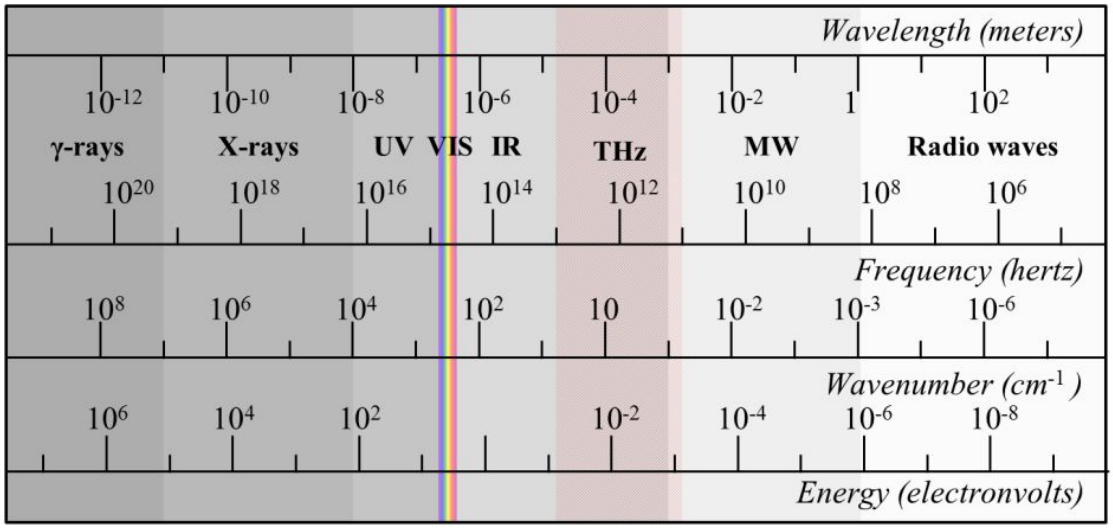

Fig. I.1-1 The EM. To calculate a photon´s quantum energy (E), Planck´s constant h (i.e. 6,626 x 10^{-34} J s^{-1} or 4,136 x 10-15 eV s^{-1}) must be multiplied by the frequency ($\nu = c / \lambda$, where λ is the wavelength and c is the speed of light. The reciprocal of the wavelength in centimeters (wavenumber, $\tilde{\nu} = 1 / \lambda$) is usually preferred in Chemistry.

Traditionally, the visualization of the inner structure of cultural heritage artifacts relies on penetrative, two-dimensional imaging techniques such as infrared reflectography (IRR) and X-ray radiography (XRR), optionally complemented with microscopic analysis of cross-sectioned samples (destructive sampling) [8].

Recently, a number of new non-invasive subsurface imaging techniques are finding application in cultural heritage inspection. The main ones will be listed in the following sub-paragraphs, and summarized in table I.1-1, on the basis of the review paper written by Alfeld and Broekaert (2013, [9]) and by Janssens et al. (2010, [8]). Imaging techniques based on large scale facilities and micro-imaging techniques will be omitted.

X-ray radiography (XRR)

XRR is the oldest scientific technique used for the investigation of paintings. It allows the internal structure of the material to be imaged. With wavelengths between 0.001 and 10 nm, the X-ray region is characterized by very energetic photons with energies between 124 keV and to 124 eV. Since they surpass the threshold of 10 eV, X-rays are considered ionizing radiation, which means they are composed of photons with enough energy to remove an electron from an atom, making it a ion.

It is a transmission technique in that absorbance of X-rays in an art-piece is imaged. The radiographic contrast depends upon the material thickness, the physical density, the electron density and the elemental composition (effective Z), as well as the energy spectrum of the x-ray beam emitted by the source [10].

To record the transmitted radiation in full-field either analogue films or digital detectors are used. In the recent years, digital radiography (DR) has largely progressed and evolved into new imaging technologies based on X-ray tube. In the *energy resolved X-ray radiography* (or K-edge imaging) the energy resolution is achieved by employing primary radiation of different energies. By subtracting images acquired with energies above and below the absorption edge of an element its distribution image can be obtained [9], [11]. *X-ray computed tomography* (CT) allows for the acquisition of three dimensional data sets reconstructed from a series of X-ray radiographs [9], [12]. It makes use of an extended series of projection images recorded under many different angles between the object and primary beam. Mathematical reconstruction then allows creation of a virtual, 3D rendition of the object's shape and (inner) density variations and visualization of its inner parts [8].

Scanning macro X-ray fluorescence (MA-XRF) and Confocal XRF (cXRF)

X-ray fluorescence spectrometry (XRF) has been used for the identification of pigments in paintings for many years. Scanning micro-XRF (mXRF) with a resolution in the micrometer range is a long established technique in the investigation of cultural heritage objects, but the construction of scanners for macroscopic objects is technically challenging, so that it was not until recently that elemental distribution images have been acquired by *scanning macro X-ray fluorescence (MA-XRF)* for the visualization of sub-surface details in artworks.

Mobile MA-XRF scanners, first described in the early 1990s, have been developed [9] and are now commercially available. They are based on X-ray tube and detectors mounted on a motorized stage and moved before the surface of a painting during a 2D scan, in reflection geometry. With a lateral resolution of about 50 µm, the main limitations of MA-XRF are the slow data acquisition as a scanning technique and the lack of species information.

Recently, developed energy dispersive cameras make full-field XRF imaging feasible. However, the camera is limited to the investigation of small areas (a few square centimeters) and is not capable of taking overview images of the whole surface of an average painting (50 × 50 cm) in a single exposure [13].

Confocal XRF (cXRF) allows for the acquisition of depth profiles with elemental contrast. Confocal XRF acts as a material probe by exciting and detecting emitted characteristic X-ray photons from within the confocal analysis volume as this volume is scanned through the sample. The confocal geometry uses two polycapillary focusing optics for enhanced applications of XRF elemental analysis. Elemental concentrations are measured within the small probe volume ("confocal volume") defined by the intersection of the output focal spot of the excitation optic and the input focal spot of the collection optic. The lateral distribution of elements is determined by moving the sample through the information volume (scanning dimension 1-3D). Confocal XRF has made a development similar to MA-XRF from synchrotron radiation sources to X-ray tube based instruments suitable for operation in conservation studios, which can achieve a depth resolution in the order of 40 µm (lateral resolution: 50 µm). Confocal XRF has several limitations. The dwell time of several tens of seconds necessitates long scans (approximately half an hour) for a single depth profile, making the acquisition of virtual cross sections and 3D data sets feasible but very time consuming. Further, only a small area is investigated. Regarding painted artworks, paint layers can be of less than 10 µm thickness, considerably smaller than the depth resolution. However, confocal XRF constitutes the only non-destructive depth profiling method with elemental contrast that can be applied in conservation laboratories [9].

- IR-reflectography (IRR) and IR reflectance imaging

IR-reflectography is based on image acquisition in the NIR and SWIR (short wave-infrared) electromagnetic regions and uses spectral bands of different width included between 700 and 2500 nm, depending on to the

detector [14]–[16]. Thanks to the capability to go through the different layers of the painting, NIR and SWIR radiations enables to image underneath features, where the contrast mechanism are the absorption properties of the materials. It is a major technique utilized to reveal preparatory drawings and *pentimenti* [7]. Carbon-based black pigments are strongly absorbing between 1 and 2.4 μm [9]. It has been investigated since the 1960s although the origins can be retraced back to the 1930s as reported by Walmsley et al. (1994) [14]. The next generation of IR reflectography systems are the multispectral scanners, consisting of acquiring the images in narrow band (some tens of nanometres) [17], and the hyperspectral scanners (few nanometers spectral sampling rate [18]).

IR reflectance imaging [14] at higher wavelengths have been exploited for paintings analysis by means of wide-band devices. The MIR reflectance imaging is dominated by the strong fundamental absorption so that the radiation is less penetrating than NIR and SWIR. Furthermore, while up to 5 μm reflected radiation is more intense than the thermal radiation emitted by a blackbody, higher wavelengths are less well suited for IRR, as images acquired in this region are always a combination of thermograms and reflectograms. Some of the IR ranges which have been recently applied to image paintings and reported in literature include:

- MWIR (3-5 μm) by combining a PtSi based camera with a MWIR source in the so called Thermal Quasi-Reflectography (TQR) [7];
- LWIR (6.9 -11 μm) by combining an hyperspectral imager HI90, developed for the remote identification and mapping of hazardous compounds12-13, with an infrared radiation source [19].
- LWIR (7.3 – 13 μm) by means of a FLIR ThermaCAM S65 which acquires thermal images from a minimum of -40 °C to a maximum of 1500 °C [20].

Infrared thermography (IRT)

The *infrared thermography* (IRT) is a technique currently used for the non-destructive characterizations in a large variety of different fields and, during the last two decades, in particular, it has evolved into a powerful nondestructive tool for the study of the conservation of cultural heritage [21]. In thermography the thermal radiation emitted by a sample, according to the blackbody radiation theory, is recorded with IR cameras sensitive in the spectral region above 3 μm in order to obtain temperature maps that reveal surface and sub-surface features and inhomogeneities in the material, where evaluation of the thermal diffusivity and/or further analysis can be

performed. *Pulsed thermography* [14] is commonly employed for the analysis of paintings. In this technique, the surface of the painting is warmed by a few degrees with a heat pulse. The air-pockets in delaminations and other discontinuities constitute thermal insulators that hinder the heat propagation, so that paint layers above them cool down slower compared to intact areas. Regarding the application on painted materials, the amount of thermal radiation emitted does not only dependent on sub-surface defects, but also on the absorption of the heat pulse in the paint layers and the emissivity of the material present. For this reason, it allows the visualization of strongly IR absorbing underdrawings and signatures.

Advanced data processing techniques such as *Pulse Phase Thermography*, *Principal Component Thermography* and *Differential Absorption Contrast* enhance the readability of the thermograms [7], [9], [21]–[23].

Optical coherence tomography (OCT)

Optical coherence tomography (OCT) is a scanning technique allowing for the investigation of objects moderately absorbing or scattering the probing light in reflection geometry. OCT employs partly coherent, polychromatic light from the NIR (0.7–1.5 µm) that is analyzed in an interferometer after being reflected by the painting. As the interfaces between layers with different absorption/scattering characteristics reflect the light back to the interferometer, OCT allows for the acquisition of depth profiles, virtual cross sections and (small) 3-dimensional data sets. OCT commonly features a lateral resolution of 10 to 30 µm and a depth resolution of 1 to 10 µm. Scanning speed and maximum imaging depth vary considerably with different excitation and detector configurations, but in general a virtual cross-section can be acquired in a few seconds. Concerning painted artworks, OCT gives a detailed insight in layering of the varnish layers and the topography of varnish and thin paint layers close to the surface. By taking the median of slices from a volume acquired by OCT with near-IR illumination allows to distinct covered layers from surface layers by selecting adequate slices. However, such investigations ask considerable more time than IRR measurements and are limited to small areas (a few square centimeters) [9], [24].

The main application area of OCT is in the medical field, so that mature instrumentation is available for the investigation of paintings [9].

Unilateral NMR

In Nuclear Magnetic Resonance spectroscopy (NMR) the relaxation of a sample's magnetization in a strong magnetic field after excitation by a radio-frequency pulse is measured. The relaxation time is dependent on the direct surroundings of the excited nuclei and thus gives insight in the sample's chemical structure. NMR has been applied in a wide range of studies in the field of cultural heritage analysis. Unfortunately, the instrumentation commonly employed for NMR measurements is not suitable for the in-situ investigation of historical paintings, as, in order to obtain a homogeneous magnetic field, the sample is placed inside the (circular) magnet of the instrument in a volume too small to contain a painting. In-situ measurements became feasible with the development of the *NMR-MOUSE*, a mobile stray-field NMR system sensitive to ^{1}H nuclei in that the investigated volume is positioned in front of the instrument. The investigated volume has a size of ca. 10×10 mm^2 and a depth resolution of less than 10 µm can be achieved. Depth profiles are acquired by changing the distance of instrument to painting via a motorized stage. The maximum sampling depth is 25 mm. The acquisition of a depth profile necessitates 30–40 min, so that 3-dimensional mapping of a painting is not practical. NMR depth profiles provide valuable information. The amplitude of the measured signal is proportional to the abundance of ^{1}H nuclei in the investigated volume, so that the distribution of organic compounds and water in covered layers can be investigated. Further, the measured relaxation times of the nuclei are related to the age of a paint layer, as its brittleness and the molecular mobility in it change over the years. So a correlation between relaxation time and age of paintings can be observed, which may be exploited to distinguish between old and recently added paint [9], [25].

Ultrasonic and acoustic imaging

Ultrasonic imaging was described in 1990s. US waves have frequencies that exceed the upper limit for audible human hearing, i.e., greater than 20 kHz. Ultrasound waves are generated in pulses (intermittent trains of pressure) that commonly consist of two or three sound cycles of the same frequency. The pulse repetition frequency (PRF) is the number of pulses emitted by the transducer per unit of time. Ultrasound waves must be emitted in pulses with sufficient time in between to allow the signal to reach the

target of interest and be reflected back to the transducer as echo before the next pulse is generated [26].

The application of ultrasonic techniques in that the propagation of sound waves in the wooden support of a panel painting is measured, was first described in 1996. The ultrasonic methods applied for the investigation of paintings have been recently reviewed and encompass next to air coupled (or non-contact) ultrasound scanning, also contact ultrasound and acoustic microscopy. Non-contact, scanning instruments that allow the visualization of defects in the structure of panel painting have been described in transmission and reflection geometry. In the obtained images delaminations and cracks in ground and wooden support can be localized. The lateral resolution is given as several millimetres, depending on the experimental conditions, while no depth information is obtained [9], [27], [28].

- Laser based holographic methods

The laser era in artwork diagnostics started in the 1970s, when holographic interferometry was applied to the detection of structural defects in panel paintings. Laser based holographic and speckle methods (*Holographic Interferometry* -HI, *Electronic Speckle Pattern Interferometry* - ESPI, *Electronic Speckle Pattern Shearing Interferometry* - ESPSI or Shearography, and *Speckle decorrelation*) allow to visualize minor displacements of a surface under stress. The methods utilize laser light in the optical range to illuminate the painting's surface and acquire images in full-field mode. In case of HI and ESPI the interference pattern of the acquired image with a reference beam is recorded, while in case of shearography the acquired image is split and the interference between the original image and its sheared version of it is recorded. Two optical representations (holograms or speckle patterns) acquired before and after the loading (i.e. putting the painting under very slight stress) are superimposed (in case of holograms) or subtracted (in case of speckle patterns) yielding correlation patterns that indicate the surface displacement. Surface and sub-surface defects, such as voids, cracks and delaminations, can be visualized in these patterns as they create discontinuities in the patterns formed by influencing the deformation of the paint surface. The loading of the painting is commonly done either by irradiation with IR radiation or a stream of warmair. The temperature change necessary is a few degrees and below normal temperature fluctuations in a museum. Also loading by sound waves and mechanically, e.g. by vibration, has been described. All of the methods mentioned above have been used for

in-situ investigations, although HI, which yields the best results of the methods mentioned, is less well suited for this due to its sensitivity to vibrations [9], [29], [30].

Another promising technique is scanning *laser doppler vibrometry* for applications in frescoes and wooden paintings. The different behavior of defective and non-defective regions is highlighted by letting the surface vibrate (by means of a hammer, loud speaker, piezo-exciters, etc.). The mean vibrational velocity is then measured for each point, providing information about the conservation state of the various regions of the surface; the vibrational velocity is related to the soundness of the surface [28].
Table I.1-1summarizes the presented techniques.

Imaging method	Radiation	Contrast type	Information imaged	Dim.	Geometry	Scanning dim.	LR (µm)	DR (µm)
XRR	X-ray	Absorption	Electron density [8], [9]	2D [8]	transmission	full-field , 1D [9]	>200 [9] >500 [8]	n.a.
ED-XRR	X-ray	Element specific absorption	Elemental distribution	2D + spectral [9]	transmission	Full-field, 1D, 2D	200	n.a
CT	X-ray	absorption	Electron density	3D [8]		Full-field [8]	>600 [8]	
(MAXRF)	X-ray	Elemental	Elemental composition	3D		Scanned beam mode	250-1000	
c-XRF	X-ray	Elemental distribution [9]	Elemental composition [8], depth profile of elemental distribution [9]	3D	reflection	1-3D	>10 [8], 50 [9]	40 [9]
IRR	NIR	absorption	Absorbing species [8], total absorption [9]	2D	reflection	Full-field [8], [9], 2D [9]	>1000 [8], 100 [9]	n.a
OCT	NIR	absorption [8], reflection, scattering [9]	Absorbing species [8], 3D datasets of interfaces [9]	3D	reflection	1D, 3D [9]	>1000 [8], 10-30 [9]	<1 ([8] 1-10 [9]
Thermography	MID-IR	heat transport	subsurface defects	time	transmission and	full field	n.a.	n.a.
NMR	magnetic field	1H abundance and molecular mobility	depth profile of 1H abundance		reflection	1D	10000	10
Laser interference techniques	optical	Deformation under stress	subsurface defects	time	reflection	full field	n.a.	n.a.
Ultrasonic	sound waves	propagation of sound waves	subsurface defects		transmission and	2D	n.a.	n.a.

Table I.1-1 Recently introduced imaging technique with subsurface inspection capabilities. XRR, Xray radiography; ED-XRR energydispersive XRR; MAXRF, Scanning macro-XRF; CT, Macroscopic computed tomography; MAXRF, Macroscopic scanning XRF; IRR, infrared reflectography; OCT, optical coherent tomography; NMR, Unilateral nuclear magnetic resonance. LR, DR, lateral and depth resolution; dim., dimensions. Adopted from [9].

I.2 Research context, aims and objectives

We have previously seen how new technologies have been rapidly adopted for artefacts inspection.

Over the last 40 years, laser-based techniques have been used to determine the composition and internal structure of objects of cultural heritage, as well as for their restoration. It should be stressed at this point that the progress achieved has strongly relied on the transfer of know-how initially developed for industrial and biomedical applications of lasers. This was adapted to the specific needs associated with the preservation of cultural heritage. In particular, since 1990 several laser materials characterization (chemical analysis and structural diagnostics) and processing techniques have inspired new approaches and investigations. The overall advances in laser technology have led to the emergence of a range of new sophisticated and powerful techniques, superseding in performance the existing methods [1].

Terahertz time-domain imaging (THz-TDI) is, in its own right, one of them.

Free space terahertz radiation became accessible only in the late 1980s, thanks to the advance in ultrafast pulsed sources and detectors based on pulsed laser excitation, [31], [32]. Practical THz imaging has been demonstrated for the first time by Hu and Nuss in 1995 [33], while the first compact THz time-domain systems was created between 2000 and 2004 [34], [35]. As a technology that can detect the amplitude and phase of coherently generated electromagnetic radiation in the THz range (0.1 – 10 THz), it may not be surprising that it is an invaluable spectroscopic tool for research in physics, chemistry and biology [36], [37]. Key applications driving the technology are in defense, security, and biosensing. In general, nonpolar, dry, and nonmetallic materials are transparent or translucent to T-ray radiation. This transparency motivates the use of THz in retection (i.e. detection of an object through concealed layer [38]), particularly useful for quality control and security applications. The strong absorption of T-ray energy by water molecules has merits in biology, where T-rays are highly sensitive to the hydration level in biological tissue [31].

Following the history of technologies in heritage science, THz-TDI has been recently transferred and adopted for artifacts inspection. The first easel painting has been THz imaged in 2006 [39], while the first wall painting in 2010 [40].

As a spectroscopic imaging, transmitted and reflected terahertz signals contain information of the absorption characteristics of the material. Further, THz pulses are reflected on the interfaces between the layers if their optical properties in the THz range are different. Therefore, the thickness of layers can be determined from the time-of-flight of the THz pulse in reflection geometry. This allows, similar to OCT, the non-destructive acquisition of depth profiles, virtual cross sections and 3D data sets and due to the more penetrative nature of THz radiation this information is not limited to the surface layers [9]. Almost as penetrating as the X-ray, THz waves are non-destructive and intrinsically safe by nature, having low photon energy (4.1 meV at 1 THz), so they can be considered as non-ionizing. In comparison, a typical X-ray photon has energy in KeV range, which is 1 million times higher than a usual THz photon [41].

Whiting this research frame, the research focus on the development of THz-TDI for artefacts inspection, providing news understandings of the use of this technology for easel, panel and wall paintings, but also lacquerwares examination. The research aims to broaden the casuistry about the application of this technology for artifacts inspection and getting new insights about the information it provides, comparing the results with those obtained by other standard imaging techniques, such as invasive cross-sectional image, infrared reflectography and X-radiography. At the same time, the presented research focused on optimizing the managing and the visualization of the large THz data set acquired by scanning large portion of artifacts (> 250 cm^2), including uneven ones, by means of customized signal processing and the adoption of advanced 2 and 3D image rendering techniques.

I.3 Overview of the dissertation

Following the preface and this introduction, chapter II acquaints the reader with the fundamentals about THz time-domain system for spectroscopy and imaging. A description of THz radiation is given, as well as an overview about broadband THz generation and detection, focusing on that based on photoconductive antennas, the one implemented in the device used for THz image acquisition. The principles of terahertz spectroscopy and imaging are also included in this chapter, which ends with the specifications about the THz-TDI device (Picometrix T-ray 4000) used for our experiments.

Chapter III deals with the application of THz-TDI to easel painting investigation, where the results obtained by scanning a Danish neoclassical easel painting are reported and compared with those obtained by invasive cross-sectional imaging and X-radiography. The hidden portrait concealed under the actual painting has been clearly imaged by THz-TDI, as well as the other subsurface constituent layers. The chapter describes the THz signal separation method developed for this application and used for the following cases. The method greatly improves the existing separation methods, facing the problematics often found when dealing with THz imaging large portions of an object, especially in case of uneven surface and inhomogeneous layers as regards to the composition, thickness and morphology. The assessed separation method allowed a clear representation of each subsurface layer in the investigated artworks.

Chapter IV shows the results obtained by scanning four different panel paintings of different age and manufacturing techniques. It highlights the capability of THz-TDI in giving important information about the presence of features hidden behind the painting surface, such as wooden structure, gilding, inclusions, degradation phenomena etc., which were also used for improving restoration interventions. A buried painting beneath the surface of a 17th century panel painting by David Teniers The Younger was imaged with THz-TDI, and again the information resulted complementary to those provided by X-radiography. THz-TDI inspection of a medieval gilded panel was placed among a multi-technical investigation campaign, emphasizing the complementarity of the information provided by this techniques with others, mainly IR reflectography, and the unicity of the information provided by THz-TDI. Above all, THz radiation was found able to inspect the panel painting internal structure by penetrating gold leafs of small thickness (close

to the skin-depth of gold). Finally, the important information obtained by THz-TD scanning three Renaissance panels made by the renowned Fra Angelico painter are presented, giving useful information about the manufacturing technique of this eminent artist.

Chapter V reports the results obtained by the on-site THz scanning of a Danish medieval absidial wall painting. Hidden anomalies detected in depth inside plaster were imaged in a 3D volume rendering for a better comprehension of their morphology and, consequently, their nature.

Chapter VI describes the outcomes we got by applying THz-TDI to lacquerwares investigation, which, to the best of our knowledge, were THz scanned for the first time. THz-TDI was found suitable for lacquer substructure identification, overcoming the limits of X-radiography in imaging organic materials; even in this case, the method gave suggestions about their manufacturing technique. In addition, THz-TDI was applied to a 17^{th} century lacquered cabinet belonging to a private collection, and it provided evidences of surface anomalies not observable in visible light by human eye.

Before the description of our results, Chapter III-VI begin reporting the state of the art of THz technology applied to the related artefact category.

Conclusions are reported in Chapter VII, while Appendix A lists the contributions that this research gave to events, conferences and publications.

Chapter II
Terahertz time-domain imaging (THz-TDI): fundamentals

II.1 Terahertz waves

The terahertz region of the electromagnetic spectrum (THz radiation, THz waves or T-rays) is loosely defined by the 0.1 to 10 THz frequency range (where 1 THz is 10^{12} cycles/s, approximately 3 mm – 30 μm in wavelength or wavenumbers in the range 3 – 300 cm^{-1} Fig. I.1-1). Situated between infrared (IR) light and millimeter wave radiation, where molecular resonances dominate, T-rays are a relatively unexplored part of the electromagnetic spectrum (terahertz gap), since inefficient generation techniques and high atmospheric absorption constrained early interest and funding for THz gap science [31], [38].

The next sub-paragraphs (II.1.A and II.I.B) will introduce the basics of broadband THz generation and detection by photoconductive antennas (PCAs). In fact, the discussion will be limited to the THz generation/detection mechanism adopted in the T-ray time-domain spectrometer used for the experiments presented in this text.

II.1.A Broadband terahertz generation and detection

Technological advances in optics and electronics have resulted in the development of different THz sources and sensors, capable of producing broadband or continuous-wave (CW) THz beam [37].

Broadband, coherent subpicosecond THz radiation can be generated in a photoconductive switch on a semiconductor substrate excited by a femtosecond laser pulse or in an electrooptic crystal by difference-frequency mixing of the frequency components of a femtosecond laser pulse [36], usually at a near-infrared (NIR) wavelength.

The femtosecond laser pulse is split into a pump beam that is used to emit a band of THz radiation and a probe beam that is used for detection of the

THz radiation. Either the pump or probe beam passes through a delay line that increases the optical path of this radiation. The resulting THz-TDS measurement corresponds to the real-time detection of the electric field vector of the THz electromagnetic wave after it propagates through the sample [42].

Changes in the position of the delay line system allow sampling of the time-domain signal in a discrete, time-gated manner (Fig. II.2-1), where the optical path length is $\Delta z = \Delta tc$, with z in the direction along the optical delay path [43].

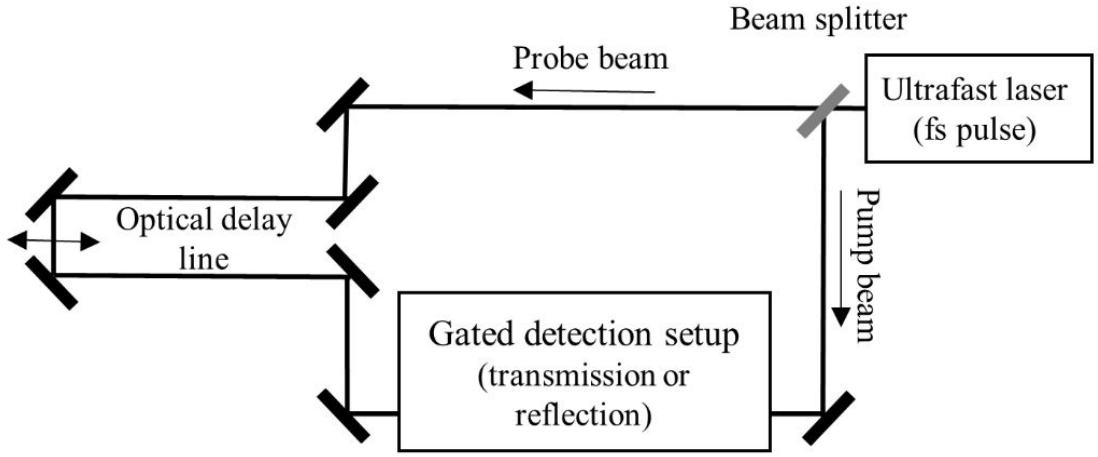

Figure II.1-1 Generalized terahertz generation and gated detection setup. Adapted from [42], [43]

Delay line and femtosecond laser present bottlenecks in the maximum attainable scan rate, scan repeatability, SNR, and instrument footprint.

Once generated, the portion of the terahertz pulse that arrives at the detection unit congruently with the probe laser pulse is sampled. The sampling window duration is defined in part by the NIR laser pulse width, because detection occurs only when birefringence modulation (electrooptic sampling, EO) or current flow (PCAs) is induced [42].

It follows that modern instrumentation for collecting a THz-TDS is analogous to a single-beam FT instrument in the sense that in both apparatus, the intensity of transmitted or reflected radiation is measured as a function of the position of a moving optical element. While a Michelson interferometer is generally used in FTIR spectroscopy, an optical delay line is used to create the TDS for THz-TDS [42].

Withayachumnankul et al. summarized the two broad classes of T-ray generation and detection relying on ultrafast laser pulses developed at commercial level [31]. The first, using photoconductive antennas (PCAs),

was reported by Mourou et al. [44] in the GHz range and then extended into the THz region by Auston et al. [45]. This method was further developed at Bell Labs [32] and the IBM Watson Research Center [46], and is now used in a commercial product from Picometrix Inc [34], [35], [47], [48]. The second method, using the nonlinear effects that exploit optical rectification (OR) and electrooptic sampling (EOS), was first observed by Hu et al. [49] and Wu et al. [50], and used in a commercial product by Zomega Terahertz Corp, NY [51]. Large-scale stand-alone imaging systems became available in 2002 from TeraView Ltd. [52] and Nikon Corp [53].

The next sub-paragraph will focus on terahertz generation and detection by photoconductive antennas.

II.1.B Photoconductive antennas (PCAs) for terahertz generation and detection

The generation of THz radiation by biased photoconductive dipole antennas (PCAs) was first described in 1989 by Grischkowsky et al. [36], [54]. It relies on the optical excitation of photoconductive dipole antennas and is now known as terahertz time-domain spectroscopy (THz-TDS) [36], [55].

A PC antenna consists of two metal electrodes (electrical switch) deposited on a semiconductor substrate (Fig. II.2-2a). It exploits electrical conductivity of semiconductors when they are exposed to light. Ultrafast current impulses are generated by impinging an ultrafast laser pulse onto a biased semiconductor surface.

When illuminated by the femtosecond laser pulse, photons with energy above the semiconductor bandgap generate electron-hole pairs into the semiconductor at a specific generation rate G(t) and the free carries are excited across the electronic bandgap of the semiconductor into the conduction band. When the pulse duration ends, the free carries finally recombine with the characteristic recombination time of the substrate, or become trapped in mid-band gap states.

The bias field applied via the metal electrodes accelerates the photogenerated free electrons and holes in opposite directions, leading to a rapid change in the current density, resulting in a changing induced dipole that produces a THz transient in the antenna. The free-space THz electromagnetic radiation is proportional to the rapid change in the photocurrent (dJ/dt) within the electric field region.

Using femtosecond laser of sub-picosecond pulse duration, such as femtosecond laser) and choosing a substrate determining a subpicosecond lifetime of the photoexcited carrier (concentration of defects at which carriers are trapped and recombined), current impulses with bandwidths well into the THz range can be generated.

The produced broadband THz pulses, whose shape resembles the optical pulse envelope [37], are then collected into a collimated beam by a substrate lens attached to the structure and radiated into free space [56]. High-resistivity silicon hyperhemispherical lenses are often used to couple the THz radiation from the emitter antenna into free space [36].

The incident THz pulse is $E_0(\omega)$ is characterized by its spectral amplitude and phase, obtained by Fourier transformation (FT) of the time-domain pulses, given that:

$$E(\omega) = |E(\omega)|e^{i\varphi} = \int E(t)e^{-i\omega t}dt \quad (1)$$

where E is a terahertz pulse, ν is the frequency, φ is the phase, $\omega = 2\pi\nu$ is the angular frequency and t the time delay.

The free-space beam is transported from the emitter to the detector with either reflective or transmissive optics. In the same way, substrate lens are used to couple the THz radiation from free space and onto the detector antenna.

Detection of the THz pulses can be done by photoconductive sampling in an antenna structure identical to the THz emitter structure (Fig. II.2-2b). A portion of the femtosecond laser pulse train, synchronized to the femtosecond pulse train used for the THz generation, is split off and used to gate the detector structure.

The detector antenna is not biased by an external circuit, and the electric field required to drive a photocurrent in the photoconductive gap is supplied by the THz pulses that arrive in synchronism with the gate pulses, which injects photocarriers. The photocurrent in the antenna circuit is then a convolution of the electric field picked up by the antenna and the transient photoconductivity induced by the gate pulse.

The induced photocurrent is proportional to the THz field amplitude. Furthermore, the shorter the photoinduced carrier trapping and recombination time and narrower the laser pulse, the more the measured terahertz signal will be closer in appearance to the radiated THz pulse.

The generated photocurrent is then amplified and measured as an electrical signal using either an oscilloscope or a data acquisition board and computer.

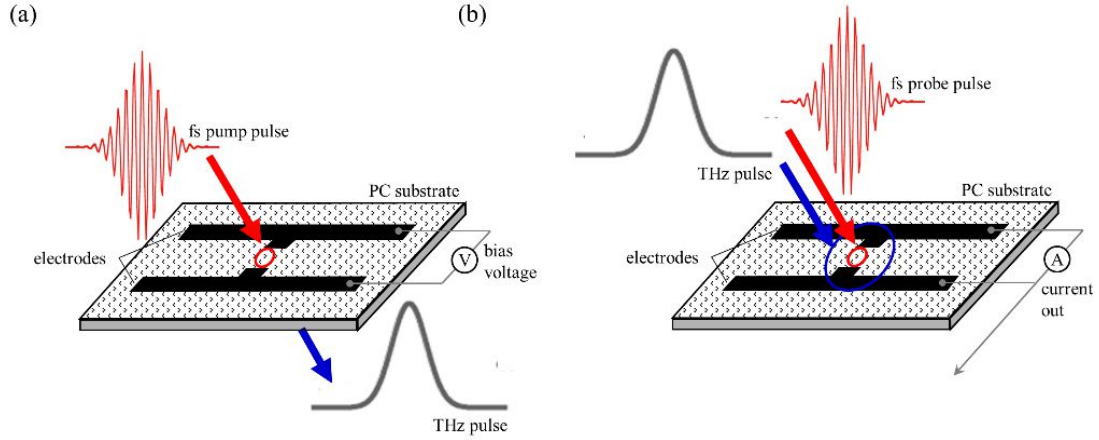

Figure II.1-2 a Photoconductive switch for the generation of terahertz transient **b** Photoconductive switch for the detection of terahertz transient

As already mentioned, the THz pulse shape is mapped out in the time domain by measuring the photocurrent while varying the time delay between the THz pulse and the optical probe. Indeed, THz detection by PC antenna is a coherent detection method, where coherent detection measures both the amplitude and phase of the field. A combined setup of broadband THz generation and detection measures changes in both the amplitude and phase of THz pulses induced by a sample, which provides enough information to simultaneously determine the absorption and dispersion of the sample [37].

II.2 Terahertz time-domain reflectometric imaging

Terahertz time-domain imaging is a spectroscopic imaging (functional imaging, where the source of contrast is the optical density of materials), meaning that is a two to three dimensional extension of terahertz spectroscopy; for this reason the two argument are strongly linked.

More than the spectroscopic potentials, the attractive property of terahertz radiation for imaging applications is its ability to penetrate optically opaque and non-conducting materials.

In the majority of the systems in use, images are obtained by simple raster scanning a terahertz beam across an object over the two lateral dimensions (x,y). The recorded quantity at each spatial coordinate is the electrical field strength of the electromagnetic pulse as a function of time (Fig. II.2-1a), recorded either in transmission or in reflection set-up, which can be Fourier transformed in frequency domain (Fig. II.2-1b, Eq.1).

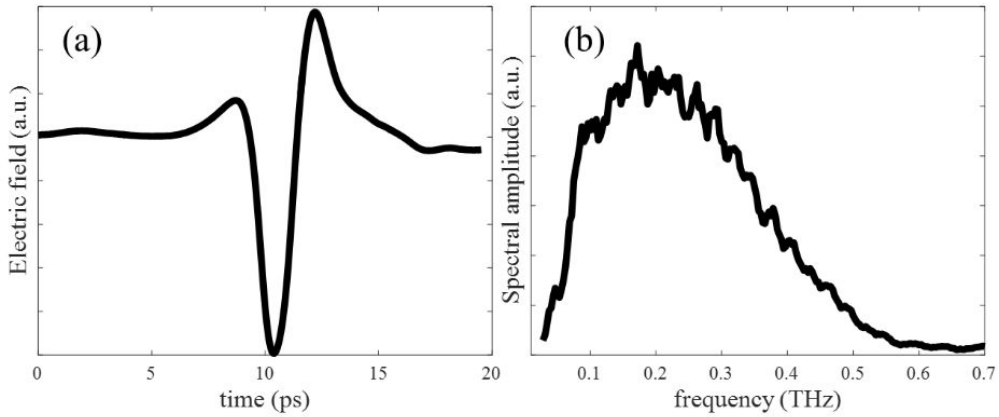

Figure II.2-1 a Terahertz pulse or time dependent electric field, E(t). **b** Terahertz pluse after FT, or frequency dependent electric field, E(ν). THz data were acquired in reflection mode at normal incidence by a metal mirror by Picometrix T-ray 4000 device (Picometrix Inc.).

The interaction of the THz incident pulse with a sample, either in transmission or reflection set-up, can be used for the extraction of the complex index of refraction of a sample, $n(\omega) = n(\omega)+ik(\omega)$, where $k(\omega)$ is the extinction coefficient, related to the absorption coefficient $\alpha(\omega)$ through $\kappa(\omega) = \alpha(\omega)c/2\omega$.

The discussion will now focus on terahertz time-domain imaging in reflection mode at normal incidence, being the set-up used for our experiments.

In a reflection geometry, the sign and amplitude of the back-reflected THz pulse can be analyzed for reflections originating from the various interfaces present between the sample layers, with a reflection amplitude at the interface determined by the terahertz refractive index mismatch at each interface, $r_{i,i+1}=(n_i-n_{i+1})/(n_i+n_{i+1})$. In general, this occurs when there is a structural or material change in the sample under investigation, which can result in strong reflections (echoes) of the incident beam even from buried layers.

Fig. II.2-2b shows the interaction between the time representation of a THz pulse at normal incidence and a layered sample.

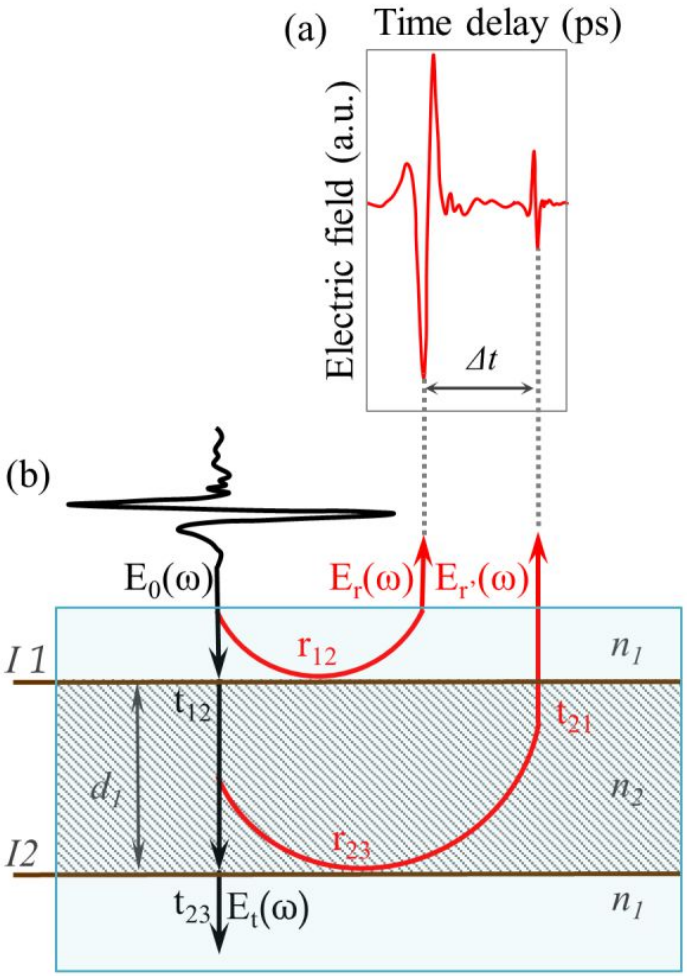

Figure II.2-2 a Terahertz waveform; Δt, temporal spacing between the first/second reflections. **b** Schematic representation of the incident terahertz beam $E_0(\omega)$ and the back-reflected signals $E_r(\omega)$, $E_{r'}(\omega)$, for a sample composed of one homogeneous layers in air investigated in reflection configuration at normal incidence; t_{ij} and r_{ij}, complex Fresnel field transmission and reflection coefficients for the different media 1 (air), 2 (homogeneous layer); n_i, refractive indices of the two different media; d_1, layer thickness; I1, I2, first and second interface respectively.

The temporal spacing between the reflections is proportional to the optical thickness of the layers (Fig.II.2-2a). Therefore, the time scale provides information about the penetrated depth *z* of the signal that is reflected at each lateral position (*x,y*), thereby enabling 3-D ToF imaging:

$$z = \frac{d}{cos\phi} = \frac{c}{n}\frac{\Delta t}{2} \qquad (2)$$

where for an angle of incidence ϑ, the angle of refraction ϕ, the refraction is determined by Snell's law

$$\phi = sin^{-1}\left(\frac{n_{air}}{n_{sam}} sin\theta\right) \tag{3}$$

and ϑ , ϕ ~ 1 in a normal incidence configuration, so that d = cΔt/2n. Ignoring, for the time being, multiple reflections in the sample, the transmitted and reflected signals are in this geometry given by

$$\begin{aligned} E_t(\omega) &= E_0(\omega)t_{12}t_{23}\, e^{-\alpha d/2}\, e^{in\omega d/c}, \\ E_r(\omega) &= E_0 r_{12}, \\ E'_r(\omega) &= E_0 t_{12} r_{23} t_{21}\, e^{-\alpha d/2}\, e^{in\omega d/c} \end{aligned} \tag{4}$$

where t_{12}, r_{12} and r_{23} are the various complex Fresnel field transmission and reflection coefficients.

In reflection mode the reference signal can be obtained by replacing the sample with a reflector such as a metallic surface.

The field reflection coefficient of a good metal far below the plasma frequency is $r_{metal} = -1$, independent of frequency. Using a metal surface as the reference reflector at normal incidence of the THz radiation the ratio of the sample reflection to the reference reflection is then [36], [57]

$$|r|e^{i\varphi} = \frac{n-1}{n+1} = \frac{n+ik-1}{n+ik+1} \tag{5}$$

where φ is the phase. This expression can be inverted to yield the index of refraction and the absorption coefficient of the sample:

$$n(\omega) = \frac{1-|r|^2}{1+|r|^2-2|r|cos\varphi} \tag{6}$$

$$\alpha(\omega) = \frac{4\pi\nu}{c}\frac{2|r|sin\varphi}{1+|r|^2-2|r|cos\varphi} \tag{7}$$

For a sample in air the generalized reflection function R(ω) proportional to the Fresnel coefficient r is

$$R(\omega) = \frac{E_{sam}(\omega)}{E_{ref}(\omega)} = \frac{n_{sam}cos\phi - n_{air}cos\theta}{n_{sam}\,cos\phi + n_{air}\,cos\vartheta} \tag{8}$$

where and ϑ , ϕ ~ 1 in a normal incidence configuration.

It follows that the conversion of pulses from time to frequency domain by means of Fourier transformation (Fig. II.2-1b and Eq. 1) could in principle allow substance identification through chemical mapping, owing to changes

in the spectral content of the reflected THz pulses, given that many solids exhibit characteristic spectral features in the 10 GHz - 4 THz frequency range. Although THz imaging has the potential to reveal information about the spatial distribution of the spectroscopic data, it is important to realize that there are many practical limitations to the capability of chemical mapping:

Firstly, even if both phase (or timing) and amplitude information can be obtained, enabling the investigation of both morphological and chemical changes, the structural and the chemical information are convolved in a single reflected pulse and can only be separated if one is known a priori.

Secondly, THz images show a reduced frequency resolution compared with purely spectroscopic investigations mainly due to limited temporal windows of the signals [58]. It can be argued that the short duration of the pulse can be used either for depth information or spectral information. For a layer separation Δd, echoes will be separated by a time $\Delta t = 2n\Delta d/c$ (Eq. 8). This time defines the available time window for spectroscopy, and thus the highest possible undisturbed frequency resolution available for spectroscopic analysis of the reflected signal from the specific interface will be $\nu = 1/\Delta t = c/(2n\Delta d)$. Thus, for any situation where depth resolution and spectroscopic resolution is required simultaneously, the general uncertainty relation

$$\Delta\nu \cdot \Delta d \geq \frac{c}{2n} \tag{9}$$

must hold. As an example, for layers with a refractive index of 1.5, separated by 0.25 mm, the best frequency resolution available will be 0.4 THz, clearly limiting the capabilities for spectral recognition in layered structures.

Thirdly, scattering of electromagnetic radiation in the THz range is considerable since the spatial scale of refractive index fluctuations – due to variations in either the surface roughness or internal structure of materials – can become comparable to the wavelength of the THz signal [59].

II.2.A Resolutions and signal-to-noise ratio in THz images

The lateral resolution (or spatial resolution) is restricted by the beam waist diameter of the focused beam, which is in turn limited by diffraction effects to approximately the wavelength of THz radiation utilized (Abbes criterium). In the frequency range from approximately 0.1 to 4 THz, the ideal lateral resolution ranges from 3 mm to 75 μm.

The ability to resolve closely spaced reflections (bandwidth-limited axial resolution or depth resolution) is determined by the temporal duration of the THz pulses. In terms of the spectral bandwidth of the terahertz pulse, the depth resolution is given by half of the coherence length of the radiation according to $L_c=c/(n\pi\Delta\nu)$, where $\Delta\nu$ is the FWHM spectral bandwidth and *c* is the speed of light in the intervening medium, with refractive index n. For a 0.5-THz FWHM spectrum in an environment with a refractive index of 1.5, the ideal depth resolution is thus approximately 65 μm. In practice, effects such as dispersion and scattering will reduce the depth resolution. Even if the depth resolution is physically limited by the spectral bandwidth of the terahertz radiation, different techniques have recently been used to improve the depth resolution [60], [61].

The signal-to-noise ratio (SNR) of the detected electric field signal is approximately given by the ratio of the signal power versus the system noise power.

II.2.B Terahertz signals separation, deconvolution and padding

THz images of interfaces between layers and connected relevant information can be extracted by separating pulses of interest (or Region of Interest, ROI) from the entire recorded THz signal by performing a series of complex signal processing steps.

Signal separation is usually performed by applying a windowing function (signal apodization) on the pulse of interest of the time-domain signal. A variety of windowing functions do exist for this purpose. The simplest apodization function is the boxcar function where the THz raw data are essentially multiplied by unity near the relevant peak and decrease toward zero nearer the extremities of the sampled time window. Other apodization functions consisting in weighting of the time-domain signal, include the following: triangular, Happ-Genzel; Hanning; Norton-Beer weak, Blackman-Harris, where the main differences are linked to the rapidity with which the function approaches its minimum value. A Tukey (tapered cosine) window is a rectangular window with the first and last r/2 percent of the samples equal to parts of a cosine, where r is the ratio of the cosine-tapered section length to the entire window length. By changing the r value of a tukey window, the weighting of samples in the time series is allowed to vary: r = 0 will gives a boxcar window, while r = 1 will give an Hanning

window. A detailed description of these functions can be found elsewhere [62].

Individual return signals may be partially or entirely overlapping in time, depending on distance between two contiguous interfaces, on the refractive index contrast between layers and on instrumental characteristics, such as temporal resolution, pulse duration and bandwidth. Furthermore, recorded signals are affected by noise due to scattering at surface, and by practical signal-to-noise limits and bandwidth reduction due to the short acquisition time required for imaging applications. Noise effect could be suppressed by repetitive averaging, but this would be time consuming and impracticable for imaging application.

Partially overlapping return signals and high noise floors make the reading of THz waveforms difficult, so that the extraction of the individual pulse signatures from the full-reflected signal may be challenging and it may requires additional processing operation.

Deconvolution is one method that help in resolving time domain features of the recorded THz signals. In fact, the measured reflected terahertz pulses are a convolution of the sample impulse response function with the incident terahertz pulse, so that a deconvolution operation is often performed to extract the impulse response function of the target sample. In the simple sense, deconvolution consists in dividing the sample by the reference spectra in the frequency domain, and inverse Fourier transform the resulting spectrum (direct inverse filtering, IF). To suppress the amplified noise affecting, the so treated waveform, coupling of filters (low pass, Wiener, double Gaussian) into IF appears an obvious choice, even if wavelet based methods, common practice for seismic signals since long time [63], [64], have been also proposed for terahertz pulses denoising since 1996 [65] for their efficient time-frequency representation. The wavelet method is continuously developing [61], [66]–[73].

A further method commonly used in THz signals processing is the zero-filling, also known as zero-padding, Fourier interpolation, or zooming. The method is commonly used to provide more spectral data points within a given frequency range. Additional data points (zeros added to the end of the TDS prior to implementing the FT calculation) represent interpolated points between the actual sampled points. Additional data points in time-domain results in additional data points in frequency domain, so that the smoothing effect is evident as the number of points increases and the point spacing decreases [42]. In the context of deconvolution, however, the zeropadding

serves a different purpose: it improves the signal-to-noise ratio in the recovered impulse response function [61].

Nevertheless, even after deconvolution and denoising, separation of single pulses of interest from the entire recorded signals is a challenging task: chapter III will introduce a simple method to proficiency address it.

II.2.C Terahertz time and frequency parametric images

Images recorded with THz-TDI can be plotted utilizing different parameters.

The THz images nomenclature generally follows the three most common formats known in the non-destructive testing (NDT), such a B-scan and C-scan presentations, while for A-scan is simply meant the representation of the THz signal as a function of time.

The B-scan presentation is a profile (cross-sectional) view of the test specimen. In B-scans, each pixel of a scan-line (entered on the horizontal axis) contains information about the strength of the reflected THz signal (visualized by a color-map) as a function of the time-delay (the vertical axis) of the signal. Since the time delay is proportional to the penetration depth of the signal which is reflected, B-scans are considered two-dimensional, cross-sectional images of the investigated sample.

In addition, in the time domain, 3D THz images can be reconstructed from measured data using the pulse delay with regard to a reference pulse (Time-of-Flight or ToF).

The C-scan provides a plan-type view of the test piece. C-scans can be displayed using different characteristics of the temporal amplitude E(t) of a pulse, such as its maximum, minimum, or peak-to-peak values, the pulse area or power over a specific time interval (time windowing) and the centroid- or weighted return time of the pulse [74]. An additional time domain parameter is the full width at half maximum (FWHM) of the pulse, which is also affected by the refractive index (especially if the medium is strongly dispersive) and frequency-dependent absorption coefficient [58].

In the frequency domain, images can be displayed by using discrete values of the amplitude, reflectivity, refractive index and absorption spectra, the spectral amplitude $E(\omega)$ at a specific frequency or the amplitude or power integrated over a specific frequency range. In principle, all the parameters usually computed on FT transformed data can be used for plotting THz images (magnitude, amplitude, power density, etc.). Further parameters which have been used in frequency domain are the reflectance

R(ω) and the corresponding reflection density, defined as the logarithm (base ten) of the reciprocal of the reflectance [75].

The table below summarizes THz time and frequency parameters based on integrals that can be used to plot a THz C-scan.

Field	$\int_s E(s)ds$	(10)
Amplitude	$\int_s \lvert E(s)\rvert ds$	(11)
Power	$\int_s \lvert E(s)\rvert^2$	(12)
Power ratio	$\frac{\lvert E(s)\rvert}{\int_s \lvert E(s)\rvert ds}$	(13)
Relative power loss	$\frac{\int_s \lvert E(s)\rvert^2 ds}{\int_s \lvert E_{ref}(s)\rvert^2 ds}$	(14)
Centroid (energy distribution of THz signal)	$\frac{\int_s \lvert E(s)\rvert^2 s\, ds}{\int_s \lvert E(s)\rvert^2 ds}$	(15)

Table II.2-1 THz time and frequency parameters based on integrals that can be used to plot a THz C-scan. S can either be frequency (ν) or time (t). Adapted from [43].

In addition to the methods used for all digital images (e.g. histogram manipulating, such as histogram equalization algorithm and its variations), effective THz contrast enhancement can be obtain by choosing the THz frequency range within which the spectral contrast among material is maximized.

II.3 Analytical instrumentation

THz-TDI measurements were performed with a portable Picometrix T-Ray 4000 device (Picometrix Inc.), consisting of a femtosecond fiber laser coupled with 5-m long umbilical cords to a photoconductive transceiver head mounted on an XY-scanning stage and a rapid-scanning pump-probe system for generating and detecting short pulses of electromagnetic radiation at terahertz frequencies [52], [76]–[79]. The photoconductive system is powered by a 100-fs laser that works between 750-850 nm and delivers at least 20 mW of optical power. Further indication about the system are found in [34], [80] and in table II.4-1.

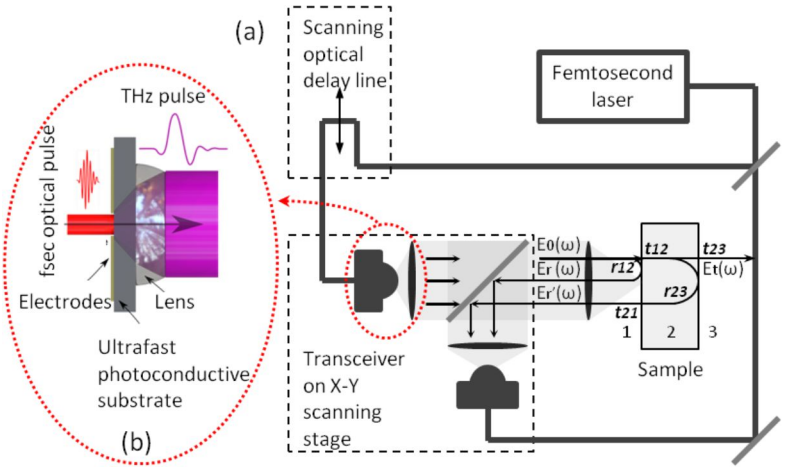

Figure II.3-1 a Schematic representation of the THz-TDI device used at normal incidence reflection geometry. **b** Photoconductive switch for generation of terahertz pulses.

We used a 320 picosecond (ps) measurement window, with a temporal resolution of 0.078 ps (sampling frequency 0.003 THz).The frequency range covered is approximately 0.01 – 3 THz, even if this frequency range is reduced by the noise floor, particularly high for imaging application (usable frequency range approximately 0.1 - 1 THz).

The system has a fundamental data acquisition rate of 100 scans/s. Further specification about the system are in table II.3-1.

System specification (RS320/100 rapid scan)

Pulse	Near single cycle (~ 7 s FWHM)
Average power	< 50-500 μW
Collimates beam diameter	1.5 inch
Focused spot size	Adjustable with optics, 200 μm – 2 mm
Signal-to-noise	>70 dB at peak pf spectral

	intensity
Bandwidth	0.01 – 3 THz
Waveform acquisition rate	100 Hz
Waveform time window	320 ps
Time domain accuracy	±10fs over 320 ps
Time-domain resolution	78 fs
Frequency resolution	3 GHz
Number of points per waveform	4096

Table II.3-1 System specification as reported in the user manual [81]

The optical resolution of the system is about 300 μm at 1 THz, which is the highest frequency considered for our applications. The optical resolution was determined independently by a knife-edge scan of the THz beam profile [82].

Terahertz raster scanner is accomplished by moving either the sensor heads or the object being imaged in a fixed pattern. The total area is broken into pixel squares. All the waveforms acquired within the pixel area contribute to that pixel representative waveform.

The user may define the scan profile, which include options such as the starting position, the heads travel, the pixel size and the acquisition rate (mm/sec), which define the acquisition rate (waveforms/pixels). The minimum rate of acquisition is approximately three waveform per pixel. At any faster rates, holes or missing data may appear in the image.

When needed, data deconvolution has been performed through the algorithm implemented in the software. The software completes data deconvolution by convolving the deconvolved signal with a Gaussian function to reduce sin-like pulse ringing [81].

Chapter III
THz-TDI applied to easel painting investigation

The ability of terahertz time-domain imaging (THz-TDI) to visualize and analyze subsurface features of artworks is nowadays established [8], [9] and THz-TDI has already shown in some cases its ability to image hidden paintings [83].

Regarding easel paintings, in 2009 A. J. L. Adam et al. demonstrated the capability of THz-TD for imaging hidden painting on canvas replicas [84], and further studies on replicas followed [85]. In 2013 THz-TDI found its application on a real work of art, when a feature with a strong resemblance to one of Goya's known signatures was imaged by THz –TDI in an 18 C painting attributed to Goya, thus showing the potential of this technique for authentication in art [86].

The following chapter reports on the results obtained by applying of THz-TDI to image a hidden portrait and other subsurface structural layers of a painting by Nicolai Abildgaard. The original article can be accessed at [87].

III.1 Reflection Terahertz Time Domain-Imaging for Analysis of an 18th Century Neoclassical Easel Painting

Terahertz time-domain imaging (THz- TDI) in reflection mode has been applied for imaging a hidden portrait and other subsurface composition layers of an 18th century (18C) easel painting by Nicolai Abildgaard, the most important 18C Danish neoclassic al painter of historical and mythological subjects. For the first time, a real hidden portrait on an easel painting has been imaged by THz-TDI, with an unexpected richness of detail. THz C- and B-scans have been compared with images obtained by x-ray radiography and invasive cross-sectional imaging, leading to a deeper

understanding of the strengths and limitations of this technique for art diagnostic purposes and defining its role among complementary tools for the investigation of art objects.

Extraction of the individual pulse signatures from the full-reflected signal may be challenging and it may requires complex processing operation (see paragraph II.2.B). A fast and effective method for separating single THz pulse from the entire recorded back-reflected waveform is presented, and it demonstrated to be suitable for processing THz images acquired from large and uneven surfaces typically encountered in practical applications of the technique. Interfaces between layers of the painting have been successfully imaged, contributing substantially to the understanding of the structure of the painting.

III.1.A Potential of THz-TDI scans as a complementary tool to X-ray radiograms

Within about one year of the discovery of X-rays (0.01 -10 nm wavelength, 3×10^{16} Hz to 3×10^{19} Hz frequency) by Conrad Wilhelm Röntgen, paintings were being examined by radiography. Indeed, radiography in transmission mode turned out quickly to be extremely useful in understanding the paintings technique and preservation state, especially in combination with paint cross-sections and infrared reflectograms, a well-established protocol to visualize the internal structure of paintings [88]. Differently, only in the recent few decades the terahertz frequency region is being filled by fundamental research on its applications, including those in artworks inspections.

One of the reasons for advocating the use of THz-TDI for art diagnostics is the concern about the ionizing effects of X-ray radiation (photon energies above 5-10 keV) and the difficulty of radiometric dating of a sample after x-ray irradiation. X-radiography also requires strict safety procedures which are not needed when dealing with low intensity THz waves (0.4 – 12.4 meV photon energy within the 3 – 0.1 mm wavelengths range) [89].

Modern digital radiography equipment for nondestructive testing typically has a lateral resolution of 100-200 μm [90], and THz imaging over large areas typically has a lateral resolution of 300 μm at 1 THz. In spite of this somewhat reduced spatial resolution compared to radiography, reflection THz-TDI, using ultrashort pulses of radiation, offers sufficient depth resolution, with the ability to image individual buried interfaces.

The complementarity of these techniques for the inspection of artefacts will be better understood with the introduction of THz-TDI in art galleries and museums, investigating actual structures, as exemplified by the case of the present study.

III.1.B Materials and methods

The investigated easel painting

The investigated painting was *The Dying Messalina and her Mother* (Fig. III.1-1a), painted by the Danish artist Nicolai Abildgaard (c. 1797, 61 x 77 cm, oil on linen canvas), a famous 18C artist known for his characteristic unorthodox painting technique [91]. Conservation and restoration of the painting was carried out in 2001. Due to the fragility of its canvas, a fabric and a paper interleaf were applied to the back of the painting as a lining to create extra support for the structure. A wax-resin mixture was applied between the two canvases at the lining treatment and melted into the structures.

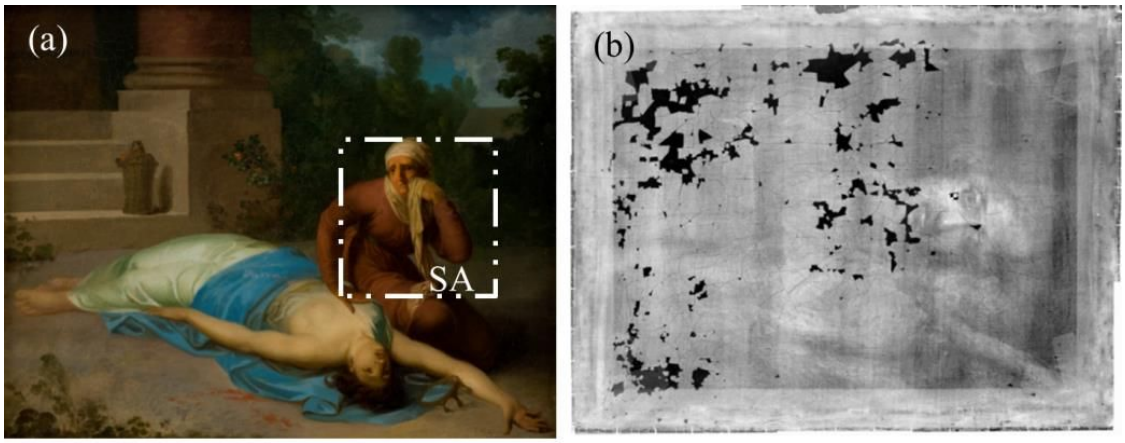

Figure III.1-1 a The Dying Messalina and her Mother by Nicolai Abildgaard (c. 1797, 61 x 77 cm, oil on canvas), Inv. No. KMS3651, Statens Museum for Kunst collection. The white dashed square indicates the area scanned by THz –TDI **b** Radiography of the painting.

Treatment, however, was also undertaken for aesthetic reasons, as the large old discolored areas of a previous restoration clearly called for a cleaning. Prior to the treatment, cross section analysis (Fig. III.1-2a-c) and X-radiography (Fig. III.1-1b) were performed.

Analytical instrumentation

THz-TDI has been performed with a Picometrix T-Ray 4000 device, and we employed a scan velocity of 15 pixel/s (6.7 scans averaged per pixel) in a reflection configuration at normal incidence. The raster scanning was performed with a resolution of 400 μm, resulting in 500x500 pixel images. The spatial step size was matched to the optical resolution of 300 μm at 1 THz (highest frequency considered here). X-radiography

Digital X-radiography was carried out with an Andrex® BW85 X-ray tube and the exposure parameters 5mA, 30kV, 60 sec. The radiography was performed on Dürr NDT CRIP3040109 digital image plates which were subsequently scanned at a lateral resolution of 100 μm in a Dürr HD-CR 35 NDT laser scanner.

III.1.C Results and Discussion

Subsurface and stratigraphic investigation by mean of radiography and cross section images

X-radiography of the painting was carried out during the restoration intervention in 2001 for an assessment of the actual state of the authentic painting underneath the old layers of restoration. The X-radiograph (Figure III.1-1b), mapping the paint losses, gave a clear picture of the extent of damage in the original painting. The recording also revealed that underneath the image of the dying Messalina was a portrait, apparently of a gentleman in a wig, painted with perpendicular orientation to the composition of the current image, indicating that Abildgaard recycled an older painted canvas for his painting. It was not possible to identify the sitter, nor could it be said to which degree the portrait was a completed painting or just an initial sketch. Though the somewhat ghostly features of the person in the X-radiograph appeared rather worked through, the image was obviously too incomplete to assess as a result of the limitations of the technique in recording elements such as areas of darker paint in the composition. Although there are other examples in which Abildgaard recycled earlier canvases with abandoned compositions, no proper portraits from his own hand are known to exist. However, one may speculate that this could also have been the reason why the portrait – if indeed painted by him - was discarded and overpainted in the first place.

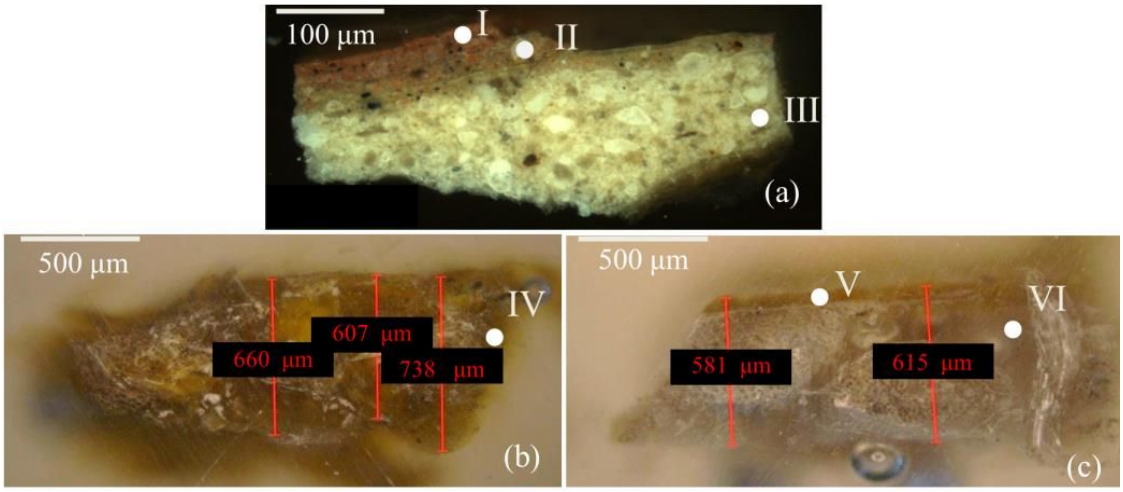

Figure III.1-2 a Cross section, showing a first pictorial layer (I), **a** second one (II) and the ground (III). **b** Cross section of the original canvas (IV). **c** Cross section of the restoration canvas (VI) with the paper interleaf. (V).

Cross-section analysis in the microscope of minute samples from different areas of the painting showed a structure with a varying number of paint layers on top of a white ground. Cross-sections of the ground and paint layers (Fig. III.1-2a) indicate that their combined thickness is in the range 100-300 µm, dimensions fairly common for paintings of the era. In addition, the cross-sections revealed that Abildgaard had not applied an intermediate ground layer on top of the portrait before painting the new composition. The original canvas (Fig. III.1-2b) has a thickness in the range 607 – 738 µm, while the lining canvas including the paper interleaf (Fig. III.1-2c) has a thickness of about 582 - 616 µm. The material used as adhesive between these two canvasses, melted and penetrated into the textile, is not detectable in the cross sections as an individual layer.

Subsurface and stratigraphic investigation by mean of THz-TDI

THz-TDI scans were performed after the last restoration intervention on the area of the painting indicated in Fig. III.1-1a. B-scans (Figure III-3a) gave non-invasively a clear picture of the stratigraphy of the painting, and six main interfaces have been found (Fig. III.1-3c). The apparent curvature of the surface is an indication of the unevenness of the painting.

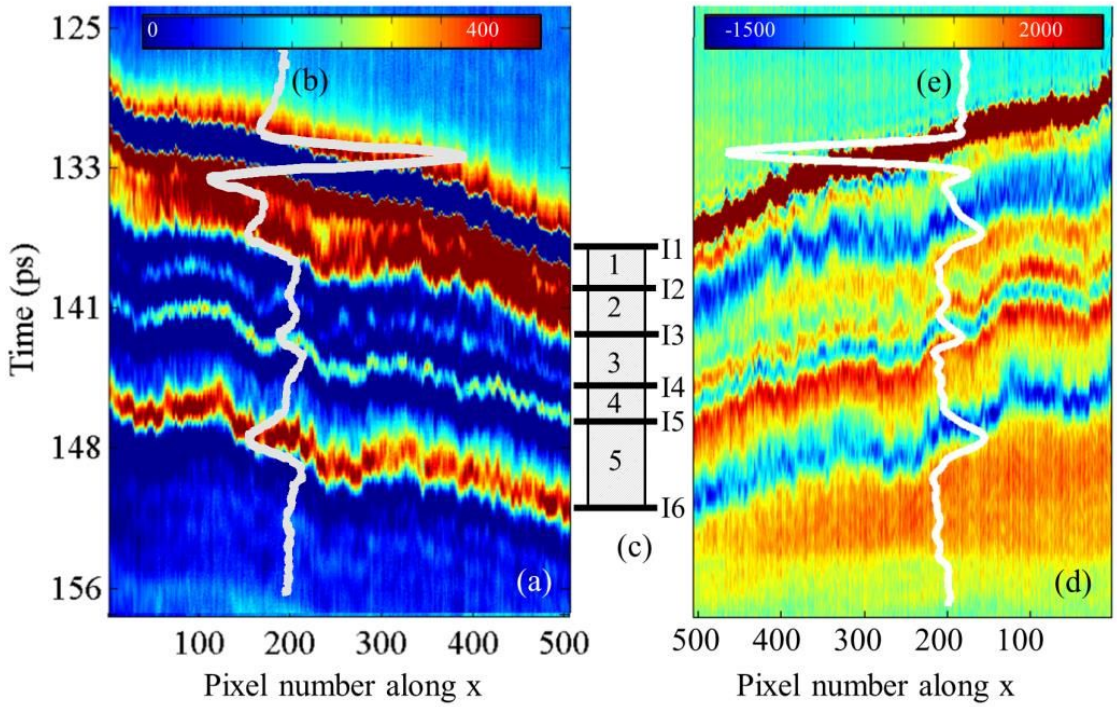

Figure III.1-3 a B-scan obtained at the scan-line indicated in dashed red in Fig. III.1-6a. **b** Waveform recorded at coordinate (200, 200) of the pixel grid, indicated by the black asterisk in Fig. III.1-6a. **c** Scheme of the stratigraphy detected by THz-TDI: I1, air/surface interface; I2 interface between various paint layers and/or the ground; I3 ground/original canvas interface; I4 interface within the original canvas, possibly at limit of the penetration depth of the wax-resin material used for the lining intervention; I5 original/restoration canvasses interface; I6 restoration canvas/air interface. **d** B-scan after deconvolution of signals combined with Wiener filter. **e** The same waveform of Fig. III.I-3a, after deconvolution.

Single THz pulses of interest, arising from the reflections at individual interfaces of the painting layers, have been separated from the full recorded waveform through recursive signal windowing and threshold clipping.

In order to handle subsurface separation for the uneven surface structure, apparent in Fig. III.1-3, the parameters used for isolating and plotting interfaces of interest (i.e. location and width of temporal windows and cut-off values for signal clipping) have been individuated by processing complete B-scans at first, instead of processing individual signals recorded at each pixel of the scanned area.

Examining B-scans instead of the single waveforms recorded at each spatial coordinate of the scanned area is crucial in choosing appropriate lower and upper cut-off values for thresholding as well as suitable location and width of temporal windows, thanks to the immediate visualization of electric field value onto the color scale, and to the overall comprehension of its simultaneous variations across the time axis and across the linear space of

the image (x direction in case of row B-scans, y direction in case of column B-scans). Individual interfaces of layers composing the painting have been imaged following the steps described below.

B-scans (Fig. III.1-4a) have been plotted after subtraction of the signal background from the system, in order to recover the recorded waveforms from noise and echoes arising from environmental and instrumental contributions which can be significant due to the small amplitude of the reflected signals. After color axis rescaling (Fig. III.1-4b), six regions of interest (ROIs) have been identified in the B-scans. Each ROI corresponds to an interface between the layers composing the painting stratigraphy. Despite the small thickness of the composing layers, the majority of the detected interfaces are temporally well resolved. To better distinguish the varying number of paint layers and the white ground, not fully resolved, deconvolution using a reflection from a plane metal surface, coupled with a Weiner filter has been applied (Fig. III-4c-d), better underscoring the presence of an additional interface within the surface and the canvas layer. Because of the complexity of the structure, it is not possible to assign this interface to that between the Abildgaard painting and the previous one, or to that between the paint layers and the ground. Consequently, the whole region included between the surface and the canvas interface has been chosen as the one of interest for imaging the hidden portrait.

First, fifth and sixth ROIs (Fig. III.1-4e, 4k, 4m) have been segmented by opening symmetric tapered cosine windows around the indices of the global maxima of the waveforms recorded at each x-coordinate of the B-scans, after preliminary windowing (Fig. III.1-4j, 4l).

When used, the tapered cosine window has been chosen for avoiding sharp discontinuity between the first and last point in the periodic time series, while the ratio of the cosine-tapered section length to the entire window length (r) has been set equal to 0.25, for not changing the weighting of samples in the time series drastically, so that almost all of them will contribute to the Fourier transform, thus reducing spectral leakage. Extraction of the second and third ROIs from B-scans turned out effective by combining apodization and threshold functions. First, the region of the B-scans which includes both those ROIs has been separated through a wide rectangular window function (Fig. III.1-4f). Rectangular window has been chosen in this case for not modifying pixels values at the extremities of the windows, which would have prevented to define the correct thresholding function.

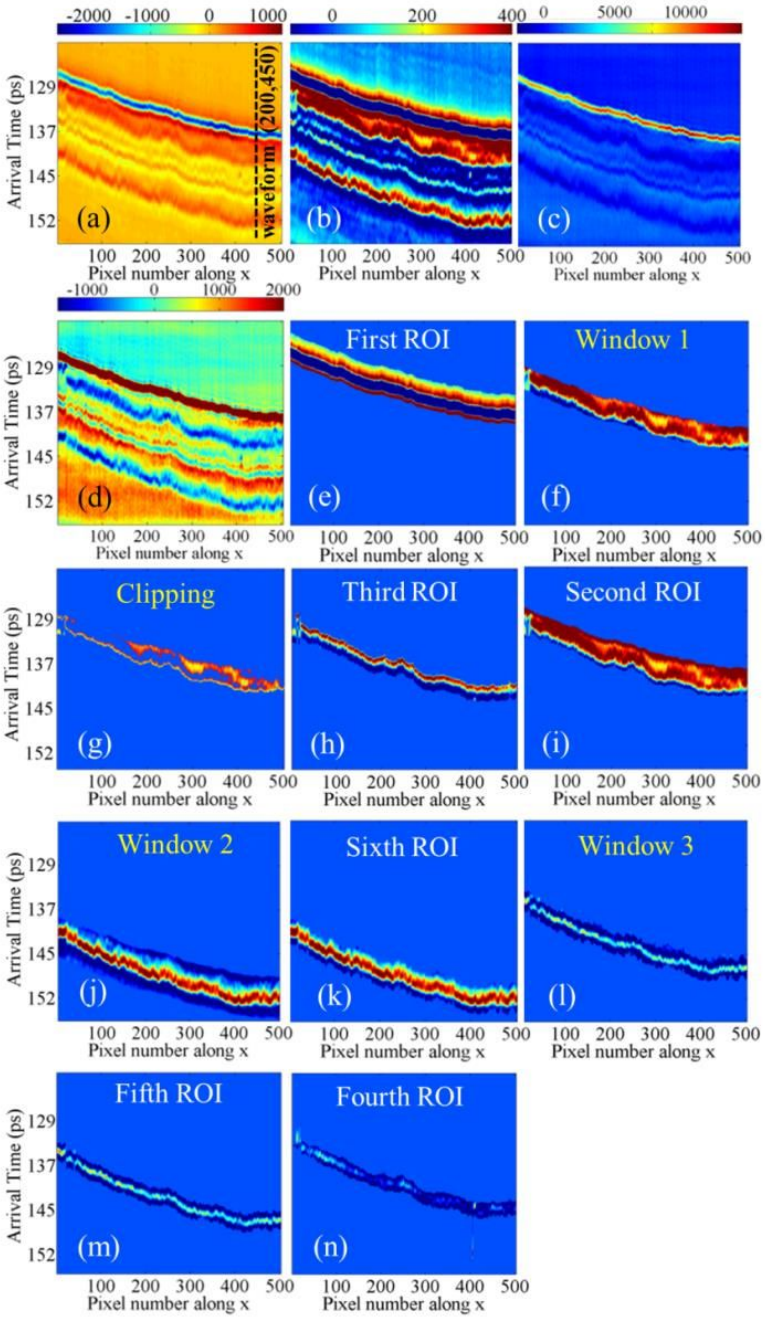

Figure III.1-4
a B-scans before and after data processing, showing the signals recorded at different spatial coordinate along x, for y fixed at 200 (dashed, black scan-line in Fig. III.1-6a). **b** B-scan after color axis rescaling. **c** B-scan after deconvolution combined with a Wiener filter. **d** B-scan after deconvolution and color axis rescaling. **e** First region of interest (ROI). **f, g, h** B-scan after windowing, after clipping and third ROI, respectively. **i** Second ROI. **j, k** windowing and sixth ROI. **l, m** windowing and fifth ROI. n Fourth ROI.

The isolated region has been further segmented by hard double thresholding, so that

$$E_f(t) = \begin{cases} 0 & if\ E_i(t) < 160 \\ 1\ if & 160 \leq E_i(t) \leq 350 \\ 0 & if\ E_i(t) > 350 \end{cases}, \qquad (16)$$

where $E_i(t)$ represents the value of the electric field recorded for each pixel, and $E_f(t)$ is the output pixel value after the threshold function has been applied (Fig. III.1-4g). Indices (along the time axis) of the nonzero pixels values within the thresholded region have been placed into index

vectors created for every spatial coordinate of the B-scans. The last linear index of each vector has been chosen as the end of the second ROI and the beginning of the third ROI. A tapered cosine window has been applied to isolate the third ROI (Fig. III.1-4h), while the second ROI (Fig. III.1-4i) has been separated by opening a window within the first and the third ROIs.

In a way similar to that used for second ROI, fourth ROI (Fig. III.1-4n) has been separated by opening a window between the third and the fifth ROI.

Once identified, the same parameters used for interfaces separation in the B-scans have been used for the processing of individual tracks recorded at each pixel (Fig. III.1-5).

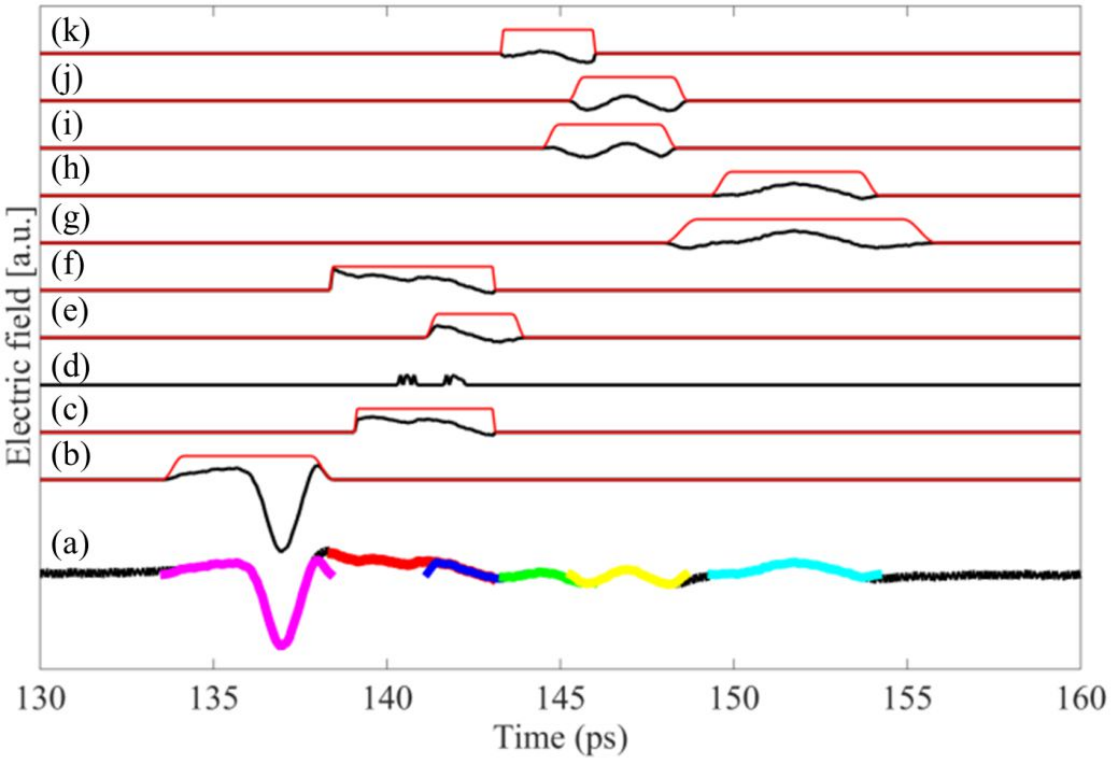

Figure III.1-5 **a** THz waveform recorded at pixel (200, 450), indicated by the red asterisk in Fig. III.1 6a, where the different isolated ROIs are plotted in different colors. **b** First ROI **c** Window 1. **d** Signal clipping. **e** Third ROIs. **f** Second ROI. **g** Window 2. **h** Sixth ROI. **i** Window 3. **j** Fifth ROI. **k** Fourth ROI

Therefore interfaces between the main layers of the painting have been imaged (Fig. III.1-6a-f), giving a substantial contribution to the understanding the structure and stratigraphy of the painting.

The detailed appearance of the interfaces (Fig. III.1-6a-f) has been imaged by integrating in the amplitude spectra of the clipped temporal

signals over the frequency range of these signals. The pixel value M is defined as

$$M = \int_{\nu_i}^{\nu_f} \left| FFT\left(E(t)\right) \right| d\nu \qquad (17)$$

where M is the pixel value, ν_i and ν_f are the limits of the exploited frequency range according to the specific parametric representation for a specific image, E is the recorded electric field in the temporal range defined as $t_i \leq t < t_f$ with t_i and t_f being the extremes of the temporal windows chosen for isolating the proper ROI.

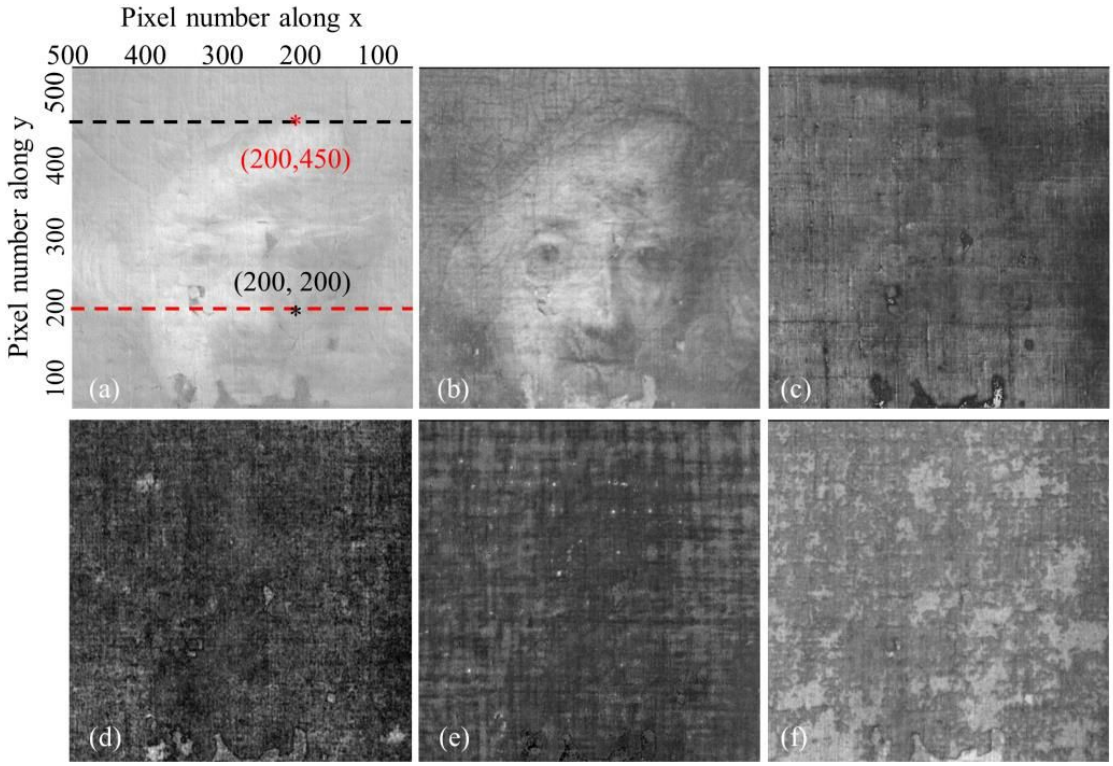

Figure III.1-6 **a** THz frequency image of first ROI. Red and black dashed lines indicate the scan lines used to plot the B-scans of Fig. III.1-3 and 4, respectively; the THz waveform plotted in Fig. III.1-5 is localized by a red, asterisks while the waveform plotted in in Fig. III.1-3b and III.1-3e by the black one. **b** THz frequency image of the second ROI. **c** THz frequency image of the third ROI, the front of the original canvas. **d** THz frequency image of the fourth ROI, possibly the interface between the structures permeated and not permeated with the wax-resin mixture used during the lining intervention. **e** THz frequency image of the fifth ROI, the front of the lining canvas with the paper interleaf. **f** THz frequency image of the sixth ROI, the back of the lining canvas.

The evidently high reflectivity values of the concealed paint layer allowed imaging the hidden portrait (Fig. III.1-6b) by using equation (17). The front of the original canvas (Fig. III.1-6c), as well as the one used for

the lining intervention with the paper interleaf (Fig. III.1-6e), have been clearly identified and imaged, underlining the capability of THz- TDI to monitor the correct adhesion between the two components, as well as their texture, thereby demonstrating that the technique is useful for the non-destructive evaluation of a lining intervention.

Fig. III.1-6d shows the interior of the original canvas, imaged by isolating the fourth ROI. The location of this interface inside the original canvas suggests it represents the penetration limit of the wax-resin mixture material melted for attaching the lining canvas to its back.

Fig. III.1-6f shows the back of the lining canvas, imaged by isolating the sixth ROI. The appearance of a material affixed on the back of the lining canvas (actually not present) restituted by the THz image, suggests that these features are due to the presence of the wax-resin material in the interior, which has the effect of changing the optical properties of the textile. This indicates that the technique is suitable for mapping the distribution of the material penetrated into the fabrics of the canvas.

Complementarity of X-radiography and THz-TDI in understanding the painting technique

Fig. III.1-7a shows the visible image of the scanned area, the corresponding X-radiograph (7b), the peak-to-peak value time-parametric THz image (7c) and different THz frequency-parametric images (7e-f).

The peak-to-peak value time-domain THz image (Fig. III.1-7c) clearly shows some features belonging to the surface layer (Messalina´s mothers dress and complexion), especially above the left eye and right ear of the portrait. Those surface features are much reduced by isolating the proper pulse in time domain before imaging (Fig. III.1-7d). We believe that the partial suppression of the painting on the upper surface is a result of a higher reflection coefficient of the pigment used for the hidden portrait than that used for the visible painting.

Highlights of the complexion show a high response both to X-ray and THz waves, appearing strongly lit. While a proper analytical methodology should be used for a validated pigment identification, these observations suggest the use of a lead white pigment, which absorbs X-rays much more than most other pigments used by 18C painters and has a high reflectivity in the THz range. Carbon based (i.e. graphite) substances would have not been detected by X-Radiography due to the low atomic number, even if in principle visible in the THz reflection image. The contrast between light and

dark areas of the face appears stronger in THz images compared to that of the X-radiograph. It is therefore likely that the unknown painter of the hidden portrait used a pigment for the mid-tones with some absorption of X-rays but of negligible reflectivity within the exploited THz range. For this reason, the shape of the face looks different according to the electromagnetic range used to record the images, as if it has been sharpened and modeled by mid-tones not seen by THz waves. The X-radiograph shows the lower lip as the most lit area of the face, while the same detail does not show particular response in THz images. This suggests the use of a pigment other than that used for the genuine highlights.

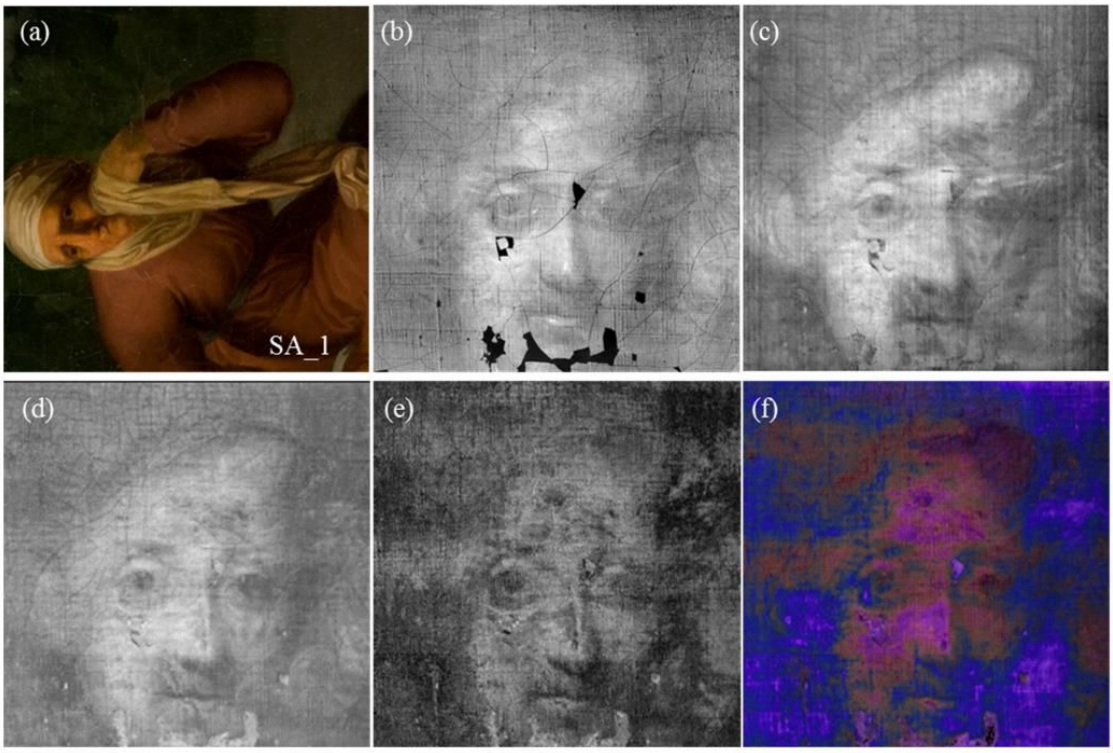

Figure III.1-7 **a** visible image of the scanned area. **b** X-radiograph of the scanned areas. **c** Peak-to-peak time parametric THz image. **d** THz frequency integrated image of interface layers included among I2 and I3. **e** THz image in 0.55 - 0.62 THz range. **f** THz false color (FC) image

Fig. III.1-7e shows the THz image realized by integrating the spectral amplitude over a restricted frequency range (0.55 - 0.62 THz). Within this frequency range lit marked lines are particularly discernible on the nose line, eyelids, eye contour and around temples, leading us to understand how the painter used them to create the backbone and main shapes from which the visage is painted. The darkest areas of the face (pupils, nostrils, upper lip and

the shadows of the upper lip) come out in THz images better than in the X-radiograph, being more contrasted to the lit ones.

Fig. III.1-7f is a THz false color (FC) image realized representing the 0.36 - 0.48 THz band by red, the 0.48 THz - 0.55 THz band by green, and the 0.22 - 0.36 THz band by blue. Pupils, more discernable from the other part of the visage in FC rendering, appear reddish-purple, while shadowed areas appear blue. This differentiation in FC supports the interpretation that different pigments have been applied for the shadows and for the realization of the pupils.

III.1.D Chapter conclusion

The painting *The dying Messalina and her mother* (1797) was scanned using THz-TDI, offering an occasion to compare the results obtained by this technique with those obtained by the more established X-radiography and cross-section imaging.

Both X-radiography and THz-TDI were able to image a hidden painting below the present one and for the first time, a real hidden composition in an easel painting has been imaged by THz-TDI, with a surprisingly richness of details. The information provided by the two techniques complement one another, offering new insight into the painting technique used by the unknown painter of the hidden portrait, and to expand the knowledge of the response of different pigments within these different electromagnetic ranges. While the hidden portrait has been imaged already in the past by X-radiography, the THz image provides a more complete representation of the features of the face, making a potential identification of the sitter more credible than if it was based solely on the X-radiograph.

B-scans gave non-invasively a clear picture of the stratigraphy of the painting, while thin layers such as the paper interleaf between the original and the restoration canvas and single paint layers, imaged by cross-section analysis, are not fully detectable in THz B-scans even after signal deconvolution.

A fast and effective method to separate individual THz pulses of interest from the entire signal recorded at each spatial coordinate of the acquired THz image has been presented. Interfaces between layers of the painting have been successfully imaged, contributing substantially to the understanding of the structure of the painting.

Both the original canvas, and the one applied with a paper interleaf to the back of the painting at the last restoration intervention, have been imaged in

their entirety (B- and C-scans) without noise or shadows due to the presence of the layers above. THz-TDI has thus demonstrated to be suitable for monitoring the preservation state of the canvas texture as well as the proper adhesion between the lining canvas and the rest of the painting structure.

Additionally, the technique was seen to be useful for mapping the distribution of the adhesive material inside the fabrics of the canvases, used at the lining intervention.

Finally, comparing THz-TDI images to the information obtained by cross-sectional imaging and X-radiography led to a deeper understanding of the strengths and limitations of this technique for art diagnostic purposes and thus to a definition of its role in a set of complementary investigation tools for the non-destructive inspection of works of art.

Chapter IV
THz-TDI applied to panel painting investigation

THz-TDI has already shown its capability in returning stratigraphic and internal structural information of artefacts non-invasively [83], [84], [92]–[96]. Within this field of application, successful results have been obtained by applying THz-TDI to the study of panel paintings.

THz-TDI has been found to be suitable for examining subsurface features of wooden supports of panel paintings, such as the wood grain lines and the presence of knots, which show a higher THz absorption than the surrounding wood, as well as defects, such as cracks or air gaps [97]–[102].

Since the wooden texture of a panel is characteristic of the wood species, THz-TDI may be an indirect aid for dating a wooden support. In fact, even though the choice of wood by local artisans was strongly influenced by questions of availability and cost, some general dating rules do exist.

Information about the type of wood used for panel painting manufacture could be also beneficial for recognizing whether or not the chosen wood was a suitable species for making the panel. Indeed, dimensional stability in the presence of humidity variations as well as shrinkage and distortion coefficients values of a panel do also depend on characteristics related to the wood species used (e.g. the presence of inhomogeneity, texture dimension, difference between earlywood and latewood, between normal wood and knots and so on). When the proper area is scanned, THz-TDI has the potential to show the way in which the wood boards were sawed (rift sawn, plain sawn, quarter sawn, etc.) or the way in which they were joined together or strengthened by imaging nails or other components (crossbeams, braces, etc.).

The possibility of obtaining stratigraphic information non-invasively within a large portion of a panel painting makes THz-TDI a suitable technique to give some insights into the construction technique of panel paintings, which is also closely connected to the provenance, age, and

attribution of the paintings. At the same time THz-TDI may provide information about the presence, the absence and the features of linens and gesso layers, elements often used for preparing the panel for the paint layer. This is advantageous in characterizing the local panel construction technique in use at the time, but also in placing this information in relation to conservation purposes, since it is related to the structural stability of the support and to the possible degradation effects which it may have on the surface painting layers [103].

In this chapter, the results obtained by applying THz-TDI to the characterization of different kind of panel paintings, are shown.

IV.1 Analysis of a 17th Century Panel Painting by Reflection Terahertz Time Domain-Imaging (THz-TDI): contribution of ultrafast optics to museum collections inspection

In this section we will show the application of THz-TDI to image a hidden painting and other subsurface composition layers on the 17th century (17C) panel painting *A Garden in front of a Country Seat* by David Teniers the Younger and belonging to the collection of the National Gallery of Denmark. Cross-sectional imaging (B-scans) has enabled a clear separation of the individual layers, thus offering visualization of the internal structure over large areas of the painting in a completely nondestructive manner.

THz plan-type images, or C-scans, have been compared with x-ray radiograms of the same subject, thus adding information on the different response and contrast mechanisms of the investigated materials at widely different regions of the electromagnetic spectrum used for imaging. The original invited paper is accessible at [104].

IV.1.A The investigated panel painting

The investigated painting was *A Garden in front of a Country Seat* (National Gallery of Denmark collection - Fig. IV.1-1a, attributed to the Flemish artist David Teniers The Younger (17C, Oil on panel, 43 x 63 cm), a prolific artist of the mid-17th century who worked in Antwerp and Brussels, where he was known for his genre scenes of peasant life.

The panel support of the painting had a horizontal grain direction and a thickness varying between 3 and 7 cm. Visual examinations of the edges showed that the panel had at some point been trimmed along the sides. X-radiography (Fig. IV.1-1b) further revealed that the artist had recycled an earlier painting for his composition, showing the existence of an escutcheon surrounded by ornamental scrolls underneath the present image.

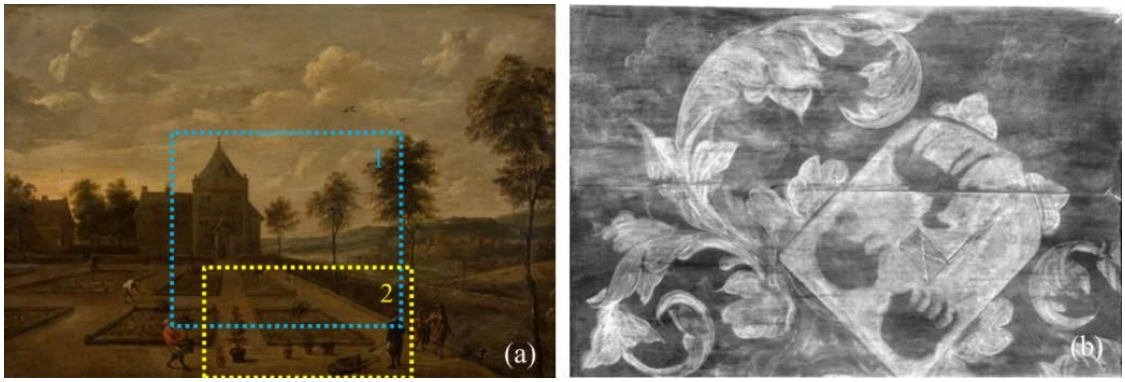

Fig. IV.1-1 a A Garden in front of a Country Seat by David Teniers the Younger, National Gallery of Denmark collection (17C, Oil on panel, 43 x 63 cm). The two areas scanned by THz-TDI are localized by dashed squares and respectively named 1 and 2 **b** X-radiograph of A Garden in front of a Country Seat

The coat of arms has heraldic bearings apparently in the shape of a flag and three different animals. A red layer observed in a few areas between the two paintings indicates that the artist most likely applied a new ground layer on top of the first painting (the coat of arms) before he painted the second composition.

IV.1.B Analytical instrumentation

THz-TDI was performed with a Picometrix T-Ray 4000 device. We employed a scan velocity of 12 pixel/s (8.3 scans averaged per pixel) in a reflection configuration at normal incidence. The raster scanning was performed with a resolution of 400 µm.

Digital X-radiography was carried out with an YXLON® MIR-201E X-ray tube and the exposure parameters 5 mA, 25 kV, 90 s. The radiography was performed on Dürr NDT CRIP3040108 digital image plates which were subsequently scanned at a resolution of 50 µm in a HD-CR 35 NDT laser scanner.

IV.1.C Results and Discussion

The THz signal incident on the painting consists of a single cycle of the electric field, with a duration of approximately 1 ps. Fig. IV.1-2 shows a representative data set obtained along a scan line of the image. The recorded return signals (Fig. IV.1-2b) show three main pulses arising from reflections at air/surface interface, at painting/wooden support and at one interface between these last two, respectively. Fig. IV.1-2a shows the resulting B-scan.

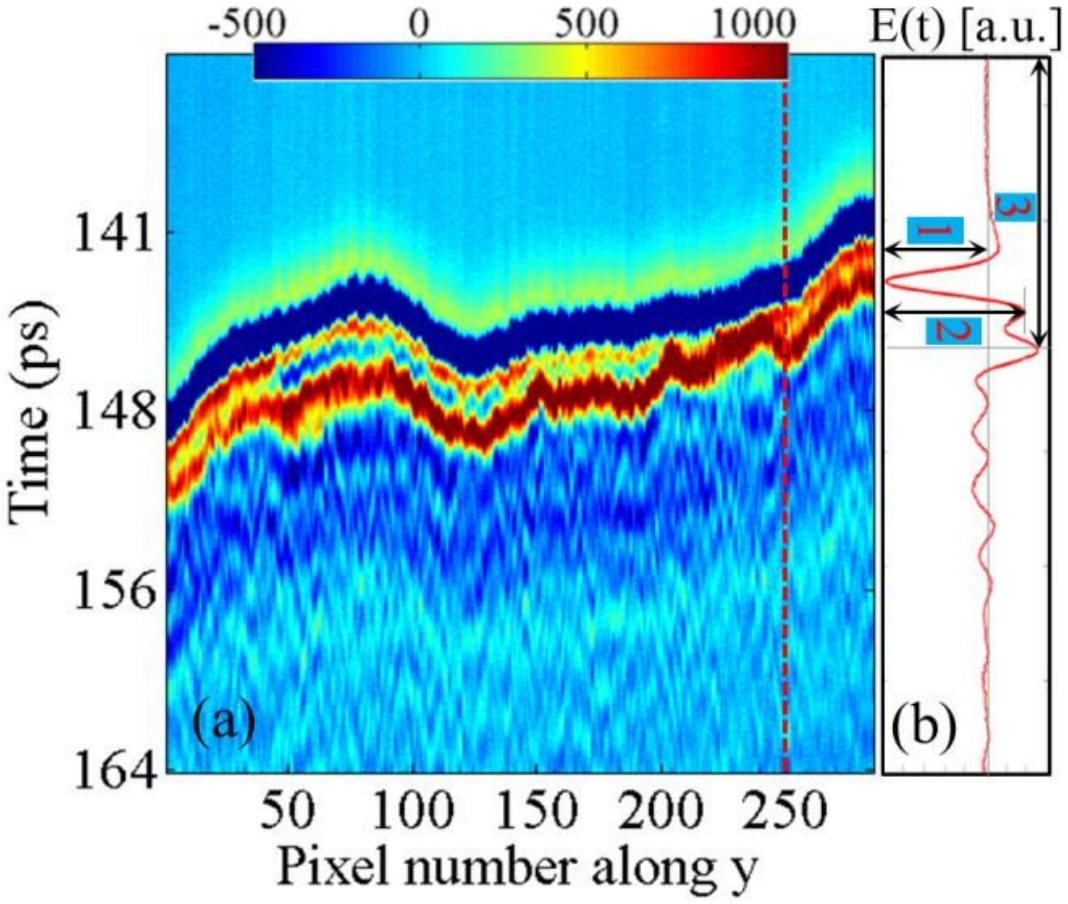

Fig. IV.1-2 a B-scan representing the electric field of the reflected THz signal as function of time, recorded along the scan-line shown in Fig. IV.1-3d. The dashed red line is the waveform shown in Fig. IV.1-2b. **b** Waveform recorded at pixel (250, 250). The horizontal axis is the recorded electric field value, while the vertical axis represents the time delay (ps), and is in common with that of Fig. IV.1-2a. The double arrows represent, respectively, (1) the peak maximum absolute value used to plot Fig. IV.1-3c, (2) the peak-to-peak or peak-to-trough amplitude value used to plot Fig. IV.1-3d, and (3) the time delay of the pulse arising from the reflection at the paint materials/wooden panel interface, used to plot Fig. IV.1-3f.

The appearance of the relevant interfaces found has been imaged using different parameters, thus providing images containing different information.

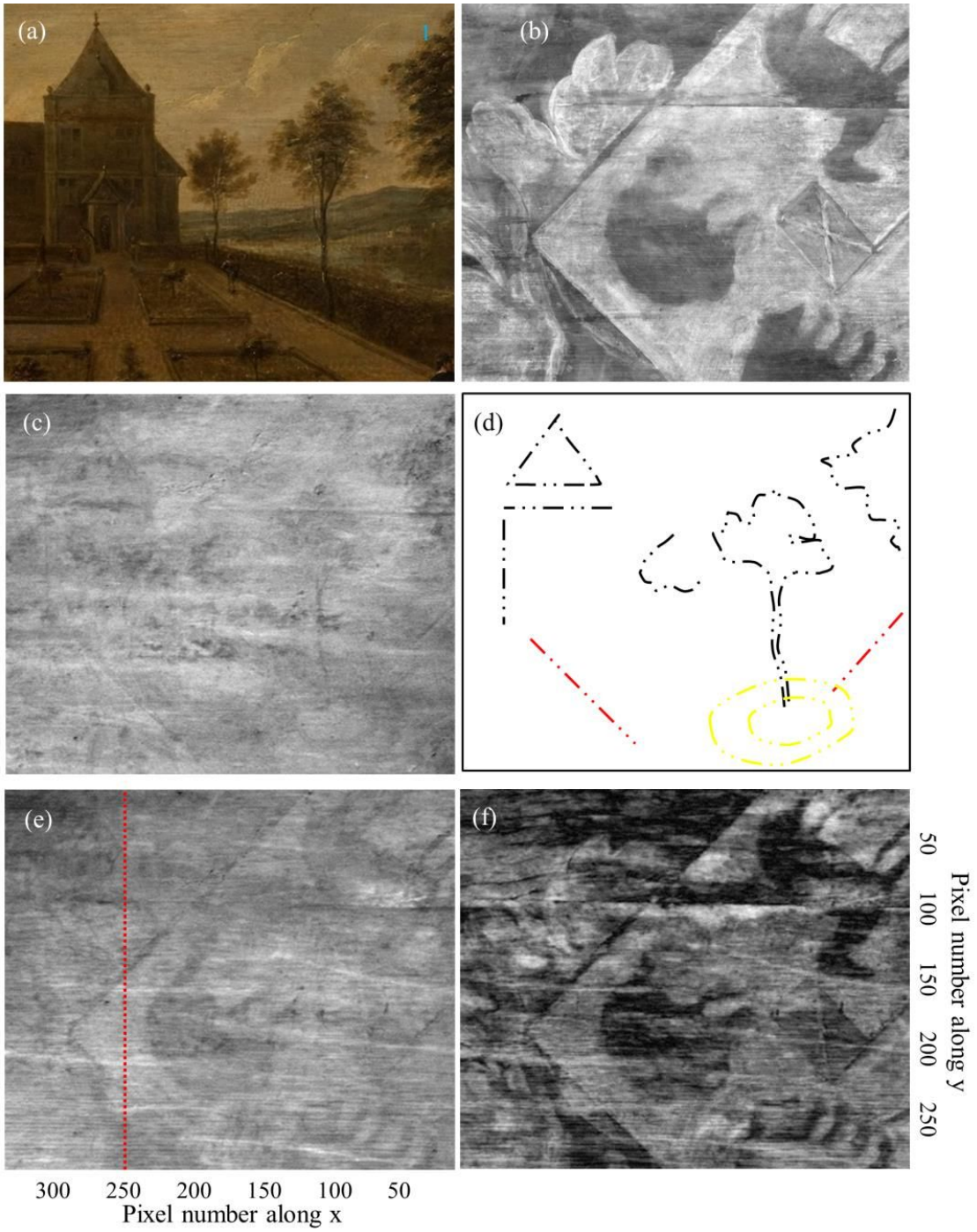

Fig. IV.1-3 a Scan area 1, located as indicated by the blue dashed square in Fig. IV.1-1a. **b** X-radiograph image of the same area.. **c** THz time-domain parametric image plotted using the maximum value of the reflected electric field at each pixel.. **d** Interpretation of the features seen in Fig. IV.1-3c: black lines: marks located on surface, yellow lines: possible construction marks, red lines: features of surface arising from subsurface components **e** Peak-to-peak THz time-domain image. The dashed red line indicates the scan-line used for the B-scan in Fig. IV.1-2a. **f** THz frequency-domain parametric image plotted by integrating the spectral amplitude over the 0.31 – 0.37 THz range, after Fourier transform of the region of interest isolated in the time domain by a window function.

Comparing the visible appearance of the scanned area (Fig. IV.1-3a) and the THz image plotted using the signal global maximum of the reflected signal (Peak Absolute Amplitude image, Fig. IV.1-3c), it may be noticed that the THz image indicates the location of marks used to trace the figures. boundaries on the surface by the painter, and also reveal features which have no counterpart in the actual composition, probably construction marks as well as a mark arising from a subsurface layer (Fig. IV.1-3d). The absolute peak value has been used instead of the relative maximum value in order to take into account phase shifts through the painting materials sufficient to cause the waveform to invert [105]. Referring to the first back-reflected main peak, the change in the peak absolute value in this case arises predominantly from the surface, where in this case is mainly related to the scattering at surface, rather than the reflection features in the paint material. In fact, lower peak values are recorded for the positions corresponding to these marks, where the optical path of the back-reflected signal increases and where the scattering angle changes abruptly in respect to that of the even surface. The deflection of the back-reflected signal causes beam decoupling at the receiver, thus reducing the recorded amplitude.

A pale appearance of the covered painting is already seen in the image formed by the THz signal peak-to-peak amplitude (Fig. IV.1-3e). The hidden painting is more visible by using this parameter since the peak separation occurred such that the point of the local maximum for the surface and the hidden painting occurs at the same time delay, where the reflection features of the hidden paint materials show significant differences [105], making the reading of the hidden composition possible. An acceptable reading of the hidden subjects is only obtained by integrating the spectral amplitude over a narrow THz frequency range (0.31 – 0.37 THz in Fig. IV.1-3f), obtained by Fourier transformation of the region of interest, windowed in time domain. In this case the contrast is enhanced by selecting the pulse arising from the reflection at the interface corresponding to the hidden painting and by choosing the frequency range where the subjects and the background composing the buried painting show the maximum difference in the reflectance spectrum.

Compared to the x-radiograph of the same scanned area (Fig. IV.1-3b), the THz image shows the features of the wood structure behind the composition more manifestly. The differences in wood density produce irregular dark and light banding that appears as longitudinal subtleties which are typical of the anisotropic structure of the wood.

Even if organic materials, such as cellulose, in general are not good absorbers of X-ray radiation, the prominent growth ring structures is usually recognizable depending on the direction of the radiograph relative to the grain of the wood [88], [106]. Anyway, in this case the wood structure is mostly hidden by the more X-ray-opaque ground and paint layers, showing details of the painting composition clearer than in the THz images.

Contrarily, the interaction between terahertz and wood originates from numerous phenomena, related to the complex structure of wood, which include strong finger-print absorption [107], as well as birefringence and attenuation that depends on orientation, attributed to preferential fiber orientation within the wood, thus resulting in polarization-dependent optical properties [108], [109]. Wood absorption is particularly strong compared to other materials composing the painting due to the water still contained even in dry wood (free water and bound water), which results in a high refractive index, and thus a higher visibility in reflection THz images. On the opposite, the presence of water may be a complication for x-radiography [109].

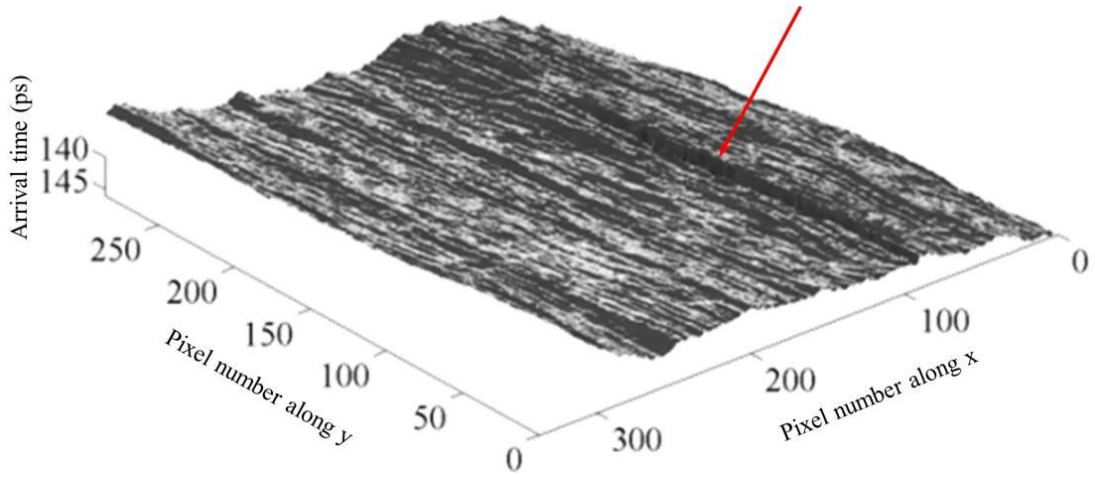

Fig. IV.1-4 ToF image clearly showing the wood grain and irregular structure, as well as the location of a crack in the wood panel supporting the painting, indicated by the red arrow.

Wood grains and irregular structures are clearly visualized by plotting the temporal position of the relevant peak (time of flight image or ToF),

$$\Delta t = \left(\frac{1}{c}\right)\int n(z)dz \qquad (18)$$

where $n(z)$ is the refractive index sampled by the THz beam along its optical path, and where the integral is taken along the path and c is the speed of light [110]. Since the wooden panel is fairly homogeneous, the presence

of a crack and its extension is definitely imaged (Fig. IV.1-4), thanks to the variation in the delay in the pulse.

The second area scanned is shown in Fig. IV.1-5a.

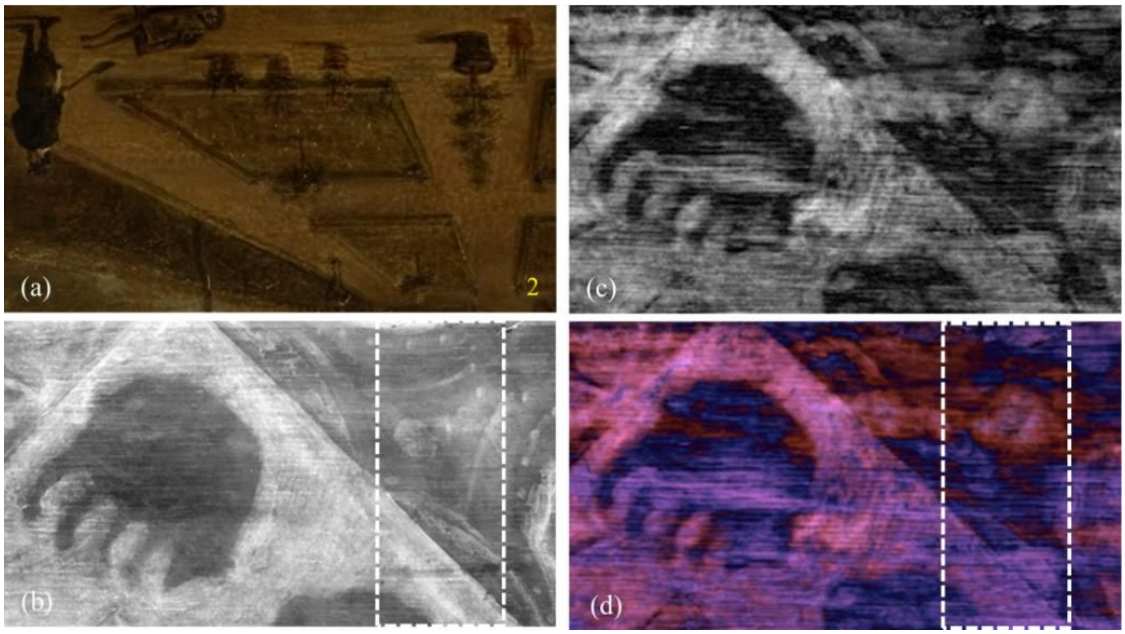

Fig. IV.1-5 a Scan area 2, located as indicated by the yellow dashed square in Fig. IV.1-1a. **b** Radiograph image of the same area. **c** THz frequency-domain parametric image of the integrated spectral amplitude over the 0.38 - 0.43 THz range, after Fourier transform of the region of interest isolated in the time domain by a window function. **d** False color terahertz image plotted with the 0.38 - 0.43 THz, 0.34 - 0.37 THz, and 0.28 - 0.34 THz bands represented as red, green and blue, respectively.

Even in this case, the THz image (the spectral amplitude integrated over the 0.38 - 0.43 THz range, after isolation of the proper pulse in time domain, Fig. IV.1-5c) shows interference due to the wood below the painting in a more prominent manner compared to the radiograph of the same region (Fig. IV.1-5b). It is likely that the change in the animal shape, resembling an additional head turned on the back, depends on these interferences instead of a significant compositional feature. The brushstrokes applied circularly around the animal Fig. are more evident in the THz image. Fig. IV.1-5c shows a THz false color image plotted by placing the 0.38 - 0.43 THz band in red, the 0.34 - 0.37 THz band in green, and 0.28 - 0.34 THz band in blue.

This rendering helped in imaging a detail (Fig. IV.1-6c) which does not follow the structural lines of the wood and has no counterpart in the surface composition.

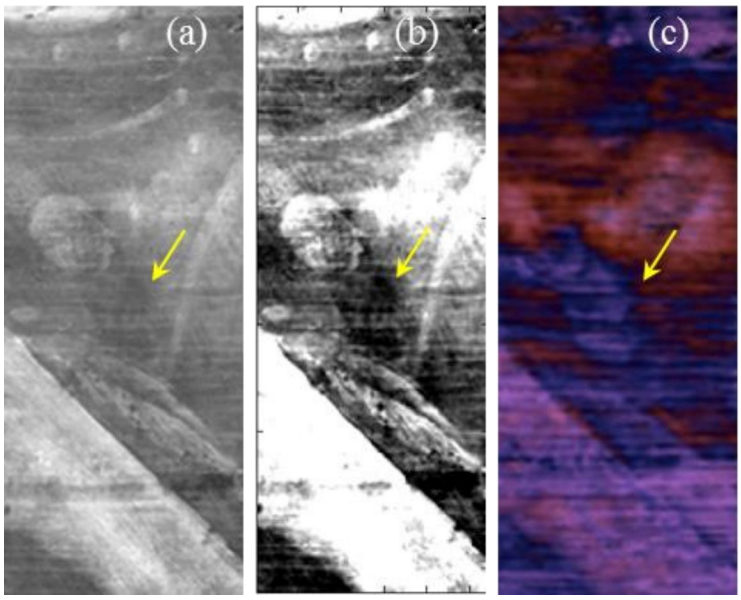

Fig. IV.1-6
a Detail of the x-radiograph, located as indicated by the white dashed square in Fig. IV.1-4b.
b Detail of the x-radiograph after contrast enhancement.
c Detail of the THz false color image of the same area (dashed line in Fig. IV.1-4d).

Even if visible, the detail is barely notable in the radiograph image (Fig. IV.1-6a), also after contrast enhancement (Fig. IV.1-6b). Its dark appearance in the x-radiograph (i.e. low radiopacity) suggests that the material is composed of low atomic number elements. This is in contrast to the bright appearance of the same feature in the THz image. Excluding the connection between this signal and the wooden panel structure, this feature may be from the hand of the unknown artist of the heraldic motives or to the presence of restoration materials at this location. While the obtained terahertz false color image cannot directly support the identification of the substance composing the detail, it helped in visualizing and localizing the feature within the concealed composition. It is auspicious that performing the hidden material mapping by means of THz-TDI will help in choosing the proper location of further spot analysis with other techniques for material identification.

IV.1.D Final considerations

Sections of the panel painting *A Garden in front of a Country Seat* by David II Teniers, National Gallery of Denmark collection (17C, Oil on panel, 43 x 63 cm), has been scanned using THz-TDI, offering an occasion to compare the results obtained by this technique with those obtained by the better developed x-radiography. Both radiography and THz-TDI were able to image an older painting hidden beneath the present painting.

The wooden structure of the panel was mostly hidden to radiographic imaging by the more x-ray-opaque ground and paint layers, while details of the painting composition were clearer than in the corresponding THz images.

We have shown that wood grains and irregular structure is better visualized by THz-TDI, especially by means of time of flight (ToF) plots, which also highlighted the presence of a crack and its extension on the wooden panel, while details of the hidden painting are optimally visualized by choosing the proper interval in THz frequency domain. The choice of the parameters used to image the THz data showed a great influence on the information provided, and thus we have been able to individually detail the surface profile, the wood grain and the hidden paint layer. At the same time, the brushstrokes made circularly around an animal figure of the hidden heraldic composition are more evident in frequency parametric THz images compared to the x-radiograph. A feature, unrelated to the panel wooden structure and barely notable in the x-radiograph, has been detected thanks to false color THz images, and can be attributed either to the unknown artist hand or to the presence of a material (including restoration material). While the THz false color image cannot support the chemical identification of the substance composing the imagined detail, it helped in localizing the feature within the concealed composition. This may help in choosing the proper location of further spot analysis for material identification.

Information provided by the two techniques are thus complementary, and the study helped in defining THz-TDI as a useful tool among the other complementary investigation tools for art pieces inspection.

IV.2 Florentine Renaissance Panel Painting structures revealed by using non-invasive Terahertz Time-Domain Imaging (THz-TDI) technique

The potentials of THz-TDI technique for a non-invasive inspection of panel paintings have been considered in detail. The THz-TD data acquired, which were processed in order to provide information on the replica of a panel painting made in imitation of Italian Renaissance panel paintings, provided insights as to the limits and potentials of the technique in detecting different kind of underdrawings and paint layers. Constituent layers, construction techniques, and anomalies were identified and localized by interpreting the extracted THz dielectric stratigraphy. We also investigated the well-known *Lamentation over the dead Christ* panel painting by Fra Angelico (ca. 1440, *San Marco Museum*, Florence). In this case, the evidence obtained from THz-TDI scans was correlated with the documented preservation history of the art piece, thus aiding in interpreting the THz-data. Erosion and damages to the wooden support, especially in the lower margin, found confirmation in the THz-TD images, which also provided a better understanding of the original construction and gilding technique as well as the plastering technique used during the 19th century restoration intervention.

IV.2.A Potentials of THz-TDI to the study of panel paintings in central Italy dating to between the 12th and 16th centuries

Panels played a particularly significant role in Italian painting between the 12th and 16th centuries, a period that corresponds to late Medieval and Renaissance Italian painting. The city of Florence in Tuscany is renowned as the birthplace of the Renaissance and, in particular, of Renaissance painting.

The pioneering THz-TDI scans performed on the *Polittico di Badia* (14th century, Giotto di Bondone, Uffizi Gallery – Florence) [111] and the *Trittico di San Giovenale* (1422, Masaccio, Masaccio Museum, Pieve of San Pietro at Cascia di Reggello (Italy) showed the potential of the methodology to curators and conservators [100], [111]. By using THz cross-section analysis (B-scans), the panel painting stratigraphy was obtained non-invasively, thus

helping in characterizing the cohesion and integrity of the constituent layers and in identifying the construction technology used by the artist in preparing the support for application of the final layers of paint. The presence of gilded areas, their application technology and their preservation conditions were monitored by means of THz images, thanks to the differences in reflection amplitudes. Furthermore, THz-TDI was found to be an aid for the identification of red areas, which were generally painted using pigments such as vermilion (high reflection coefficient), red earths, and red lakes (both showing low reflection amplitude values) [100].

The supports of Tuscan paintings that were produced until approximately 1250–80 possibly derive from Gothic retables and are made primarily of coniferous wood. During the late 13th, 14th, and early 15th centuries, poplar, a suitable species for panels, was the main species used. Regarding the construction technique, *de facto*, within Central Italy up until the 14th century, great care was taken in preparing the ground layer, which was basically made of glue, cloth, *gesso grosso*, and *gesso sottile*. The cloth, which was generally made of large, overlapping pieces, was often applied over the whole panel and over the frame as well. In the 15th century, cloth strips were often applied only on the most sensitive areas, whereas in later years parchment or vegetable fibers mixed with glue were used. Increasingly, less care was devoted to gessoing [103]. Moreover, information on gessoing has great relevance for conservation purposes. Indeed, a complex of uniformly applied pieces of cloth will lead the whole ground layer to separate from the support in the case of wood movements, thus preserving the painting at best [103].

A number of other measures were often taken in order to reduce the negative consequences of defects in selected boards, defects which may be highlighted by THz-TDI scans (i.e. cavities plugged with paste) [103]. A flat surface was sometimes reconstructed prior to the application of cloths and the ground layer, as has been found in the *Trittico di San Giovenale* by Masaccio [100] by means of THz-TDI scanning. Furthermore, THz-TDI scanning can also provide information about defects, such as leavage and layer detachment, delaminations, insect damage, wormholes, cracks, knots, and other type of imperfections.

In this section, the results obtained by applying THz-TDI to the characterization of both the replica of a panel painting, fabricated by following the traditional technique in use in Tuscany between the 13th and

16th centuries, and the "*Lamentation over the dead Christ*" panel painting (ca. 1440) by Fra Angelico are presented.

IV.2.B Instrumentation and Analytical methods

THz-TDI was performed using a portable Picometrix T-Ray 4000 device. The relevant area was scanned using a 320 picosecond (ps) measurement window and we employed a scan velocity of 12.5 pixel/s (8 full temporal waveforms averaged per pixel) in a reflection configuration at normal incidence. The raster scanning was performed with a lateral resolution of 400 μm.

IV.2.C Artworks investigated

The panel painting replica

The panel painting replica investigated was prepared by conservators of the *Polo museale regionale della Toscana*, Italy using materials and methods in use from the 12th to the 16th-centuries.

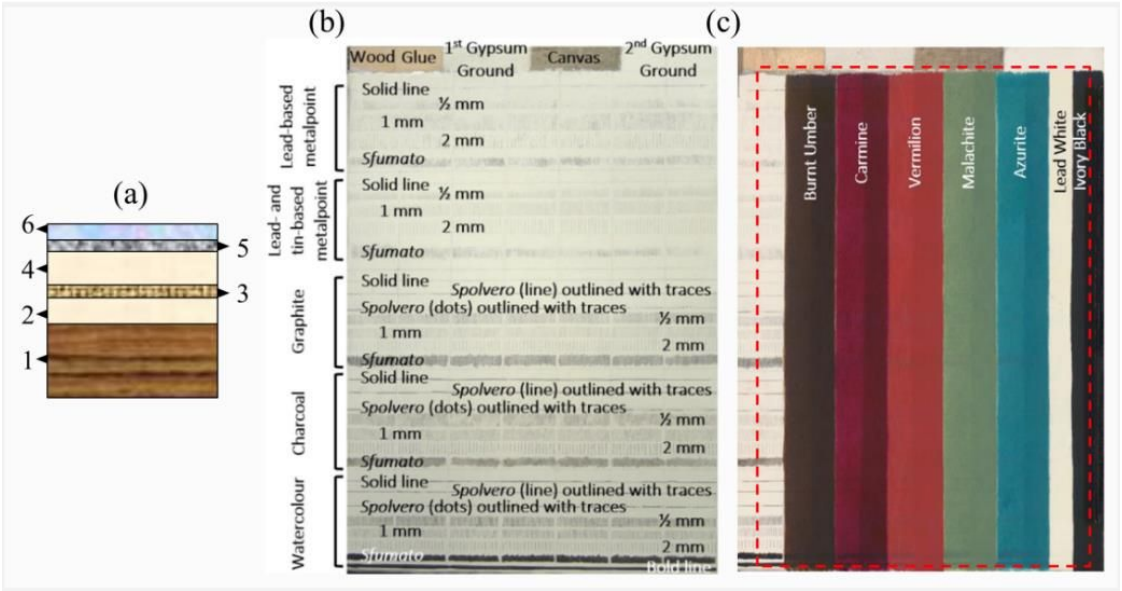

Fig. IV.2-1 a Scheme of the stratigraphy of the replica of the panel painting. **b** Picture of the panel painting replica after the underdrawings were made**. c** Picture of the panel replica. The red dashed square localizes the scanned area.

The panel replica was made with a wooden support covered by modern industrial cloth placed between a ground layer and a primer layer (mixture of *gesso* and animal glue, nr. 1-4 in Fig. IV.2-1a). The first gesso layer was applied with the function of levelling out the uneven surface of the wood, as

was used for the *Trittico di San Giovenale* by Masaccio [112]. On the top of the second gesso layer, underdrawings (nr. 5 in Fig. IV.2-1a) had been sketched using different historical materials (metal-points, graphite, charcoal, watercolor), dimensions (from 0,5 to 2 mm) and techniques (*sfumato, spolvero, solid lines, engravings*), as shown in Fig. IV.2-1b. Lastly, the paint layer was applied on the top of the preliminary drawings (nr. 6 in Fig. IV.2-1a). Seven different pigments (burnt umber, carmine, vermillion, malachite, azurite, lead white and ivory black) were applied to a strip of two different superimposition thicknesses (Fig. IV.2-1c) in an egg-based binder. The dimensions of the scanned area (Fig. IV.2-1c) are approximately 18.8 cm x 28.4 cm, corresponding to a 471 x 711 pixel grid.

The "Lamentation over the dead Christ" panel painting

The panel painting *The Lamentation over the Dead Christ* by Fra Angelico (sometime referred to as *The Deposition* or *The Piety,* Fig. IV.2-2) was studied using the THz-TDI system. The painter Fra Angelico (original name Guido di Pietro, also called Fra Giovanni da Fiesole or Beato Angelico, 1400 – 1455) is considered to be one of the greatest painters within the framework of early Renaissance style. In addition to the influence that he had on his followers, Fra Angelico exerted a significant influence in Florence, and was mentioned in Vasari's famous *Lives of the Most Eminent Italian Painters, Sculptors, & Architects* (16th century) [113].

The panel painting is the only extant altarpiece from the oratory of *Santa Maria della Croce al Tempio*. Known as "*Il Tempio*", in the 15th century the oratory was the final devotional space in which a condemned criminal was spiritually repentant for his crime. The altarpiece was commissioned in 1436 by the lay confraternity that governed the structure, and its mission was to prepare condemned persons for the afterlife [114]. The confraternity was suppressed in 1785, when the death penalty was abolished by the Grand Duke of Tuscany [115], and in 1786 the panel painting was moved to the *Galleria dell'Accademia* in Florence, where it was extensively repainted by an unknown purist artist around 1850 [116] and also later on.

Fig. IV.2-2 *The Lamentation over the Dead Christ* by Fra Angelico. Tempera panel, 109 x 165 cm, San Marco museum collection (Florence, Italy). The white squares localize the two scanned areas.

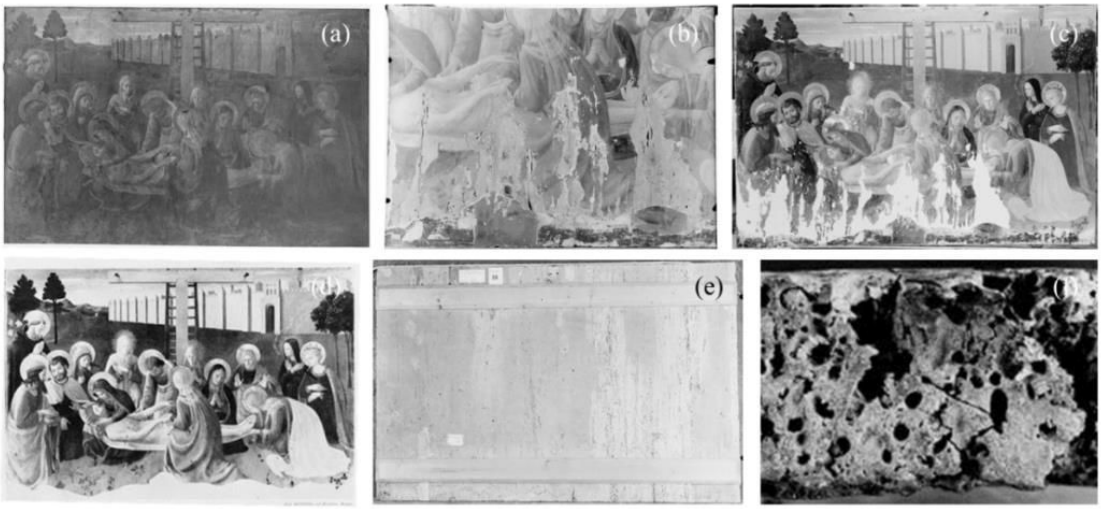

Fig. IV.2-3 Pictures of the panel painting before and after the restoration intervention of the 1950s (ISRC photographic archive). **a.** The panel before the intervention, FG862. **b.** Detail of the panel during the intervention, showing the major *lacunas* that reached the support, FG5470 **c**. The panel during its restoration, showing the new priming layers, FG5485. **d.** The panel after the restoration intervention, with the movable mask applied to the lowest margin, FG3403 **e.** Back of the painting after the restoration, FG5466 **f**. Detail of the wooden support and the wormholes, FG5463

The panel underwent several restoration interventions in the past. The major recent restoration was carried out between 1950 and 1953 (Fig. IV.2-3a-d), when the copious 19th century inpaintings were removed, with the exception of the lowest margin where the later restoration materials were left [26]: due to damages possibly caused by fire [116], no original matter was left. A movable parchment mask was applied to the top of this part (Fig. IV.2-3d), so that *"(...) it can be shown at any time a whole collection of stucco layers and overpaintings and inpaintings, tempera or oil"*[116]. The painting support, consisting of two poplar axes, was found to be affected by wood-boring beetles (Fig. IV.2-3e-f), while a non-original priming layer was individuated in the reconstructed areas of the lower portion of the panel [116].

Two areas were selected on the panel surface for THz TDI investigations. The dimensions of the two scanned areas are approximately 13.8 cm x 8.4 cm (346 x 210 pixel grid, area 1 in Fig. IV.2-2) and 14.6 cm x 10.6 cm (366 x 266 pixel grid, area 2 in Fig. IV.2-2), respectively.

IV.2.D Results and Discussion

The panel painting replica

Fig. IV.2-4 shows the grayscale peak-to-peak THz image of the scanned area, both before (Fig. IV.2-4a) and after (Fig. IV.2-4b) local contrast enhancement (CLAHE method [117], [118]).

The underdrawings sketched by metal-points on the primer were not detected by the system when these were made by tin-lead points, while they were in fact detected when these were made by lead points. In the latter case, the solid lines were discerned even when spaced at distances of 0.5 mm, while the *sfumato* technique was detected only at a higher concentration (i.e. where the line was not faded). When dealing with carbon and graphite drawing tools, both of which depend on the pressure and concentration of the tool, most of the underdrawings traced by graphite appeared whiter in the gray scale values as compared with the gray-values of underlying primer. This was due to the high THz reflection caused by the high electrical conductivity of this semimetal, which is a naturally-occurring allotrope of carbon [119], [120].

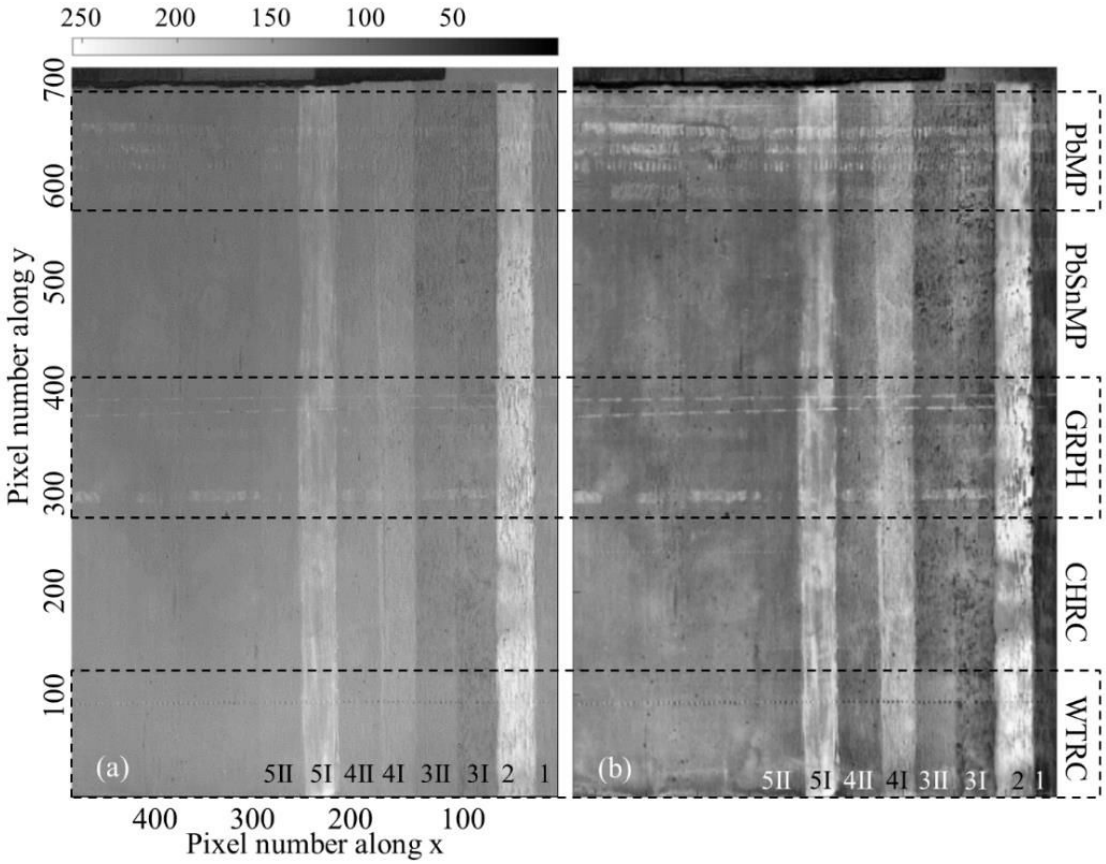

Fig. IV.2-4 THz peak-to-peak image **a** before and **b** after local contrast enhancement. PbMP lead metal point, PbSnMP tin-lead metal point, GRPH graphite, CHRC charcoal, WTRC watercolor. 1 ivory black, 2 lead white, 3 azurite, 4 malachite, 5 vermilion. I lower concentration, II higher concentration.

While the presence of the underdrawings sketched by charcoal did not seems to affect the THz reflectivity values of the underlying *gesso* primer and were not detected by the system, the presence of ivory black pigment was intuited after contrast enhancement (Fig. IV.2-4b). This was due to the lower overall reflectivity value of this paint layer compared to that of the primer. It is known that totally or partially amorphous carbon compounds (e.g. charcoal pencil and ivory black) do not usually exhibit distinct spectral features below 2.25 THz (75 cm^{-1}), but rather a difference in overall absorbance from one pigment to another [121]. The different behavior of the carbon-based pigments used to make the panel under investigation may depend upon differences in the concentration, the amorphousness degree, or to the presence of calcium phosphate and calcium carbonate in the ivory black. Underdrawings traced by water colors were not identified by the system. Due to the different optical path in the THz range, the underdrawings outlined by engravings, even dotted ones, appeared in the THz images. In fact, according to the grayscale images, variations in the

THz image reflect not only the variations in the material composition, but also those in the sample thickness [119]. Furthermore, the electric field values recorded vary according to the amount of scattering on the surface caused by irregular features.

Forming the image by using the spectral amplitude values at single THz frequencies helps in defining the behavior of the pigments (Fig. IV.2-5 a-h).

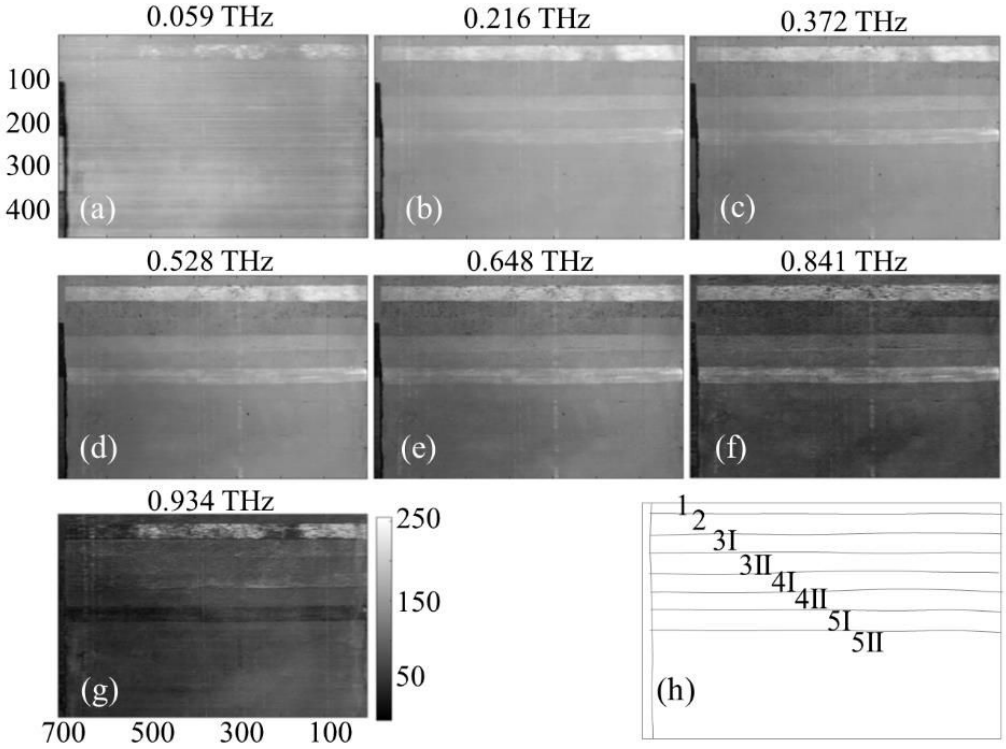

Fig. IV.2-5 a-g THz images plotted by using the value of the spectral amplitude at single THz frequencies. **h**. Scheme of the scanned area according to the nomenclature described in paragraph IV.1.D

The spatial resolution in the images depends greatly on the frequency range used for imaging (diffraction-limited beam waist ~600 μm at 0.5 THz, ~300 μm at 1 THz [122]). In fact, due to smaller diffraction limits, THz higher-frequency components reproduce higher spatial frequencies better than do THz lower-frequency components, even though at a higher frequency the granular nature of pigments causes frequency-dependent scattering, which tends to mask the spectral feature [123]. In addition, the low signal-to-noise ratio limits the usable bandwidth to 0.15 - 0.94 THz. When applied at a higher concentration, lead white and vermilion showed the highest reflection amplitude values, while azurite showed the lowest in both concentrations. Carmine and burnt umber did not show any particular reflection features compared to that of the primer layer. Malachite applied in a higher concentration reflected THz radiation more than the underlying

primer layer did. This was particularly visible after contrast enhancement of the acquired signal (Fig. IV.2-4b) [40], [124], [125].

The whole stratigraphy of the painting was visualized by means of non-invasive cross section analysis. Fig. IV.2-6a shows the raw B-scan as plotted starting from the scan-line y = 202. The main composition layers (Fig. IV.2-6b) are imaged thanks to the demarcated differences in the dielectric material parameters (wood panel [126], gesso [126], cloth [127], paint layers [124]). An additional interface was recorded within the primer layer (I3 in Fig. IV.2-6b).

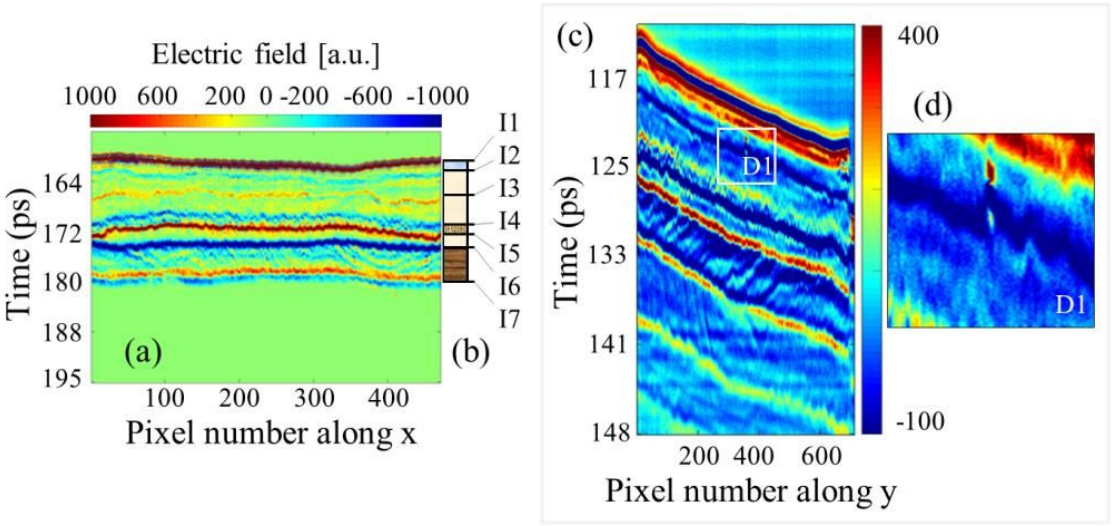

Fig. IV.2-6. a. Raw B-scan at y = 202, after signal deconvolution and windowing around the relevant optical path of the signals (from the surface to the bottom of the wooden panel). **b.** scheme of the stratigraphy: I (interfaces) where n is the labeling number according to 1,air/surface; 2, paint layers/primer; 3, separation interface within the primer layer; 4, primer/cloth; 5, cloth/ground; 6 ground/wooden panel; 7 wooden panel/air. **c** Column B-scan at x = 301. **d** Detail of the white square area D1 of the B-scan.

According to the conservators who made the replica of the panel, there was no difference in the material that they used, but rather in the application technique: a wooden slat was used to fit the plaster inside the fiber pattern of the cloth during the first applications, while a brush was used for the following applications. As a consequence the detected interface I3 is the separation edge of the same gessoing material applied using different degrees of compaction. Fig. IV.2-6c shows the column B-scan plotted at x = 301 scan-line, and displays an anomaly inside the priming layer (Fig. IV.2-6d) just behind the paint layers, which have the appearance of a red spot relative to the chosen color-map.

Using the method described in [87], signals were processed in order to separate pulses of interest from the entire signal recorded for extracting THz

images of single regions of interest (ROI) and related relevant information. Fig. IV.2-7a-c highlights the separated pulses of interest, while the associated images are displayed in Fig. IV.2-7d-f.

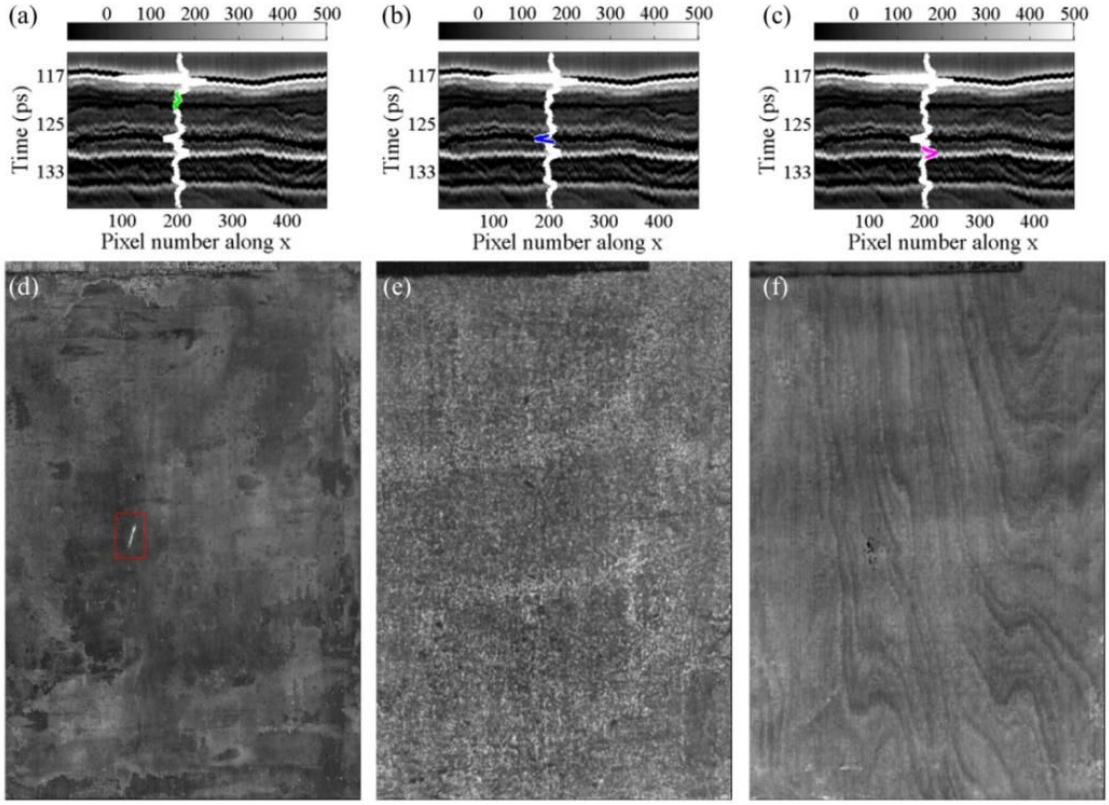

Fig. IV.2-7 a-c Grayscale B-scans plotted starting from the scan-line y = 202. The waveform (200,202) is plotted in white, while the separated pulses are highlighted by the colored lines within the waveforms. **d-f** Frequency parametric THz image of the primer layer (where the inclusion found is circumscribed by the dashed red rectangle), the cloth, and the wooden panel, which correspond respectively to the separated signals in B-scans a-c.

The image of the primer layer (Fig. IV.2-7d) clearly shows the position and extension of the inclusion found. Its high reflectivity value suggests that it is a metal object, and its sharp shape indicates that it can be a metal point used by the conservator to engrave the underdrawings, which had accidentally fallen into the wet plaster. The cloth has been imaged (Fig. IV.2-7e) where the pattern appears blurred due to of the reduced lateral resolution at the cloth plane, below the focal one (the painting surface). Lastly, the wooden surface of the panel is shown in Fig. IV.2-7f.

The "Lamentation over the dead Christ" panel painting

Fig. IV.2-8a shows the first scanned area of the panel painting. It was located in the lower margin of the painting, where the restoration materials applied prior the last restoration intervention have been left. The scanned area includes three different regions belonging to three different restoration interventions: the restoration of the 1950s, that of the 19th century, and a previous one, which was not attributed to a specific time (respectively, R3, R2 and R1 in Fig. IV.2-8a). The corresponding THz peak-to-peak image is shown in Fig. IV.2-8b.

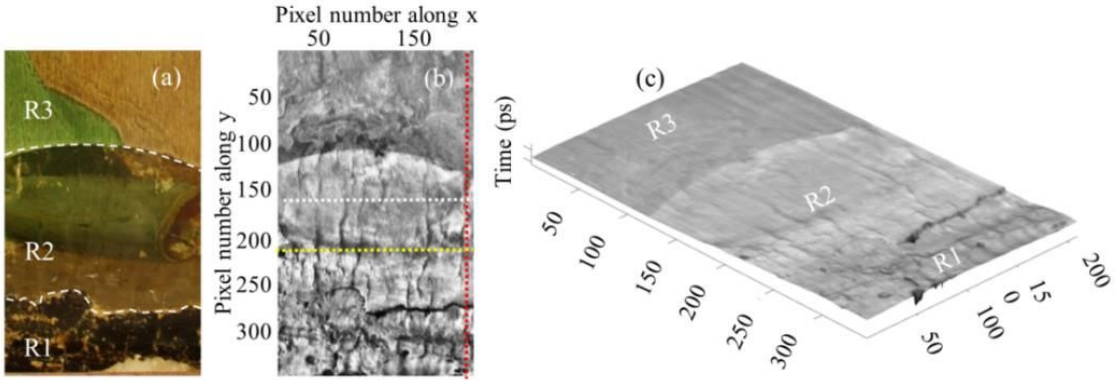

Fig. IV.2-8 a Visible appearance of the first scanned area D1. **b** THz peak-to-peak image after contrast enhancement (CLHAE); the dashed white, yellow and red lines are the scan-lines used for plotting the B-scans, respectively, y = 168, y=208 and x=208 shown in Fig. IV.2-9. **c** Time-of-Flight plot

In plotting the Time-of-Flight image (Fig. IV.2-8c), it was noted that the R1 plaster appeared slightly below the R2 one.

The dielectric stratigraphy of the scanned area was restituted by B-scan plots, which clearly showed that no cloth was found between the surface and the wooden support of the painting. In many raw B-scans, an interface is detected between the surface and the ground/wooden panel interface (red arrow in the B-scan from the y = 168 scan-line, Fig. IV.2-9a), meaning that the R2 plaster had been frequently placed on top of the previous one (R1). However, this fact does not seem to have been a strict rule, since other raw B-scans did not display this interface so markedly. Fig. IV.2-9b shows the raw B-scan plotted from the scan-line y = 208. The separation line between R1 and R2 plasters in this case is not identifiable for the entire length of the B-scan, but is only limited to a region close to it, in which the outline resembles the cross-section of a plaster patch. Fig. IV.2-9c shows the waveform (208,150) that displays the pulses arising from the reflections on the R2 surface, at the patch border, and on the wood interfaces.

Consequently, it can be hypothesized that the R2 conservator first tried to even out R1 by removing the unstable parts, and then applied the R2 so as to level out the new filler up to the original plaster. The result was that R2, when it existed, is of varying thicknesses, depending on the presence, absence, and thickness of the underlying ground R1.

Column B-scans give a clear picture of the differences in the dielectric stratigraphy of the three different R areas (Fig. IV.2-9d, B-scan plotted for x = 206).

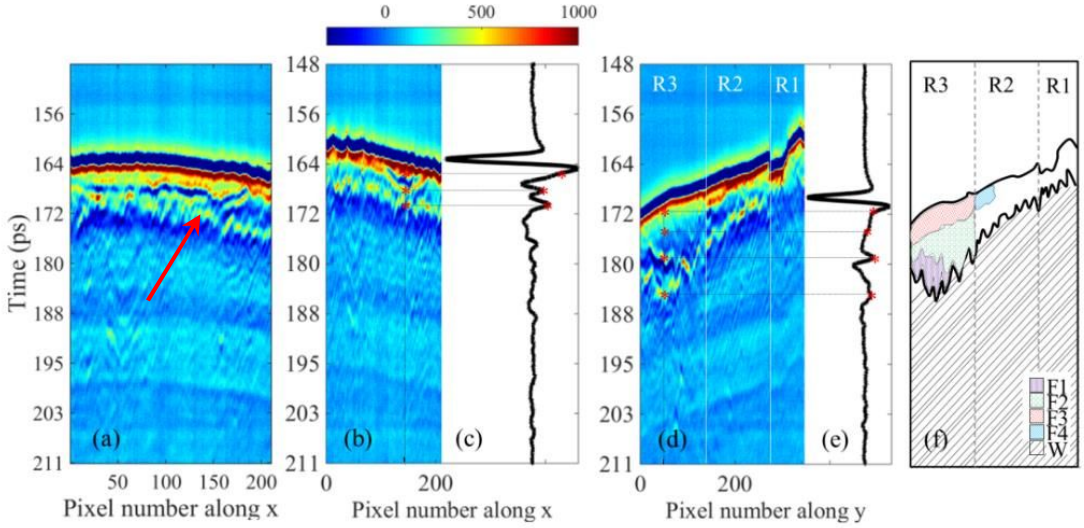

Fig. IV.2-9 Raw B-scan y=168. **b** Raw B-scan y = 208; **c** waveform (150, 208). **d** Column B-scan x = 206. **e** waveform (206, 50). **f** B-scan x = 206. Simplified scheme made by interpreting the back-reflected signals at the main dielectric changes observed in the B-scan x = 206. W, wooden panel; F1-3, different dielectric regions found in the B-scans within the R3 area. F4, filling borders within the R2 area.

The wood boundary appeared extremely uneven, thus giving an indication of the erosion which it had suffered because of a fire in the past (Fig. IV.2-9d and W in Fig. IV.2-9f). The thickness of the ground layer on top of the wood increased from the R1 to the R3 areas, depending on the amount of loss in the wood support.

A pronounced depression in the wood was found within the R3 area. By following the changes in the amplitude of the reflected electric field (color changes in Fig. IV.2-9d and waveform (206, 150) in Fig. IV.2-9e), it was possible to observe two additional interfaces between the surface and the wood boundary, which corresponded to the reflections at the interfaces named F2/F3 and F1/F2 in Fig. IV.2-9f. The one at F2/F3 appeared to be particularly intense. The hypothesis that three different materials have been applied seems weak, while it is likely that the wood depression was filled first in order to reconstruct a flat surface and that the primer layer was then

applied. Changes in the dielectric properties between the patching material and the covering primer layer could, for instance, be due to variations in the plaster composition, degree of compaction, and/or application time. The signal at the interface referred to as F2/F3 did not appear as a sharp pulse yielded by a strong dielectric contrast among materials, but rather as a smooth variation in amplitude and polarity. The photographic records of the intervention of the 1950s showed how conservators had applied a completely new gesso-based primer to the top of the wood panel in the R3 area (Fig. IV.2-3b-c), and they themselves documented that only one product was used for the plastering operations (a mixture of *gesso* and animal glues). Consequently, the THz signal variations observed were produced by minor dielectric changes between the top and bottom parts of the same material. This may have been caused by sedimentation in the heavy component of the primer on the bottom part and / or to the penetration of fluids applied on the surface down to a certain depth (e.g. pictorial binders or coating materials). Column B-scans also show the spot fillings in the R2 area, as already discussed before (Fig. IV.2-9d and F4 in Fig. IV.2-9f).

The time parametric image of the primer layer is shown in Fig. IV.2-10a. Its appearance recalls the description given in the restoration report regarding the presence of a whole collection of stucco layers constituting the lower margin of the panel painting. Fig. IV.2-10b shows the time parametric THz image of the wooden support.

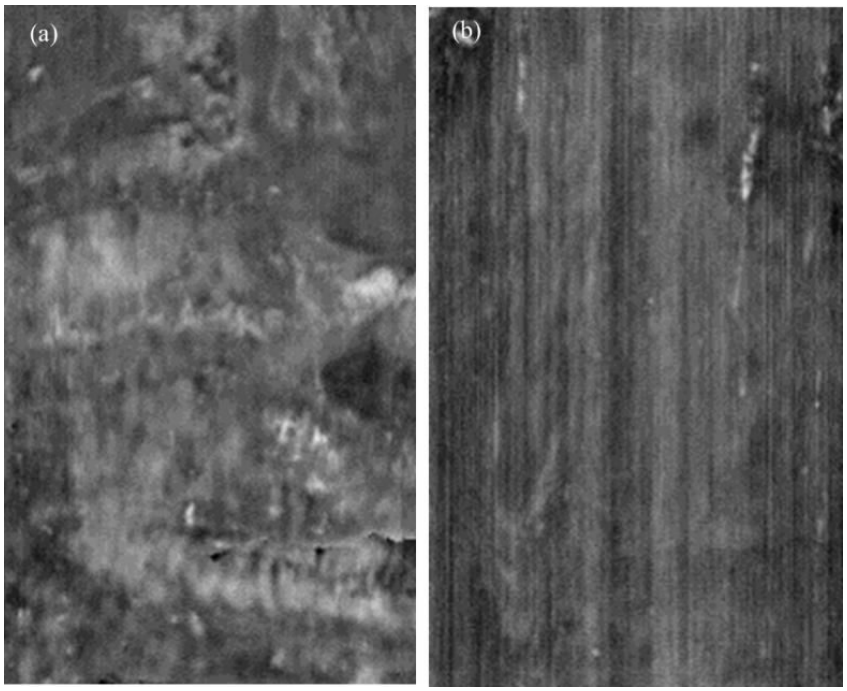

Fig. IV.2-10 a THz image of the primer layer. **b** THz image of the wooden support.

Fig. IV.2-11a shows the visible image of the second scanned area, while Fig. IV.2-11b is the corresponding peak-to-peak THz image.

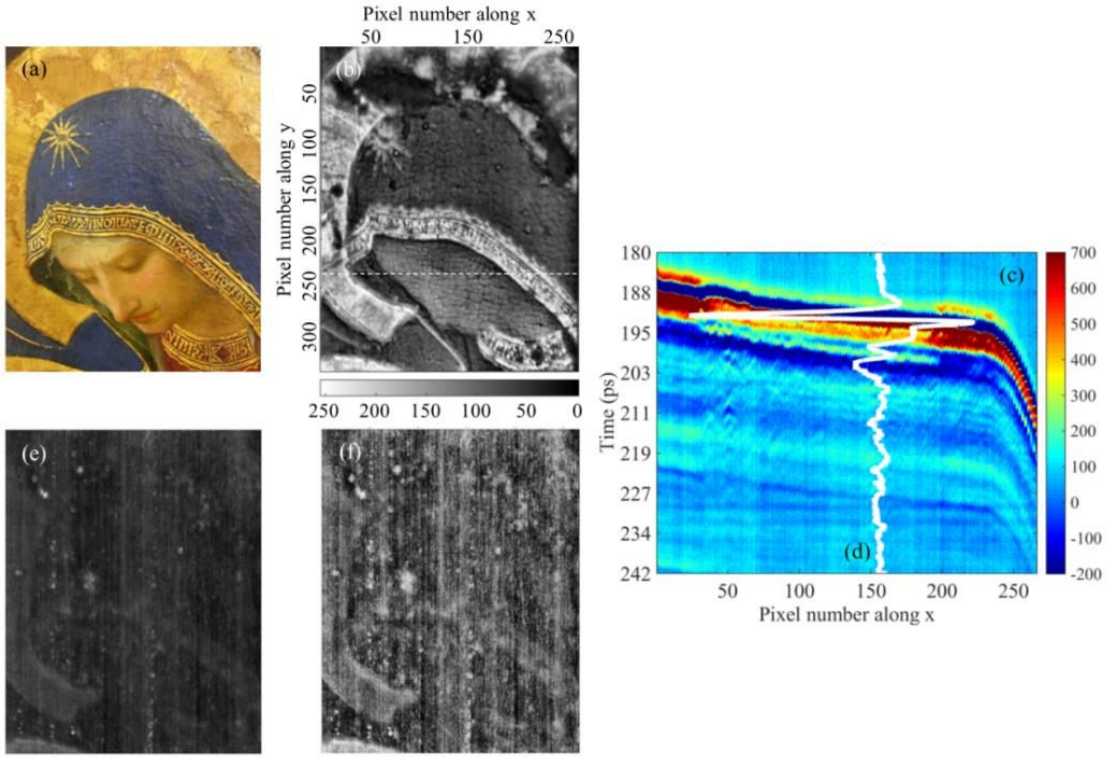

Fig. IV.2-11 a Visible image of the second scanned area (white square n. 2 in Fig. IV.2-2) **b** Peak-to-peak THz image; the dashed white line represents the scan-line used to plot the B-scan shown in Fig. IV.2-2c. **c** raw B-scan at y = 230. **d** waveform(150,130)**. e** THz peak-to-peak images of the wooden support before contrast enhancement. **f** THz peak-to-peak images of the wooden support after contrast enhancement (CLAHE)

The THz image helps in defining the damaged areas of the gilded halo of the Virgin, where the gilding had been replaced by a golden paint that had to match the color of the previous interventions. Indeed, those areas appeared as dark spots in the grayscale THz image. The boundaries of the gilded aureole match the perimeter of the face of the Virgin, a fact that confirmed the high level of Angelico's technical skills in the preparation of the areas depicted. In fact, it is common to find the presence of closely spaced square leaf pieces behind the paint layers, which are usually detected in THz-TD images (see sections IV.4-5). Instead, the matching between the halo and the visage boundaries suggests the use of a fine brush for the painted areas which end perfectly at the boundaries with the gold metallic leaves. Following the temporal evolution of the signals by plotting B-scans (Fig. IV.2-11c-d) demonstrates how the signal is almost entirely reflected back by the gilded areas, suggesting a gold thickness that is much greater than that of

the skin depth of the metal at THz frequencies (~250 nm at 0.1 THz, ~80 nm at 1 THz in case of pure gold [128], [129] (see sections IV.4-5)..

THz peak-to-peak images of the wooden support are shown, before and after contrast enhancement, in Fig.s IV.2-10e-f, respectively. The white spots individuated on the wood structures seemed to be connected to wood damages (worm holes, losses and cracks, as shown in Fig. IV.2-3f). Finally, no cloth was identified between the wooden support and the painting surface.

IV.2.E Final considerations

In this section the potential of using THz-TDI applied to panel painting investigations, with a special focus on the Italian Renaissance paintings, was carefully analyzed.

The creation and investigation of the replica of a panel painting contributed to individuating the underdrawings which can be detected by the system as concerns materials, sketching technique, and line thickness, as well as the possibility of detecting the presence of paint layers in the replica by THz imaging. Thus, valuable insights from an imaging point of view are added to the already existing studies on artistic pigments. By carefully interpreting the THz dielectric stratigraphy of the panel, the constituent layers and the construction technique have been identified. Furthermore, THz-TDI was shown to be capable of detecting the separation line between the same gessoing material applied with different degrees of compaction, thus giving an indication regarding different application techniques of the same material used. After signal separation, single composition layers were imaged and an in-depth anomaly (metal inclusion in the priming layer) was located and imaged within both the painting stratigraphy and the areal position.

Selected areas of the famous *Lamentation over the dead Christ* panel painting by Fra Angelico (ca. 1440) were scanned by THz-TDI for the first time. In this case, THz-TDI helped to depict the preservation history of the panel painting in the form of images. The wooden panel boundaries appeared to be extremely uneven in the dielectric stratigraphy obtained by scanning an area of the lower margin of the panel. This information, which was obtained non-invasively, matches very well with the preservation history of the panel which, according to the existing documentation, suffered severe erosion in the lower side because of a fire in the past. Furthermore THz-TDI helped in defining the plastering technique used during the 19th

century restoration intervention. By detecting the presence, absence, changes in thickness and extension of the hidden earlier plaster layer in the B-scans, it was concluded that the 19th century conservator first tried to even out the existing grouting layer, removing the unstable parts, and subsequently leveled the new filler out to the original plaster. Furthermore, by correlating the existing information about the restoration operation performed during the intervention of the 1950 with the THz-TDI data, it was concluded that gessoing was performed in two steps. First the surface was flattened by filling existing depressions and holes in the wooden support, that then the grouting layer was applied. Furthermore, dielectric variations were detected by THz-TDI between the top and the bottom parts of this grouting material, known to be made by animal glue and *gesso*. This fact indicates that the minor dielectric change is due to the sedimentation of the heavy component of the primer on the bottom part and / or to the penetration of fluids applied on the surface (e.g. pictorial binders or coating materials), until a certain depth. Detailed images of both the primer and the wooden panel textures were obtained after signal separation. The second area scanned included the face of the Virgin and the contouring gilded aureole. In addition to showing the repairs made in the golden aureole, the borders matching between it and the visage suggests that the gilding was applied by a thin brush. Furthermore, the evidence that THz signals appear almost entirely reflected back by the gilded areas, suggests that the gold thickness is comparable or higher than that of the skin depth of the metal at THz frequencies. Spot-like defects were observed in the THz C-scan of the wooden panel within this scanned area. This matches with the records about the important damages affecting the wooden support of the painting, primarily caused by insect attacks.

IV.3 Insights on the side panels of the *Franciscan Triptych* by means of Terahertz time-domain imaging (THz-TDI)

Within the framework of Italian Renaissance panel paintings inspection, THz-TD data have been acquired and processed to get insights about the two side panels (*Saints Jerome, John the Baptist and the Archangel Gabriel* and *Saints Francis, Onofrio and the Virgin Annunciate*) of the so called *Franciscan Triptych*, by Fra Angelico. Constituent layers, construction, gessoing and gilding techniques, subsurface cracks and anomalies were identified and localized by interpreting the extracted THz dielectric stratigraphy and the THz C-scans.

IV.3.A Panel paintings description

The investigated panel paintings, one depicting *Saints Jerome, John the Baptist and the Archangel Gabriel* (Fig. IV.3-1a), the other *Saints Francis, Onofrio and the Virgin Annunciate* (Fig. IV.3-2), are believed to be the side panels of the so-called *Franciscan Triptych*, painted by Fra Angelico before 1429 [130]. The three items were dismembered in an unspecified period and the side compartments have followed a historical and conservative history quite different from that of the better known central panel (*The Virgin and Child Enthroned,* San Marco museum, Florence).

The side panels are intended to be exposed at San Marco museum together with the central panel and their restoration in imminent. For this reason an extensive diagnostic campaign was performed during 2004-2006, where the analysis were performed by several Italian research institutes, such as SMAArt[1] and CNR-ISTM[2], (XRF, reflectance mid FTIR, reflectance UV-Vis spectroscopy, microfluorimetry, Fig. IV.3-1a), CNR-ICVBC[3] (cross section analysis by optical and SEM microscopes, diamond cell FT-IR), M2ADL[4] (multispectral imaging, including reflected Vis, reflected UV, Vis fluorescence induced by UV, reflected IR and false color IR), the Chemistry

[1] Center of Excellence Scientific Methodologies Applied to Archaeology and Art, c/o Chemistry Department, University of Perugia

[2] Institute of Molecular Science and Technologies, c/o Chemistry Department, University of Perugia

[3] Institute for the Conservation and Valorization of Cultural Heritage, Sesto Fiorentino

[4] Microchemistry and Microscopy Art Diagnostic Laboratory, University of Bologna

Department of Pisa University (gas chromatography) and a private company (PanArt sas, X-radiography, Fig. IV.3-1b).

The two areas scanned by THz-TDI on the *Saints Jerome, John the Baptist and the Archangel Gabriel* panel painting, G1 and G2 (8,4x5,4 cm and 13,8x9 cm) are located in Fig. IV.3-1a; Fig. IV.3-1b is the X-ray radiography.

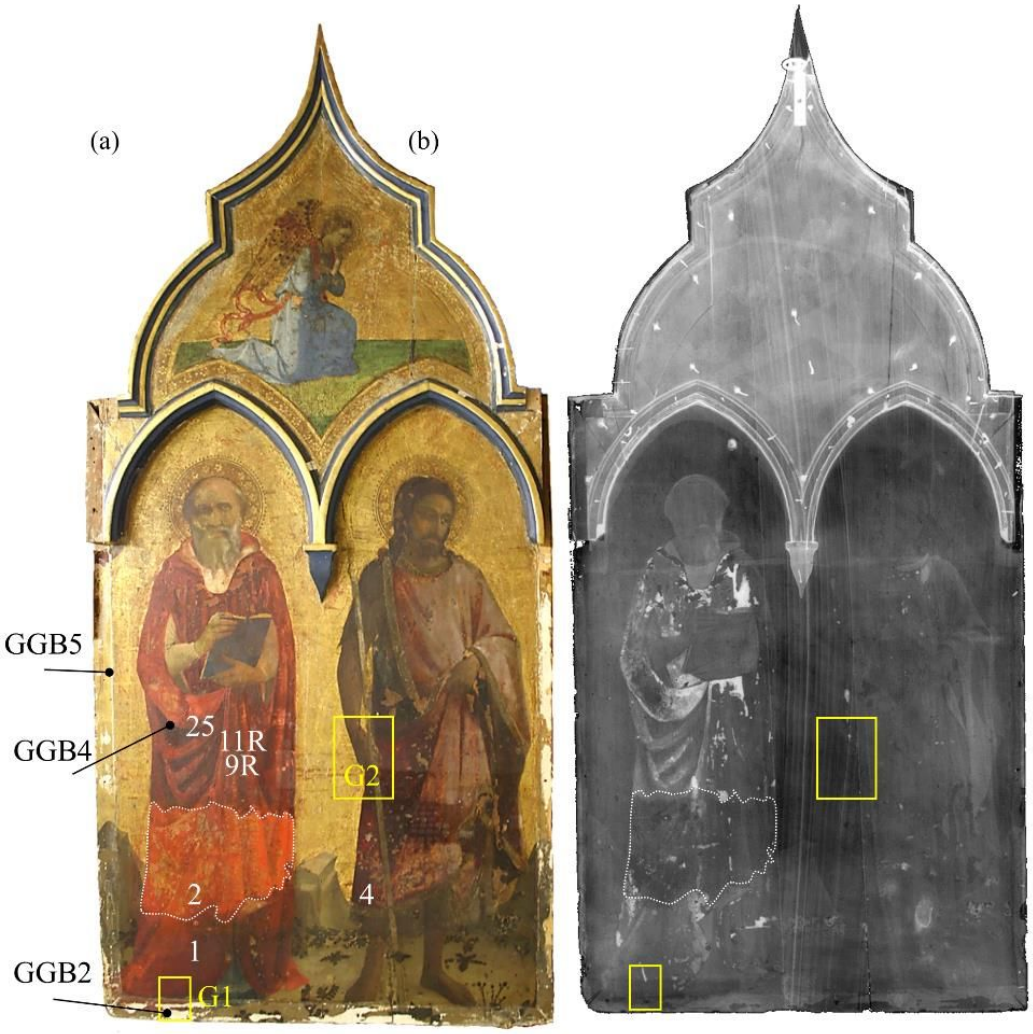

Fig. IV.3-1 a *Saints Jerome, John the Baptist and the Archangel Gabriel* panel painting, visible image; the yellow squares localize the two areas scanned by THz-TDI; the dashed white line delimited the area of the dress where the overpaints were removed; The white number 1,2,4 indicate the spots analyzed by XRF, 9R, 11R by micro-fluorimetry,; GBB2 and GBB4 are the sampling locations of the relevant cross sections **b.** Single x-ray projection image, digital editing of 14 RX plates (made by PanArt sas)

The two investigated areas on the *Saints Francis, Onofrio and the Virgin Annunciate* panel painting, O1 and O2 (8,2x11,4 cm and 10x8,4 cm) are located in Fig. IV.3-2.

Fig. IV.3-2
Saints Francis, Onofrio and the Virgin Annunciate panel painting, visible image; the yellow squares localize the two areas scanned by THz-TDI; SFO2 is the sampling locations of the relevant cross sections image

IV.3.B Instrumentation and analytical methodology

THz-TDI was performed with a portable Picometrix T-Ray 4000 device. We employed a scan velocity of 15 pixel/s (6,67 full temporal waveforms averaged per pixel) in a reflection configuration at normal incidence. The raster scanning was performed with a lateral resolution of 400 μm.

IV.3.C 3 Results and Discussion

Saints Jerome, John the Baptist and the Archangel Gabriel

Fig. IV.3-3a shows the visible appearance of the scanned area, while the corresponding THz and RX images are plotted respectively in Fig. IV.3-3b and c. Paint layer lacunas appear of lower grayscale intensity than the painted area in the THz image. While the visible image does not show any diversity within the scanned red area, both the THz image and the X-radiograph show a high grayscale-intensity area on the top right corner (anomaly).

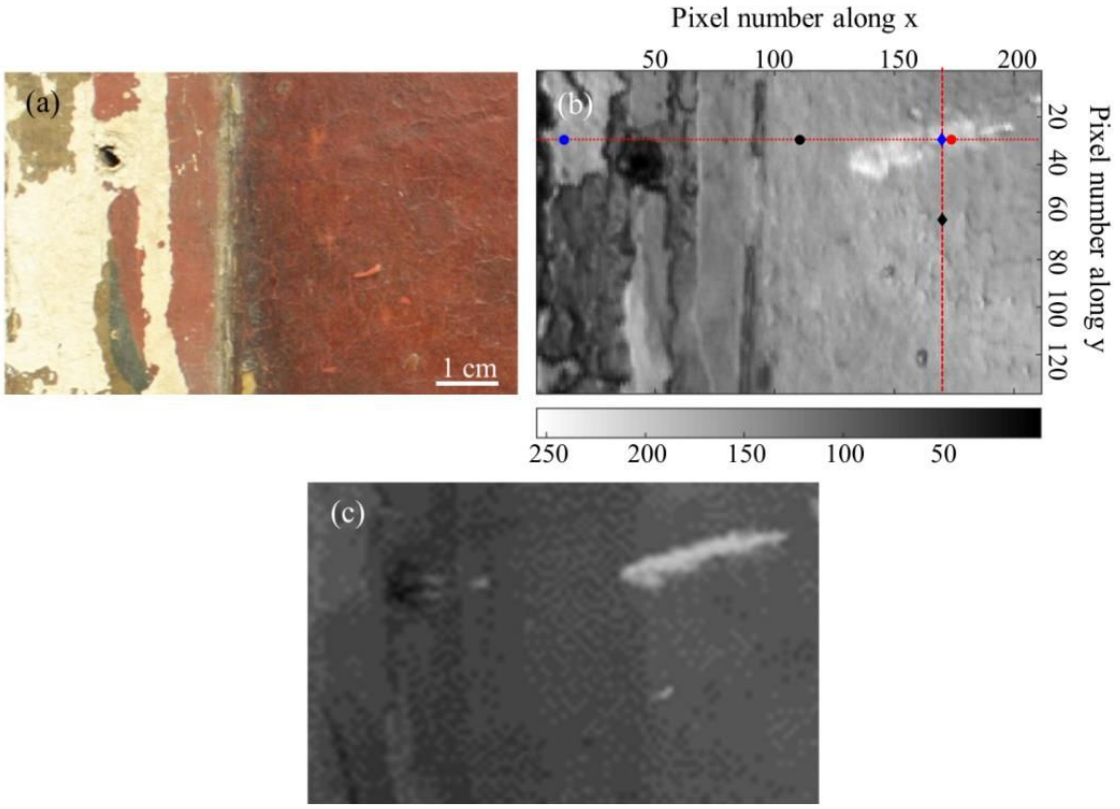

Fig. IV.3-3 Visible image of the area named G1 in Fig. IV.3-1a. b. Peak-to-peak THz image of the scanned area. Blue, red and black points are the location of the waveforms plotted in Fig. IV.3-4 b and e. **c**. Zoom on a detail of the radiograph shown in Fig. IV.3-1b**.**

B-scans plotted in Fig. IV.3-4a and 4d display the optical stratigraphy of the painting respectively at the scanline x=171 and y = 29 (red dashed lines in Fig. IV.3-3). The oblique trend of the surfaces is due to an imperfect alignment of the transceiver head in respect to the surface of the painting, which was kept tilted for safety reasons.

Waveforms are displayed for locations of the raw and column B-scans which include (wfm 171,29 in Fig. IV.3-4b and 173,29 in Fig. IV.3-4e, Fig.

IV.3-4f, where wfm is the abbreviation of waveforms) and do not include (wfm171,75 in Fig. IV.3-4b and wfm 109,29 in Fig. IV.3-4e) the detected anomaly.

The stratigraphic schemes of the panel deducted from the main THz amplitude variation are plotted in Fig. IV.3-4c and f-g. The air/surface, paint layers/ground, ground/canvas, canvas/support interfaces are distinctly detected, while it can be observed how the cloth does not cover the whole scanned area (Fig. IV.3-4d, wfm 12,29 in Fig. IV.3-4e and Fig. IV.3-4g), leaving the external margin of the panel uncovered.

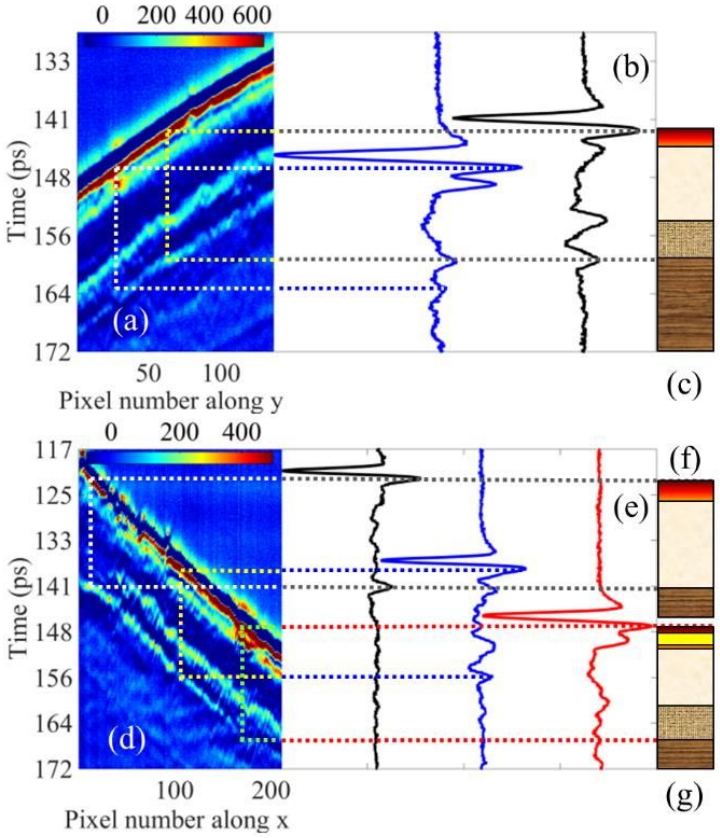

Fig. IV.3-4
a. Column B-scan at x=171.
b. wfm 171,29 (blue) and 171,75 (black).
c. scheme of the deducted panel painting stratigraphy.
d. Raw B-scan at y = 29. **e.** wfm 12,29 (black), 109,29 (blue) and 173,29 (red)

Minor signal variations are detected between the pulses arising from the reflections at the painting surface and at the grounding layer, meaning that the layer included between these two interfaces is inhomogeneous. The temporal location of the pulses arising from the reflection at the anomaly interfaces in the B-scans indicates that it is located inside this last layer, although, according to the spatial position, it is sometime found in contact with the ground layer (Fig. IV.3-4a and d).

Information about the paint layers composition can be obtained at first instance by inspecting the visible aspect of the painting (Fig. IV.3-1a): a dark red overpainting is on the top of a vivid red. The XRF analysis made in

2005 [131] recorded Hg in three selected spots on the red robe of Saint Jerome (spots n. 1, 2, 25, as shown in Fig. IV.3-1a), situated both in the overpainted and cleaned area, suggesting the use of Cinnabar (HgS) for both the red paints. The FC infrared photography and the micro-fluorescence analysis (9R and 11R spots in Fig. IV.3-1a, [131]) advocated the diffuse presence of a red lake in correspondence of the mantle shading and finishing [132]. Due to the extremely confined nature of the anomaly recorded in THz and X-ray images, it follows that it does not depend on the presence of any of these materials, which contrarily are spread over the whole figure. While the presence of a waxy coating and a thin lead white priming layer was deducted by means of portable FT-IR and XRF analyses, the cross section images [133] demonstrated that those materials are not present for the entire extension of the panel painting, since missing the in the observed cross-sections of the GGB4 and GGB2 samples (Fig. IV.3-1a).

The evidences obtained by THz-TDI stratigraphic analysis cannot exclude the presence of a waxy coat within the scanned area. The fact that no high THz-reflectivity interfaces were detected on the top of the ground layer, which usually characterizes the lead white layers, suggests that if present, the lead-white based priming layer is of very small thickness within the scanned area. This is confirmed by the X-radiograph which, distinctly showing the cloth and the wooden structure under the ground layer, points that no significant radiopaque layers are present on the top of them.

The THz stratigraphic analyses highlights that the anomaly is a material applied locally under the dark red overpainting. The fact that it is sometime found in contact with the ground layer suggests that, depending on the presence or absence of the supposed thin primer layer, it can either be a paint layer roughly applied in correspondence of paint losses of the vivid red layer before the dark red application, or a material used as integration of the primer layer, where missing, before the overpainting with the dark red paint layer. Furthermore, its strong radiopacity in the RX image (Fig. IV.3-1b and c) may indicate that the material contains elements with a high atomic number.

Fig. IV.3-5 shows the THz images of the scanned area G1 at different temporal position of the signals and four different region of interests have been imaged (frequency THz images in Fig. IV.3-6b,e,h,l and ToF in c,f,m) after signal separations by window function (Fig. IV.3-6a,d,g,i).

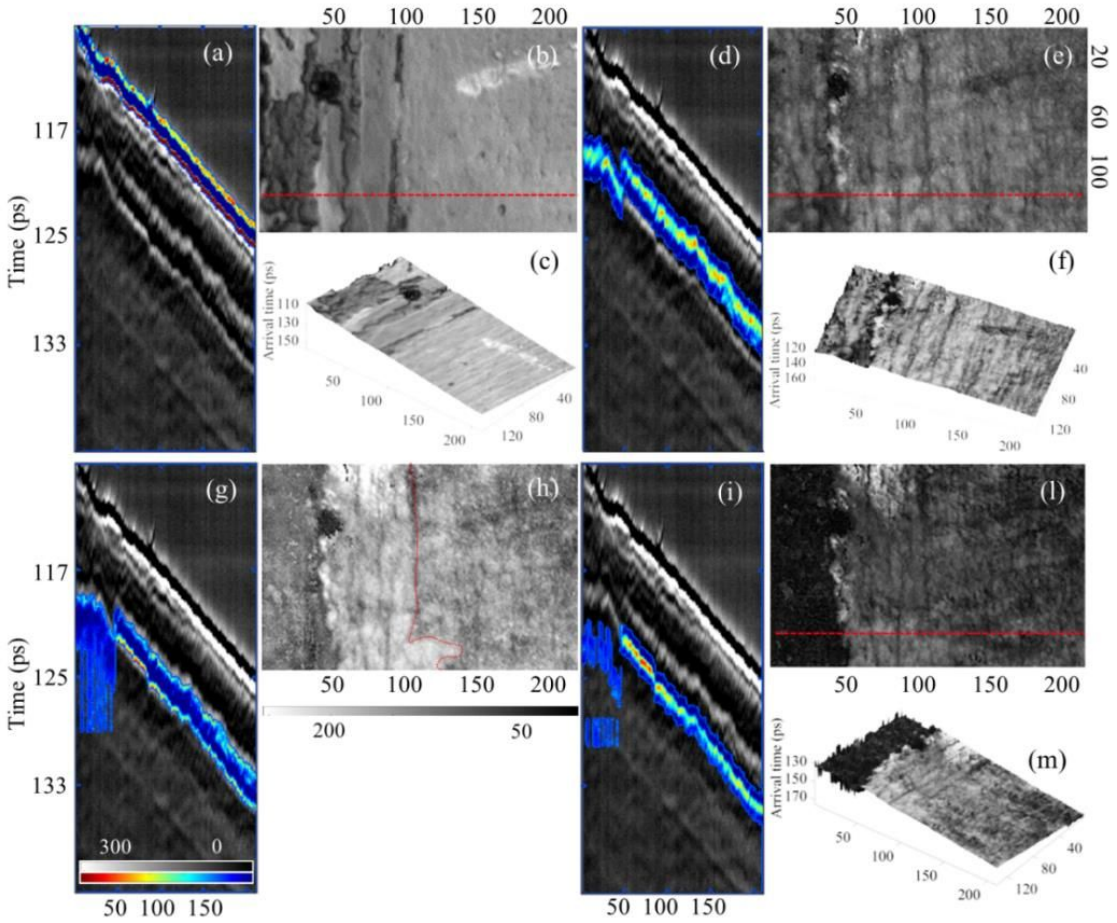

Fig. IV.3-5 a,d,g,i. Grayscale raw B-scans at y = 120; the colored areas of the B-scans individuate the portion of the signals separated by window function and used to plot the associated frequency THz images. **b,e,h,l.** THz frequency images of the regions of interest corresponding to the colored areas imaged in a,d,g,i. **c,f,m.** Time-of-Flight images of the regions of interest highlighted in a,d,i.

The cloth cover the scanned area approximately until where the nail is located, leaving the external margin uncovered (Fig. IV.3-6e). By imaging the region included between the ground/cloth and cloth/panel interfaces (Fig. IV.3-6h) it appears how the textile was applied by assembling more cloth pieces, which can be identify by the different grayscale intensities between the superimposed and the single cloth pieces in the THz image.

The second scanned area (G2 in Fig. IV.3-1a), which includes the background gilding, in shown in Fig. IV.3-7a and the corresponding THz peak-to-peak image is plotted in Fig. IV.3-7b.

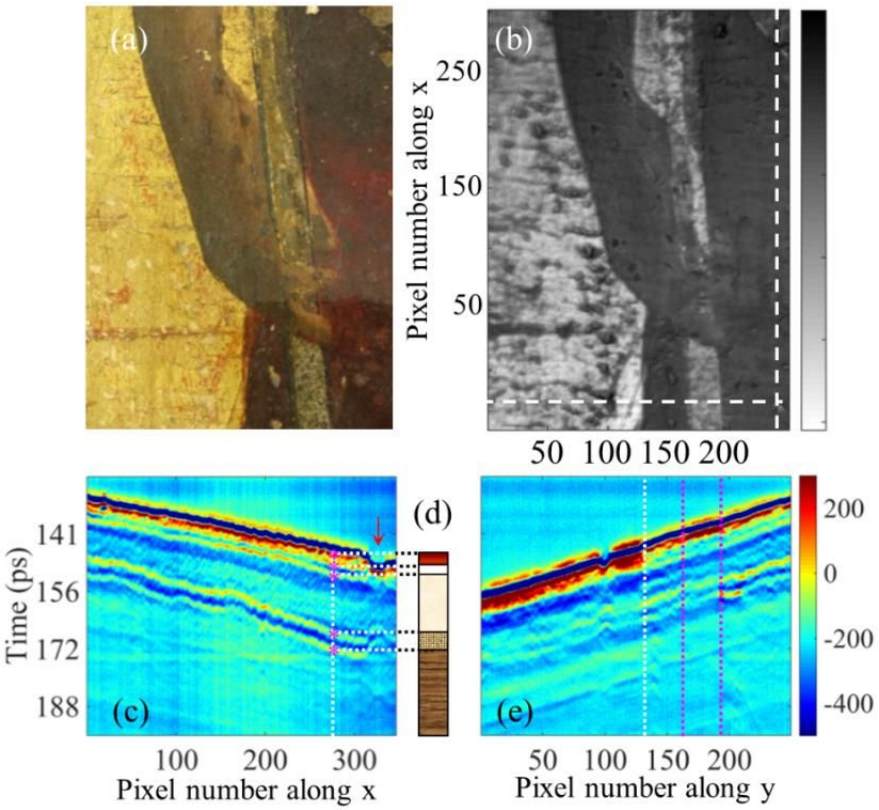

Fig. IV.3-6
a. Visible image of the area named G2 in Fig. IV.3-1a. **b.** Peak-to-peak THz image of the scanned area. **c.** Raw B-scan at y = 242. **d.** scheme of the panel painting stratigraphy as deducted from Fig. IV.3-7c. **e.** column B-scan at x = 24.

Raw and column B-scans are plotted in Fig. IV.3-6c and 7e. Fig. IV.3-6d shows the scheme of the painting stratigraphy as deducted from the column B-scan of Fig. IV.3-6c. The major interfaces wooden panel/cloth, cloth/ground, ground/paint layers are clearly visible in the B-scan, while a well-defined interface is detected within the pain layers (separation between the white and the red boxes in the scheme of Fig. IV.3-6d), indicating that at least two well dielectrically contrasted layers are place on the top of the ground (either two pigments, primer and pigment, or pigment and varnish). It can be noticed how the subsurface interfaces (e.g. ground/cloth and cloth/wooden panel) reflect back the THz incident radiation even when covered by the gold finishing. In fact, in Fig. IV.3-6e the subsurface interfaces are visible, in reduced amplitude, on the left of the dashed white line and within the dashed purple lines of the B-scan, areas which respectively correspond to the gilded background and to the silver baton). This evidence suggests that very thin metal layers are found at surface (see sections IV.4-5).

The very thin nature of the gold finishing is confirmed by the cross section image taken by sampling at point, GGB5 in Fig. IV.3-1a [133].

The THz image shows how the boundaries of the gilded background do match very well the perimeter of John the Baptist ´s limb (Fig. IV.3-6b),

feature already observed in the other investigated panel painting by Fra Angelico, presented in section IV.2. This highlights how the painter either shaped the gold leaves with high accuracy, either applied the gold finishing by brush in correspondence of the perimeters of the figures, in both case meaning that he worked in a material saving manner. Furthermore the THz image (Fig. IV.3-6b) reveals that the Saint John's silver baton, covering the paint layers, was drawn on the top of paint layers defining the Saint: the covered portions of the subject are visible under the silvering layer in the THz image.

Saints Francis, Onofrio and the Virgin Annunciate

Fig. IV.3-7a shows the first scanned area (O1 in Fig. IV.3-2), Fig. IV.3-7b the corresponding THz peak-to–peak image, Fig. IV.3-7c-f the raw B-scans respectively at y = 2, 76, 124 and 176 and Fig. IV.3-7g the stratigraphic scheme of the panel painting deducted by crossing the THz data with the cross-section image of the sample sampled within scanned area (SFO2 in Fig. IV.3-2, [133]).

While the separation between the upper paint layers is not clearly discernable in the THz B-scans, the priming layer on the top of the ground is detected thanks to the back-reflected amplitude variations of signals at that interface. Even in this case, the cloth was applied so that the lower margin of the panel painting was left uncovered (Fig. IV.3-7c). The THz peak-to-peak image highlights a small crack visible at surface in the lower margin of the scanned area. Nevertheless, by looking at the B-scans it can be observed how the crack origins on the wooden panel and it broads almost for the entire length of the scanned area underneath the painted surface. The cloth seems split into two non-combining parts at the crack line, while the ground layer does not appear traversed by it, looking well adhered to the cloth (no THz interfaces due to air-gaps are found within this region in B-scan). This suggests that this defect was present in the wooden panel before the gessoing operation and that, as structural weak point, it generates the surface crack later.

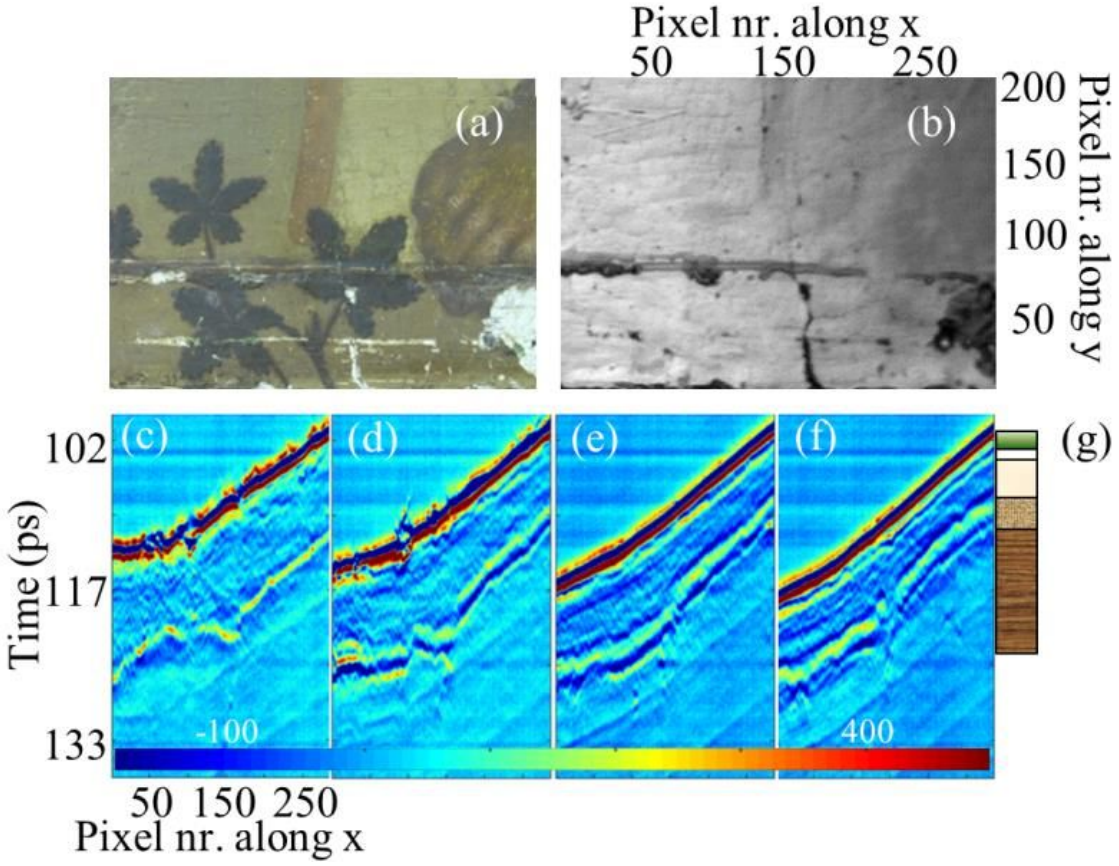

Fig. IV.3-7 a. Second scanned area, visible image. **b.** THz peak-to-peak image. **c-f.** raw B-scans at scanlines y = 2, 76, 124 and 176.

By isolating the pulses arising from the reflections at the wooden panel or cloth interface, the cloth extension and positioning is better comprehended and the development of subsurface crack it is better visualized, as well as the presence of further minor cracks in addition to (Fig. IV.3-8a-b).

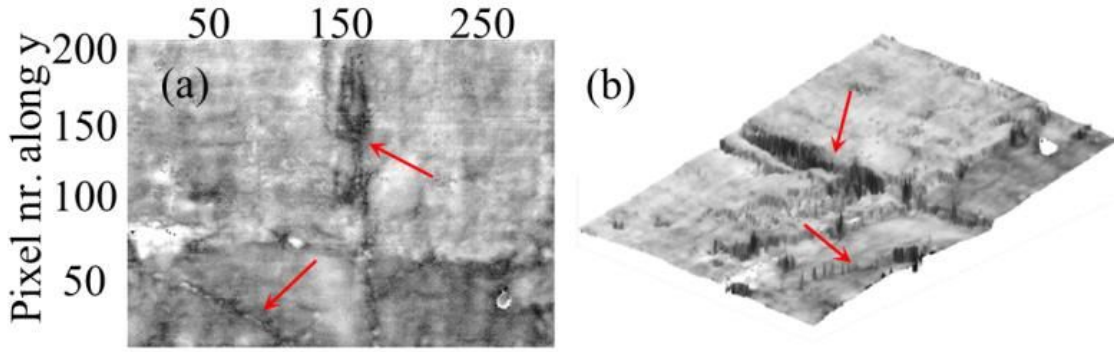

Fig. IV.3-8 a. THz image of the interface between the canvas or the wooden panel and the ground layer. The red arrows localize the cracks. **b.** ToF image of the same interface. The red arrows localize the cracks.

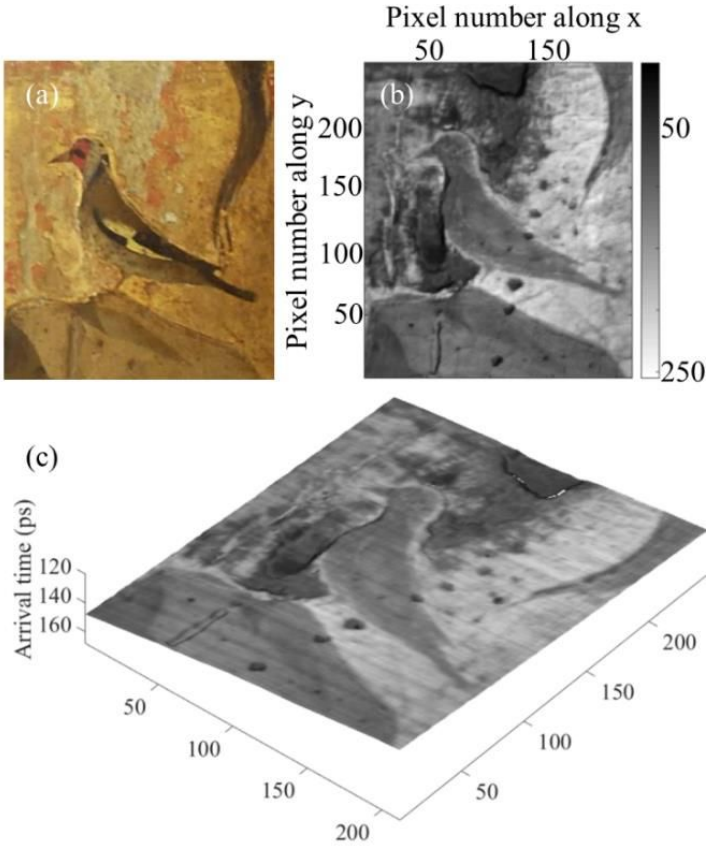

Fig. IV.3-9
a Second scanned area, located as indicated in Fig. IV.3-2.
b. Corresponding THz peak-to-peak image.
c. ToF image

Fig. IV.3-9a shows the second scanned area (O2 in Fig. IV.3-2), Fig. IV.3-9b the corresponding peak-to-peak THz image and Fig. IV.3-9c the time-of-flight image (ToF). Even in this case it is possible to observe that the boundaries of the gilded background do match very well the perimeter of bird. At the left side of the THz image in can be better estimate that the background gilding suffers several losses, appearing darker in the THz grayscale image. In the same left side of the THz image, it can be furthermore observed how the gilding at the boundaries of the subject's perimeter is much better preserved. According to the conservators this evidence can be related to past cleaning operations, widely performed in areas far from the painting's subject, while more careful close to the subjects.

The black spots which cross longitudinally the THz peak-to-peak image (Fig. IV.3-9b) are connected to paints lacunas, as better defined by ToF image (Fig. IV.3-9c).

IV.3.D Final considerations

The side panels of the *Franciscan Triptych* (Fra Angelico, before 1429) were scanned by means of THz-TDI.

Concerning the *Saints Jerome, John the Baptist and the Archangel Gabriel* panel painting a localized high grayscale-intensity zone was identified in the THz C-scan of the area scanned on the red *Saints Jerome's* robe. The THz stratigraphic analyses highlights that the anomaly is a material applied locally under the dark red overpainting. By integrating the THz results with those obtained by previous diagnostic analyses performed in the past, two hypotheses on the material identity were formulated: it can either be a paint layer roughly applied in correspondence of paint losses of the original red layer, or a material used ad integration of the primer layer, where missing, where in both cases it was applied before the dark red overpainting. The scheme of the panel painting stratigraphy was deducted from the THz B-scans. The cloth covering the wooden panel was imaged, highlighting that the external margin of the panel is uncovered within the scanned area. Furthermore, by imaging the proper temporal range of the THz back-reflected pulses, it appeared how the textile was applied by assembling more cloth pieces.

The second scanned area was located in the background gilding. THz B-scans showed how the subsurface layers reflect back the THz incident radiation even when covered by the gold finishing, suggesting that a very thin gold layer was applied. The THz C-scan showed how the boundaries of the gilded background do match very well the perimeter of the figures. This points out that the painter either shaped the gold leaves with high accuracy, either applied the gold finishing by brush in correspondence of the perimeters of the figures, in both case meaning that he worked in a material saving manner. In addition the THz image reveals that the silver baton held by Saint John was drawn on the top of the figure paint.

Regarding the *Saints Francis, Onofrio and the Virgin Annunciate* panel painting, two areas were scanned, one located in the background vegetation of the lower margin and the other one in the gilded area, including the central bird. The stratigraphy of the panel was deducted by THz B-scans and, even in this case, the cloth was applied so that the lower margin of the panel painting was left uncovered. Looking at the THz B-scans it was observed how the crack visible at surface originated in the wooden panel, extending for the entire length of the scanned area underneath the painted surface. The crack is present of the cloth but not the ground layer, suggesting that this defect was present in the wooden panel before the gessoing operation. The presence of further minor crack was fully comprehended by

imaging the THz back-reflected pulses arising from the reflections at the wooden panel or cloth interfaces.

The second scanned area was located in a gilded part of the panel painting. Even in this case it was observed that the boundaries of the gilded background do match very well the perimeter of bird. In addition, it was observed that the gilding at the boundaries of the subject's perimeter is much better preserved.

IV.4 Inspection of Panel Paintings behind Gilded Finishes with Terahertz Time-Domain Imaging (THz-TDI)

This section focuses on the use of THz-TDI for inspection of gilded panel paintings. The extremely high reflectivity of metals at submillimeter wavelengths generally precludes the transmission of electromagnetic waves through metallic films. A non-negligible direct transmission through metal films occurs due to the skin effect. The typical thickness of a thin gold leaf, a fraction of a micrometer, may match the skin depth of gold in the terahertz frequency range covered by THz-TDI devices. We therefore investigated and imaged subsurface features of panel paintings through gilded finishes with THz-TDI. Subsurface layers of three gilded panel paintings have been successfully imaged behind gold finishes with THz-TDI. The original research article can be accessed at [128].

IV.4.A Panel paintings and gilded finishes in Europe: an overview

Panels were used as main supports of European paintings from antiquity to the 16th century, when they have been almost completely replaced by canvas with the introduction of easel paintings.

In the Byzantine world, panel paintings were largely in use before and after the iconoclastic periods (8th and 9th centuries), while in Europe they reached the widest diffusion in the 13th century. It is believed that this diffusion is related to the new liturgical practices of Mass celebration introduced by the Fourth Council of the Lateran (1213), which sees the priest now faced *ad orientem* (East) and not *versus populum*, incentivizing the use of the altar as frame for sacred images, and thus the production of altarpieces [134].

Given the widespread religious use of panel paintings, they are often found to be adorned by gilded finishes. Gold was particularly appreciated in Christian sacred subjects for its mystical effect, the liturgical function and for a purely devotional purpose, and the high cost of the material was seen as an offering to the God [135].

Gilding finishes are not a Christian invention. Thin gold films have been applied to objects with a decorative function more than 6000 years ago. The

desired thickness of gold films was obtained by artisans though different steps of gold thinning, such as hammering (ancient process) or rolling (modern process) to obtain foils, or beating to obtain leaves. The term foil is used when the gold film can be handled easily (i.e. several μm thick), and the term leaf is used when the gold film is so thin that it cannot sustain its own weight (i.e. less than 1 μm).

Gold foils were the first being applied for decorative purposes, but rapidly the thickness of the foil was decreased, mostly to reduce costs. Decoration of sarcophagi by gold leaves less than 1 μm thick is attested already in Egypt during the 3rd millenary B.C. Pliny the Elder (23-79 A.C.), in his famous book *Naturalis Historiae*, mentions that the gold artisans were able to obtain gold leaves less than 0.4 μm thick [136]. Gold can be beaten without any special difficulty to a thickness of about 100 nm [137], [138].

IV.4.B THz-TDI as investigation tool for gilded panel paintings

The high reflectivity of metals at submillimeter wavelengths generally precludes the transmission of electromagnetic waves through metallic films, perhaps leading to the belief that the inspection of subsurface structures of panels covered by gilded finishes would be impossible. Despite this, a small but non-negligible direct transmission through metal films occurs if the film thickness is of the order of the skin depth of the metal in the terahertz range, due to the skin effect. The skin effect is a well-known electromagnetic effect which refers to the tendency of an alternating electric current to distribute within a conductor so that the current density is largest in a thin layer with a thickness denoted the skin depth near the surface. The value of the skin depth for electromagnetic waves in a metal is determined by the penetration distance at which the electric field falls to 1/e. The skin depth is a direct consequence of the finite conductivity of the metal, and is a frequency-dependent quantity which decreases at higher frequencies [129], [139], [140].

In the terahertz region the direct transmission through gold films of sub-micrometer thickness is consistent with a skin depth of 250 nm at 0.1 THz and 80 nm at 1 THz [129], [141], [142]. These penetration depths may approach the thickness of thin gold leafs applied to panel paintings or other gilded artifacts, and thus some transmission can be expected. The complementary technique of radiography, which is typically used for

inspection of the internal structure of art artifacts, uses x-rays for transmission imaging. The absorption coefficient of gold at x-ray wavelengths is typically so that gold leaves will be virtually invisible in radiography images, so that inspection of the gold leaf deposition itself is difficult using x-rays. Thus, THz-TDI may be a versatile and unique technique to image subsurface features of panel paintings through gilded finishes.

IV.4.C Analytical Instrumentation and Methodologies

Terahertz time domain imaging (THz-TDI) has been performed with a Picometrix T-Ray 4000 device. The investigated artifacts have been scanned in 500 μm steps, using a 320 picoseconds (ps) measurement window, a time increment of 0.078 ps (detector time-resolution) and a reflection configuration at normal incidence. Since we were interested in testing the capability of THz-TDI in imaging subsurface features behind gold finishes, the investigated panels were raster scanned from the front. Furthermore, if scanned from the back, the wooden panels would have attenuated the THz beam significantly, due to the high absorption of wood within the THz range, especially at ambient conditions, due to the moisture content.

IV.4.D The investigated panel paintings

The 14th Century icon represents *the Virgin with the Child and a Saint* (Fig. IV.4-1). The paint layer seems to be applied on a thin primer lying directly on the wooden support. The figures have been depicted on a gold background. Gold has been used to traces some details of the robes and aureoles. The precious icon, belonging to the Public Library of Taormina (Sicily), is at the moment under restoration at Angelo Cristaudo conservation laboratory (Acireale, Sicily). Loss of material was affecting the icon largely, from the paint layers to the ground and wood panel. For this reason, the main features of the stratigraphy of the panel painting could be observed at the edges of the losses, leading the conservator to believe that cross section analysis was unnecessary.

The panel painting n.1 (Fig. IV.4-2a) faithfully reproduces the indications of the famous *Cennino Cennini* treatise, the *Book of Art*, written at the beginning of the 15th Century. The replica has great value for evaluation of the THz-TDI technique since all the constituent layers were intentionally left exposed. A cloth piece was applied on the wooden support, and then covered

by the primer layer (animal glue and plaster mixture). The ultramarine pigment was applied mixed with egg on a first drawing sketched by pencil. A golden finish, made through the application of gold leafs on a red bole layer, frames the pictorial scene.

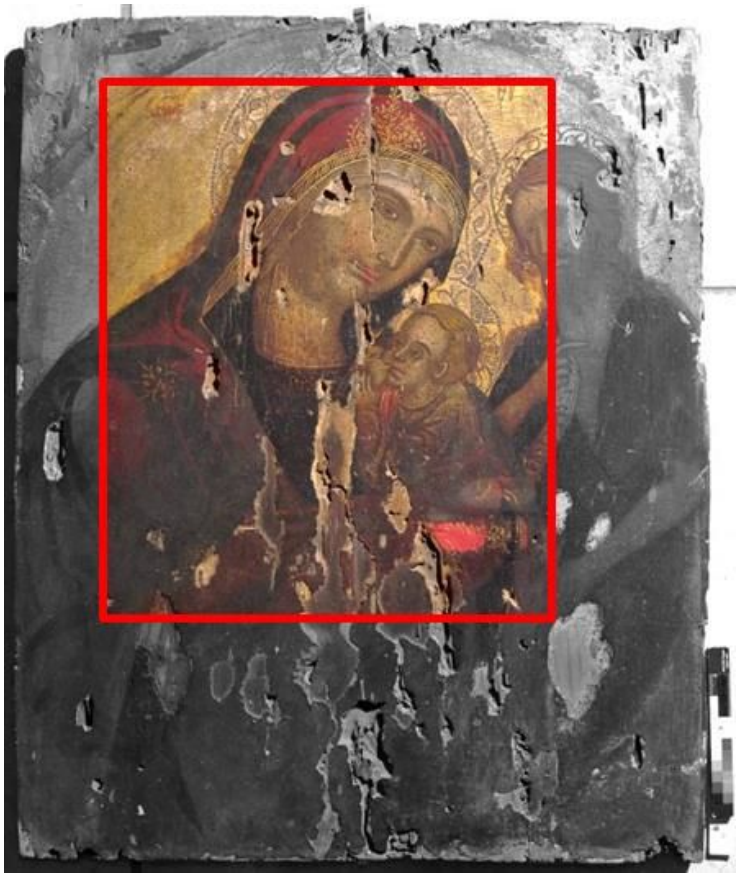

Fig. IV.4-1
14th icon representing the *Virgin with the Child and a Saint*; the scanned area of the panel is represented in true color.

The panel painting replica n.2 (Fig. IV.4-3a) is also made on a wooden support covered by the primer layer. The gilding and the paint layer have been applied on this stratum. The pictorial scene is more complex, since the gilding has been used extensively as decorative theme together with the painting material to represent textile. Engravings on the gilding are used to represent geometrical and floral motives. Also in this case the constituent layers were intentionally left exposed, so that the main stratigraphy of the panel was known is its main features, even without the use of cross sections.

Decorative engravings made by scratch awl and burin on the gilded decorations are present on all the three investigated panels.

IV.4.E Results and discussion

Panel paintings replicas

Fig. IV.4-2a shows the visible image of the panel painting replica n.1, while Fig. IV.4-2b shows the acquired terahertz time-parametric image.

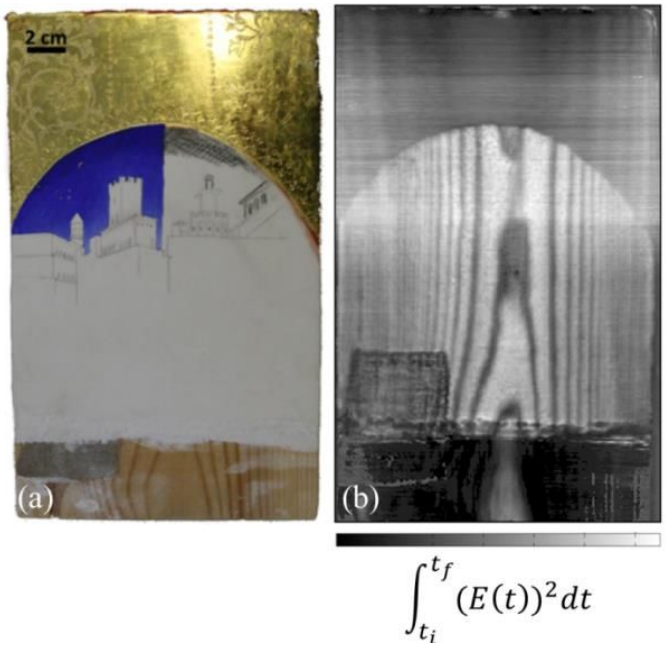

Fig. IV.4-2
a Panel painting replica n.1, visible image.
b Panel painting replica n.1, time-parametric THz image showing the location and extension of the cloth piece covered by the ground layer and applied on the wooden panel. The digital image varies from black to white representing the integral of the power of signals on a linear scale, recorded in the time interval included within t_i and t_f, where E(t) in the colorbar is the recorded temporal amplitude. The grain of the wood located behind the ground layer is visible, also partially on the areas covered by the surface gilding.

As can be seen in Fig. IV.4-2b, THz-TDI aids in identifying the location and extension of the cloth piece covered by the ground layer and applied on the wooden panel. The grain of the wood located behind the ground layer is visible, also partially on the areas covered by the surface gilding, due to the skin effect in the gold film.

Fig. IV.4-3a shows the visible image of the panel painting replica n.2, while Fig. IV.4-3b-d show terahertz frequency-parametric images of the air/surface, paint/plaster and plaster/wood interfaces, respectively.

THz images have been plotted by integrating the spectral amplitude over the full frequency range (0,05 – 0,56 THz) after the Fourier transform of the single pulses of interest, isolated from the waveform by temporal windowing.

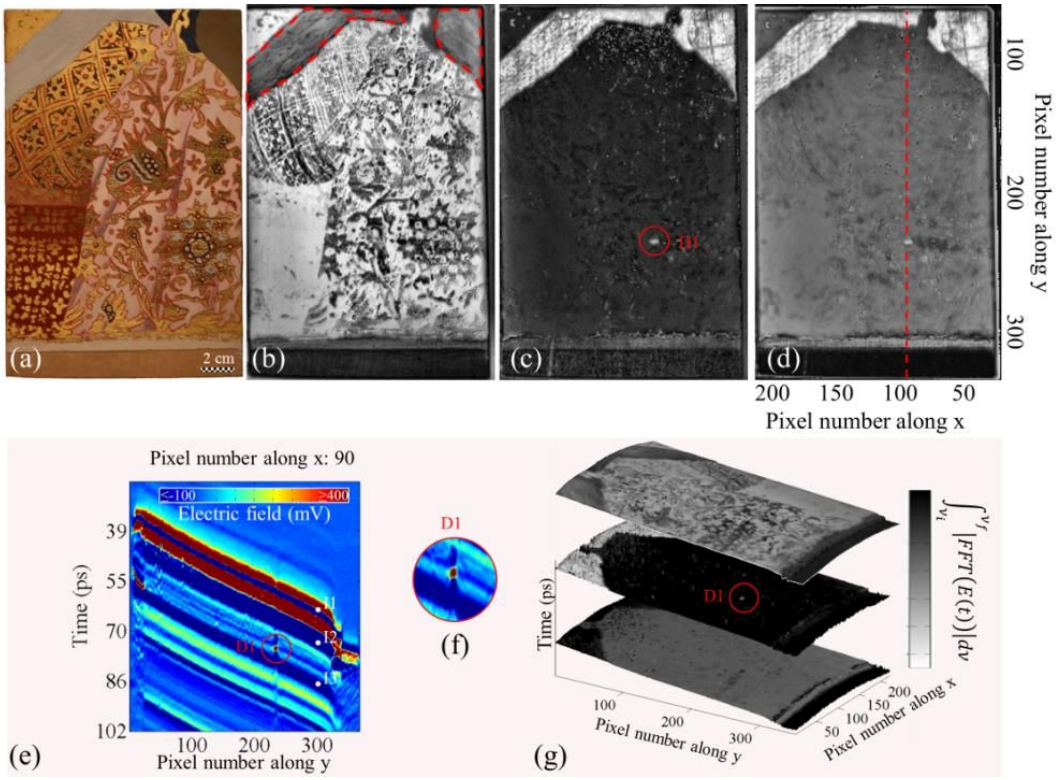

Fig. IV.4-3 Visible, gray-scale THz C- and B-scans of the panel painting replica n.2. When used, the gray color-map varies from black to white representing the spectral amplitude (E(t) in the color-bar) on a linear scale, integrated within the frequency range 0,05 – 0,56 THz (ν_i - ν_f in the color-bar) in the time interval (t) where the relevant peak is located. **a** Panel painting replica n.2, visible image. **b** Panel painting replica n.2, gray-scale frequency-parametric THz image of the air/surface interface. **c** Panel painting replica n.2, gray-scale frequency-parametric THz image of the paint/plaster interface. The red circle indicates the location of the anomaly (D1) **d** Panel painting replica n.2, gray-scale frequency-parametric THz image of the plaster/wood interface. **e** Panel painting replica n.2, B-scan representing value (color-map) and time of-flight (vertical axis) of the recorded electric signal along the scan-line (horizontal axis) indicated by the red line of Fig. IV.4-3c; the three main interfaces (I1-3) are found; the circled area indicates the location of a defect inside the plaster layer, compatible with an air bubble. **f** A zoom on the defect (D1) revealed by the B-scan of Fig. IV.4-3e). **g** Panel painting replica n.2, Time-of-Flight plots of the detected interfaces (from top to bottom: air/surface, paint layer/plaster, plaster/wood interfaces).

THz-TDI gives information about the painting technique used for the panel manufacturing. The THz image of the surface proves that the paint layer has been applied on the gold background, which covers almost the total area of the ground layer, except for the parts delimitated by the dashed red line in Fig. IV.4-3b, where the paint layer has been applied directly on the ground, without the presence of the gilding in between. This has been assessed based on the lower reflectivity that these zones exhibit compared to the adjacent ones (appearing darker in the THz grayscale plan-type image),

and highlighted by the B-scans (see Fig. IV.4-3e), which display that the strength of the pulses arising from the reflections at the subsurface interfaces are stronger compared to the uncovered areas, where no gilding at the surface is applied.

On the other hand, the strength of pulses arising from the reflections at subsurface interfaces in the gilded zones is high enough to be detected, and to enable the separation of single regions of interest from the whole temporal waveform by window function. The time-of-flight plots of the individuated regions of interest (air/surface interface, paint/plaster interface and plaster/wood interface) are shown in Fig. IV.4-3g.

The engravings made on the gold surface for tracing decorative motives appear darker in the THz image of the surface layer because of deflections of the incident beam caused by the irregularities (engravings themselves) at the surface. According to this, smoother gold areas appears whiter (i.e. higher reflectivity) compared to the other areas.

THz gray-scale images of the subsurface layers, (paint/plaster and plaster/wood interfaces, shown in Fig. IV.4-3c and IV.2-3d, respectively) indicate that areas covered by surface gilding are darker compared to the uncovered ones, due to higher reflection at the surface metal film, which consequently reduces the direct transmission of radiation in depth.

The reading of the texture of the layers in these THz-images is difficult because of their dark appearance, especially in the regions corresponding to the surface engravings, where the detected beam is reduced significantly in intensity because of deflection of the reflected beam away from the normal direction to the detector.

Despite this, a white spot (circled with red line in Fig. IV.4-3c) is visible in both the THz-images of the subsurface layers. Inspection of the B-scans shows how this spot (circled with red line in Fig. IV.4-3e and zoomed in Fig. IV.4-3f) is located in the middle of the plaster layer. For location, size and extension, and due to its high reflectivity value, the spot individuated by the THz-scan may be attributed to an air bubble inside the plaster layer, which is quite common to found inside ground layers. The internal defect has been localized in the interior of a layer located beyond the surface gilding, proving again the ability of THz radiation to penetrate thin gold leaf layers.

The 14th Century icon

The frequency-parametric terahertz image of the surface of the scanned area of the tempera panel is shown in Fig. IV.4-4b, and may be compared to the visible image (Fig. IV.4-4a).

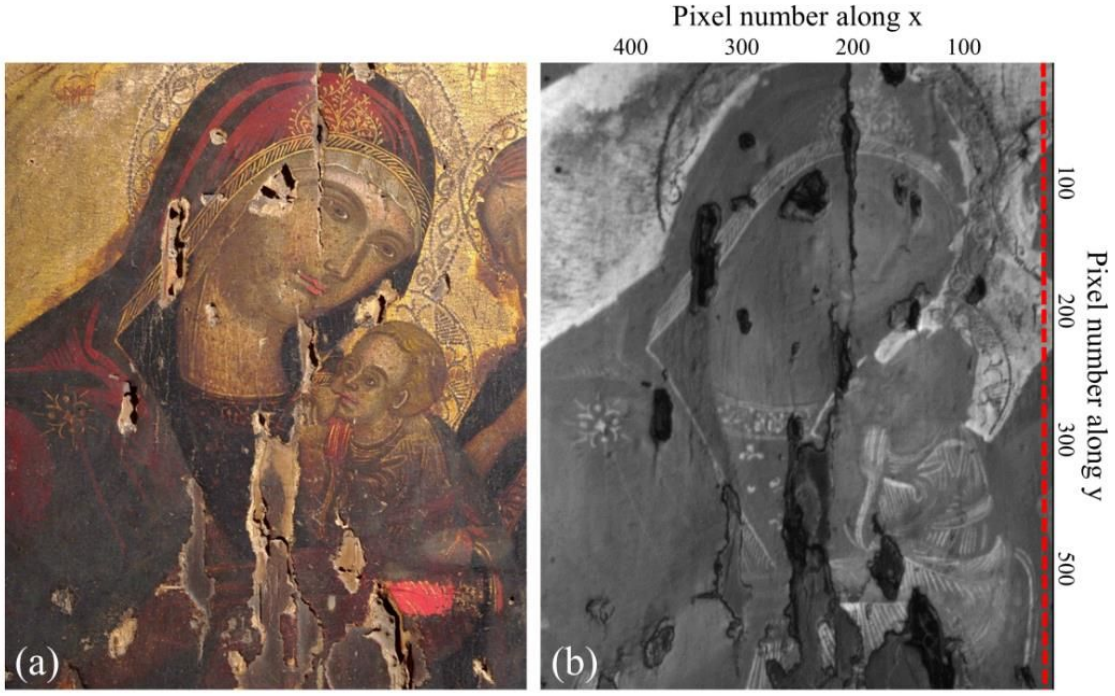

Fig. IV.4-4 a Scanned area of the 14th icon representing the *Virgin with the Child and a Saint,* visible image. **b** 14th icon, grayscale frequency-parametric THz image of the air/surface interface- The monochromatic colormap varies from darker to lighter tonalities according to the value of spectral amplitude on a linear scale

The image has been plotted by integrating the spectral amplitude over the full frequency range after the Fourier transform of pulse of interest, isolated from the temporal waveform by window function. The high reflectivity of the metal in the THz range makes the background gold located under the painting layer clearly visible. At the contours of the faces of the figures, in the vicinity of the aureoles, it´s possible to identify the squared edges of the applied gilding, evidence that leads to assume that the Painter used gold leafs for the gilded background. Thus, the THz-TDI investigation immediately gives a substantial contribution in understanding the gilding technique utilized by the Master for the gold background.

Furthermore, THz-TDI facilitates the localization of the gilding used for tracing decorative motives on the figures dresses (straight lines on the Child garment and at the border of the Virgin veil, floral motives of the Virgin mantle), not clearly perceptible looking at the visible image because of the

intense browning of the surface varnish layer, which impedes a correct reading of the image details.

In addition, the THz imaging contributes to the understanding of the pigments used by the Master painter. The bright red highlights used on Virgin's mantle and on her lips, appear distinguishable in the THz image thanks to a reflectivity greater than that of adjacent pigments. It is well known that among the red pigments, the cinnabar (HgS) is characterized by a high reflectivity within the THz range used, distinctive from other red pigments [111], [124].

Thanks to the high reflectivity within the explored THz range of the white pigment used to enlighten the Madonna and Child faces, the volumes and features of visages are clearly defined in the THz grayscale images, with their lighter tones of gray. Among white pigments which use is contemporary to the painting, it is the lead white ($Pb_3(CO3)_2(OH)_2$ or $PbCO_3$) that has the highest reflectivity in the used THz range [124], [143] indicating that this pigment, as expected, has been used. Concerning pigments characterization, THz-TDI has helped in mapping the distribution of pigments on the surface, localizing areas of interest for further punctual non-invasive analysis, or sampling sites for chemical analysis of pigments (i.e. red areas of the Virgin's robe having a different THz response, enlighten of Madonna and Child faces).

Fig. IV.4-5a shows the column B-scan displaying the time-of-flight of the electric field recorded along the scan-line drawn in Fig. IV.4-4b, with the colors of the color map related to the strength of the recorded signals. Accentuated by the chosen color-map (ranging from blue to red through cyan, yellow, and orange for increasing strength of the recorded signal), it is clearly visible that pulses arising from reflections at the paint/plaster and plaster/wood interfaces are strong enough to be detected on areas covered by the gilding located at the surface, even if the strength of the recorded electric field is lower than the areas not covered by the gilding. After having isolated the detected interfaces (Fig. IV.4-5b), THz time-of-flight plots have been imaged (Fig. IV.4-5c), while Fig. IV.4-6a-b show the THz C-scans of the interfaces paint/plaster and plaster/wood.

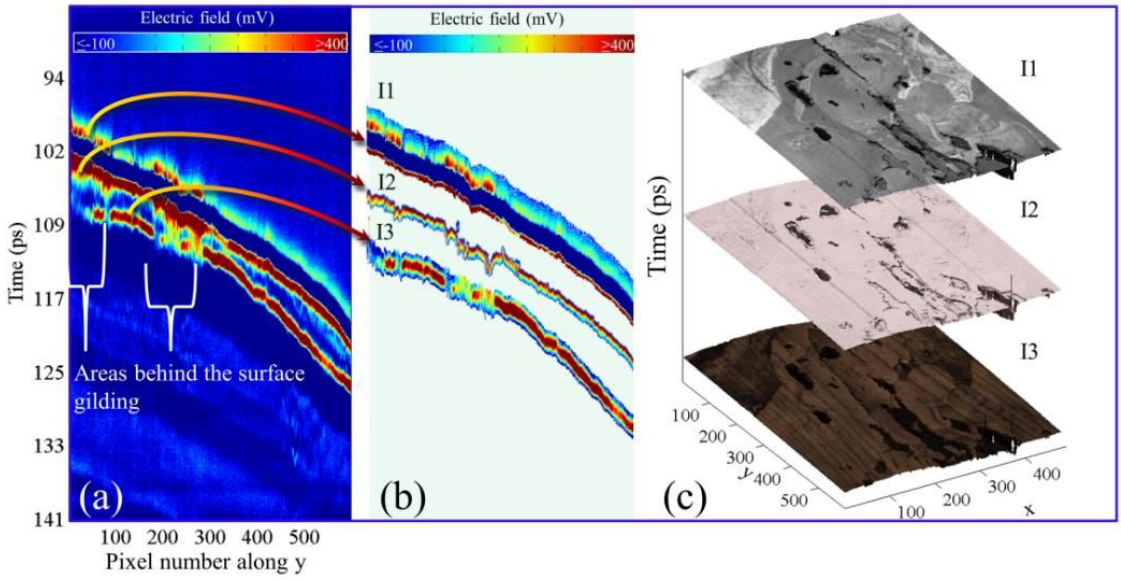

Fig. IV.4-5 a B-scan representing value and time-of-flight of the recorded electric signal recorded along the scan-line indicated by the red line of Fig. IV.4-4b). **b** Single interfaces (air/surface, paint/plaster, plaster/wood) found, isolated from the B-scan of Fig. IV.4-5c). **c** 14th icon, Time-of-Flight plots related to the three interfaces found (air/surface, paint/plaster, plaster/wood).

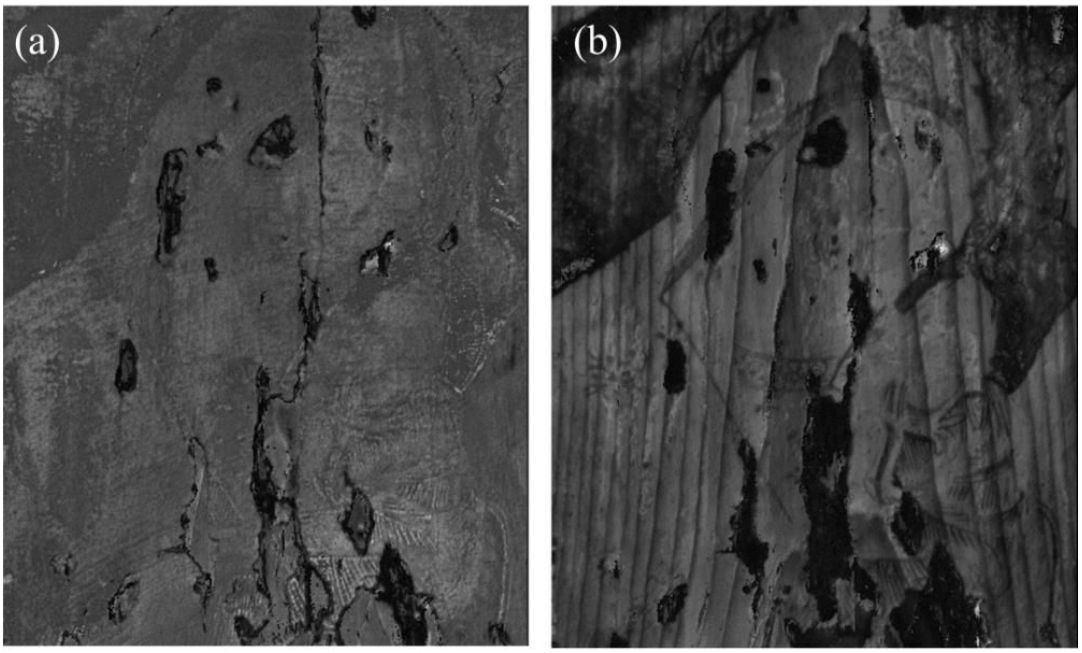

Fig. IV.4-6 a 14th icon, gray-scale frequency-parametric THz image of the paint/plaster interface. **b** 14th icon, gray-scale frequency-parametric THz image of the plaster/wood interface.

The texture of the subsurface interfaces, as appear in the corresponding plan-type images, can still be recorded for the areas covered by the surface gilding, even if less clearly that for the uncovered ones.

IV.4.F Final considerations

We have shown that investigation of subsurface features of gilded panel paintings and the characterization of their internal structure by means of THz-TDI in reflection geometry is possible, and in particular, we have demonstrated that the investigations are also possible behind the gold finishes. Despite the very high reflectivity of metals at submillimeter wavelengths, a small but non-negligible direct transmission through gold leafs occurs if the gold leaf thickness is of the order of the skin depth of gold films in the terahertz range, due to the skin effect.

THz-TDI applied on the two panel painting replicas gave important information about the execution technique.

Concerning the panel painting n.1, THz-TDI aided in individuating location and extension of the cloth piece covered by the ground layer and applied on the wooden panel. The grain of the wood located behind the ground layer is visible in the THz image, also partially on the areas covered by the surface gilding.

THz-TDI investigation of the panel painting replica n.2 proves that the paint layer has been applied on the gold background, which covers almost the total area of the ground layer, except for small areas where the paint layer has been applied directly on the ground, without the presence of the gilding in the middle. An internal defect, compatible with the presence of an air bubble inside the primer layer, has been localized by imaging the subsurface interfaces, proving again the ability of THz radiation to penetrate thin gold leaf layers.

THz-TDI investigation of the 14th Century icon representing *the Virgin with the Child and a Saint* gave a substantial contribution in understanding the gilding technique utilized by the Master for the gold background. The squared edges of the gilding located behind the paint layers, only visible in the THz images, indicate the use of gold leaves.

Furthermore, THz-TDI facilitated the localization of the gilding used for tracing decorative motives on the figures dresses (straight lines on the Child garment and at the border of the Virgin veil, floral motives of the Virgin mantle), not clearly perceptible by inspection of the visible image owing to the intense browning of the surface varnish layer, which impedes a correct reading of the image details.

Concerning pigments characterization, THz-TDI indicated the possible use of cinnabar for the red highlights used on Virgin's mantle and lips and lead-white for the figure visages. Thus, it helped in mapping the distribution

of pigments on the surface, localizing areas of interest for further punctual non-invasive analysis, or possible sampling sites for further invasive analysis aimed towards pigment identification.

The THz pulses arising from reflections at the subsurface paint/plaster and plaster/wood interfaces are strong enough to be detected even on areas covered by the surface gilding, allowing these interfaces to be imaged by c-scans and modeled by time-of-flight plots.

Based on our findings we finally conclude that the unique possibility of seeing through gilding layers while recording 3D information about the internal structure of an object makes THz-TDI is a very powerful technique which can complement radiography techniques in inspection of valuable art artifacts.

IV.5 Diagnostics pre and post conservation on a 14th century gilded icon from Taormina, Sicily

This section reports parts of the pre and post conservation diagnostics made on the 14th century icon, *the Virgin with the Child and a Saint*, already discussed in the previous section. The original article can be accessed at [144].

We implemented the THz-TDI scanning made before the restoration intervention (section IV.4) with a further set of non-invasive imaging techniques, before and after the restoration treatment. The methods used included technical photography (Vis fluorescence induced by UV light - UVF, reflected UV - UVR, reflected IR - IRr, IR luminescence induced by Vis light - IRF), infrared reflectography (IRR) and multispectral imaging (MSI). At the end of the investigation, an identification of the palette has been attempted, crossing the results obtained by reflectance spectra analysis with those obtained by the other imaging techniques. THz-TDI examination gave a substantial contribution to the understanding of the gilding technique. An accurate examination of the surface has been performed with infrared Reflectance Transformation Imaging (IR-RTI) and with THz-TDI to localize cracks, flacking, incisions and material losses. Subsurface layers have been imaged by THz-TDI imaging. This study is a valid example of the application of non-invasive imaging methods before and after the conservation treatment of a work of art.

The multi-technique approach has been used in order to identify the materials and technique of the original painting, to detect previous restoration and additions as well as the nature and extent of the alterations present. The intention of these pre-conservation diagnostics was to provide key information to the conservator for the development of an appropriate conservation treatment. The diagnostics after conservation provided further information on painting materials thanks to the removal of the thick dirt deposit from the painting surface, and allowed to evaluate the accuracy of the conservation treatment itself. This case of study highlights the importance of a non-invasive diagnostics approach for artefact comprehension and for the evaluation of a conservation intervention. It wants also to contribute to the literature regarding scientific examinations of medieval icons [145]–[147].

IV.5.A The 14th century icon: preservation state

The 14th century icon has been already described in section IV.4. Fig. IV.5.1a and b shows the icon before (pre- within the text) and after (post- within the text) the restoration treatment.

Fig. IV.5-1 The investigated icon **a** before (pre-) and **b** after (post-) the cleaning and conservation treatment. The dashed frame indicates the cleaning test on the vest of Jesus.

The icon was affected by extensive damages: losses and detachments of the paint as well as lacunae in the wooden support. The significant accumulation of surface dirt was substantially reducing the brightness of the gold background. The painting's figures were barely recognizable, as well as the complexity of colors and details, which characterized the original aspect of the painting. A cleaning test (Fig. IV.5-1a) revealed the intense red pigment of the vest of Jesus under the soil layer, suggesting the color richness which was eventually revealed with the cleaning completed.

IV.5.B Analytical Instrumentation and Methodologies

Technical photography was performed with a Nikon D800 DSLR camera (36 MP, CMOS sensor) modified for full spectrum acquisition. These methods and the related imaging equipment and calibration procedures are extensively described elsewhere [148]. Infrared reflectography (IRR) was performed with an InGaAs camera (320×256 pixels) Merlin NIR by Indigo

Systems. THz-TDI measurements were performed as described in section IV.4.B. Reflectance Imaging Spectroscopy was performed with a CCD camera (PixelTeq SpectroCam VIS) and 12 interferential bandpass filters also commercialized by PixelTeq. The method is referred to as MSI-12 and the filters used are (center wavelength/bandwidth nm): 425/50, 475/50, 532/16, 578/10, 620/10, 669/10, 680/10, 717/10, 740/10, 750/10, 780/20, 800/10.

IV.5.C Results and discussion

Ultraviolet Imaging (UVF, UVR)

Because of the surface thick layer of dirt, the pre-UVF image (Fig. IV.5-2a) turned uniformly dark and featureless. The post-UVF image (Fig. IV.5-2b and e) revealed a strong pale white fluorescence in correspondence of the white areas of the painting, a weak reddish fluorescence in correspondence of some red areas (red robe of Infant Jesus and red highlights of Madonna's mantle).

Fig. IV.5-2 a Pre-UVF, **b** post-UVF, **c** post-UVR. Details: **d** post-VIS, **e** post-UVF and **f** post-UVR. The dashed frame localizes the cleaning test on Jesus' vest.

Retouches were detected thanks to their fluorescence, when placed close to a non-fluorescent area of the original painting, and to their lack of

fluorescence, when placed on an original paint area with characteristic fluorescence.

UVR (Fig. IV.5c) was acquired just after the cleaning intervention was completed, and it highlights surfaces defects (e.g. the edges of the filling parts, Fig. IV.5f).

Infrared Imaging (IRr, IR-FC, IRF, IRR)

The pre-IRr image allowed a clear understanding of the details of the composition even before the cleaning treatment (Fig. IV.5-3b, Fig. IV.5-5b).

A notable detail is that the greenish dress of the small Jesus appear IR-transparent in both the IRR and IRr images

Infrared photography and reflectography were indispensable for inspecting the painting for underdrawings and *pentimenti*; they were both used because of the different detectors sensitivity and response, where IRR can penetrate further acquired (Fig. IV.5-3c-d, Fig. IV.6-4c-d) through the pictorial layer compared to IRr.

Fig. IV.5-3 a Pre VIS, **b** pre IRr, **c** post IRr and **d** post IRR

The brushworks done with *verdaccio* on the Virgin's neck (green earth based paint used to outline the figure's skin), partially visible in the post-VIS image, become more distinct in the IRr image (Fig. IV.5-4a-b,d). The IRr image shows a *pentimento* on the left arm of the Saint: the forearm was larger and eventually covered by the green paint of the vest of the Saint (Fig. IV.5-4c,e).

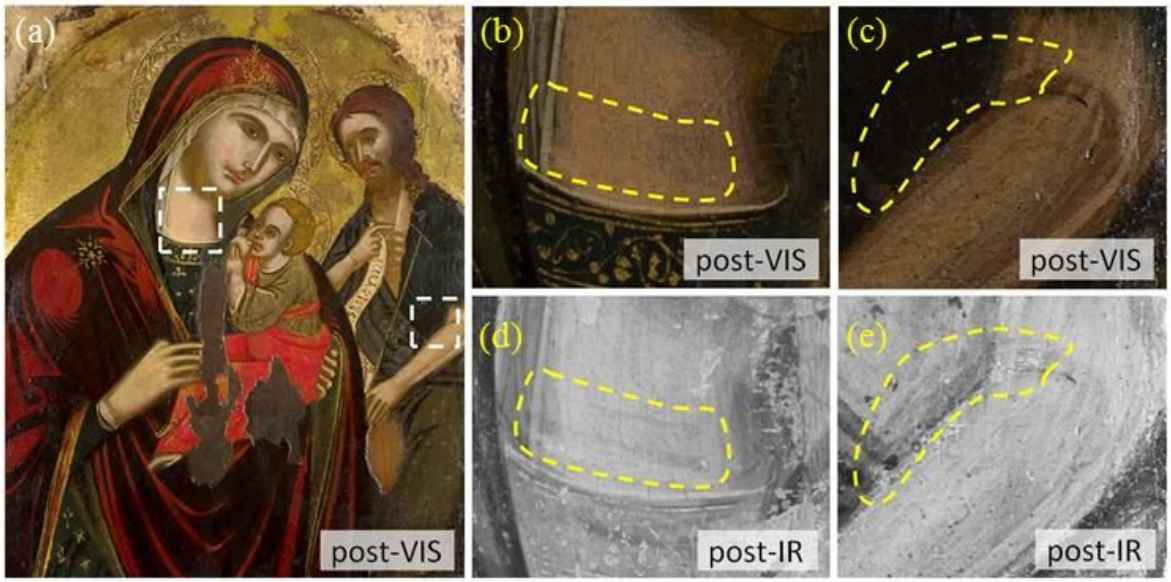

Fig. IV.5-4 a Areas where the underdrawings and the *pentimenti* were detected. **b, c** relevant details in Vis image **d, e** relevant details in IRr image

Once the thick veil of dirt was removed the contrast between IR-absorbing pigments and those allowing the radiations to pass through to the substrate is enhanced (Fig. IV.5-5c).

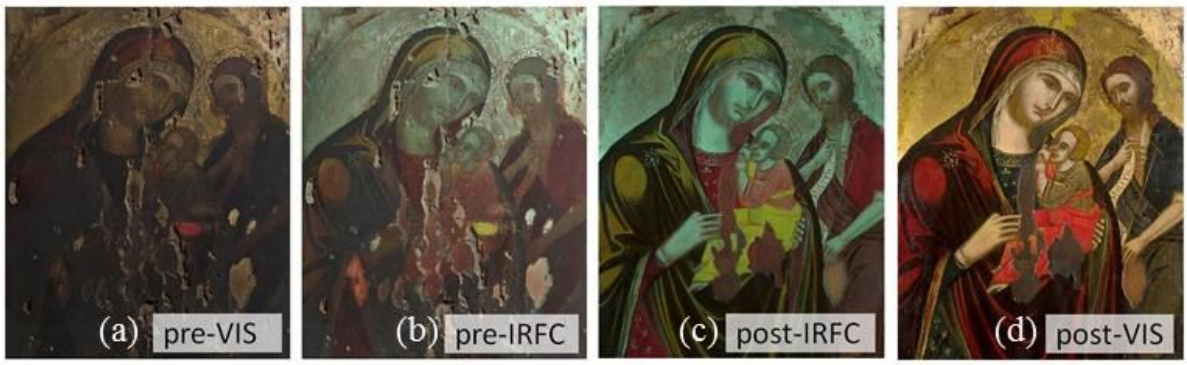

Fig. IV.5-5 Pre-VIS **a**, pre IRFC **b**, post IRFC **c** and post-Vis **d**.

The red highlights of the Virgin's mantle appear orange in IRFC, while the red vest of Jesus shows a bright yellow false color in IRFC, demonstrating the different composition of these red areas of the painting. The gilded dress of the Virgin and those of the Saint show a similar response, appearing both deep green in Vis light, while red in IRFC. Thus, the post-IRFC image provided useful information which, combined with the results obtained by the other non-invasive inspection methods, aided in attempting pigments identification.

Very few pigments exhibit IR fluorescence induced by visible light: cadmium red, cadmium yellow and Egyptian blue [149], [150]. The bright

spots visible in the post-IRF image (Fig. IV.5-6a) highlight the retouches made with cadmium-based pigments.

Fig. IV.5-6 **a** post-IRF. **b** post-VIS

Terahertz Time-Domain Imaging (THz-TDI)

Thanks to THz-TDI the gilding technique utilized by the artist for the background, has been cleared (gold leafs, see section IV.5).

It is important to point out that the identification of the gold leaves under the paint was possible only with THz imaging and, indeed, even IRR could not penetrate as much deep into the paint (Fig. IV.5-7c,d).

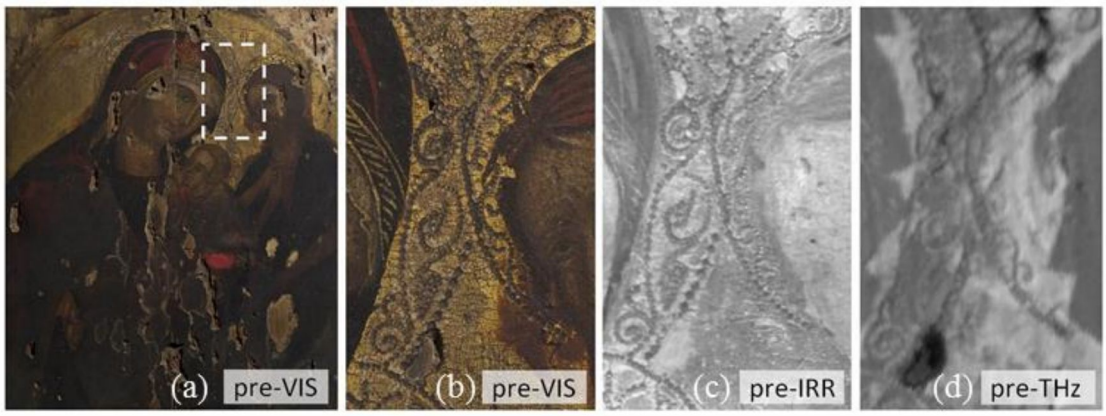

Fig. IV.5-7 **a** Pre-VIS. Detail: **b** pre-VIS, **c** pre-IRR and **d** pre-THz images

The technique facilitates the localization of the gilding used for tracing decorative motives on Jesus´s dress (Fig. IV.5-8c), not clearly noticeable by naked eye inspection owing to the thick dirt layer (Fig. IV.5-8a). This helped in preserving them by aggressive cleaning agents during the restoration intervention (Fig. IV.5-8d). Even in this case, only THz-TDI images

localized the gildings, while they were not seen by IRr images (Fig. IV.5-8b,c).

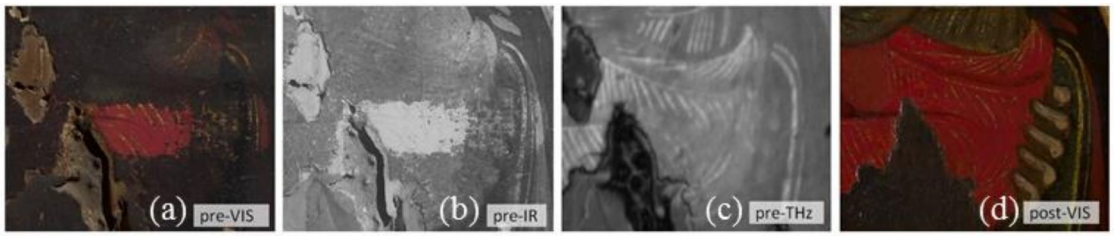

Fig. IV.5-8 Details of the vest of Jesus. **a** Pre-VIS, **b** pre-IR, **c** pre-THz and **d** post-VIS images

Before the cleaning treatment some areas of the gilding appeared darkened (Fig. IV.5-9a,b). The same areas appeared bright in the THz image (Fig. IV-5-9c), suggesting the presence of a firm gold leaf under a darkened coat. This has been confirmed after the restoration intervention, when the original gilding came out after the dark varnish removal (Fig. IV.5-9d).

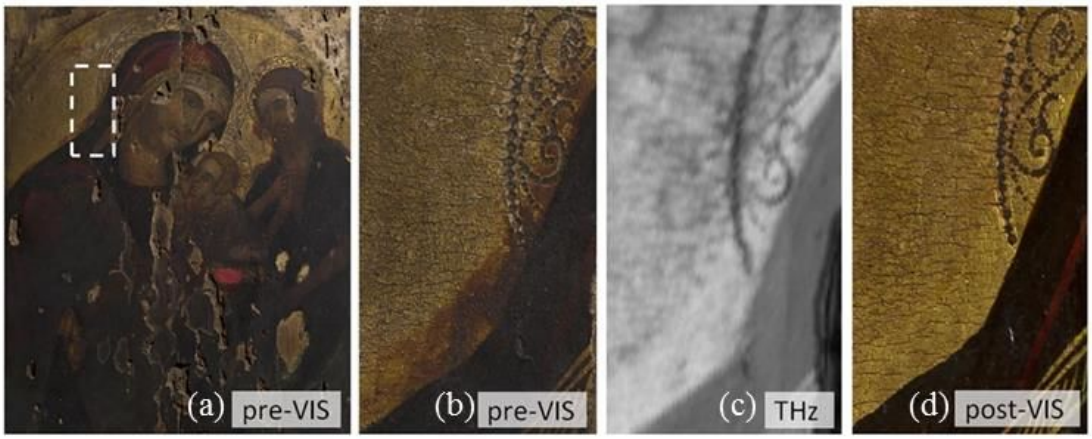

Fig. IV.5-9 a pre-Vis image of the icon. Details of the background gilding. **a** Pre-VIS, **b** pre-IR, **c** pre-THz and **d** post-VIS images

Subsurface interfaces have been successfully imaged (Fig. IV.5-10d,e).

The THz image of the wooden panel support allows the identification of the wood grains, which was not possible by seeing the panel from the back (Fig. IV.5-10f). THz imaging also contributed to pigments identification thanks to the different reflectivity of some pigments within the THz range frequency examined [124], as discussed later in the text. IRr image is shown in Fig. IV.5-10b for a comparison between IRr and THz-TDI images.

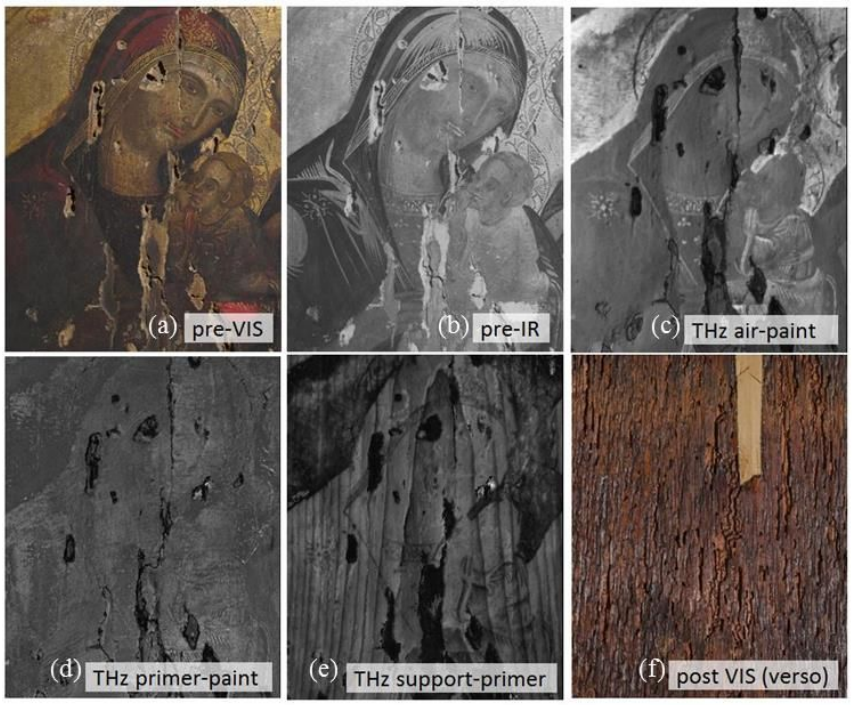

Fig. IV.5-10
a Pre-VIS image.
b Pre-IRr image
c THz image (air –paint interface),
d THz image (primer-paint interface),
e THz (support-primer interface),
f back of the wooden support.

Reflectance Transformation Imaging (IR-RTI)

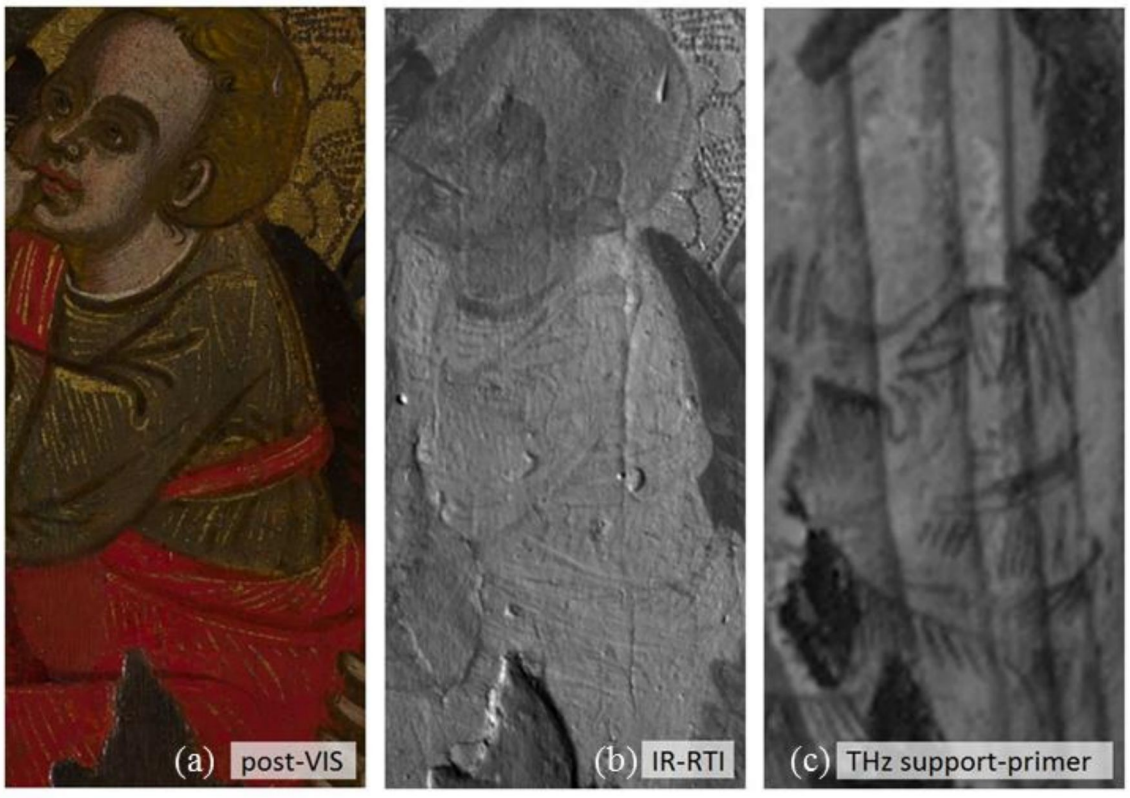

Fig. IV.5-11 Detail. **a** Post VIS, **b** IR-RTI, **c** THz (interface support-primer) images

RTI was used to inspect the icon for incisions and retouchments and surface features.

The IR-RTI image of a detail of the icon shows a number of retouches, recognizable by their lower profile. No incisions were detected by IR-RTI, but it revealed some raised vertical lines that follow the length of the painting. Fig. IV.5-11b shows one of them going across the vest of Jesus. This line is located between two grains of the wooden support as seen in the THz support/primer interface image and, therefore, can be explained as a consequence of stress inside the panel.

Multispectral imaging (MSI-12)

MSI provided reconstructed reflectance spectra (Fig. IV.5-8b) which are used for pigments mapping and introductory identification.

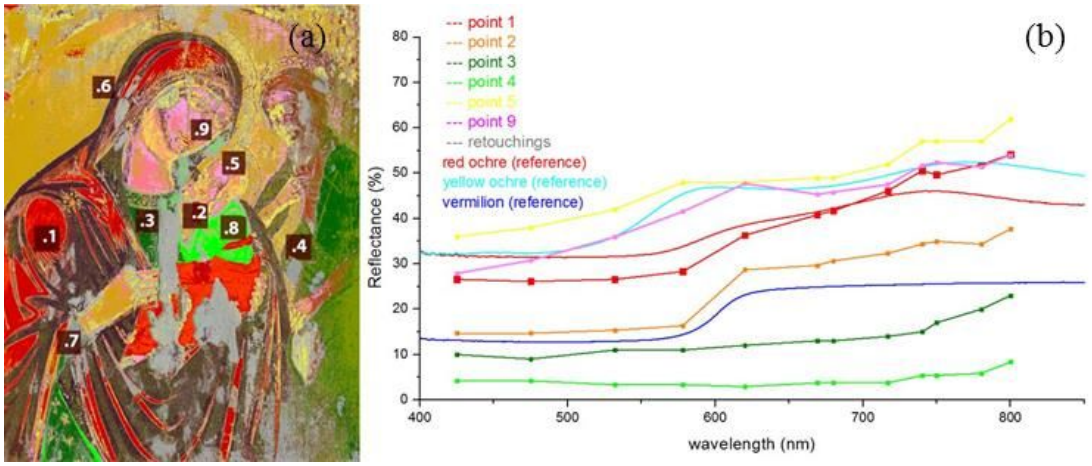

Fig. IV.5-12a MSI-12 classified image and **b** reflectance spectra of 6 points, with the relevant reference spectra

It furthermore provided a classified image (Fig. IV.5-8a), meaning that pixels with similar reflectance spectra are clustered and assigned to a specific false color. The classified image aided in examining the painting, distinguishing original pigments from retouching (grey false color, Fig. IV.5-8a). A purposive discussion about the MSI reflectance spectra follows below.

- *Point 1. The red mantle of the Virgin*

The MSI-12 reflectance spectrum (point 1 in Fig. IV.5-7b) shows the S-shape which is characteristic of the ochres and an inflection point at about 600 nm, characteristic of the vermilion. This suggests the use of vermilion mixed with red ochre. The brighter appearance of the highlights of the

Virgin´s mantle in the grayscale THz image (Fig. IV.5-6c) cannot discount this interpretation [124].

•*Point 2. The scarlet red mantle of the infant Jesus*

Its reflectance spectrum suggests the presence of vermilion because of its sharp inflection point at 600 nm. The classified image (Fig. IV.5-12a) successfully maps the distribution of this pigment at surface (orange false color) and differentiates it from the mixture with red ochre (dark red false color). This hypothesis is supported also by the THz imaging where this area appear even brighter than that the one where point 1 is localized. The different compositions of the red decorations on the Virgin's veil and of the red vest of Jesus was already suggested by the IRFC image, which showed different false colors for the vest of Jesus and for the Virgin's mantle (Fig. IV.5-5c). When investigated by UVF the red vest of Jesus exhibits a weak reddish fluorescence, which can also be attributed to vermilion laid with tempera (Fig. IV.5-2b).

•*Point 3. The dark green vest of the Virgin*

The Virgin green garment and the green vest of the Saint show a similar response in the IRFC images, both appearing bright red. The reconstructed reflectance spectrum is flat in the visible with an increased reflectance in the near infrared region. These features rule out the typical medieval green pigments used for the panel painting construction. In fact, malachite and verdigris have a strong reflectance maximum in the green region of the visible spectrum and, together with the green earth, absorbs the near infrared light. Consequently, this green is more likely to be mixture of yellow and blue.

•*Point 4. The light green mantle of the Saint*

This light green shade seems to be a green earth because of its flat reconstructed reflectance spectrum all over the visible and near infrared regions and because it shows a brownish color in the IRFC rendering (Fig. IV.5-5c).

•*Point 5. The hair of Jesus*

The reconstructed reflectance spectrum features the S-shape of yellow ochre. This hypothesis is sustained by the images obtain with the other imaging techniques, showing no special features for this area.

•*Point 8.The green shirt of Jesus*

It appears extremely bright in IR and IRR, excluding the presence of an inorganic green pigment (Fig. IV.5-c,d). The reconstructed reflectance spectrum is characterized by a sharp inflection point at about 725 nm, suggesting a mixture of indigo, responsible for this inflection point, and a yellow pigment.

•*Point 9. The Figures complexion*

Concerning the white pigment used to enlighten and define the complexion of figures, complementary information provided by the imaging techniques pointed to lead white. This is the white pigment which has the highest reflectivity in the used THz range and indeed the white highlights are moderately bright in the THz image (Fig. IV.5-10c). The other two common modern white pigments, zinc white and titanium white, could be excluded observing the UVR image (Fig. IV.5-2c,f) because these pigments absorb the UV and appear as dark areas in the UVR image. Also lithopone could be ruled out thanks to the reconstructed reflectance spectrum which does not show the pigment's characteristic absorption bands in the near infrared region.

IV.5.D Final considerations

We have presented a comprehensive non-invasive imaging diagnostics of a 14th century gilded icon before and after its conservation treatment, highlighting the importance of combining different methods to achieve convincing conclusions about painting composition and condition, through its detailed inspection from the paint surface to the wooden support.

Pigment identification has been attempted crossing the results from reflectance spectroscopy imaging (MSI-12) and those obtained from the other imaging techniques (UVF, UVR, IRr, IRFC, IRR, THz-TDI). The applied methods successfully designated most of the pigments in the

painter's palette with reasonable confidence. We can assume that lead white, vermilion, red ochre, yellow ochre and green earth were used.

For a more confident materials identification, the imaging methods used have demonstrated to be advantageous for identifying areas of interest for further studies with non-invasive and invasive analytical methods, being capable of mapping the surface distribution of pigments.

The original gilding technique used by the artist has been identified by THz-TDI scanning: the square edges of the gilding imaged behind the pain layers led to the conclusion that the gilding background was made by gold leaves.

Immediately behind the surface paint layer, brushworks sketched by *verdaccio* to outline the figures skin become more distinct on the Virgin's neck by IR inspection, while on the left arm of the Saint a *pentimento* has been observed.

By means of THz-TDI, subsurface layers (primer and wooden support) have been imaged. The primer layer does not seem to be affected by significant alterations. Imaging wood grain has been possible with THz-TDI, which is effective for understanding the nature of the longitudinal crack on the paint surface, highlighted in detail by IR-RTI investigation. Located between two wood grains, the origin of the crack appears to be connected with mechanical stress arising from the interior of the panel.

Our study has shown the utility of performing diagnostic imaging prior to restoration intervention, since it provided key information to the conservator about the composition and condition of the icon from the surface paint film down to the support and it allowed him to develop an appropriate conservation treatment. In this context, THz-TDI facilitated the localization of the gilding covered by a thick soil layer. This allowed him to protect them properly from aggressive cleaning agents, permitting their preservation. Furthermore THz-TDI helped in excluding serious structural problem thanks to the images of the primer and the wooden support layers.

This section illustrates also the importance of diagnostic imaging even after the cleaning treatment. The thick dirt layer limits information obtained by pre-UVF, pre-UVR and pre-IRFC images regarding painting materials while, after the cleaning, these images returned a number of information on original pigments and binder.

IV.6 Chapter conclusion

Chapter IV reports about the results obtained by scanning with THz-TDI three panel painting replicas and different typologies of valuable panel paintings. Those include *A Garden in front of a Country Seat* painting by David Teniers the Younger (17th century), the *Lamentation over the dead Christ* by Fra Angelico (ca. 1440), the two side panels of the *Franciscan Triptych* (the *Saints Jerome, John the Baptist and the Archangel Gabriel* and *Saints Francis, Onofrio and the Virgin Annunciate,* before 1429*)* and an original medieval icon (*the Virgin with the Child and a Saint,* 14th century*)* by an unknown artist.

THz-TDI gave precious insights about manufacturing technique used to create the scanned painting concerning wooden panel preparation, gessoing and gilding.

Regarding the panel support preparation, THz B-scans made on the *Saints Francis, Onofrio and the Virgin Annunciate* showed the presence of a cloth covering the wooden panel, furthermore highlighting that the external margin of the panel is uncovered within the scanned area. The same was deducted for the *Saints Jerome, John the Baptist and the Archangel Gabriel* panel painting. In addition, by imaging the proper temporal range of the THz back-reflected pulses, it appeared how the textile in this last case was applied by assembling more cloth pieces. The presence of a cloth between the wooden panel and the ground was revealed also for the panel painting replican.1 (section IV.4), while the cloth was clearly THz imaged between the two priming layers located the top of the wooden panel for the replica discussed in section IV.2. No cloths were found for the medieval icon, where the paint was directly applied on the wooden support. The same was concluded for the panel painting replica n. 2 (section IV.4).

Regarding gessoing, by carefully interpreting the THz B-scans it was concluded that the 19th century conservators of the *Lamentation* panel first tried to even out the existing grouting layer, removing the unstable parts, and subsequently leveled the new filler out to the original plaster. This data interpretation found confirmation in the conservation report made by the conservators of that time. Furthermore, the THz-TDI data set recorded on the panel painting replica discussed in section IV.2, indicated how THz-TDI was

capable of detecting the separation line between the same gessoing material applied with different degrees of compaction, as said by the conservators who made it, thus giving an indication regarding different application techniques of the same material used.

THz-TDI is furthermore able to provide impressive information about the gilding technique used for panel finishing. In addition to showing the repairs made in the golden aureole of the Virgin represented in the *Lamentation*, the precise borders matching between it and the visage suggests that the gilding was applied by a thin brush at the figures borders.

The same evidence was obtained by the investigation made on the *Franciscan Triptych* side panels. Different gilding technique has been found for the 14th century icon, where the squared edges of the gilding imaged behind the paint layers indicate the use of gold leaves.

In addition, the THz images reveal that the silver baton held by Saint John, on the *Saints Jerome, John the Baptist and the Archangel Gabriel* was drawn on the top of the figure paint. The opposite conclusion was deducted by scanning a gilded panel painting replica (panel painting replica n.2 in section IV.4), where THz-scans showed how the paint layer was applied on the gold background except for small areas where the paint layer was applied directly on the ground, without the presence of the gilding in the middle.

Furthermore, the evidence that THz signals appear almost entirely reflected back by the gilded areas in the B-scans made on the *Lamentation*, suggests that the gold thickness is higher than that of the skin depth of the metal at THz frequencies. Differently, B-scans obtained from gilded parts of the *Franciscan Triptych* side panels and from the Medieval icon indicate an opposite behavior, showing THz reflections at subsurface layers even when covered by the gold finishing, suggesting that the gold is of a very small thickness, either because original choice or because later abrasion. Consequently, we have demonstrated that the characterization of the internal structure of gilded panel paintings by means of THz-TDI in reflection geometry is possible, also though very thin gold finishing.

In fact, the grain of the wood located behind the ground layer was partially imaged in the THz image of the gilded panel painting replica n.1 (section IV.4), and so was for the Medieval icon, where priming layer and wooden panel were individually THz-image despite the presence of a surface gilding. An internal defect, compatible with the presence of an air bubble inside the priming layer, has been localized by imaging the subsurface

interfaces of the panel replica n. 2 of section IV.4, proving again the ability of THz radiation to penetrate thin gold leaf layers.

The technique proved suitable for detecting and localization of hidden cracks or defects of the wooden panels, providing precious information concerning the preservation state of the paintings.

The wooden panel boundaries of the *Lamentation* appeared to be extremely uneven in the dielectric stratigraphy obtained by scanning an area of the lower margin of the panel and confirmed the known preservation history of the panel which suffered severe erosion in the lower side because of a fire in the past. Spot-like defects were observed in the THz C-scan of the wooden panel within the scanned area of the *Lamentation*. This matches with the records about the important damages affecting the wooden support of the painting, primarily caused by insect attacks.

THz B-scans showed a crack on the wooden panel of *Saints Jerome, John the Baptist and the Archangel Gabriel*, which is extending for the entire length of the scanned area underneath the painted surface. The absence of air gaps in the plaster layer furthermore suggests how the crack was in the wooden panel originally, before the gessoing operation. On the other hand, the origin of the crack visible on the surface of the medioeval icon has be explained thanks to the THz image of the wooden support: in fact, it is located between two grains of the wooden support and it is therefore originating by stress within the wooden panel.

Other information of interest within the conservation issue are the in-depth anomaly found by THz-TDI in the upper layers composing the art pieces.

Concerning the *Saints Jerome, John the Baptist and the Archangel Gabriel* the THz stratigraphic analyses highlights an anomaly, related to a material applied locally just behind the paint surface. Similarly, after THz signal separation, single composition layers were imaged and an in-depth anomaly (metal inclusion in the priming layer) was located and imaged within both the painting stratigraphy and the areal position of the panel painting replica described in section IV.2

Besides, THz-TDI facilitated the localization of the gilding used for tracing decorative motives on the figure dresses of the medioeval icon, not clearly perceptible by inspection of the visible image owing to the intense browning of the surface varnish layer, therefore allowing the conservator to

protect them from aggressive cleaning agent during the conservation intervention.

Relating to pigments characterization, where the pigment combination offered a THz contrast with the exploited frequency range, THz-TDI helped in mapping the distribution of pigments not only on the surface (e.g. the medieval icon), but also on subsurface layer (e.g. *A Garden in front of a Country Seat*).

This study offers the occasion to compare the THz-TDI scanning with reflected infrared image and X-radiograph, highlighting the importance of combining different methods to achieve convincing conclusions about painting composition and condition.

Both radiography and THz-TDI were able to image an older painting hidden beneath the actual *A Garden in front of a Country Seat* painting by David Teniers the Younger (17^{th} century); comparison between the two images showed how wood grains and features are better visualized by THz-TDI compared to X-radiography, including subsurface cracks. Small variation in the thickness of the hidden paint brushstroke and painting details of the concealed composition were found also to be more evident in frequency parametric THz images compared to the X-radiograph.

Based on our findings we also conclude that the unique possibility of seeing through gilding layers and the gilding layers themselves in a unique scan makes THz-TDI a very powerful technique, which can complement standard X-ray and reflected IR technique. At the same time, THz-TDI cannot replace the IR reflectography in detecting the underdrawings: the *verdaccio* brushstrokes made before the application of the paint used for the skin tone of the figures of the medieval icon were only revealed by IR reflectography. Limitations in detecting underdrawings were also found for the panel painting replica described in section IV.2: of the five historical materials used for underdrawings (lead metal-point, tin-lead metal point, graphite, charcoal, watercolor), only lead metal-point, and graphite at thicker lines were detected by THz-TDI scans, while the ability of IR reflectography in detecting all the proposed underdrawings is well known.

Chapter V
THz-TDI applied to wall painting investigation

To the best of our knowledge, the first interest in building materials characterization by means of terahertz radiation was addressed to typical office environment, for obtaining realistic model for propagation channels in terahertz communication systems (2005 [151]) approximately ten years after the first terahertz time-domain imaging system was realized [33]. Simultaneously with the development of studies on the characterization of building materials for indoor wireless communication systems [126], GHz and THz frequencies started to be exploited for building materials investigation within the context of non-destructive testing and civil structures damage detection. Imaging of concrete with microwaves (6-10 GHz) [152] and with terahertz imaging systems [153], [154], proved the ability to image metallic, dielectric objects and cracks inside concrete and building block unite samples. Systematic studies on the application of terahertz spectroscopy and imaging to construction, ground terrain and building materials are still developing in the recent years [155], [156]. In the meanwhile in 2006 the first attempt to investigate artworks by means of terahertz imaging systems was made [39], thus calling attention to the application of this technology to art investigation. Being the crossing points between paintings and building materials, the application of terahertz time-domain systems to the investigation of wall paintings followed rapidly [94]. The first attempt in the world to image an ancient real wall painting fragment was made in 2010 [40]. A number of case studies about terahertz imaging of wall painting took place between 2013 and 2014, including mock-up samples [83], [157], [158] and real wall paintings of different age (Neolithic [159], Paleolithic [160], ancient Roman [161], Medieval [162]).

V.1 Inspection of Subsurface Structures Buried in Historical Plasters: the Medieval wall painting of Nebbelunde Church

Within this research frame this section will show the use of terahertz time-domain imaging (THz-TDI) to image subsurface features of different nature until approximately 1 cm depth over an extended area of a real medieval wall painting (the apsidal wall painting of Nebbelunde Church, Rødby, Lolland, Denmark, 54.709079ºN, 11.385661ºE). By combining customized signal processing and advanced 3D visual rendering the system provided a substantial contribution in substructures characterization and identification. The original article can be accessed at [59].

V.1.A Subsurface imaging of wall paintings: the conservation issue

The long term preservation of mural paintings is linked not only to the preservation status of the surface pictorial layers [163], but also to the state of the building substrate on which they are applied. A detailed knowledge of the internal structure supporting a wall painting may be considered the key to a successful restoration project. For preservation purposes, localization of cracks and detached areas, as well as identification of regions where filling or consolidation is needed is as important as localization of buried or concealed structures inside the plaster. The presence of degrading, deforming or moving components inside plaster layers can affect their integrity, and consequently also affect the condition of the painting layers themselves. Furthermore, brick examination is at the basis of *mensiochronology*, while the analysis of stratigraphic units constituting walls and their reciprocal relationship is the fundament of relative chronological analysis of buildings and decorative surfaces, such as wall paintings. Accordingly, the characterization of subsurface features of wall paintings and position, geometry and appearance of internal structural elements is essential for understanding building history and its construction phases, and thus important in conservation and technical art history as well as in building archaeology and other architecture areas.

There are a large number of well-developed nondestructive methods for investigation of wall paintings subsurface features, including infrared

reflectography, thermography, ground penetrating radar [164], acoustic impact method (sounding), ultrasonic pulse velocity method, ultrasonic pulse-echo method [163]. Advanced non-destructive testing (NDT) methods such as radar, ultrasonic and sonic methods are mainly suited for detection and characterization of large inhomogeneities at depths larger than 2 to 10 cm. Thermography is mainly used for testing the near-surface region to a depth of up to 10 cm [165], while IR reflectography is a suitable method for detecting features, underdrawings or engravings sketched by the artist on the preparation layer immediately behind the paint layers [166].

THz-TDI has recently proven its utility as a means of investigating wall paintings [40], [83], [94], [157]–[162], panel paintings [104], [128] and easel paintings [87], and in reflection configuration it has the prospects of being a complementary non-invasive technique for subsurface features investigation of historical plasters. Due to the extremely short electromagnetic pulses being emitted from a THz-TDI system, time-of-flight measurements are feasible, thereby allowing for 3D reconstruction of the subsurface structures. The technique may provide subsurface information to a depth of a few centimeters, at depths greater than IR reflectography, but lesser than thermal imaging. This intermediate depth range is of course important to explore since many classes of damage originate from defects which are close to the surface, such as delamination of plaster, surface and subsurface cracks, voids, spalling, soiling, efflorescence and microbiological attack.

This issue is particularly relevant in relation to investigation of wall paintings, since THz-TDI measurements in reflection geometry are strongly influenced by the scattering of THz-waves caused by irregularity, grain-like and uneven structures typically found in such paintings. Recently, an image processing technique for the visualization of buried layers through uneven wall painting surfaces has been reported and the method is in progress [159].

V.1.B Instrumentation and analytical methods

THz-TDI was performed with a Picometrix T-Ray 4000 device. The relevant area has been scanned using a 320 picosecond (ps) measurement window, with a temporal resolution of 0.078 ps. We employed a scan velocity of 12.5 pixel/s (8 full temporal waveforms averaged per pixel) in a reflection configuration at normal incidence. The raster scanning was performed with a lateral resolution of 400 μm, comparable to the optical resolution of the system (300 μm) at 1 THz [82].

We have examined a region (approximately 18 x 14.6 cm, corresponding to 457 x 371 pixels) of the apsidal wall painting of Nebbelunde Church (Rødby, Lolland, Denmark). The investigated medieval wall painting (Fig. V.1-1a) is of Gothic style and depicts Saint Anne, sitting on a bench with the infant Mary, holding a book on her left hand, and the Christ in glory on the right. The pictorial technique used is the traditional medieval Danish one, which typically employs copper based green pigment, carbon-black and earths. After the Protestant Reformation (16th and 17th century) the wall painting was covered by a thick layer of lime-wash. Despite the past uncovering intervention, some lime-based mortar remains are still present on the surface.

V.1.C Results and discussion

Results and discussion of surface inspection

Fig. V.1-1b shows the visible image of the investigated area. The value of the electric field recorded at each spatial coordinate (x,y) of the scanned areas has been used to generate both frequency and time domain parametric terahertz images by a custom-written script for the computational program Matlab.

Fig. V.1-1c shows the grayscale plan-type terahertz reflection image, based on the peak-to-peak value of the reflected THz signal. Despite the characteristic high reflectivity of carbon-based pigment in the terahertz range [121], the outlines of the figures, painted with carbon-black, are not always visible in the terahertz image due to strong scattering of the reflected signal by the irregular and uneven surface, which cause unquantified signal losses due to the imperfect coupling between the detector and the reflected beam. Regardless of this, it is possible to identify the carbon-black distribution in some painting details, including the outlines of Mary's fingers (especially the index), the normal outlines which define the bottom of the book (particularly the one of the open page) and, even if pale, the two curved outlines defining the draperies of the dress that falls to her knees. The reflection image clearly localizes the incisions made on the wet lime-based plaster by a blunt point as preparatory drawing for the outlines of Mary's fingers (specially marked for the little finger) before the pigment application, which do not always overlap with the final painted outlines. This proves that the artist has changed his mind as to the composition during the process of painting (*pentimenti*). All the surface scratches appear highlighted, with an

effect similar to that of grazing visible light. The lower, middle part of Fig. V.1-1c shows a dark "Γ" shape mark that has no counterpart in the visible image.

Three-dimensional ToF plot of the surface (Fig. V.1-1d) reveals that this mark is related to an abrupt shallow depression of the wall at that point. The difference in return time of the signal between the depression and the surrounding area (5-10 ps) indicates a depth of approximately 0.75 – 1.5 mm of the depression. The uncovered regions of the wall painting are characterized by a smooth appearance, whereas the regions still covered by lime wash appear much more uneven in the THz image. This correlates well with the visual appearance of the area.

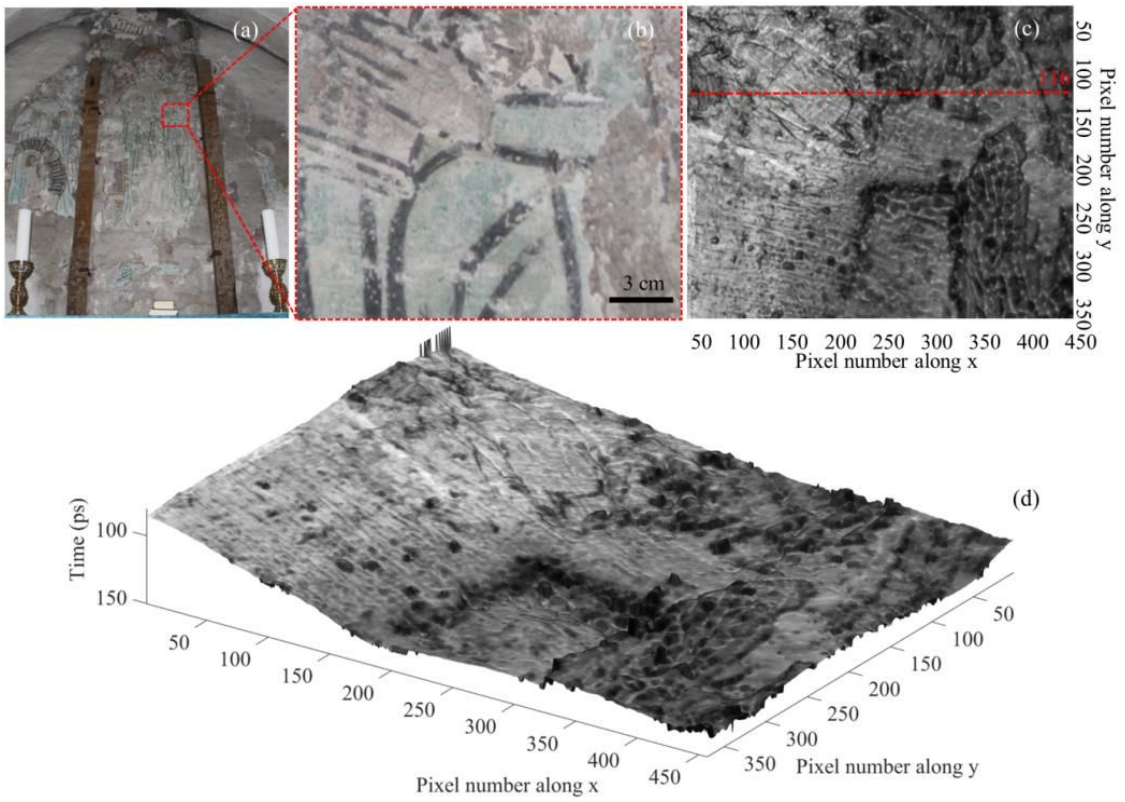

Figure V.1-1 **a** Apsidal wall painting in Nebbelunde Church - Rødby, Lolland, Denmark. **b** The relevant detail of the painting. **c** THz reflection image of the detail. The red dashed line indicates the scan-line used for the B-scans shown in Fig. V.1-2. **d** THz ToF image of the surface.

Results and discussion of subsurface inspection

B-scans (non-invasive cross-section images) have been realized displaying the time-of-flight (travel time) of the electric field along the

vertical axis and the (*x*,*y*) linear positions of the transceiver along the horizontal axis.

The B-scans reveal the presence of two major in depth anomalies. Fig. V-.1-2a shows the B-scan image obtained by scanning the investigated area along the red scan-line y = 116 in Fig. V.1-1c, and Fig. V.1-2b is the associated waveform at position (*x*,*y*) = (175,116). Fig. V.1-2c shows a zoom-in on the detail D1 where an in-depth interface is located. A waveform from the right edge of D1 is plotted in Fig. V.1-2d. Within this temporal interval, from 150 ps after the arrival time of the main pulse until the limit of the scan window (320 ps), the anomalous interface is detected transverse to the plaster, highlighted by the white arrow in Fig. V.1-2c. The systematic features that run across the B-scan image (Fig. V.1-2a and c) parallel to the surface profile are in fact system echoes, and not related to the internal structure of the wall. These features could, in principle, be suppressed by deconvolution techniques using a reference reflection signal from a metallic surface. However, these artifacts are easily recognizable, and are discarded in the following discussion.

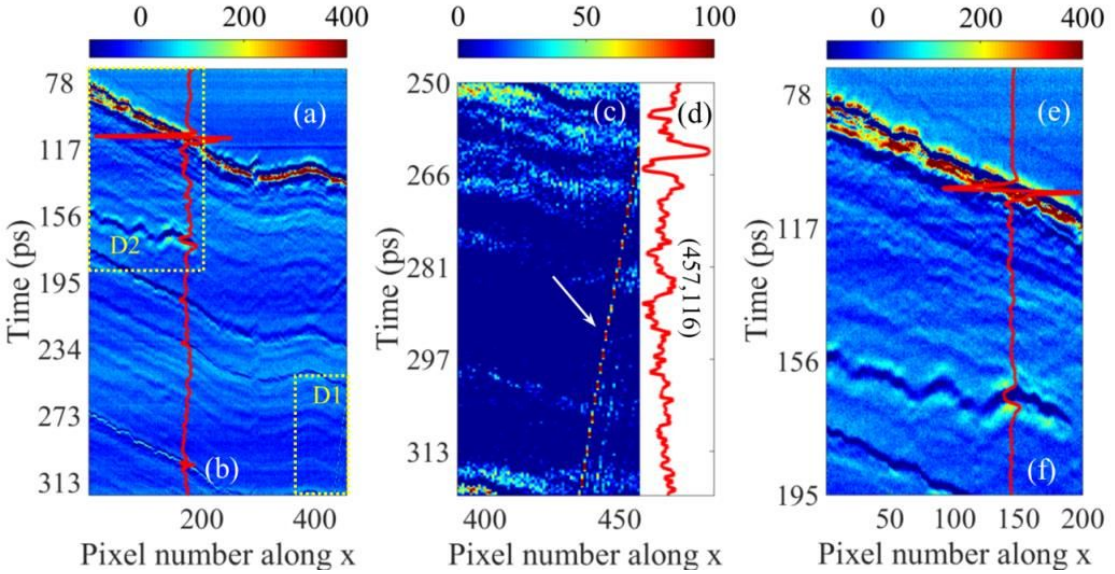

Figure V.1-2 a B-scan along the red line named 116 in Fig. V.1-1c; the yellow rectangles D1 and D2 indicate the details plotted in panel c and e. **b** Waveform at position (175,116). c Detail D1 of the B-scan. d Waveform at position (457, 117). e Detail D2 of the B-scan. f Waveform at position (145,116).

Assuming a reasonable average index of refraction $n = 2$ [17] for the building material, the data show that the anomaly is located at about 1 cm from the surface ($\Delta x = c\Delta t / (2n)$). Closer inspection of the waveform in Fig. V.1-2d shows that the reflected signal from the anomaly in D1 is of opposite

sign than the reflection from the surface. Thus, the material related to the anomalous interface must be with a lower refractive index than the surrounding mortar [60].

ToF imaging again offers additional insight when interpreting the B-scans plots. Zooming in on the anomaly identified in Fig. V.1-2 (region D1), we clearly visualize the relevant interface, located transversely at a steep angle into the wall. Detail of its surface morphology is shown in Fig. V.1-3a. The extremely sharp and regular texture of the buried interface makes it most probable not an accidental air gap, but rather a building structure. The interface is found to be in close contact with a further interface that, given its characteristic surface texture (Fig. V.1-3b), may be attributed to a further building element.

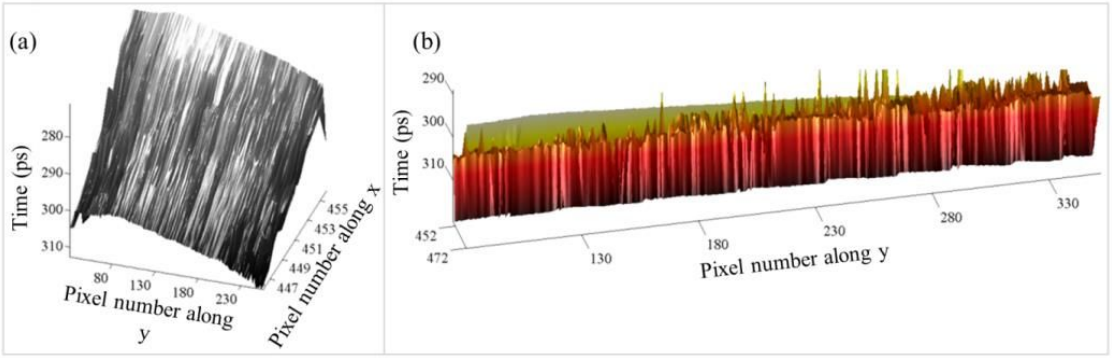

Figure V.1-3 a Detail of the ToF plot of the first buried anomalous interface found. **b** Detail of the ToF plot of the second buried interface found

The other anomaly (D2 in Fig. V.1-2a and Fig. V.1-2e) is found at about 7-8 mm depth inside the plaster. This feature is present in all the raw B-scans for *x* pixel 1-250 and *y* pixel 50-224. Due the complex and the varying shape of this hidden feature, the recorded data are best visualized in a volume rendering, as shown in Fig. V.1-4a-c. The locations of the anomaly is given by the time at which the maximum values of the temporal signals are located, where the data-set was first processed by windowing to isolate the proper regions of interest before the volume rendering. The color-map of the volume has been rescaled so that the internal feature visibility is maximized compared to the surroundings [167]. Fig. V.1-4d-g shows the location of this last anomaly found within the wall painting with respect to the surface. Here the anomaly has been colored in yellow/orange tones to allow an easy differentiation from the surface, shown in green hues.

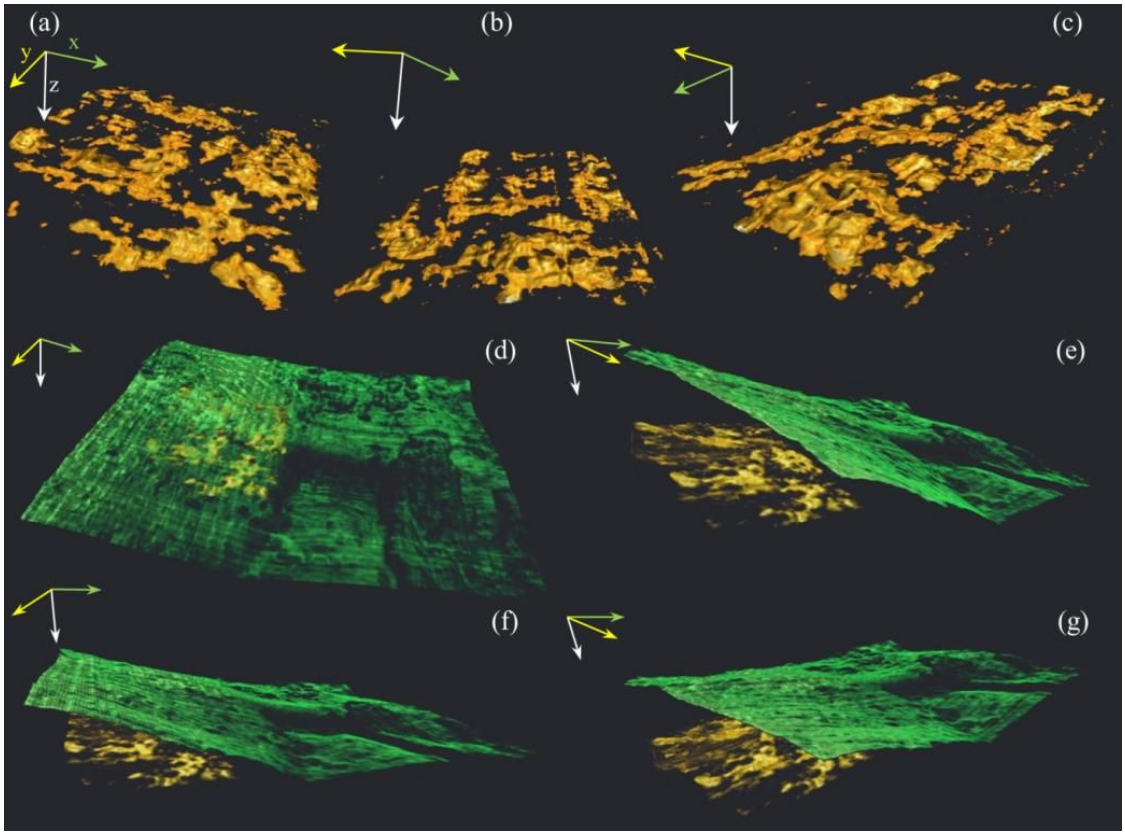

Figure V.1-4 a-c, 3D representation from different viewing angles of the in depth anomaly detected. **d-g**, 3D representations from different viewing angles of the anomaly found in relation with the location of the surface wall painting.

The exact nature of the detected anomaly is difficult to assign to a particular material. However, in contrast to the anomaly in D1, it seems that the polarity of the signal reflected from the anomaly D2 is the same as that reflected from the surface (Fig. V-2e), indicating that this anomaly has a higher refractive index than the material above it. This could indicate that the inclusion consists of a material with a higher density than the mortar [60]. An air gap or a material of low refractive index, even of sub-wavelength thickness, would lead to a reflected signal of opposite polarity compared to the surface reflection, as observed for the anomaly in region D1 of Fig. V-2a and c [60].

V.1.D Chapter conclusion

The apsidal wall painting of Nebbelunde Church (Rødby, Lolland, Denmark) has been investigated by means of non-invasive Terahertz time-domain imaging (THz-TDI). An anomalous interface characterized by high reflectivity values has been found at a depth of approximately 1 cm inside the lime-based plaster of the wall painting and imaged by B-scans and time-

of-flight plots. The identified structure appeared to be in contact with a building element of different surface morphology, which has been clearly 3D imaged. A second anomaly is found at about 7-8 mm in depth inside the mortar, as observed in the B-scans and visualized by 3D volumetric rendering. The sign of the reflected signal from the anomaly with respect to that from the surface indicates that the inclusion is a material with a higher refractive index than the surrounding mortar.

The interpretation of the building elements found in depth in plaster is rather difficult, and further scans over extended areas should be performed for certain identification of these elements. Despite this, the surface textures which characterize the structures found have been 3D imaged in detail by THz-TDI. This demonstrates how the proper THz data-set processing combined with the use of advanced 3D visual rendering make the THz-TDI technology interesting not only for identifying the presence of hidden subsurface inclusions in lime-based plaster of similar composition but also in understanding their surface texture. Given that the readability of the surface morphology of buried structures is an important step for attempting their identification, it follows that THz-TDI may provide information beneficial

Chapter VI
THz-TDI applied to lacquerware investigation

Lacquering is a traditional manufacturing used in Japan and Asia since ancient time to protect and decorate a wide variety of objects. It is recognized as one of the most representative Asian artistic techniques. Their manufacturing implies the use of a lacquer on a substructure, which can be considered the backbone of the object itself.
However, very little about lacquering technique is clarified from a scientific basis, and there is a great interest in applying new technologies to fill this gap [95], [168].

VI.1 Analysis of Asian lacquer Substructures by Terahertz Time-Domain Imaging (THz-TDI)

Three different kind of Asian lacquer-wares have been examined by THz-TDI, with the aim of contributing to the understanding of lacquers manufacturing technique, with a special focus on lacquerware substructures, and assessing strengths and limitations of this technology for lacquerware inspection. The results have been compared with those obtained by standard X-radiography. In fact, since lacquerwares are mostly composed by organic materials, such as *urushi* (lacquer), wood, carbon black, and fabrics, which are very x-ray transparent, X-ray-radiography poses some problems in achieving clear x-ray radiographic images. THz-TDI demonstrates to provide unique information on lacquerwares substructures, aiding in the comprehension of their manufacturing technology.

Interpretation of terahertz data required a deep knowledge of the lacquering technique, which will be therefore presented in details in the following paragraph.

VI.1.A The production of Asian Lacquer-wares

The world's earliest lacquerware products, according to the archaeological remains found up to now (*Kakinoshima* Site B, Hokkaido, Japan), can be traced back to 7000 year ago (Japanese *Jomon* period) [169].

Lacquerwares manufacturing involves building up layers of lacquer, which can be embedded with precious materials, or carved. In Japan, the raw material (*urushi* in Japanese), is collected as a milky sap from trees (*Rhus verniciflua*), much as rubber is tapped. The refined sap or lacquer is applied in thin coats on a substructure. A layer of lacquer hardens as the result of a complex internal chemical reaction which occurs in the presence of high humidity. It is then polished and another layer is applied. An object may have only a few or more than a hundred layers, progressing to a very refined final lacquer surface. Plant fibers are often found in the individual layers, especially when *urushi* was not filtered [168].

Different grades of lacquer are appropriate for specific tasks. The sap that has fermented is called *ki urushi* (raw *urushi*). It is used in *mugi-urushi* and *nori-urushi*, or in making *urushi shitaji* (*urushi* foundation). After collection, the sap is stirred, heated and filtered. Stirring *ki urishi* to reduce the moisture inside from 10 to 20% produces *suki urushi* (translucent *urushi*) for coating. Adding iron hydroxide to suki *urushi* and filtering it produces *kuro urushi* (black *urushi*), while *Iro urushi* (colored *urushi*) is made by adding pigments. Cinnabar and iron oxide were used to make red and black lacquers, orpiment for yellow lacquer. Until the development of synthetic colors, white, blue and green were not used, as these natural pigments are unstable in lacquer. Oils and other ingredients are added as dictated by various recipes. Different techniques can then be used to create the ornamental parts of a lacquer-ware.

VI.1.B Substructure of Asian Lacquers

To create a lacquer-ware, the liquid lacquer must be brushed onto a substructure which determines the shape of the object. Even if to a large extent, the life of the lacquerware depends on the substructure's stability, there is very little published about these substructures, how they are manufactured, and what materials are used. Reports on lacquer substructures in English have been written by B. Milam and H. Gillette [170] and by Hiroshi K. [171] and they will be summarized here.

There are many core materials used for the substructure: wood (*Kiji)*, bamboo (*Rantai)*, cane, leather (*Shippi, nurikawa* or *urushi kawa*; in Japan, mostly deer or cow leathers were used), cloth (*Kanshitsu*), paper, shell, ceramic (*Totai*), glass (*Ruritai*), horn, fish skin, metal (*Kintai*) or any lightweight material.

The most popular substrate is *kiji* (wood) and can be made in several ways. *Sashimo* is made by assembling wood boards; it is used to make object such as chests, shelves, trays and multi-tiered *urushi* boxes. *Hikimono* is made by shape-forming a block of wood on a turning wheel. It is used to make objects composed of concentric circles such as bowls, urns and kettles. *Magemono* is made by immersing thin boards of coniferous tree in water or hot water to make them flexible so that they may be bent. It is used to make thin and light object such as lunch box, trays and food containers.

Many variations on *Kiji* techniques can be found, such a single piece of wood forming the central section with added handles, feet, sides, and/or foot ring. The substructure of the central base can also be fabricated from different types of wood sections mechanically joined by dowels, cleats, split bamboo canes, fabric saturated with *urushi*, and/or with *urushi* used as an adhesive. Reinforcements such as wood dowels, cleats, and split bamboo canes were used for joining and strengthening the wood substructure of the base in *urushi* pieces. Various metal strips, sheets, fabrics or wires were used to reinforce the rim, foot, or edges of *urushi*.

Score lines found on the base appear to be associated with the wood substructure. There is no visible evidence of these lines on the *urushi* surface. Woodworkers score wood either to align sections during gluing or to position a pattern for tracing a design. However, many score lines are found to be totally out of alignment or following no visible pattern surface, so that their purpose is not known with certain. The centering point was made by a sharp instrument or resulted from turning the bowl on a lathe.

Sabi (*urushi* mixed with pulverized ceramic, clay, or rice flour), was often used as a filling material of seams or holes in the wood substructure, including score lines and centering point. Grooves can also be carved and filled with *kokuso* (sawdust and hemp fibers, *urushi* and flour mixture).

Fabric was often used to hold the wood sections together or to reinforce the rim and the foot ring, to give tooth or texture to the subsequent *urushi* layers and as a substructure in the *dry lacquer technique (kanshitsu)*.

Kanshitsu is a technique whose origin is in China during the Han dynasty. From the Asuka to the Nara period in Japan, coffins of aristocrats

were commonly made by *kanshitsu* technique. Historically, the technique developed in two ways. First, fabric saturated with lacquer is molded or modelled over a wood or clay core. Once the latter is removed, the resulting sculpture is hollow, with perhaps a wood frame or armature added for strength [172]. Later, layers of hemp cloths were applied over a wooden substrate to make *mokushin kanshitsu*. In Nara period, *kanshitsu* was widely used as the newest technique imported from China in making Buddha statues. Coiled or bent wood/bamboo laminated or tied together strips can be used to form the flared sides of Oriental lacquerware, as well as basket weave of reeds, grasses, or bamboo, sometimes forming the entire substructure of an object, as described below.

Rantai consists of winding a thin strip of bamboo or coniferous tree around a core. It is a technique originally used during Han dynasty in China and still a very popular in many part of Asia. In Japan it is manufactured in Hita (Oita prefecture) and Takamatsu (Kagawa prefecture). There are two kind of *rantai*: *amiage* and *makiage* (or *kentai*). *Amiage* substrate is made by weaving thin, split bamboo to form a basket-like shape. In more elaborated case, a wooden mold is made first and a bamboo is woven around it. Then the object is further decorated by using a special weaving technique. *Kentai* is made by using thin pieces of bamboo on whose ends triangular incisions are made. These incisions are assembled to make a loop. Then another piece of bamboo is wound along the inside of the first loop. This is repeated, resulting in an object with gradually decreasing diameter. In Aomori (Aomori prefecture), a thin strip of Japanese beech is used to make *makiage* known as *bunako* urushiware. Wire was often used to tie together the coiled wood strips and bundles of reed, grass, or bamboo in basket weave pieces.

The substructure may be primed with ground layers, until it is smooth and without any flaws which would disrupt the lacquer coating. Ground can also be mixed with coarse minerals (mostly with black additives).

Japanese traditional lacquering techniques include the *shitaigatame* process, which consists of two sub-processes, *nunokise* and *jigatame*. *Nunokise* is a process for protecting the substrate and serves as a *komai* (base) for the subsequent process. Cloth is attached to the substrate with *nori-urushi*, a mixture of rice paste and raw *urushi*. Today, hemp, silk, and cotton cloths are used for *nunokise* but it is said that in the old days hemp cloth was mainly used for this purpose. In the case of dry lacquer (*kanshitsu*), *nori-urushi* is made by mixing flour into raw *urushi*, producing what is called *mugi urushi*. *Jigatame* serves to protect and thermally insulate

wooden substrates. Typical *jinoko* (fired, ground, and screened clays) used for *jigatame* include *Wajima-jinoko* and *Yamashina-jinoko*, named for the places of origin of the clay. These two kinds of *jinoko* are usually mixed with rice paste, and the term *kiriko* means the mixture of *ji* and *sabi*.

VI.1.C X-ray radiography and THz-TDI for imaging analysis of Asian Lacquers substructures

X-radiography is used as standard technique to image the internal structure of Oriental lacquer-wares.

The dark areas in the radiograph are formed by x-ray transparent materials, such as the *urushi* itself. The lighter areas in the radiograph are formed by the more x-ray opaque materials. These last can be centering points, grouting, and worm holes, where the opacity is caused by a build-up of fill material (*sabi*). In fact, because of the pulverized ceramic contained in the *sabi*, it is more x-ray opaque than wood or textile. Occasionally these features appear dark in the radiograph. This could be due to the type of *sabi* material used or even to the lack of a *sabi* layer.

Furthermore radiographs reveal areas of additions, alterations and repairs as they generally have different densities due to the different resins and/or pigments used in these restorations. Also, they will sometimes reveal inscriptions or design motifs that are covered by later layers of *urushi*, if x-ray opaque pigments were used in these motifs. Metal reinforcements, being among the most x-ray opaque materials being, can also be distinguished in an x-ray radiograph, appearing light areas in the radiographic image. Most red *urushi* and some multicolored *urushi* have very x-ray opaque pigments incorporated in the *urushi*. These pigments include litharge (lead oxide), orpiment (yellow arsenous sulfide), realgar (orange arsenic sulfide), ochers (iron compounds), and vermilion (mercuric sulfide) [170].

According to literature [170], X-ray-radiography poses some unique problems in achieving sharp, high contrast x-ray radiographic images. Organic materials commonly used in Oriental lacquerware, such as *urushi* itself, wood, carbon black, and fabrics are very x-ray transparent.

Differently, THz-TDI already showed its potentiality in analyzing such kind of organic materials. Due to textiles and wood characteristic response at THz wavelengths, THz-TD spectroscopy has already been introduced into the differentiation of these materials [93], [108], [109], [173]–[177].

X-ray radiography it is of course advantageous in mapping the distribution of opaque pigments (i.e. strongly absorbing x-rays incorporated in the *urushi* but, for the same reason, the graining of the wooden base is very difficult to identify with this technique, while its strong interaction with THz waves let it be easily detected and imaged. On the other hand, organic and low-atomic number pigments (such as many carbon-based black pigments), while transparent in the X-radiograph, show high reflectivity in THz range.

Lastly, reading of the radiograph can be complicated by the fact that light or opaque areas can sometimes be the result of overlapping or differing thicknesses of components within the object. Oriental lacquerwares can be three or more colored layers of *urushi* carved to varying depths. Since each of these areas would require different energy levels or the use of filters to achieve detail in all areas, only multiple x-ray radiographs or multiple x-ray exposures on a single film sheet can give satisfactory results [170]. Differently, THz-TD imaging in reflection geometry, using pulses of radiation, is consistent with depth resolution, having the ability to image single buried interfaces with a single measure.

VI.1.D The investigated lacquer-wares

Three different kinds of lacquer-wares have been examined.

Lacquer-ware n.1 (Fig. VI.1-1) is a contemporary shallow bowl with the annexed cover, original from Myanmar. The interior is divided in three parts by partition walls (Fig. 1a), and the base consists in a foot ring (Fig. 1c). A knob is positioned in the center of the cover. The visible parts are decorated with anthropomorphic and abstract motives painted with modern colors.

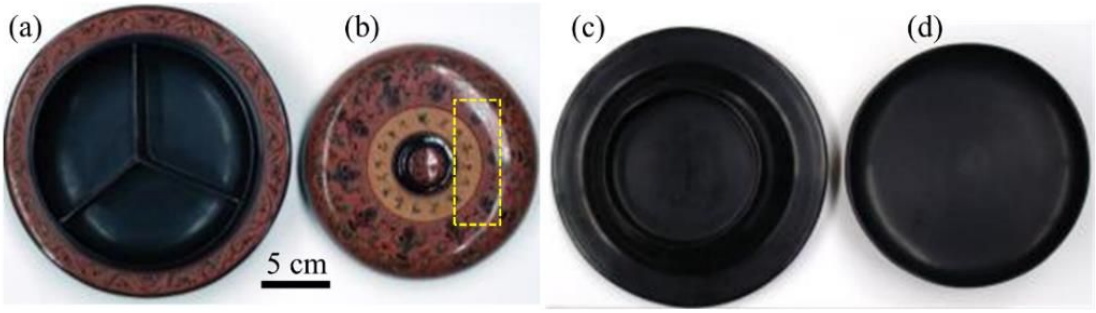

Figure VI.1-1 Lacquerware n.1, **a** front of the shallow bowl. **b** Lacquer-ware n.1, front of the cover. The dashed yellow rectangular localized the THz scanned area. **c** Lacquer-ware n.1, back of the shallow bowl. **d** Lacquer-ware n.2, back of the cover.

Lacquer-ware n.2 is a rectangular tray (Fig. VI.I-2) for food use, supported by four feets.

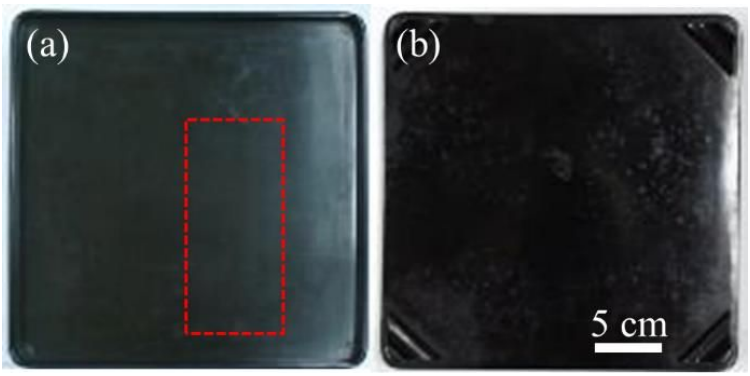

Figure VI.1-2
Lacquer-ware n. 2,
a front. The dashed red rectangular localized the THz scanned area.
b Lacquer-ware n. 2, back.

The tray is lacquered with green pigmented *urushi* on the front (Fig. VI.I-2a) and black pigmented *urushi* on the bottom (Fig. VI.I-2b). A single piece of wood (about 5,2 mm in thickness) has been used for the base. The lacquer has been applied on a ground layer and their combined thickness is about 1,2 mm, where the lacquer coat thickness is less than 0,05 mm.

Lacquer-ware n.3 (Fig. VI.I-3 a-d) consists in a pair of bowls (bowls a and bowls b), with foot rings at the bases. Differently than bowl b (VI.I-3b, 3d), the rim of bowl a (VI.I-3a, 3c) foot ring is gilded. They are decorated with *makie*[5] technique on the external sides with floral and zoomorphic motifs of oriental trees, tortoises and exotic birds on a black background.

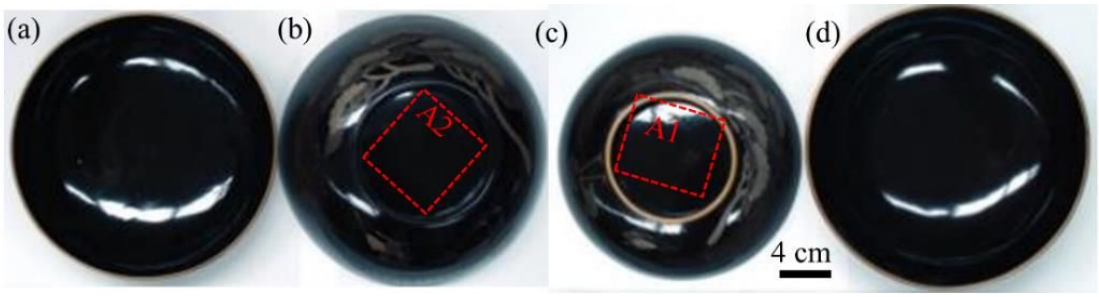

Figure VI.1-3 Lacquer-ware n.3. **a** Interior of the shallow bowl a. **b** Exterior of the shallow bowl b. The dashed red rectangular localized the THz scanned area named A2. **c** Exterior of the shallow bowl a. The dashed red rectangular localized the THz scanned area named A1. **d** Interior of the shallow bowl b.

[5] Japanese *Makie* consists in drawing patterns (*nurihada*) with *urushi* lacquer on the surface and, before the *urushi* dries, sprinkling gold or silver powder over it.

VI.1.E Analytical instrumentations

THz-TDI

THz-TDI has been performed with a Picometrix T-Ray 4000 device. The scanned areas (localized on the objects by dashed rectangles in Fig. VI.1-1b, VI.1-2a, VI.1-3b, VI.1-3c) have been scanned using a 320 picosecond (ps) measurement window, a time increment of 0.078 ps (sampling frequency 0.003 THz). We set the scan-velocity at 5 pixel/s, pixel size 0,5 mm and a reflection configuration at normal incidence. Impulse response functions have been extracted from waveforms recorded on lacquer-ware n.1 and lacquerware n. 2 by means of deconvolution function, while the uneven surface of the lacquer-ware n.3 leads the application of this method impractical for an acceptable S/N ratio.

X-radiography

Lacquer-ware n.1 and Lacquer-ware n.3 have been imaged by standard X-radiography, where the exposure parameters for lacquer-ware n. 3 are FR film, 30 kV, 180 s, 2mA, while for lacquer-wares n.1 are FR film, 35 kV, 2mA, 120 s.

VI.1.F Results and discussion

Fig. VI.1-4a shows the peak-to-peak THz image of the scanned area of lacquer-ware n.1. Concentric circular strips of higher reflectivity within the THz range can be detected.

B-scans (Fig. VI.1-4b) revealed the hidden structure of the cover, where the air/lacquer, the lacquer/ground and the ground/substructure interfaces are detected. An additional minor interface is found inside the ground layer. This can be either interpreted as the use of two different materilas or the application of two main layers of the same material for the ground manufacturing, where in the last case the separation among them is remarcable.

The profile of the substructure is not flat, but it raises at the borders of the cover, probably to reinforce and give shape to the flared sides.

Fig. VI.1-4c show the appearance of the lacquer/ground interface, where grains inclusions are imaged. This morphology suggests the use of the traditional grounting material, a mixture of *jinoko* (clay) and sawdust.

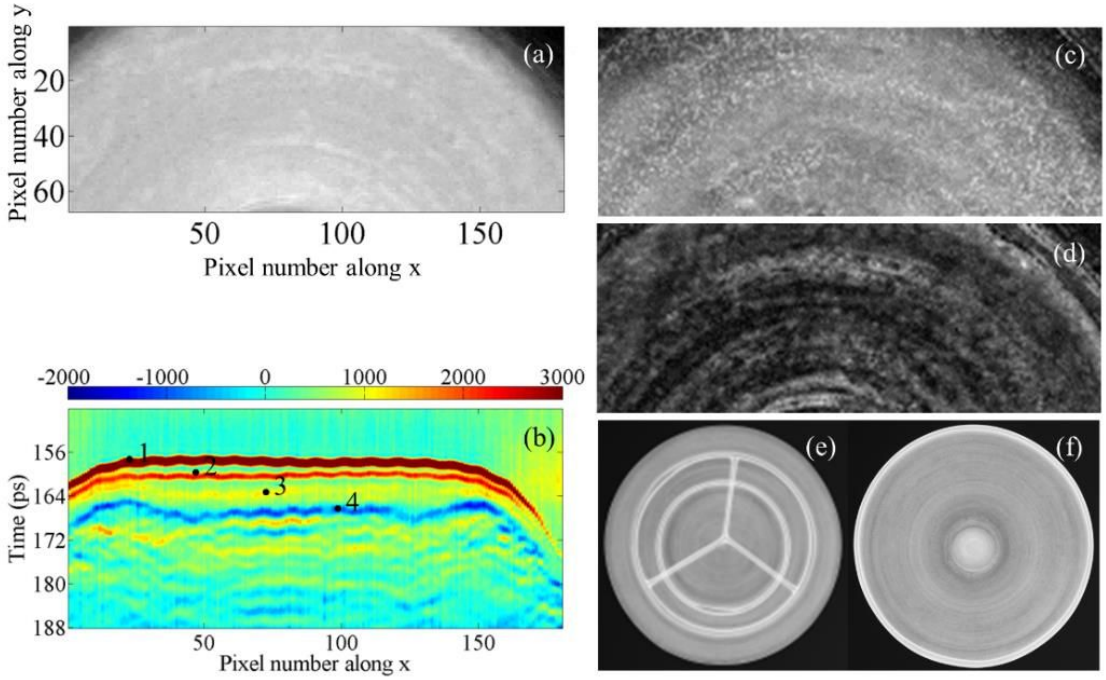

Figure VI.1-4 a Peak-to-peak image of the scanned area of the lacquer-ware n.1. The dashed red line localizes the scan-line used to image the B-SCAN of Fig. VI.1-3b. **b** Raw BSCAN plotted by using the value of the electric field recorded along the pixel of the horizontal axis, for y fixed at 13. Black dots indicate the interfaces found: the air/lacquer interface (1), the lacquer/ground interface (2), interface within the ground layer (3), the ground/substructure interface (4). **c** THz image of the lacquer/ground interface. **d** THz image of the filler/ground interface. **e** X-radiograph of the bottom of lacquer-ware n.1. **f** X-radiograph of the cover of lacquer-ware n.1.

The appearance of the substructure is better understood by imaging the interface found within the ground layer, as shown in Fig. VI.1-4d. The concentric shape of the looped strips reveals the use of *Kentai* technique. The looped strips are detected by the X-radiograph of the lacquerware (Fig.VI.1-4e-f). Fig. VI.1-5a shows the peak-to-peak THz image of the scanned area of lacquerware n.2.

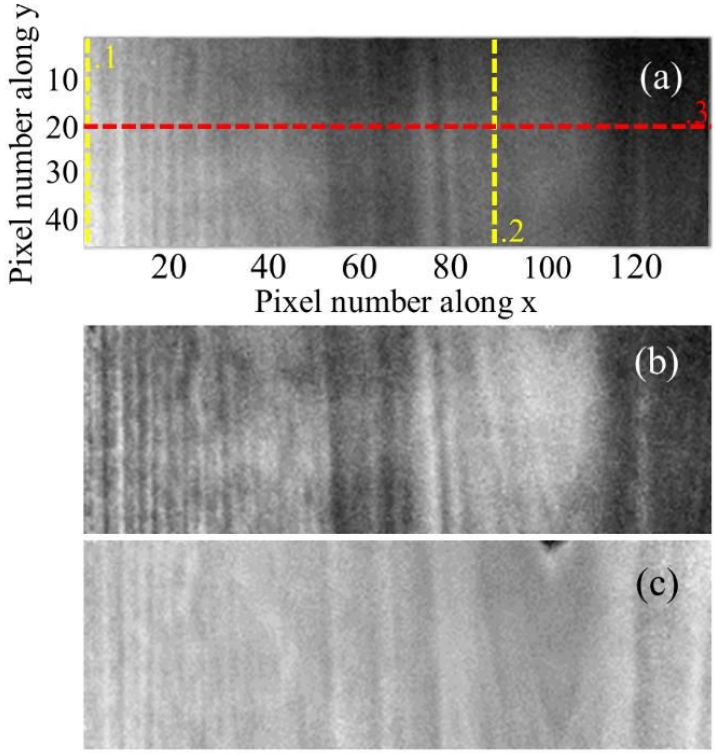

Figure VI.1-5 Scanned area of the lacquer-ware n.3.
a Peak-to-peak THz image. Dashed lines (named 1, 2 and 3) localize the scan-lines used to realize the B-scans of Fig. V.I-4a, 4b and 4c respectively.
b THz image plotted by integrating the spectral amplitude of the signal at 5 ps after the global maximum.
c THz image plotted by integrating the spectral amplitude of the signal at 8 ps after the global maximum.

The grain of the wood is clearly visible (*Kiji* technique). The almost parallel trend of the annual rings allows deducing that the lacquerware substructure has been realized by a single piece of wood, where a cut has made longitudinally close but outside of the center of the trunk (flamed tangential plain sawn). Optically nice, so cut wooden boards usually tend to considerable swelling and shrinkage.

Furthermore, it is possible to distinguish between the heart wood, where no annual rings are detected, from the sap wood, where the annual rings appear and become more frequents from the hard wood to the exterior. Plotting the integral of the THz signal amplitude for increasing time delay allow to visualize subsurface aspect of the wood board, localizing the areas closer to the wood pith, where the rings become visible in the shape of a parabola (Fig. VI.1-5b-c). B-scans plots show both the lacquer coat and the ground applied on the wood; specifically, the air/lacquer, lacquer/ground and ground/wood interfaces are imaged, named I1, I2 and I3 respectively in the column B-scan of Figure VI.1-6.

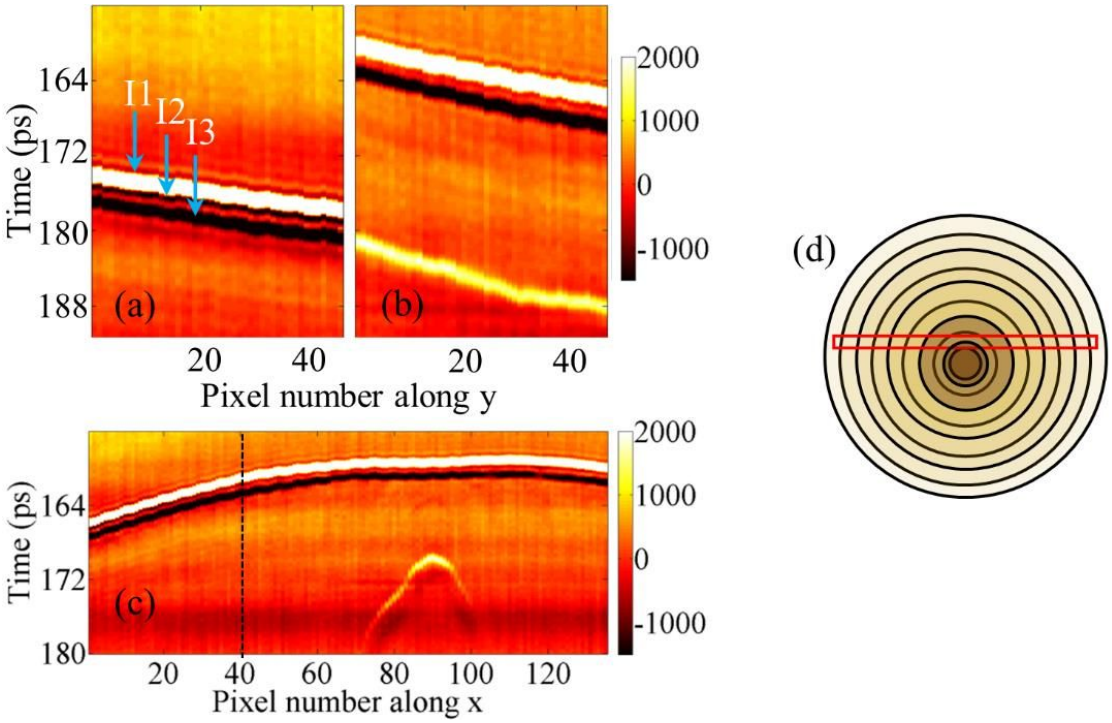

Figure VI.1-6 B-SCAN recorded along x =1; **a** I1, I2, I3 are the air/lacquer, lacquer/ground, ground/wood interfaces. **b** B-SCAN recorded along x =87. **c** B-SCAN recorded along y = 20; the lacquer/ground interface is only visible on the left of the dashed black line. **d** Scheme of the plain sawn of the lacquer-ware substructure. Transversal section of a trunk and approximate localization of the plain sawn of the board.

Due to the variability of the lacquer coat thickness, the lacquer/ground interface is not detected on the whole scanned area (Fig. VI.1-6b): the thinner parts of the layer are clearly at the frontier of the depth resolution limit of the THz-TD device for this material.

An additional interface at about 180 ps in depth has been detected in the column B-scans (representing the tangential sections of the scanned area of the board) within 80-100 pixel numbers along the x-axis (Fig. VI.1-6b). This feature is better identified by looking at the raw B-scans (transverse sections of the scanned area of the board, Fig. VI.1-6c), which show how this interface is related to the profile of the wood core, as shown in the scheme of Fig. VI.1-6d. Raw B-scan also revealed that the board is convex, where the maximum height is in proximity of the hard wood location. The fact that the lacquer/ground interface is only detectable on the sloping areas of the base leads to assume that the board shrinkage occurred prior of the lacquer application: the lacquer, applied liquid, accumulated at the slopes minima.

Fig. VI.1-7 shows the X-radiograph of lacquer-ware n.3.

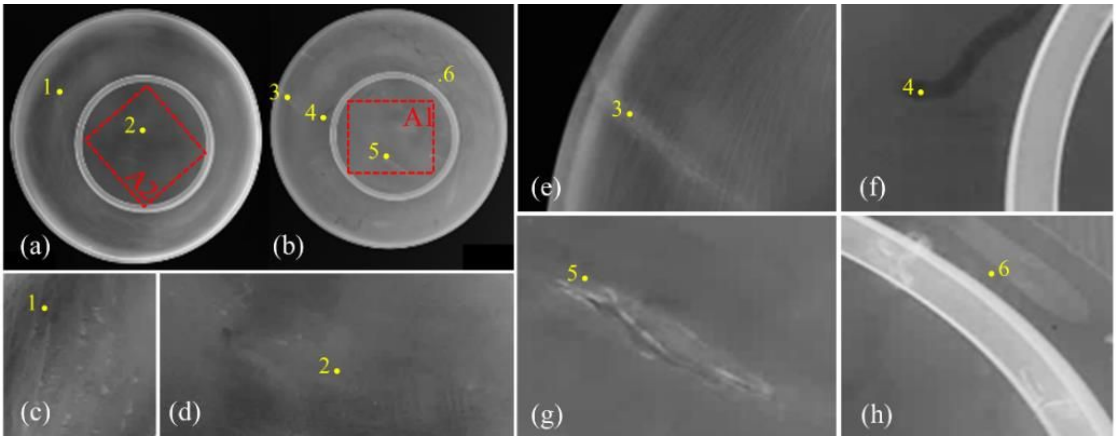

Figure VI.1-7 a X-radiograph of the shallow bowl b. The red dashed square localized the THz-scanned area named A2. **b** X-radiograph of the shallow bowl a. The red dashed square localized the THz-scanned area named A1. The numbered point in yellow localized the areas detailed in the following images. **c** Detail n.1 of the shallow bowl b. **d** Detail n.2 of the shallow bowl b. **e** Detail n.3 of the shallow bowl a. **f** Detail n.4 of the shallow bowl a. **g** Detail n.5 of the shallow bowl a. **h** Detail n.6 of the shallow bowl a.

The substructure is not clearly imaged, apart from the annual rings on the flared sides (Fig. VI.1-7c). Details of the base (Fig. VI.1-7d) show a complex structure difficult to interpret. Radiopaque features are connected to the presence of repairs (Fig. VI.1-7e, g,-h), while wood-boring beetle emergence holes and galleries appear X-ray transparent (Fig. VI.1-7f). The rims of the foods of the shallow bowls appear very radiopaque, leading to assume the use of metal rings as reinforcement.

Peak-to-peak THz image of the scanned area of the foot of the bowl a underscores the complexity of the structure behind the surface coat (Fig. VI.1-8a). Multiple interfaces are detected looking at the column and raw B-scans (Fig. VI.1-8b and c respectively).The grain of the wood is clearly visible at the bottom of the B-scans. The parts of the wood closer to the surface show different dielectric proprieties compared to that of the wood in depth, where the interface between these two dielectric behaviors of the wood appears clearly marked. The reason of this is not clear, but it is compatible with an impregnation of the wood by applying a coating layer.

On the top of the wood, several thin discontinuous, rippled and overlapping interfaces are found in B-scans. The terahertz image obtained by plotting the value of the integral of the recorded signals about 3 ps after the signal global maxima (Fig. VI.1-8d) shows how these interfaces appear as overlapping pieces of a light, thin and semi-rigid material resembling paper, even if other similar materials, including fabrics, cannot be excluded.

Moreover it looks like additional sheets have been added in correspondence of wood grooves (see Fig. VI.1-8b-c), to even out the surface.

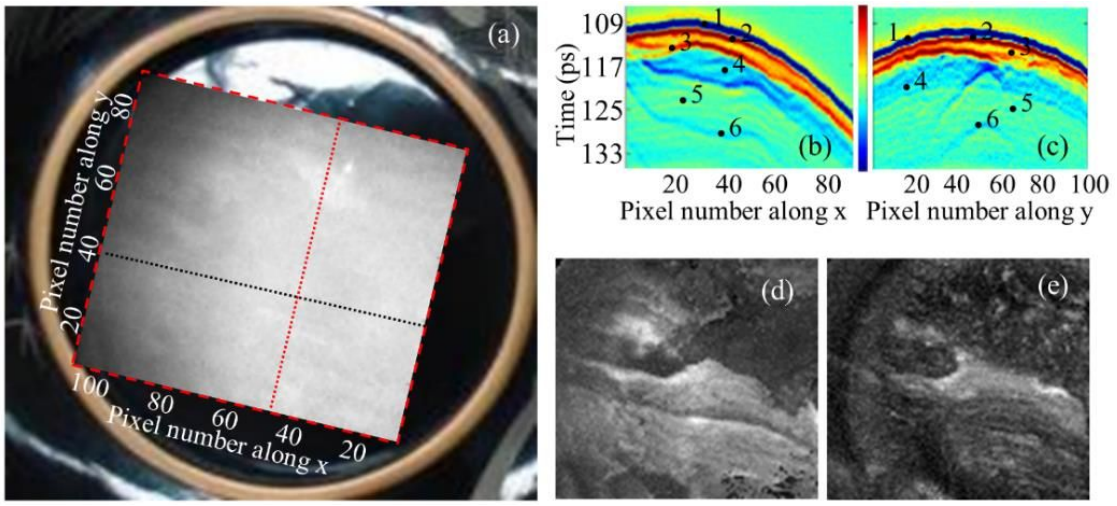

Figure VI.1-8 a Peak-to-peak THz image of the scanned area of the foot of the bowl a. The dashed lines inside the image indicate the scanlines used to realize the raw B-SCAN of Fig. VI.1-6b (black), and the column B-SCAN of Fig. VI.1-6c (red). **b** Raw B-SCAN realized by using the values of the Electric field recorded at every pixel of the x-axis, for y fixed at 42. Black dots indicate the air/lacquer interface (1), the lacquer/ground interface (2), the ground/patches interface, in correspondence of an overlapping point (3), layer of impregnated wood (4), wood (5), interface between different wood densities, in correspondence of the wood grain (6). **c** Column B-SCAN realized by using the values of the Electric field recorded at every pixel of the x-axis, for y fixed at 46. Black dots indicate the air/lacquer interface (1), the lacquer/ground interface (2), the ground/patches interface, in correspondence of an overlapping point (3), layer of impregnated wood (4), wood (5), interface between different wood densities, in correspondence of the wood grain (6). **d** THz map of the value of the recorded signals about 3 ps after the signal maxima. **e** THz map of the value of the recorded signals about 7 ps after the signal maxima.

Both the ground layer and the lacquer layer are visible in the B-scans (Fig. VI.1-8b-c), immediately after the air/lacquer interface. Plotting the value of the recorded signals about 7 ps after the signal maxima (Fig. VI.1-8e) allows to visualize the wood grain seen as a parabolic feature in the wood structure imaged in the B-scans. Additionally, on the left of the same figure (Fig. VI.1-8e), a circular score line used to trace the border of the foot of the bowl is found.

Fig. VI.1-9a shows the peak-to-peak image of the area scanned on the foot of the bowl b.

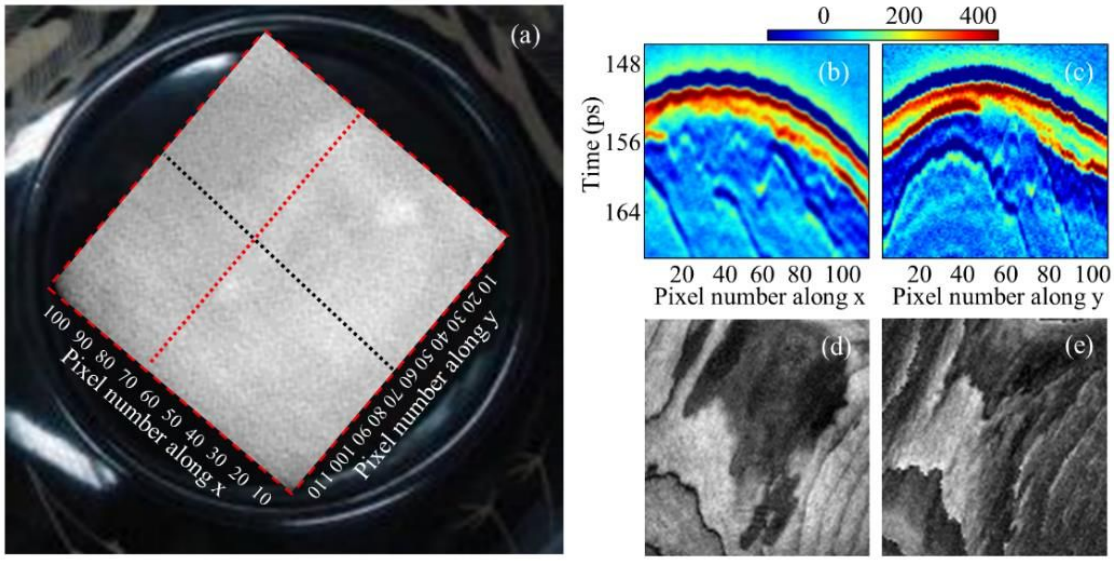

Figure VI.1-9 a Peak-to-peak THz image of the scanned area of the foot of the bowl b. The dashed lines inside the image indicate the scanlines used to realize the raw B-SCAN of Fig. VI.I-8b (red), and the column B-SCAN of Fig. VI.1-7c (red). **b** Raw B-SCAN realized by using the values of the electric field recorded at every pixel of the x-axis, for y fixed at 42. Black dots indicate the air/lacquer interface (1), the lacquer/ground interface (2), the ground/patches interface, in correspondence of an overlapping point (3), layer of impregnated wood (4), wood (5), interface between different wood densities, in correspondence of the wood grain (6). **c** Column B-SCAN realized by using the values of the Electric field recorded at every pixel of the x-axis, for y fixed at 46. Black dots indicate the air/lacquer interface (1), the lacquer/ground interface (2), the ground/patches interface, in correspondence of an overlapping point (3), layer of impregnated wood (4), wood (5), interface between different wood densities, in correspondence of the wood grain (6). **d** THz map of the value of the recorded signals about 3 ps after the signal maxima. **e** THz map of the value of the recorded signals about 7 ps after the signal maxima.

B-scans (Fig. VI.1-9b-c) reveal a sequence of interfaces similar to that observed on bowl a, where, even in this case, the interfaces of the unknown patched material do not always adhere to the wood behind. The appearance of these interfaces is seen as dark areas in the center of Fig. VI.1-9d (THz integral map of the value of the recorded signals about 3 ps after the signal maxima), where the wood grain texture can also be observed. This last it´s fully imaged in Fig. VI.1-9e (THz integral map of the value of the recorded signals about 7 ps after the signal global maxima).

Combining the information obtained from the X-radiographs with those obtained by THz, it can be advance the hypothesis that the bowls are made by *Hikimono* technique.

VI.1.G Final considerations

For the first time, Asian lacquer-wares have been examined by THz-TDI. The results have been compared with those obtained by standard X-radiography, allowing to assess the potentiality of this technique for the comprehension of lacquer-wares manufacturing.

The cover of lacquer-ware n.1 resulted manufactured by lacquering a substructure made by *Kentai* technique, and the thin looped wooden strips have been imaged by THz-TDI. The substructure is found to rise at the borders of the to cover to reinforce and shape its flared sides. The THz image of the ground shows the presence of grain inclusions in the material, leading to assume that use of the traditional Asian grounting material (mixture of *jinoko* and sawdust). The lacquer coat is found to be very thick.

Lacquer-ware n.2 resulted built on a single board of *Kiji,* where the grain of the wood is clearly visible in the THz images, allowing to understand the provenance of the board respect to the trunk (flamed tangential plain sawn just above the pith of the wood). Both the lacquer coat (thickness ~0,05 mm) and the ground applied on the wood have been identified by realizing non-invasive cross-sections (B-scans), while the whole board itself appears convex. THz-TDI allowed to assess that the board shrinkage occurred prior of the lacquer application: the lacquer coat is detectable in the B-scans only on the sloped sides of the board, where it amassed for gravity after the application. This leads to assume that deformation process are currently not occurring.

The feets of the pair of bowls composing the lacquer-ware n.3 resulted of high complexity structure. The grain of the wood is clearly visible in the THz images, while it hasn´t been detected by X-radiography, which, on the other hand, has detected the wood grain on the sides of the bowls. By combining X-radiography and THz-TDI information the substructure used for manufacturing (*Hikimono)* has been identified. Several thin, discontinuous, rippled and overlapping interfaces, undetected by X-radiography, are found in THz B-scans just above the wood layer, as if sheets have been superimposed especially in correspondence of wood grooves to even out the surface. This artifice could be either original or related to later repairs. While indistinguishable in X-radiographs, a circular score line used to trace the border of the foot of the bowl has been detected by THz-TDI.

The study showed the capability of THz-TDI in imaging hidden lacquerwares substructures and features, overpassing the limit of standard X-radiography in imaging organic and low atomic number materials.

VI.2 Characterization of European Lacquers by Terahertz (THz) Reflectometric Imaging

Deeply appreciated by Western countries, Asian lacquerwares had a large influence on the world's arts and crafts. Starting from the sixteenth, they have been imported, collected and, finally, imitated in Europe. Techniques of production and materials used vary a lot depending on lacquered objects historical and geographical context. Being composite objects, the preservation of lacquerwares is particularly complex [178].

In this study a European lacquerware replica has been investigated by terahertz (THz) reflectometric imaging. The inspected lacquerware is a wooden panel covered by multiple complex layers of lacquers and plaster. Utilizing pulsed Terahertz Time-Domain Imaging (THz-TDI) in reflection mode, we observe non-invasively buried layers of the lacquerware replica, including the internal structure of the wooden panel itself. We find that non-invasive terahertz reflectometric imaging analysis of lacquerware can provide conservators with important information about the condition of the compositional layers, potentially aiding in the development of appropriate conservation treatments. With the same technique we have performed a surface material mapping. The material distribution has been enhanced through reflected THz composite RGB false color rendering, where RGB mapping allows distinction between different materials and textures on the surface of the lacquerware. The contrast between different textures is enabled by wavelength-dependent scattering from the surface, as well as differences in the composition of the surface layer.

The original article can be accessed at [95].

VI.2.A Analytical Instrumentation and Methodologies

The laquerware replica has been scanned in 0.5 mm steps, using a 320 ps measurement window, a time increment of 0.078 ps (4096 data points in each time trace) and a reflection configuration at normal incidence.

VI.2.B The Lacquerware Replica

The investigated European lacquerware (Fig. VI.2-1a) belongs to The Royal Danish Academy of Fine Arts (School of Architecture, Design and Conservation - Copenhagen, Denmark).

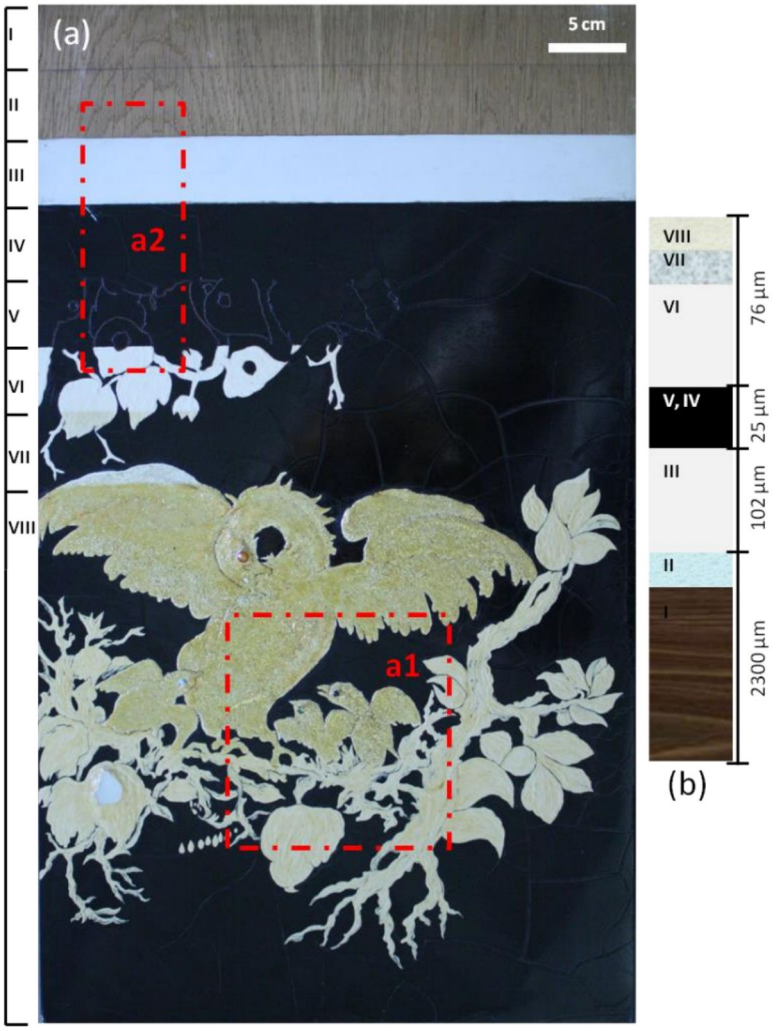

Figure VI.2-1
a Visible-light photograph of the European lacquerware replica; the red lines outline the scanned areas (a1, a2).
b Schematic stratigraphy of the lacquerware, with the indications of the average thicknesses measured.

The replica is a decorative piece made of a wood panel covered with several layers of plaster and lacquers to depict floral and zoomorphic motifs. The wooden panel (layer I) is covered by a thin layer of lacquer (layer II) and a second layer of plaster (layer III) on which it has been applied a thick glossy black lacquer (layer IV). Engravings have been made on this surface and then marked out with Dragon's Blood (layer V) to trace the drawing of the figurative bas-reliefs realized with plaster (layer VI) inlaid with mother of pearl and beads. A lacquer layer coats the reliefs (VII), to hold silver-like glitters, which are then sealed under a layer of yellow colored lacquer (VIII), an imitation of gold.

VI.2.C Results and discussion

Plan-type Terahertz Reflection Images: C-scans

The value of the electric field measured for each spatial coordinate (x, y) of the scanned areas has been used for the bi-dimensional visualization of the lacquerware. A Matlab routine was coded to generate both frequency and time domain parametric terahertz images, shown in Fig. VI.2-2 for the scanned area a1 of Fig. VI.2-1a.

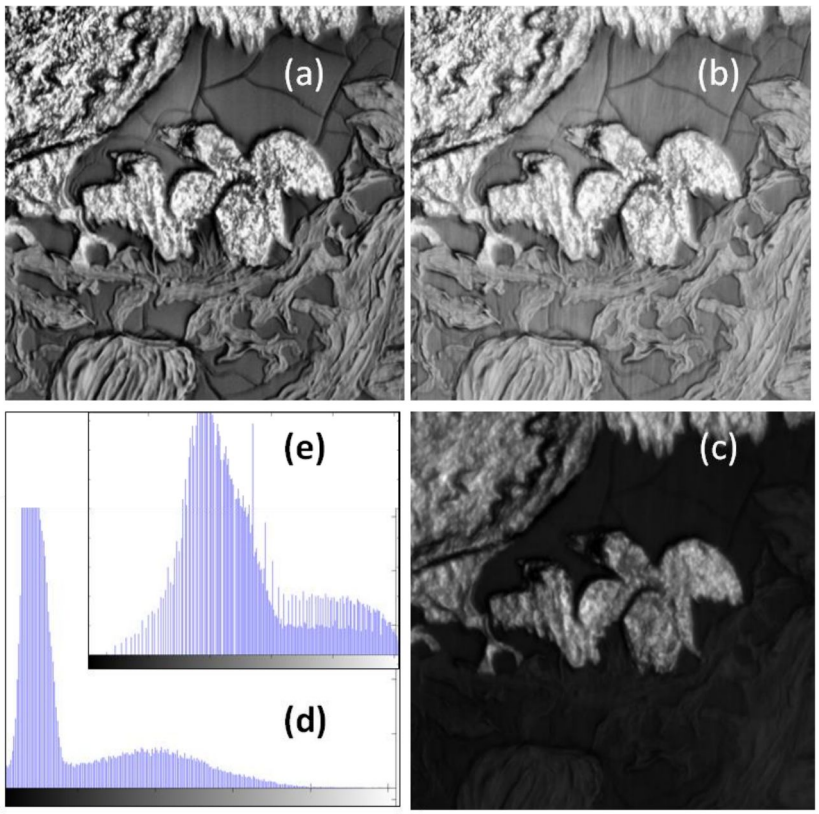

Figure VI.2-2 **a** THz time image (maximum of temporal amplitude) after logarithmic transformation (log), contrast-limited adaptive histogram equalization (CLAHE) and gamma correction (γ). **b** THz frequency image (integral of the spectral amplitude over the whole frequency range) after log transformation, CLAHE and γ correction. The location of the scanned area is indicated in Fig. VI.2-1a. **c** THz time image (maximum of temporal amplitude) before log transformation, CLAHE and γcorrection. **d** Histogram of Fig. VI.2-2c. **e** Histogram of VI.2-2b.

Using the parameter maximum of temporal amplitude (Fig. VI.2-2a), the information displayed arise predominantly from the first interface (air/ surface), so that the grain of the wood behind the surface are not as visible as using the parameter spectral amplitude integrated over the whole frequency range (Fig. VI.2-2b).

Contrast and detail enhancement has been obtained through histogram modifications (Fig. VI.2-d-e), realized applying well developed image processing techniques such as logarithmic transformation, contrast-limited adaptive histogram equalization or gamma correction

The terahertz reflection images in Fig. VI.2 are displayed by assigning a single intensity value for each pixel, resulting in different shades of gray from black to white proportional to the value of the parameter used (grayscale or intensity images). Another displaying method used in terahertz imaging application is pseudo-coloring (some time referred as false-color). It consists in assigning arbitrary colors to the gray levels of an intensity image through a pseudo-color scale (or color-map), where high pixel values are assigned to one color (for example, red), and low pixel values are assigned to another color (for example, blue), with other colors assigned to intermediate values (pseudo-color mapping) [179].

All the terahertz reflection images show a good terahertz optical contrast among the materials (black lacquer of the background, plaster of the floral reliefs, plaster covered by lacquer and glitters of the animal reliefs). To improve this contrast, we have utilized composite RGB false color rendering to create reflected THz composite images. Two of them are shown in Fig. VI.2-3.

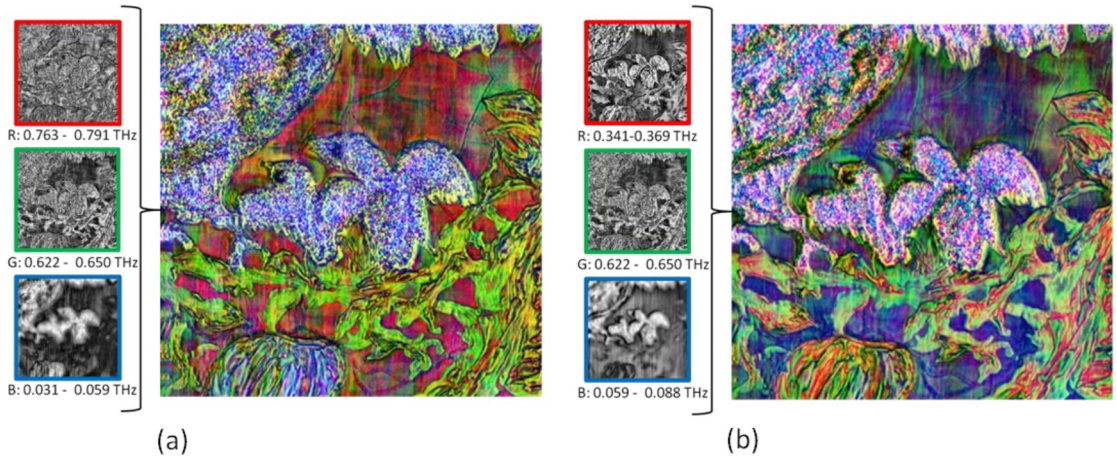

Figure VI.2-3 a Terahertz reflection composite image obtained inserting the spectral amplitude integrated over the 0,0763 – 0,791 THz range image in the red channel, the spectral amplitude integrated over the 0,622 – 0,650 THz range image in the green channel and the spectral amplitude integrated over the 0,0031 – 0,059 THz range image in the blue channel. **b** Terahertz reflection composite image obtained inserting the spectral amplitude integrated over the 0,341 -0,369 THz range image in the red channel, the spectral amplitude integrated over the 0,622 – 0,650 THz range image in the green channel and the spectral amplitude integrated over the 0,059-0,088 THz range image in the blue channel.

The 0.031 - 0.819 THz spectral window (9.67 - 0.819 mm in wavelength), characterized for having an acceptable signal to noise ratio, has been divided into twenty-five different frequency intervals (bands) and the integral of the spectral amplitude over each frequency interval has been calculated and used to form the images. All the possible permutations of sets of three images have been arranged into the RGB channels, obtaining the composite images.

Putting the three different bands together in one color composite gives a better visual impression of terahertz reflectivity contrast than displaying one band at a time or a unique band (whole frequency window). RGB false color rendering allows distinction between different materials and textures on the surface of the lacquerware. The contrast between different textures is enabled by wavelength-dependent scattering from the surface, as well as differences in the composition of the surface layer. An improvement is particularly evident for the animal reliefs, where reading of the dotted-like texture given by the metallic glitter inclusions in the lacquer is much clearer, thanks to the different RGB color of the metal grains with respect to the adjacent areas.

Plan-type Terahertz Reflection Images: B-scans

B-scans (non-invasive cross section images) have been realized by displaying the time-of-flight (travel time) of the electric field along the vertical axis and the (x,y) linear position of the transceiver along the horizontal axis.

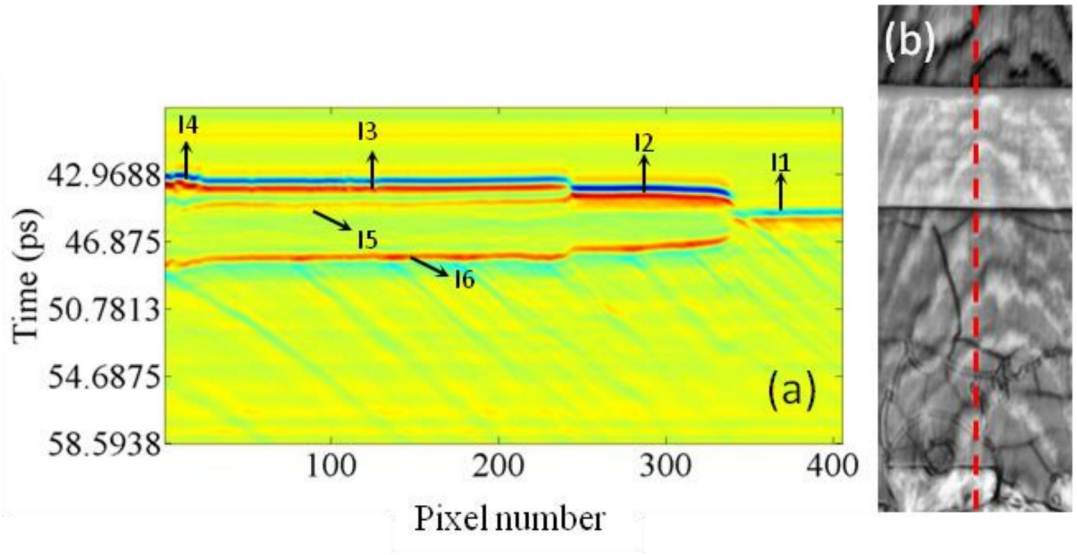

Figure VI.2-4 a B-scan image. The six main interfaces found are I1 (air/wood interface), I2 (air/layer III interface), I3 (air/layer IV interface), I4 (air/layer VI

interface), I5 (layer IV/layer III interface), I6 (layer III/wood interface). **b** THz reflection image of the power of the electric field integrated over the whole time window; the dashed red line represent the scanline used to plot the B-scan of Fig. 5(a).

Fig. VI.2-4a shows a B-scan image obtained from the scan-line dashed in red on the terahertz time domain parametric image of Fig. VI.2-4b, showing the area a1 of VI.1-4a. Six main interfaces have been imaged: I1 (air/wood interface), I2 (air/layer III interface), I3 (air/layer IV interface), I4 (air/layer VI interface), I5 (layer IV/layer III interface), I6 (layer III/wood interface). Additional minor interfaces are the ones formed because of inhomogeneities inside the wood and plaster layers. The wood grain is clearly visible in the lower part of the b-scan image.

Time-of-Flight Plots (ToF)

Fig. VI.2-5 shows the time-of-flight plots of the two scanned areas. Different buried layers have been individuated by plotting the maximum of the electric field for increasing time delay, in different time windows.

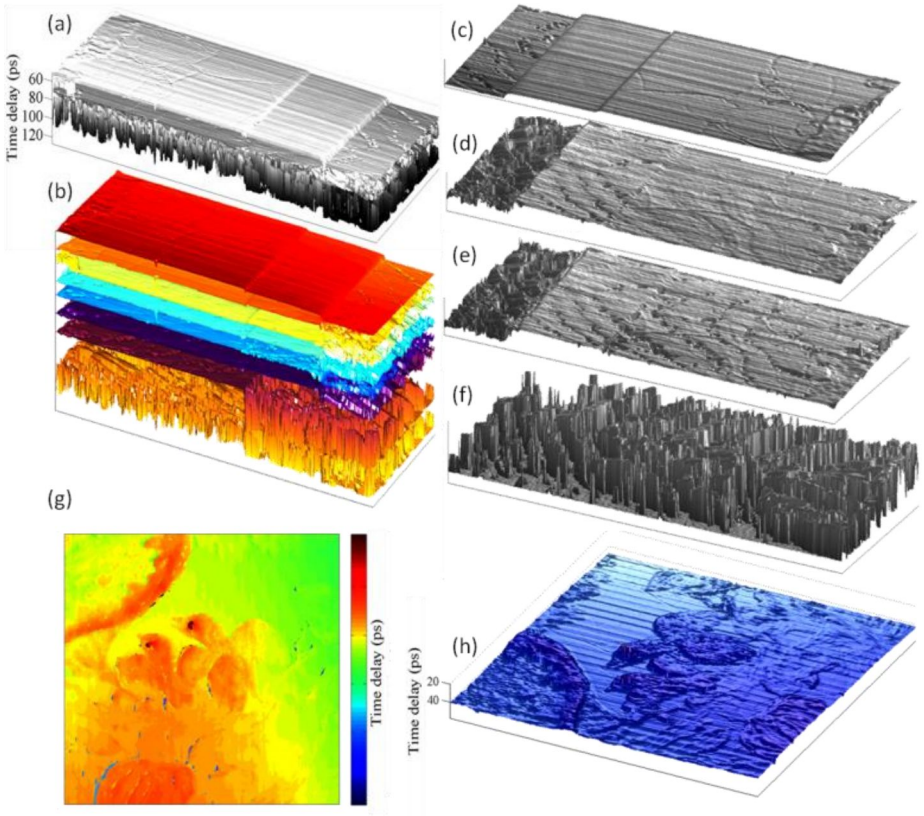

Figure VI.2-5 a ToF image of the layers found for the area a2 of Fig. VI.2-1a in the real time-scale. **b** Arbitrary separation of the layers for a better comprehension. **c** ToF image of the surface. **d** Layer IV/layer III interface (interface I5 of Fig. VI.2-4a.

e Layer III/wood interface (interface I6 of Fig. VI.2-4a). **f** Internal structure of the wood, plotted thanks to the optical inhomogeneities inside the panel due to the wood grain. **g** ToF image of the surface of the area a2 of Fig. VI.2-1a, plan-type rendering. **h** ToF image of the surface of the area a2 of Fig. VI.2-1a, 3D rendering

Fig. VI.2-5a shows the layers found for the area a2 indicated in Fig. VI.2-1a)using the real time-scale of he reflected signal, while in Fig. VI.2-5b the layers have been arbitrary separated for a better comprehension. Fig. VI.2-5c is the ToF image of the surface, Fig. VI.2-5d the layer IV/layer III interface (interface I5 of Fig. VI.2-4a), Fig. VI.2-5e the layer III/wood interface (interface I6 of Fig. VI.2-4a), Fig. VI.2-5f is the internal structure of the wood, plotted thanks to the optical inhomogeneities inside the panel due to the wood grain. Fig. VI.2-5g-h represent the ToF images of the surface of the area a2 of Fig. VI.2-1a, respectively a plan-type plot and a 3D plot.

VI.2.D Final considerations

Utilizing pulsed Terahertz Time-Domain Imaging (THz-TDI) in reflection mode, we observe non-invasively buried layers of the laquerware replica, including the internal structure of the wooden panel itself. With the same technique we have performed a surface material mapping. Surface topology mapping of hidden layers allowed by the THz-TDI technique has a great importance in the field of artworks inspection for conservation or art-history purposes, enabling the detection of defects or characteristic features of the surface of buried layers. The possibility to visualize the internal structure of the wooden support allows the inspection of its integrity.

Reflected THz composite RGB false color rendering allowed for surface material distribution, where RGB mapping allowed distinction between different materials and textures on the surface of the lacquerware.

VI.3 Terahertz time-domain imaging of a 17th century lacquered cabinet: a contribution to European lacquerwares characterization

A late 17th century white European lacquered cabinet, attributed to the Gérard Dagly workshop and belonging to the Barbara Piert-Borgers private collection of Far-East and European lacquerware, has been investigated by means of terahertz time domain imaging (THz-TDI), giving new insights into its composition.

In context of an interdisciplinary research project on European lacquers, called 'European Lacquer in Context', THz-TDI [100], [110], [180] was considered as a useful tool to investigate the internal structure, stratigraphy and condition of surface or subsurface layers of this complex multi-layered object. The original article can be accessed at [181].

VI.3.A Materials and methods

The examined cabinet was realized by applying a European lacquer layer on the top of paint layers. Those were applied on a ground layer and on the respective wooden support.

Figure VI.3-1 Visible image of the examined cabinet. The red square indicates the first scanned area

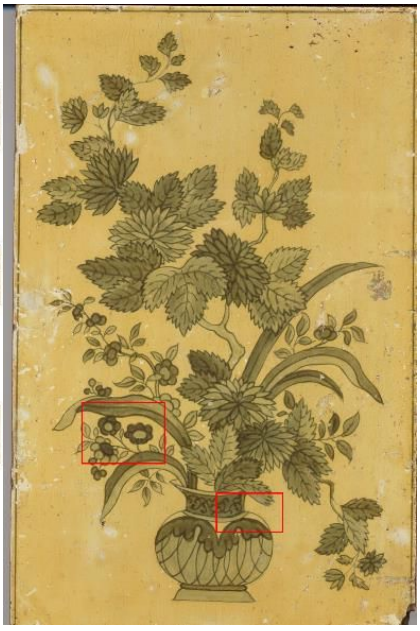

Figure VI.3-2 Visible image of the examined cabinet's door (back side). The red squares indicates the second and third scanned areas

An area of the cabinet's right door has been scanned using a Picometrix T-ray 4000 system (Fig. VI.3-1), while two further scans were made on the back of the cabinet door (Fig. VI.4-2). All the areas have been scanned in 0.5 mm steps, using a 320 ps measurement window, a time increment of 0.078 ps (4096 data points in each time trace) and a reflection configuration at normal incidence.

VI.3.B Results and discussion

The visible image of the first scanned area of the cabinet's door is shown in Fig. VI.3-3a, while the corresponding peak-to-peak THz image is shown in Fig. VI.3-3b. The peak-to-peak THz image highlights certain heterogeneity within the area (dark greyish areas), not connected to the decoration apparatus of the art-piece.

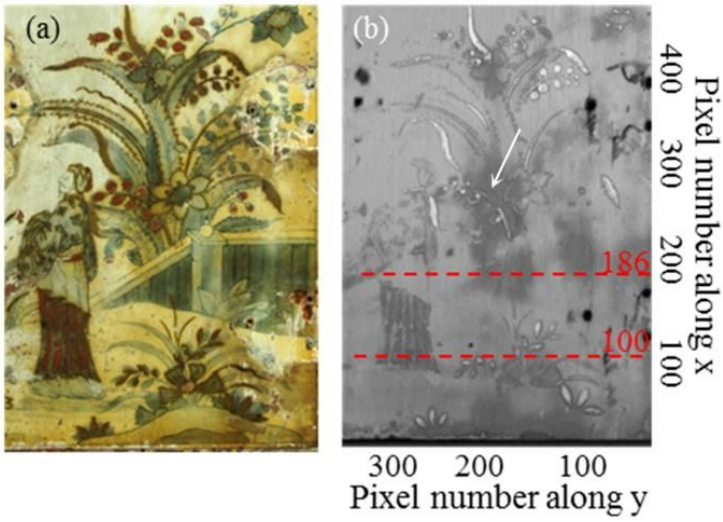

Figure VI.3-3
a Visible image of the scanned area of the lacquered cabinet.
b Terahertz peak-to-peak image of the scanned area; the scanlines used to plot the B-scans of Fig. VI.3-4 are indicated by dashed red lines. The white arrow points at one of the stain-like heterogeneities.

A frequency analysis of the THz image confirms that these stains have a different behavior compared to the adjacent areas (Fig. VI.3-4).

To gain a better understanding of the true nature of these stains, and to relate and to localize them within the lacquer's stratigraphy, B-scans have been realized after signal deconvolution (Figs. VI.3-5a-b). The recorded THz waveforms are composed of four main peaks, which indicate the presence of at least four different layers with dielectric contrast. An additional peak is detected where further decorations were applied on the top of the background (waveform 100, 280 in Fig. VI.3-5a).

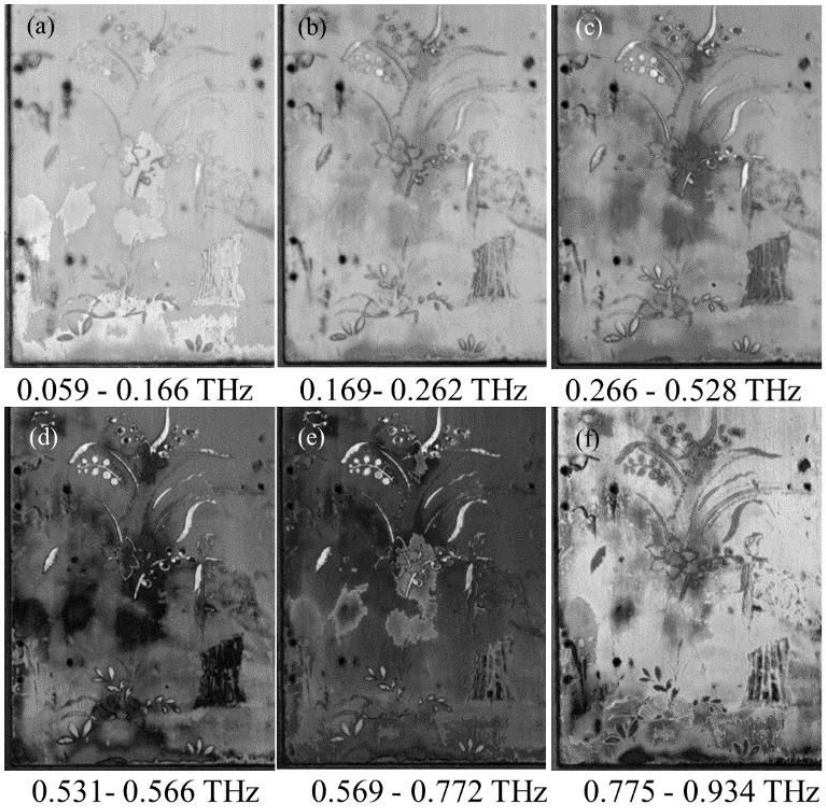

Figure VI.3-4
a-f Terahertz frequency images of the scanned area

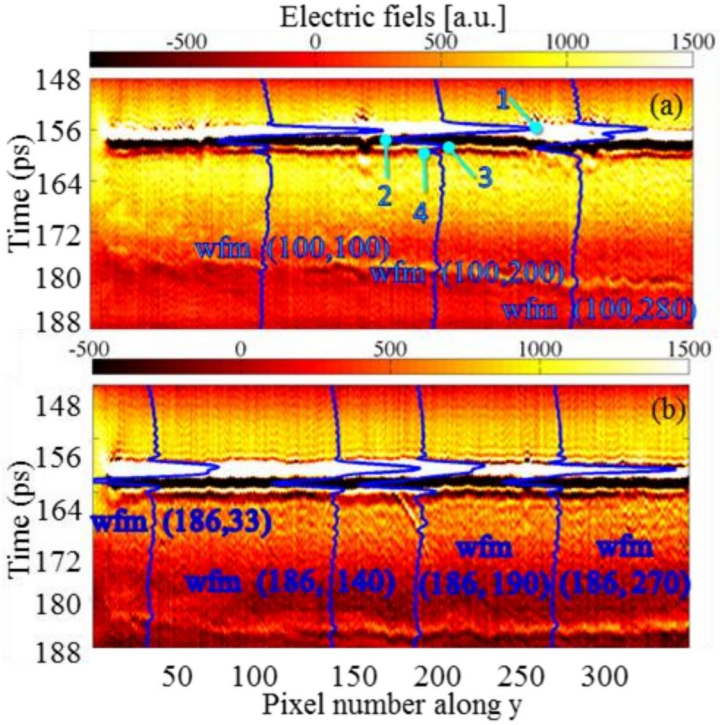

Figure VI.3-5
a B-scan corresponding to the electric field value recorded along the scanline 100 of Fig. VI.3-2a; three representative waveforms are plotted within it.
b B-scan corresponding to the electric field value recorded along the scanline 186 of Fig. VI.3-2a; three representative waveforms are plotted within it.

The raw B-scan along scanline 186 as a function of the arrival time shows no significant changes in the cabinet's stratigraphy where the stains are located, compared to that of the adjacent stainless areas. The THz signals arising from the reflection at the air/cabinet interface are often observed to

split at the locations of the stains (waveform 186, 22 and 186,190 of Fig. VI.3-5b). This suggests the presence of additional surface material in those areas. Furthermore, changes in the moisture content within the wooden panel cannot be excluded.

Finally, the THz image of the wooden support located underneath the lead-white ground layer has been clearly imaged (Fig. VI.3-6).

This confirms the capability of THz-TDI in imaging subsurface features behind dense lead-white layers with a high refractive index, differently than the traditional X-radiography, where the lead-white efficiently shields X-rays because of high Pb stopping power.

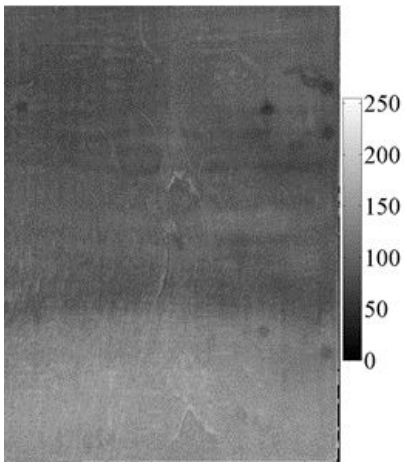

Figure VI.3-6 THz frequency image of the wooden panel

False color rendering technique has been used to enhance the contrast between materials at surface for the second and third scanned areas.
Fig. VI.3-7a show the second scanned area and Fig. VI.3-7b the THz peak-to-peak image. Contrast enhancement between the green areas and the white background of the door has been obtained by frequency analysis (value of the integral of the spectral amplitude within different frequency range, Fig. VI.2-7c). In particular, by integrating the amplitude values within the interval 0.56 - 0.86–THz, the contrast is maximized. The amplitude integrated within the 0.30 – 0.56 THz range shows a further contrast between the dark green lines used to trace the border of the light green motives. By choosing the proper images combination, the contrast between the three materials (light green of the motives, dark green of the borders and white of the background) is combined in a single image (Fig.VI.3-7d).

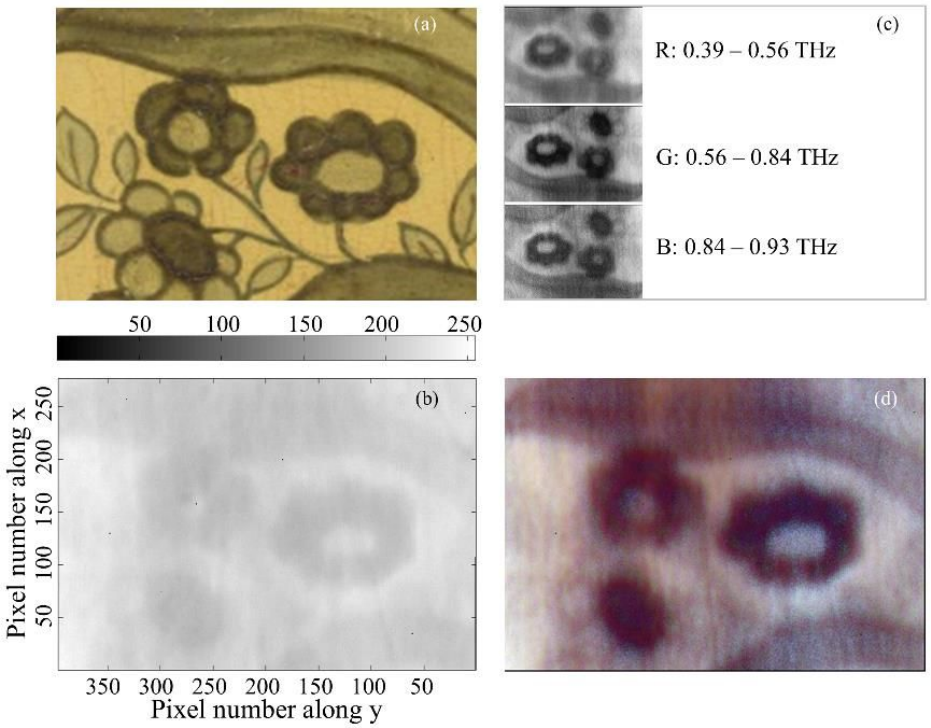

Figure VI.3-7 a the second scanned area.**b** THz peak-to-peak image. c integral of the spectral amplitude integrated within three different THz frequency ranges. **c** false color rendering

The same was made for the third scanned area, as shown in Fig. VI.3-8a-c.

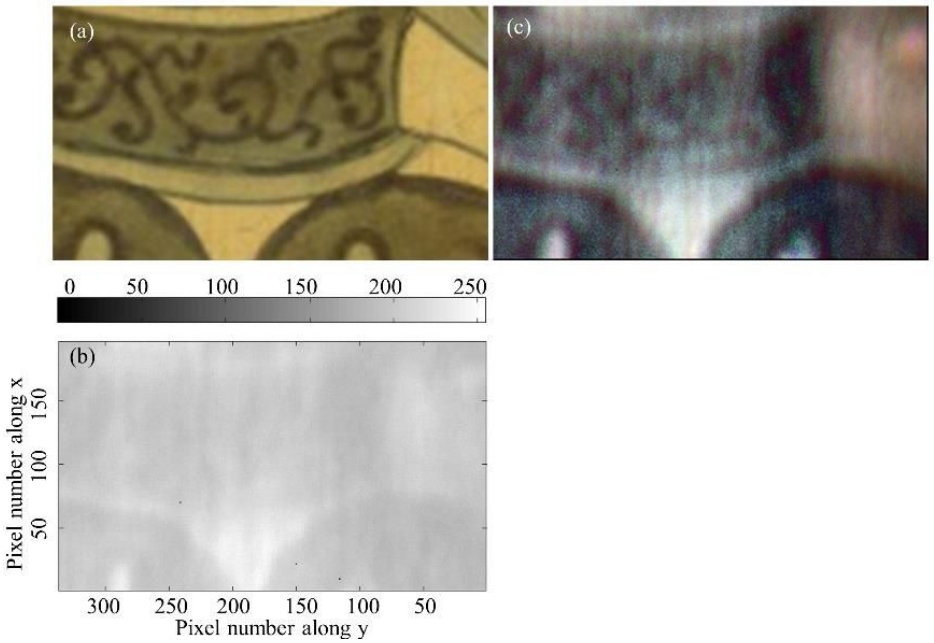

Figure VI.3-8 a the third scanned area.**b** THz peak-to-peak image. **c** false color rendering

For the false color rendering the three THz images combined were those obtained by integrating the amplitude over the 0.47 – 0.61, 0.62 – 0.82, 0.82 – 0.93 THz ranges.

VI.3.C Final considerations

Three different areas of a lacquered cabined doors were scanned by THz-TDI. Regarding the first scanned areas, THz-TDI gave a non-invasive picture of the lacquered cabinet stratigraphy and preservation condition of hidden layers and support. Furthermore, it highlights stain-like heterogeneities on the lacquerware surface. While their nature could nott be understood, the finding has encouraged the conservators to take a set of diagnostic measurements to further understand their nature and cause.

The false color rendering which followed the frequency analysis of the second and third scanned areas on the back side of the door, allowed to discriminate between three paint layers of different color present at surface, which were not clearly discriminated in the peak-to-peak THz images of the same subject.

VI.4 Chapter conclusion

For the first time, Asian lacquer-wares have been examined by THz-TDI.

Manufacturing technique of the support of three different Asian lacquerware have been individuated by THz-TDI scans: *kentai* for lacquerware n.1 (section VI.1), a single board of wood (*kiji*) for lacquerware 2 and *Hikimono* for lacquerware n.3

Further information extracted from THz data are highly important for the conservation issue. THz images of the wood grains of lacquer-ware n.2 allowed to understand the provenance of the board respect to the trunk (flamed tangential plain sawn just above the pith of the wood) and to evaluate the board convexity.

Ground layer on the top of the wood was THZ imaged, where for lacquerware n.1 its granular aspects, according to conservators, lead to suspect the use of a traditional Asian grounting material (mixture of *jinoko* and sawdust).

THz images plotted after scanning the lacquerware n. 3 (a pair of bowls) have been compared with those obtained by standard X-radiography: the grain of the wood is clearly visible in the THz images, while it hasn´t been detected by X-radiography. Several thin, discontinuous, rippled and overlapping interfaces, undetected by X-radiography, were found in THz B-SCANS just above the wood layer. While indistinguishable in X-radiographs, a circular score line used to trace the border of the foot of the bowl has been detected by THz-TDI.

The study showed the capability of THz-TDI in imaging hidden lacquer-wares substructures, overpassing the limit of standard X-radiography in imaging organic materials.

Proving its ability in detecting lacquerwares substructures, THz-TDI also showed its ability in recording surface anomalies. The THz-scans performed on a 17th century European lacquered cabined highlight stain-like heterogeneities on the lacquerware surface. While their nature could nott be understood, the finding has encouraged the conservators to take a set of diagnostic measurements to further understand their nature.

Within surface lacquerware inspection, false color rendering (FC) allowed to better discriminate among surface material of lacquerwares.

Concerning the 17th century cabinet, FC rendering allowed to discriminate between three paint layers of different color present at surface, which were not clearly discriminated in the peak-to-peak THz images of the

same subject. The same contrast enhancement has been obtained by creating reflected THz composite RGB false color image on a European lacquerware replica, where RGB mapping allowed distinction between different materials and textures on the surface of the lacquerware (section VI.2).

Chapter VII
Conclusions, future work and outlooks

The ability of terahertz time-domain imaging (THz-TDI) to visualize and analyze subsurface features of artworks has recently been established.

An important aspect of practical THz-TDI operating in reflection mode is the capability to handle subsurface separation, also in the typical situation where the surface is not flat, where the hidden layers vary in nature, thickness and morphology, and when the scanned areas are of notable areal dimensions. A fast and straightforward method that handles these problems and allows a clear representation of each subsurface layer in the artwork is presented in this research work (chapter III). The assessed optimization in managing large THz data set was used to get insights the artistic technique and preservation state of both replicas and real valuable artefacts, where the rendering of the imaged surface and subsurface structures composing the investigated objects was also optimized (chapter V).

THz-TDI scans were performed on two inestimable paintings belonging to the *Statens Museum for Kunst* collection (Copenhagen, Denmark): *The dying Messalina and her mother*, by the Danish Nicolai Abildgaard (1797, chapter III) and *A Garden in front of a Country Seat*, by the Flemish David Teniers The Younger (17th century, chapter IV). A wall painting subjected to the *National Museum of Denmark* vigilance, the medieval absidial wall painting of the Nebbelunde Church (Denmark), was also investigated (chapter V). Three Renaissance panel paintings by the well-known Florentine Fra Angelico painter were investigated (chapter IV): the *Lamentation over the dead Christ* painting, and the two side panels of the *Franciscan Tryptic*, known as the *Saints Francis, Onofrio and the Virgin Annunciate* and the *Saints Jerome, John the Baptist and the Archangel Gabriel*, all belonging to the *San Marco Museum* collection (Florence, Italy). A medioeval icon by an unknown author belonging to the public library of Taormina was examined by THz-TDI (chapter IV). To the best of our

knowledge, for the first time lacquerwares have been imaged by THz-TDI (chapter VI). Those included contemporary Asian lacquered objects belonging to the National Research Institute for Cultural Properties (Nara, Japan) and a European lacquered cabinet from the 17th century attributed to artisans close to the environment of the famous decorator Gerard Dagly (Barbara Piert-Borgers private collection of Far-East and European lacquerware, Köln - Germany).

It follows that this research work broadened the comprehension of the capabilities of THz-TDI applied to artifacts inspection, also comparing the information it provided with that obtained by other standard imaging techniques.

THz-TDI gave precious insights about artifacts manufacturing and restoration non-invasively.

Hidden paintings below the present ones have been THz-TDI imaged both for easel painting *The dying Messalina and her mother*, and for panel painting *A Garden in front of a Country Seat*, with a surprising clearness of details.

The THz-TDI scans performed on different panel paintings provided essential records for understanding differences in the original support-making techniques.

The non-invasive cross section analysis performed on the renaissance side panel of the *Franciscan Triptych*, the *Saints Francis, Onofrio and the Virgin Annunciate*, showed that the famous Fra Angelico artist covered the wooden support with a cloth before applying the preparation layer. The same was deducted for the *Saints Jerome, John the Baptist and the Archangel Gabriel* side panel, made by the same artist, where, in this last case, the cloth was applied by assembling more overlapping pieces. No cloths were found for the medieval icon, where the paint layers were directly applied on the wooden support.

Three different manufacturing techniques of three different contemporary Asian lacquerware have been individuated by THz-TDI scans: *kentai*, *kiji* and *hikimono*. Furthermore, by THz imaging the wood grains of the *kiji*-made lacquerware the provenance of the board respect to the trunk was understood and the board convexity evaluated. Further details regarding lacquerwares manufacturing were discovered thanks THz plots, such as the presence of thin, rippled and overlapping interfaces just above the wooden

substructure and the circular score line used to trace the border of the foot the *hikimono*-based lacquerware.

Regarding gessoing technique, the THz B-scans performed on the *Lamentation over the dead Christ* panel painting gave indication about the plastering operations performed during the 1950s by conservators to repair the original priming layer.

In addition, the THz data set recorded on the panel painting replica discussed in section IV.2, indicated how THz-TDI is capable of detecting separation lines between the same gessoing material applied with different degrees of compaction, thus giving an indication regarding different application techniques of the same material used.

No ground was found between the actual and the hidden compositions of *The dying Messalina and her mother* easel painting and *A Garden in front of a Country Seat* panel painting, indicating how both Nicolai Albildgaard and David Teniers The Younger painted directly on the previous paintings for composing their artworks.

THz-TDI furthermore helped in characterizing the ground layers applied on the top of the wooden substructure used for lacquerwares manufacturing. Particularly, the granular aspect of the ground composing the *kentai*-made lacquerware lead to suspect the use of a traditional Asian grounting material (mixture of *jinoko* and sawdust).

Limitations of the technique in detecting underdrawings were found by THz scanning the panel painting replica described in section IV.2: of the five historical materials used for underdrawings (lead metal-point, tin-lead metal point, graphite, charcoal, watercolor), only lead metal-point, and graphite at thicker lines were detected by THz-TDI scans. Also, while detected by means of IR reflectography, the *verdaccio* brushstrokes made before the application of the paint used for the skin tone of the figures of the medieval icon were not revealed by the technique.

Relating to pigments characterization, where the pigments combination offered a THz contrast with the exploited frequency range, THz-TDI helped in mapping the distribution of pigments not only on the surface (e.g. the medieval icon), but also on subsurface layer (e.g. *A Garden in front of a Country Seat* and *The Dying Messalina and her mother* paintings). Within this context, the THz frequency analysis and false color rendering (FC)

allowed to better performing materials areal mapping and discrimination by enhancing contrast. Concerning the 17th century cabinet, FC rendering allowed to discriminate between three paint layers of different color present at surface. The same contrast enhancement has been obtained by creating reflected THz composite RGB false color image on a European lacquerware replica, where RGB mapping allowed distinction between different materials and textures on the surface of the lacquerware (Section VI.2). In addition, frequency analysis and FC rendering helped in differentiating pigments and artistic materials of the hidden paintings found behind the *A Garden in front of a Country Seat* and *The Dying Messalina and her mother* paintings.

THz-TDI was found to be able to provide impressive information about the gilding technique used for artworks finishing.

In addition to showing the repairs made in the golden aureole of the Virgin represented in the *Lamentation over the Dead Christ*, the precise borders matching between it and the visage suggests that the gilding was applied by a thin brush at the figures borders. The same evidence was obtained by the investigation made on the *Franciscan Triptych* side panels. This experimental evidences are in line with the historical ones, since it is known that Fra Angelico was initially trained as a manuscript illuminator, thus gaining confidence with the application of gold finishing by thin brushes. A different gilding technique has been found for the 14th century icon, where the squared edges of the gilding imaged behind the paint layers indicate the use of large gold leaves. The THz plan-type rendering is furthermore able to reveal when the paint layers are applied on the top of a gilding or vice-versa. Fra Angelico drawn the silver baton held by Saint John on the top of the figure paint (*Saints Jerome, John the Baptist and the Archangel Gabriel* panel painting), while the unknown artist of the medieval icon painted directly on the gold background.

Indications about the gilding thickness can also be obtain by THz scanning an art-piece. THz signals appeared almost entirely reflected back by the gilded areas of the *Lamentation* panel painting, suggesting that the gold thickness is higher than the skin depth of the metal at THz frequencies. Differently, data obtained from the scanned areas of the *Franciscan Triptych* side panels and from the medieval icon show THz reflections at subsurface layers even when covered by the gold finishing, suggesting that the gold is of a very small thickness, either because original choice or because later abrasion.

Consequently, we have demonstrated that a detailed characterization of the internal structure of gilded object by means of THz-TDI in reflection geometry is possible, also though very thin gold finishing.

The technique resulted suitable for detecting and localize hidden structural defects and/or anomalies, providing precious information concerning the preservation state of the paintings.

Cracks are a wide spread damage typology affecting artworks manufactured by means of rigid support. A crack was THz imaged on the wooden panels of *A Garden in front of a Country Seat* and of the *Saints Jerome, John the Baptist and the Archangel Gabriel*. In this last case, the cracks was extending for the entire length of the scanned area underneath the painted surface. The integrity of the plaster layer (lack of significant dielectric changes at the corresponding crack location) furthermore suggested that the crack was in the wooden panel originally, before the gessoing operation. On the other hand, the origin of the crack visible on the surface of the medieval icon was explained thanks to the THz C-scan of the wooden support: in fact, it is located in correspondence of two grains of the wooden support and it is therefore originated by stress within the wooden panel.

Further typologies of damage affecting the wooden support have been imaged thanks to THz-TDI scanning.

The wooden panel boundaries of the *Lamentation* panel painting appears extremely uneven in the THz dielectric stratigraphy; additionally, spot-like defects were imaged in the THz C-scan of the region of interest. Those evidences are confirmed by the preservation history of wooden support of the painting, which see it suffering severe erosion in the lower side because of a fire in the past and important damages mainly caused by insect attacks.

Other information of interest within the conservation issue are the anomalies found at different depth within the objects dielectric stratigraphy.

An anomaly related to a material applied locally just behind the paint surface. has been individuated by THz stratigraphic analyses of the *Saints Jerome, John the Baptist and the Archangel Gabriel* panel. Similarly, an in-depth anomaly (metal point inclusion in the priming layer) was located and imaged within the panel painting replica described in section IV.2. The THz-scans performed on the 17th century European lacquered cabined highlight

stain-like heterogeneities on the lacquerware surface. The finding has encouraged the conservators to take a set of diagnostic measurements to further understand their nature. Two anomalous interfaces of different nature were found at different depth inside the lime-based plaster of the apsidal wall painting of Nebbelunde Church (Rødby, Lolland, Denmark) and imaged by B-scans, time-of-flight plots and 3D volume rendering, thus allowing the comprehension of their morphology. This makes the THz-TDI technology interesting not only for preservation but also for typological analysis purposes.

Within the preservation context, THz-TDI technique proven its ability in monitoring conservation interventions.

THz-TD imaging was proven advantageous in monitoring the correct adhesion between the original and the restoration canvas applied during a lining intervention to *The Dying Messalina and her mother* easel painting. Besides, THz-TDI facilitated the localization of the gilding used for tracing decorative motives on the figure dresses of the medioeval icon, not owing to the intense browning of the surface varnish layer, therefore allowing the conservator to protect them from aggressive agents during the cleaning operations.

Furthermore this study offered the occasion to compare the THz-TDI scanning with reflected infrared images and X-radiographs, highlighting the importance of combining different methods to achieve convincing conclusions about painting composition and condition. The study showed the capability of THz-TDI in imaging hidden lacquer-wares substructures, overpassing the limit of standard X-radiography in imaging organic materials. Based on our findings we also conclude that the unique possibility of seeing through gilding layers and the gilding layers themselves in a unique scan makes THz-TDI a very powerful technique, which can complement standard X-ray and reflected IR technique. Comparison between radiographic and THz images showed how wood grains and features are better visualized by THz-TDI compared to X-radiography, including subsurface cracks. Small variation in the thickness of the hidden paint brushstroke and painting details of the concealed composition were found also to be more evident in frequency parametric THz images compared to the X-radiograph (e.g. *A Garden in front of a Country Seat*). At

the same time, THz-TDI cannot replace the IR reflectography in detecting the underdrawings and *pentimenti*.

The possibility to use THz-TD systems for art materials identification is very attractive, so that future works should focus on the real capacity of THz-TDI systems in performing spectroscopic imaging and extracting spectral data from surface and subsurface layers composing an object, which at the moment looks quite inaccessible. To achieve this objective, a first easy step would be to broaden the only existing THz spectral database of artistic materials (http://thzdb.org/), while bands assignments should also be attempted. A better development of contrast enhancement methods is desirable, by means of digital image processing techniques but also by using supplementary parameters to those already in use for plotting THz image, especially the chemometrics ones. Lastly, attention should be paid to the development of optimized deconvolution methods for imaging applications as well as a further optimization of signal separations methods.

References

[1] D. Tornari, V. Fotakis, C. Georgiou, S. Zafiropulos, V. Anglos, "1. Introduction," in *Lasers in the Preservation of Cultural Heritage - Principles and Applications*, Taylor & Francis, 2006, pp. 1–2.

[2] P. . Camiz, P.; Barilli, R.; Curi , U.; Bartocci , C.; Rossi, "ARTE E SCIENZA - Rai Scuola." [Online]. Available: http://www.raiscuola.rai.it/articoli/arte-e-scienza/9708/default.aspx. [Accessed: 18-Aug-2015].

[3] J. Wouters, "Chemistry international," *Reflections on the Position of Science in Multidisciplinary Approaches*, 2008. [Online]. Available: http://www.iupac.org/publications/ci/2008/3001/1_wouters.html. [Accessed: 06-Aug-2015].

[4] Iccrom, "Conservation Science in Context," 2013. [Online]. Available: http://conservation.gu.se/infoglueCalendar/digitalAssets/1785685748_BifogadFil_Review-of-Strategic-Documentsv4[2].pdf. [Accessed: 06-Aug-2015].

[5] The Getty Conservation Institute, "Science at the Getty Conservation Institute." [Online]. Available: http://www.getty.edu/conservation/about/science/index.html. [Accessed: 06-Aug-2015].

[6] C. D´Amico, "Una riflessione sulle scienze per i beni culturali, archeometria e conservazione," in *Atti Acc. Rov. Agiati, a. 254, ser. VIII, vol. IV, B*, 2004, pp. 23–36.

[7] C. Daffara, D. Ambrosini, L. Pezzati, and D. Paoletti, "Thermal quasi-reflectography: a new imaging tool in art conservation," *Opt. Express*, vol. 20, no. 13, pp. 14746–14753, Jun. 2012.

[8] K. Janssens, J. Dik, M. Cotte, and J. Susini, "Photon-based techniques for nondestructive subsurface analysis of painted cultural heritage artifacts," *Acc. Chem. Res.*, vol. 43, no. 6, pp. 814–825, 2010.

[9] M. Alfeld and J. a C. Broekaert, "Mobile depth profiling and sub-surface imaging techniques for historical paintings - A review," *Spectrochim. Acta - Part B At. Spectrosc.*, vol. 88, pp. 211–230, 2013.

[10] B. H. Hasegawa, *The Physics of Medical X-ray Imaging: (or the Photon and Me,*

how I Saw the Light). 1991.

[11] K. Krug, J. Dik, M. Den Leeuw, a. Whitson, J. Tortora, P. Coan, C. Nemoz, and a. Bravin, "Visualization of pigment distributions in paintings using synchrotron K-edge imaging," *Appl. Phys. A Mater. Sci. Process.*, vol. 83, no. 2, pp. 247–251, 2006.

[12] M. P. Morigi, F. Casali, M. Bettuzzi, R. Brancaccio, and V. D'Errico, "Application of X-ray Computed Tomography to Cultural Heritage diagnostics," *Appl. Phys. A*, vol. 100, no. 3, pp. 653–661, 2010.

[13] M. Alfeld, J. V. Pedroso, M. van Eikema Hommes, G. der Snickt, G. Tauber, J. Blaas, M. Haschke, K. Erler, J. Dik, and K. Janssens, "A mobile instrument for in situ scanning macro-XRF investigation of historical paintings," *J. Anal. At. Spectrom.*, vol. 28, no. 5, pp. 760–767, 2013.

[14] a Bendada, S. Sfarra, C. I. Castanedo, M. Akhloufi, and J. P. Caumes, "Subsurface imaging for panel paintings inspection : A comparative study of the ultraviolet , the visible , the infrared and the terahertz spectra," *Opto-electronics Rev.*, vol. 23, no. 1, pp. 88–99, 2015.

[15] M. Gargano, N. Ludwig, and G. Poldi, "A new methodology for comparing IR reflectographic systems," *Infrared Physis Technol.*, vol. 49, no. November 2006, pp. 249–253, 2007.

[16] C. M. Falco, "High-resolution infrared imaging," in *SPIE Optics + Photonics Conference*, 2010, no. August.

[17] C. Bonifazzi, P. Carcagnì, R. Fontana, M. Greco, M. Mastroianni, M. Materazzi, E. Pampaloni, L. Pezzati, and D. Bencini, "A scanning device for VIS–NIR multispectral imaging of paintings," *J. Opt. A Pure Appl. Opt.*, vol. 10, no. 6, p. 064011, 2008.

[18] C. Cucci, A. Casini, M. Picollo, and L. Stefani, "Extending hyperspectral imaging from Vis to NIR spectral regions: a novel scanner for the in-depth analysis of polychrome surfaces," in *Optics for Arts, Architecture, and Archaeology IV, Proc. of SPIE*, 2013, vol. 8790, pp. 879009–9.

[19] F. Rosi, C. Miliani, R. Braun, R. Harig, D. Sali, B. G. Brunetti, and A. Sgamellotti, "Noninvasive analysis of paintings by mid-infrared hyperspectral imaging," *Angew. Chemie - Int. Ed.*, vol. 52, no. 20, pp. 5258–5261, 2013.

[20] C. Daffara, L. Pezzati, D. Ambrosini, D. Paoletti, R. Di Biase, P. I. Mariotti, C. Frosinini, I. I. Nazionale, L. E. Fermi, U. Aquila, P. E. Pontieri, I.-M. Roio, and L. Aquila, "Wide-band IR imaging in the NIR-MIR-FIR regions for in situ analysis of frescoes," in *Proc. of SPIE*, 2011, vol. 8084, pp. 1–12.

[21] F. Mercuri, U. Zammit, N. Orazi, S. Paoloni, M. Marinelli, and F. Scudieri, "Active infrared thermography applied to the investigation of art and historic artefacts," *J. Therm Anal Calorim*, vol. 104, no. 2, pp. 475–485, 2011.

[22] D. Gavrilov and D. P. Almond, "A review of imaging methods in analysis of works of art: Thermographic imaging method in art analysis," *Can. J. Phys. - NRC Res. Press*, vol. 92, pp. 341–364, 2014.

[23] N. P. Avdelidis and A. Moropoulou, "Applications of infrared thermography for the investigation of historic structures," *Journal of Cultural Heritage*, vol. 5, no. 1. pp. 119–127, 2004.

[24] P. Targowski and M. Iwanicka, "Optical Coherence Tomography : its role in the non-invasive structural examination and conservation of cultural heritage objects — a review," *Appl. Physic A*, vol. 106, pp. 265–277, 2012.

[25] D. Capitani, V. Di Tullio, and N. Proietti, "Progress in Nuclear Magnetic Resonance Spectroscopy Nuclear Magnetic Resonance to characterize and monitor Cultural Heritage," *Prog. Nucl. Magn. Reson. Spectrosc.*, vol. 64, pp. 29–69, 2012.

[26] V. Chan and A. Perlas, "Basics of Ultrasound Imaging," in *Atlas of Ultrasound-Guided Procedures in Interventional Pain Management*, S. N. Narouze, Ed. New York, NY: Springer New York, 2011.

[27] A. M. Siddiolo, L. D'Acquisto, A. R. Maeva, and R. G. Maev, "Wooden panel paintings investigation: An air-coupled ultrasonic imaging approach," *IEEE Trans. Ultrason. Ferroelectr. Freq. Control*, vol. 54, no. 4, pp. 836–846, 2007.

[28] R. G. Maev, R. E. G. Jr, and A. M. Siddiolo, "Review of Advanced Acoustical Imaging Techniques for Nondestructive Evaluation of Art Objects," *Res. Nondestruct. Eval.*, vol. 17, no. 4, pp. 191–204, 2006.

[29] V. Tornari, "Laser interference-based techniques and applications in structural inspection of works of art," *Anal Bioanal Chem*, vol. 387, pp. 761–780, 2007.

[30] "GLOSSARY OF PAINT TERMS." [Online]. Available: http://www.goldenglowpaints.com/Articles/GeneralArticles/GLOSSARYTERMS.htm. [Accessed: 12-Aug-2015].

[31] W. Withayachumnankul, G. M. Png, X. Yin, S. Atakaramians, I. Jones, H. Lin, S. Y. Ung, J. Balakrishnan, B. W. H. Ng, B. Ferguson, S. P. Mickan, B. M. Fischer, and D. Abbott, "T-ray sensing and imaging," *Proc. IEEE*, vol. 95, no. 8, pp. 1528–1558, 2007.

[32] P. R. Smith, D. H. Auston, and M. C. Nuss, "Subpicosecond photoconducting dipole antennas," *IEEE J. Quantum Electron.*, vol. 24, no. 2, pp. 255–260, Feb. 1988.

[33] B. B. Hu and M. C. Nuss, "Imaging with terahertz waves.," *Opt. Lett.*, vol. 20, no. 16, p. 1716, 1995.

[34] D. A. Z. James V. Rudd, Matthew W. Warmuth, Steven L. Williamson, "Compact fiber pigtailed terahertz modules," 09-Nov-2004.

[35] D. Zimdars, J. V. Rudd, and M. Warmuth, "A Compact, Fiber-Pigtailed, Terahertz Time Domain Spectroscopy System." [Online]. Available: http://web.eecs.umich.edu/~jeast/zimdars_2000_7_15.pdf. [Accessed: 01-Nov-2015].

[36] P. U. U. Jepsen, D. G. G. Cooke, and M. Koch, "Terahertz spectroscopy and imaging - Modern techniques and applications," *Laser Photon. Rev.*, vol. 5, no. 1, pp. 124–166, 2011.

[37] Y. S. Lee, *Principles of terahertz science and technology*. 2009.

[38] D. Abbott and X. C. Zhang, "Scanning the issue: T-ray imaging, sensing, and retection," *Proc. IEEE*, vol. 95, no. 8, pp. 1509–1513, 2007.

[39] W. Köhler, M. Panzer, U. Klotzach, and S. Winner, "Non-destructive investigation of paintings with THz-radiation," in *9th ECNDT, Berlin, ...*, 2006, pp. 1–7.

[40] K. Fukunaga, I. Hosako, Y. Kohdzuma, T. Koezuka, M. J. Kim, T. Ikari, and X. Du, "Terahertz analysis of an East Asian historical mural painting," *J. Eur. Opt. Soc.*, vol. 5, pp. 10024–1 – 100244, 2010.

[41] A. Younus, "Imagerie Terahertz 2D at 3D: Application pour l´etude des materiaux du patrimoine culturel," Unibersite´ de Bordeaux.

[42] R. M. Smith and M. a. Arnold, "Terahertz Time-Domain Spectroscopy of Solid Samples: Principles, Applications, and Challenges," *Appl. Spectrosc. Rev.*, vol. 46, no. 8, pp. 636–679, 2011.

[43] J. B. Jackson, "Terahertz Time-Domain Reflectometry of Multilayered Systems," The University of Michigan, 2008.

[44] G. Mourou, "Picosecond microwave pulses generated with a subpicosecond laser-

driven semiconductor switch," *Appl. Phys. Lett.*, vol. 39, no. 4, p. 295, Aug. 1981.

[45] D. H. Auston, K. P. Cheung, and P. R. Smith, "Picosecond photoconducting Hertzian dipoles," *Appl. Phys. Lett.*, vol. 45, no. 3, p. 284, Aug. 1984.

[46] C. Fattinger and D. Grischkowsky, "Terahertz beams," *Appl. Phys. Lett.*, vol. 54, no. 6, p. 490, Feb. 1989.

[47] D. A. Zimdars, G. Stuk, and Steven L. Williamson, "Terahertz imaging system for examining articles," 11-Nov-2008.

[48] I. DULING and D. ZIMDARS, "TERAHERTZ IMAGING: Compact TD-THz systems offer flexible, turnkey imaging solutions - Laser Focus World." [Online]. Available: http://www.laserfocusworld.com/articles/print/volume-43/issue-4/features/terahertz-imaging-compact-td-thz-systems-offer-flexible-turnkey-imaging-solutions.html. [Accessed: 01-Nov-2015].

[49] B. B. Hu, X.-C. Zhang, D. H. Auston, and P. R. Smith, "Free-space radiation from electro-optic crystals," *Appl. Phys. Lett.*, vol. 56, no. 6, p. 506, Feb. 1990.

[50] Q. Wu and X.-C. Zhang, "Free-space electro-optic sampling of terahertz beams," *Appl. Phys. Lett.*, vol. 67, no. 24, p. 3523, Dec. 1995.

[51] A. M. Li, X.-C. Zhang, G. D. Sucha and D. J. Harter, "Portable THz system and its applications," in *Proc. SPIE Commercial and Biomedical Applications of Ultrafast Lasers*, 1999, pp. 126–135, 1999.

[52] M. C. Nuss, "Method and apparatus for terahertz imaging," 21-Aug-1996.

[53] M. Usami, M. Yamashita, K. Fukushima, C. Otani, and K. Kawase, "Terahertz wideband spectroscopic imaging based on two-dimensional electro-optic sampling technique," *Appl. Phys. Lett.*, vol. 86, no. 14, p. 141109, Apr. 2005.

[54] M. van Exter, C. Fattinger, and D. Grischkowsky, "Terahertz time-domain spectroscopy of water vapor," *Opt. Lett.*, vol. 14, no. 20, p. 1128, Oct. 1989.

[55] P. U. Jepsen, R. H. Jacobsen, and S. R. Keiding, "Generation and detection of terahertz pulses from biased semiconductor antennas," *J. Opt. Soc. Am. B*, vol. 13, no. 11, p. 2424, 1996.

[56] M. Komatsu, R. Sato, M. Mizuno, K. Fukunaga, and Y. Ohki, "Feasibility study on terahertz imaging of corrosion on a cable metal shield," *Jpn. J. Appl. Phys.*, vol. 51, no. 12, pp. 72–75, 2012.

[57] P. U. Jepsen and B. M. Fischer, "Dynamic range in terahertz time-domain transmission and reflection spectroscopy.," *Opt. Lett.*, vol. 30, no. 1, pp. 29–31, 2005.

[58] E. Berry, J. W. Handley, A. J. Fitzgerald, W. J. Merchant, R. D. Boyle, N. N. Zinov'ev, R. E. Miles, J. M. Chamberlain, and M. a. Smith, "Multispectral classification techniques for terahertz pulsed imaging: An example in histopathology," *Med. Eng. Phys.*, vol. 26, no. 5, pp. 423–430, 2004.

[59] C. L. K. Dandolo and P. U. Jepsen, "Wall Painting Investigation by Means of Non-invasive Terahertz Time-Domain Imaging (THz-TDI): Inspection of Subsurface Structures Buried in Historical Plasters," *J. Infrared, Millimeter, Terahertz Waves*, 2015.

[60] M. Schwerdtfeger, E. Castro-Camus, K. Krügener, W. Viöl, and M. Koch, "Beating the wavelength limit: three-dimensional imaging of buried subwavelength fractures in sculpture and construction materials by terahertz time-domain reflection spectroscopy.," *Appl. Opt.*, vol. 52, no. 3, pp. 375–80, 2013.

[61] G. C. Walker, J. W. Bowen, J. Labaune, J.-B. Jackson, S. Hadjiloucas, J. Roberts, G. Mourou, and M. Menu, "Terahertz deconvolution.," *Opt. Express*, vol. 20, no. 25, pp. 27230–41, 2012.

[62] F. J. Harris, "On the Use of Windows for Harmonic Analysis with Discrete Fourier Transform," in *Proceedings of the IEEE*, 1978, vol. 51, pp. 172–204.

[63] N. Crump, "Techniques for the deconvolution of seismic signals," in *1975 IEEE Conference on Decision and Control including the 14th Symposium on Adaptive Processes*, 1975, pp. 2–8.

[64] V. Matz, M. Kreidl, and R. Šmíd, "Signal Separation in Ultrasonic Non-Destructive Testing," *Acta Polytech.*, vol. 47, no. 6, pp. 3–9, 2007.

[65] D. M. Mittleman, S. Hunsche, L. Boivin, and M. C. Nuss, "T-ray tomography.," *Opt. Lett.*, vol. 22, no. 12, pp. 904–906, 1997.

[66] B. Ferguson and D. Abbott, "De-noising techniques for terahertz responses of biological samples," *Microelectronics J.*, vol. 32, no. 12, pp. 943–953, Dec. 2001.

[67] Y. Chen and E. Pickwell-MacPherson, "Stationary-wavelet regularized inverse filtering: A robust deconvolution approach for terahertz reflection imaging," *2009 34th Int. Conf. Infrared, Millimeter, Terahertz Waves*, pp. 1–2, 2009.

[68] Y. Chen, S. Huang, and E. Pickwell-MacPherson, "Frequency-Wavelet Domain Deconvolution for terahertz reflection imaging and spectroscopy.," *Opt. Express*, vol. 18, no. 2, pp. 1177–1190, 2010.

[69] R. Neelamani, H. Choi, and R. Baraniuk, "ForWaRD: Fourier-Wavelet Regularized Deconvolution for Ill-Conditioned Systems," *IEEE Trans. Signal Process.*, vol. 52, no. 2, pp. 418–433, Feb. 2004.

[70] Y. Chen, Y. Sun, and E. Pickwell-MacPherson, "Total variation deconvolution for terahertz pulsed imaging," *Inverse Probl. Sci. Eng.*, vol. 19, no. 2, pp. 223–232, 2011.

[71] Y. CHEN, Y. SUN, and E. PICKWELL-MACPHERSON, "Improving Extraction of Impulse Response Functions Using Stationary Wavelet Shrinkage in Terahertz Reflection Imaging," *Fluct. Noise Lett.*, vol. 09, no. 04, pp. 387–394, 2010.

[72] a Heidari, "Signal recovery in pulsed terahertz integrated circuits," *Prog. Electromagn. Res.*, vol. 107, no. May, pp. 269–292, 2010.

[73] N. Cai, "The Study on Wavelet De-noising in Terahertz Time-Domain Spectroscopy," in *2009 International Conference on Information Technology and Computer Science*, 2009, vol. 1, pp. 618–621.

[74] J. B. Jackson, J. Bowen, G. Walker, J. Labaune, G. Mourou, M. Menu, and K. Fukunaga, "A survey of terahertz applications in cultural heritage conservation science," *IEEE Trans. Terahertz Sci. Technol.*, vol. 1, no. 1, pp. 220–231, 2011.

[75] C. L. K. Dandolo and P. U. Jepsen, "THz reflectometric imaging of contemporary panel artwork," in *2013 38th International Conference on Infrared, Millimeter, and Terahertz Waves (IRMMW-THz)*, 2013, pp. 1–2.

[76] R. H. Jacobsen, M. C. Nuss, and D. M. Mittleman, "Systems and methods for processing and analyzing terahertz waveforms," 13-May-1998.

[77] I. M. Brener and D. R. Dykaar, "Terahertz generators and detectors," 17-Mar-1998.

[78] M. C. Nuss, "Optical system employing terahertz radiation," 04-Aug-1998.

[79] I. M. Brener and M. C. Nuss, "Near field terahertz imaging," 13-Apr-1999.

[80] D. Zimdars, J. Rudd, and M. Warmuth, "A Compact, Fiber-Pigtailed, Terahertz Time Domain Spectroscopy System," *Elev. Int. Symp. Sp. Terahertz Technol.*, vol. 1, p. 423, 2000.

[81] Picometrix, "T-Ray 4000 Imaging and Spectroscopy System."

[82] J. D. Buron, D. H. Petersen, P. Bøggild, D. G. Cooke, M. Hilke, J. Sun, E. Whiteway, P. F. Nielsen, O. Hansen, A. Yurgens, and P. U. Jepsen, "Graphene conductance uniformity mapping.," *Nano Lett.*, vol. 12, no. 10, pp. 5074–81, Oct. 2012.

[83] R. Radpour, N. Bajwa, J. Garritano, S. Sung, M. Balonis-Sant, P. Tewari, W. Grundfest, I. Kakoulli, and Z. Taylor, "THz imaging studies of painted samples to guide cultural heritage investigations at the Enkleistra of St. Neophytos in Paphos, Cyprus," in *Terahertz Emitters, Receivers, and Applications V, Proc. of SPIE*, 2014, vol. 9199, p. 91990Q.

[84] A. J. L. Adam, P. C. M. Planken, S. Meloni, and J. Dik, "Terahertz imaging of hidden paint layers on canvas," *Opt. Express*, vol. 17, no. 5, pp. 3407–3416, 2009.

[85] E. Abraham, A. Younus, J. C. Delagnes, and P. Mounaix, "Non-invasive investigation of art paintings by terahertz imaging," *Appl. Phys. A*, vol. 100, no. 3, pp. 585–590, Mar. 2010.

[86] C. Seco-Martorell, V. López-Domínguez, G. Arauz-Garofalo, A. Redo-Sanchez, J. Palacios, and J. Tejada, "Goya's artwork imaging with Terahertz waves.," *Opt. Express*, vol. 21, no. 15, pp. 17800–5, Jul. 2013.

[87] C. L. Koch-Dandolo, T. Filtenborg, K. Fukunaga, J. Skou-Hansen, and P. U. Jepsen, "Reflection terahertz time-domain imaging for analysis of an 18th century neoclassical easel painting," *Appl. Opt.*, vol. 54, no. 16, p. 5123, 2015.

[88] R. Newman, "Applications of x rays in art authentication: radiography, x-ray diffraction, and x-ray fluorescence," in *Photonics West '98 Electronic Imaging*, 1998, pp. 31–41.

[89] M. Bessou, B. Chassagne, J.-P. Caumes, C. Pradère, P. Maire, M. Tondusson, and E. Abraham, "Three-dimensional terahertz computed tomography of human bones," *Appl. Opt.*, vol. 51, no. 28, p. 6738, 2012.

[90] KG Dürr NDT GmbH & Co., "TreFoc Technology | Digital Radiography | Non-Destructive Testing." [Online]. Available: http://duerr-ndt.com/index.html. [Accessed: 15-Oct-2015].

[91] T. Filtenborg, *Between formula and freestyle : Nicolai Abildgaard and 18th-century painting technique /*. 2014.

[92] G. Filippidis, M. Massaouti, a. Selimis, E. J. Gualda, J.-M. Manceau, and S. Tzortzakis, "Nonlinear imaging and THz diagnostic tools in the service of Cultural Heritage," *Appl. Phys. A*, vol. 106, no. 2, pp. 257–263, 2012.

[93] K. Fukunaga, T. Ikari, Y. Kohdzuma, M.-J. Kim, and K. Shinozawa, "THz reflection imaging for internal structure analysis of artworks," pp. 1–3.

[94] J. B. Jackson, M. Mourou, J. F. Whitaker, I. N. Duling, S. L. Williamson, M. Menu, and G. a. Mourou, "Terahertz imaging for non-destructive evaluation of mural paintings," *Opt. Commun.*, vol. 281, no. 4, pp. 527–532, 2008.

[95] C. L. K. Dandolo, P. U. Jepsen, and M. C. Christensen, "Characterization of European lacquers by terahertz (THz) reflectometric imaging," in *2013 Digital Heritage International Congress (DigitalHeritage)*, 2013, vol. 1, pp. 89–94.

[96] D. Giovannacci, D. Martos-Levif, G. C. Walker, M. Menu, and V. Detalle, "Terahertz applications in cultural heritage: case studies," in *Fundamentals of Laser Assisted Micro- and Nanotechnologies 2013*, 2013, p. 906510.

[97] R. M. Groves, B. Pradarutti, E. Kouloumpi, W. Osten, and G. Notni, "2D and 3D non-destructive evaluation of a wooden panel painting using shearography and terahertz imaging," *NDT E Int.*, vol. 42, no. 6, pp. 543–549, 2009.

[98] I. Duling and D. Zimdars, "Terahertz imaging: Revealing hidden defects," *Nat. Photonics*, vol. 3, no. 11, pp. 630–632, 2009.

[99] I. Hosako and K. Fukunaga, "Non destructive observation of defects in dielectric materials and prospects for diagnostics of infrastructure and cultural heritage," *2011 30th URSI Gen. Assem. Sci. Symp. URSIGASS 2011*, pp. 2–5, 2011.

[100] M. Picollo, K. Fukunaga, and J. Labaune, "Obtaining noninvasive stratigraphic details of panel paintings using terahertz time domain spectroscopy imaging system," *J. Cult. Herit.*, pp. 1–8, 2014.

[101] A. S. Skryl, J. B. Jackson, M. I. Bakunov, M. Menu, and G. a. Mourou, "Terahertz time-domain imaging of hidden defects in wooden artworks: application to a Russian icon painting," *Appl. Opt.*, vol. 53, no. 6, p. 1033, 2014.

[102] N. Kamba, Y. Tsuchiya, O. Akiko, and K. Fukunaga, "INTERNAL STRUCTURE OBSERVATION OF A JAPANESE PANEL PAINTED SCREEN BY TERAHERTZ IMAGING TECHNIQUE." [Online]. Available: http://www.ndt.net/article/art2011/papers/FUKUNAGA - NDT 41.pdf.

[103] L. Uzielli, Z. Véliz, J. Wadum, and P. Walker, "History of panel-making

techniques," in *The structural conservation of panel paintings - Proceedings of a symposium at the J. Paul Getty Museum, April 1995*, 1998, vol. Part two, pp. 109–185.

[104] C. L. Koch Dandolo, T. Filtenborg, J. Skou-Hansen, and P. U. Jepsen, "Analysis of a seventeenth-century panel painting by reflection terahertz time-domain imaging (THz-TDI): contribution of ultrafast optics to museum collections inspection," *Appl. Phys. A*, vol. 121, no. 3, pp. 981–986, 2015.

[105] W. E. Baughman, "Terahertz spectroscopic imaging," 2014.

[106] S. O'Connor and M. Brooks, *X-Radiography of Textiles, Dress and Related Objects*. Routledge, 2007.

[107] Y. Liul, J. Tanl, L. Jiang, S. Shi, B. Jin, and J. Ma, "Study on Terahertz Time Domain Spectroscopy of pine wood nematode disease," pp. 271–275.

[108] T. M. Todoruk, I. D. Hartley, and M. E. Reid, "Origin of birefringence in wood at terahertz frequencies," *IEEE Trans. Terahertz Sci. Technol.*, vol. 2, no. 1, pp. 123–130, 2012.

[109] M. Reid and R. Fedosejevs, "Terahertz birefringence and attenuation properties of wood and paper.," *Appl. Opt.*, vol. 45, no. 12, pp. 2766–2772, 2006.

[110] D. . Mittelman, "Sensing with terahertz radiation," in *Springer Series in optical science*, Springer-V., .

[111] K. Fukunaga and M. Picollo, "Terahertz spectroscopy applied to the analysis of artists' materials," *Appl. Phys. A*, vol. 100, no. 3, pp. 591–597, 2010.

[112] M. Picollo, "Application of THz-TDS imaging technology to the investigation of panel paintings," pp. 289–294, 2014.

[113] M. Salmi, "Fra Angelico | Italian painter | Britannica.com," *Encyclopaedia Britanica*, 2014. [Online]. Available: http://global.britannica.com/biography/Fra-Angelico. [Accessed: 17-Oct-2015].

[114] T. Allie, "Criminal vision in early modern Florence: Fra Angelico´s altarpiece for 'Il Tempio' and the Magdalenian gaze," in *Renaissance theories of vision*, 2010, pp. 45–62.

[115] Regione Toscana, "Visit the Places of Faith in Tuscany - Ex Oratorio della Compagnia di Santa Maria Vergine della Croce al Tempio." [Online]. Available:

http://web.rete.toscana.it/Fede/ricerca.jsp. [Accessed: 17-Oct-2015].

[116] Portale ARES, "Portale ARES," 1953. [Online]. Available: http://www.iscr-ares.beniculturali.it:8080/ares/ricerche.do?formAction15&idintervento=3752&type=DOC. [Accessed: 17-Oct-2015].

[117] S. M. Pizer, E. P. Amburn, J. D. Austin, R. Cromartie, A. Geselowitz, T. Greer, B. ter Haar Romeny, J. B. Zimmerman, and K. Zuiderveld, "Adaptive histogram equalization and its variations," *Comput. Vision, Graph. Image Process.*, vol. 39, no. 3, pp. 355–368, Sep. 1987.

[118] A. M. Reza, "Realization of the Contrast Limited Adaptive Histogram Equalization (CLAHE) for Real-Time Image Enhancement," *J. VLSI Signal Process. Signal, Image, Video Technol.*, vol. 38, no. 1, pp. 35–44, Aug. 2004.

[119] E. Abraham, a. Younus, a. El Fatimy, J. C. Delagnes, E. Nguéma, and P. Mounaix, "Broadband terahertz imaging of documents written with lead pencils," *Opt. Commun.*, vol. 282, no. 15, pp. 3104–3107, 2009.

[120] M. B. Johnston and J. Lloyd-Hughes, "Pump-Probe Spectroscopy at Terahertz Frequencies," in *Terahertz Spectroscopy and Imaging*, vol. 171, K.-E. Peiponen, A. Zeitler, and M. Kuwata-Gonokami, Eds. Berlin, Heidelberg: Springer Berlin Heidelberg, 2013.

[121] T. Bardon, R. K. May, P. F. Taday, and M. Strlič, "Systematic study of terahertz time-domain spectra of historically informed black inks.," *Analyst*, pp. 4859–4869, 2013.

[122] a J. Fitzgerald, E. Berry, N. N. Zinovev, G. C. Walker, M. a Smith, and J. M. Chamberlain, "An introduction to medical imaging with coherent terahertz frequency radiation.," *Phys. Med. Biol.*, vol. 47, no. 7, pp. R67–R84, 2002.

[123] G. Sundberg, L. M. Zurk, S. Schecklman, and S. Henry, "Modeling rough-surface and granular scattering at terahertz frequencies using the finite-difference time-domain method," *IEEE Trans. Geosci. Remote Sens.*, vol. 48, no. 10, pp. 3709–3719, 2010.

[124] NiCT and RIKEN, "Terahertz Database." [Online]. Available: http://thzdb.org/. [Accessed: 17-Oct-2015].

[125] "Terahertz Time-domain and Fourier-transform Infrared Specroscopy of traditional Korean Pigments," *J. Korean Phys. Soc.*, vol. 64, no. 5, pp. 727–731, 2014.

[126] R. Piesiewicz, C. Jansen, S. Wietzke, D. Mittleman, M. Koch, and T. Kürner,

"Properties of building and plastic materials in the THz range," *Int. J. Infrared Millimeter Waves*, vol. 28, no. 5, pp. 363–371, 2007.

[127] M. Naftaly, J. F. Molloy, G. V Lanskii, K. a Kokh, and Y. M. Andreev, "Terahertz time-domain spectroscopy for textile identification.," *Appl. Opt.*, vol. 52, no. 19, pp. 4433–7, 2013.

[128] C. L. Koch Dandolo, A. Cosentino, and P. Uhd Jepsen, "Inspection of panel paintings beneath gilded finishes using terahertz time-domain imaging," *Stud. Conserv.*, vol. 60, no. supplement 1, 2015.

[129] A. K. Azad and W. Zhang, "Resonant terahertz transmission in subwavelength metallic hole arrays of sub-skin-depth thickness," *Opt. Lett.*, vol. 30, no. 21, p. 2945, Nov. 2005.

[130] J. Henderson and J. Joannides, "A Franciscan triptych by Fra Angelico," *Arte Cris.*, vol. 79, pp. 3–6, 1991.

[131] F. Presciutti, C. Ricci, F. Rosi, L. Cartechini, C. Miliani, B. G. Brunetti, and A. Sgamellotti, "Indagini spettroscopiche non invasive sulla Pala Santa Croce del Beato Angelico," 2005.

[132] M2ADL – Laboratorio diagnostico di microchimica e microscopia and Ravenna, "INDAGINI DIAGNOSTICHE SUL TRITTICO FRANCESCANO DI SANTA CROCE DEL BEATO ANGELICO - Studio dei materiali costitutivi e delle tecniche mediante imaging multispettrale," 2005.

[133] CNR ICVBC - Istituto per la Conservazione e la Valorizzazione dei Beni Culturali, "Prelievi Tavole GGB e SFO- Schede prelievi BA," 2005.

[134] J. H. Stoner and R. Rushfield, *Conservation of Easel Paintings*. Routledge, 2013.

[135] M. G. T. Antonelli, *La pittura su tavola*. 2003.

[136] E. Darque-Ceretti and M. Aucouturier, "Gilding for Matter Decoration and Sublimation. A Brief History of the Artisanal Technical Know-how," *1st International Conference on Innovation in Art Research and Technology*, vol. 4, no. special issue. pp. 647–660, 10-Jul-2013.

[137] K. Nassau, "The feefteen causes of color," in *Color for Science, Art and Technology*, K. Nassau, Ed. Elsevier, 1997, p. 144.

[138] P. T. Bishop and P. A. Sutton, "Decorative gold materials," in *Gold: Science and*

Applications, CRC Press, 2009, p. 357.

[139] F. Kadlec, P. Kuzel, and J.-L. Coutaz, "Study of terahertz radiation generated by optical rectification on thin gold films.," *Opt. Lett.*, vol. 30, no. 11, pp. 1402–1404, 2005.

[140] N. Laman and D. Grischkowsky, "Terahertz conductivity of thin metal films," *Appl. Phys. Lett.*, vol. 93, no. 5, pp. 1–3, 2008.

[141] M. a Ordal, R. J. Bell, R. W. Alexander, L. L. Long, and M. R. Querry, "Optical properties of fourteen metals in the infrared and far infrared: Al, Co, Cu, Au, Fe, Pb, Mo, Ni, Pd, Pt, Ag, Ti, V, and W.," *Appl. Opt.*, vol. 24, no. 24, p. 4493, 1985.

[142] M. A. Seo, H. R. Park, S. M. Koo, D. J. Park, J. H. Kang, O. K. Suwal, S. S. Choi, P. C. M. Planken, G. S. Park, N. K. Park, Q. H. Park, and D. S. Kim, "Terahertz field enhancement by a metallic nano slit operating beyond the skin-depth limit," *Nat. Photonics*, vol. 3, no. 3, pp. 152–156, Feb. 2009.

[143] K. Fukunaga and Picolllo Marcello, "Characterization of works of art," in *Terahertz Spectroscopy and Imaging*, Springer, 2012.

[144] A. Cosentino, C. L. Koch-Dandolo, A. Cristaudo, and P. Uhd Jepsen, "Diagnostics pre and post Conservation on a 14th Century Gilded Icon from Taormina , Sicily," *e-conservation J.*, vol. 3, pp. 1–7, 2015.

[145] S. Sotiropoulou, "Diagnostic methodology for the examination of Byzantine frescoes and icons. Non-destructive investigation and pigment identification," in *Comprehensive Analytical Chemistry XLII*, Elsevier., V. Janssens and Grieken, Eds. 2004.

[146] M. C. Buoso, G. Scarabottolo, and D. Zafiropoulos, "Analysis of the Sant'Agata Post-Byzantine Icon from the Hellenic Institute of Byzantine and Post-Byzantine Studies, Venice. A Multi-Method Approach," *LNL Annual Report - Applied and Interdisciplinary Physics*. [Online]. Available: http://www.lnl.infn.it/~annrep/read_ar/2008/contributions/pdf_singles/84.pdf. [Accessed: 18-Oct-2015].

[147] M. Avillez and C. Vourvopoulou, "Conservation of a Greek Icon. Technological and Methodological Aspects - Icon Network," 2010. [Online]. Available: http://www.icon-network.org/Conservation-of-a-Greek-Icon,183.html. [Accessed: 18-Oct-2015].

[148] A. Cosentino, "A practical guide to panoramic multispectral imaging," *e-conservation Mag.*, no. 25, pp. 64–73, Jan. 2013.

[149] G. Accorsi, G. Verri, M. Bolognesi, N. Armaroli, C. Clementi, C. Miliani, and A. Romani, "The exceptional near-infrared luminescence properties of cuprorivaite (Egyptian blue).," *Chem. Commun. (Camb).*, no. 23, pp. 3392–4, Jun. 2009.

[150] A. Cosentino, "Identification of pigments by multispectral imaging; a flowchart method," *Herit. Sci.*, vol. 2, no. 8, 2014.

[151] T. . Pieseewincz, R.; Kleine-Ostmann, T.; Krumbholz, N.; Miettelman, D.; Koch, M.; Kurner, "Terahertz characterisation of building materials," *Electron. Lett.*, vol. 41, no. 18, 2006.

[152] T. Kurabayashi, L. Zhen, P. Plotka, M. Watanabe, Y. Oyama, and J. I. Nishizawa, "Sub-terahertz imaging for construction materials," in *33rd International Conference on Infrared and Millimeter Waves and the 16th International Conference on Terahertz Electronics, 2008, IRMMW-THz 2008*, 2008, pp. 3–4.

[153] J. Dash, S. Ray, K. Nallappan, S. Sasmal, and B. Pesala, "Non-destructive inspection of internal defects in concrete using continuous wave 2D terahertz imaging system," *Int. Conf. Infrared, Millimeter, Terahertz Waves, IRMMW-THz*, pp. 0–1, 2013.

[154] Y. Oyama, L. Zhen, T. Tanabe, and M. Kagaya, "Sub-terahertz imaging of defects in building blocks," *NDT E Int.*, vol. 42, no. 1, pp. 28–33, 2009.

[155] D. a. DiGiovanni, a. J. Gatesman, R. H. Giles, and W. E. Nixon, "Backscattering of ground terrain and building materials at submillimeter-wave and terahertz frequencies," in *Passive and Active Millimeter-Wave Imaging XVI, Proc. of SPIE Vol. 8715*, 2013, vol. 8715, pp. 871507–1.

[156] A. Abina, U. Puc, A. Jeglič, and A. Zidanšek, "Applications of Terahertz Spectroscopy in the Field of Construction and Building Materials," *Appl. Spectrosc. Rev.*, vol. 50, no. 4, pp. 279–303, 2015.

[157] K. Fukunaga, T. Meldrum, W. Zia, M. Ohno, T. Fuchida, and B. Blumich, "Nondestructive investigation of the internal structure of fresco paintings," *Proc. Digit. 2013 - Fed. 19th Int'l VSMM, 10th Eurographics GCH, 2nd UNESCO Mem. World Conf. Plus Spec. Sess. fromCAA, Arqueol. 2.0 al.*, vol. 1, pp. 81–88, 2013.

[158] J.-L. Bodnar, J.-J. Metayer, K. Mouhoubi, and V. Detalle, "Non destructive testing of works of art by terahertz analysis," *Eur. Phys. J. Appl. Phys.*, vol. 64, no. 2, p. 21001, 2013.

[159] G. C. Walker, J. W. Bowen, J.-B. Jackson, J. Labaune, G. Mourou, M. Menu, W. Matthews, and I. Hodder, "Sub-surface Terahertz Imaging through Uneven Surfaces: Visualizing Neolithic Wall Paintings in Çatalhöyük," *Conf. Lasers Electro-Optics 2012*, vol. 1, p. CTu3B.4, 2012.

[160] J. B. Jackson, G. Walker, J. Roberts, A. Pike, V. Detalle, G. Mourou, M. Menu, and J. Bowen, "Terahertz Pulse Investigation of Paleolithic Wall Etchings," in *Infrared, millimeter, and terahertz waves (IRMMW-THz), International conference on*, 2014, pp. 5–6.

[161] "Ancient Roman man hidden beneath famous painting at the Louvre -- ScienceDaily." [Online]. Available: http://www.sciencedaily.com/releases/2013/04/130410154622.htm. [Accessed: 24-Aug-2015].

[162] G. C. Walker, J. B. Jackson, D. Giovannacci, J. W. Bowen, B. Delandes, J. Labaune, G. a Mourou, M. Menu, and V. Detalle, "Terahertz analysis of stratified wall plaster at buildings of cultural importance across Europe," *Proc. SPIE*, vol. 8790, p. 87900H–87900H–8, 2013.

[163] R. Letellier, *Recording, Documentation, and Information Management for the Conservation of Heritage Places: Guiding Principles*. 2007.

[164] V. Pérez-Gracia, D. Di Capua, R. González-Drigo, O. Caselles, L. G. Pujades, and V. Salinas, "GPR resolution in Cultural Heritage applications," in *Proceedings of the 13th Internarional Conference on Ground Penetrating Radar, GPR 2010*, 2010, pp. 389–393.

[165] F. Weritz, R. Arndt, M. Röllig, C. Maierhofer, and H. Wiggenhauser, "Intestigation of concrete structures with pulse phase thermography," *Mater. Struct.*, vol. 38, no. 9, pp. 843–849, Nov. 2005.

[166] C. et al. Maierhofer, "Investigating historic masonry structures at different depths with active thermography," in *10th International Conference on Quantitative InfraRed Thermography*, 2010, vol. 1, pp. 5–6.

[167] ZIB and FEI, "AVIZO 8 user´s guide." [Online]. Available: http://www.vsg3d.com/sites/default/files/AvizoUsersGuide.pdf. [Accessed: 27-Sep-2015].

[168] A. Burmester, "Technical Studies of Chinese Lacquer," in *Urushi: Proceedings of the 1985 Urushi Study Group*, 1988.

[169] "Kakinoshima Site | Jomon Archaeological Sites in Hokkaido and Northern Tohoku." [Online]. Available: http://jomon-japan.jp/en/jomon-sites/kakinoshima/. [Accessed: 21-Oct-2015].

[170] B. Milam and H. Gillette, "X-ray radiography in the study of oriental lacquerware

substructures," in *Urushi: Proceedings of the Urushi Study Group, June 10–27, 1985, Tokyo*, 1988, p. 272.

[171] K. Hiroshi, "The story of Japanese urushiware," in *Urushi 2003: International Course on Conservation of Japanese Lacquer*, 2003.

[172] B. Museum, "Lacquer," 1996. [Online]. Available: http://www.bishopmuseum.org/research/pdf/cnsv-lacquer.pdf. [Accessed: 25-Oct-2015].

[173] J. F. Molloy and M. Naftaly, "Terahertz characterization of textiles," in *2013 6th UK, Europe, China Millimeter Waves and THz Technology Workshop (UCMMT)*, 2013, pp. 1–2.

[174] J. Molloy and M. Naftaly, "Wool textile identification by terahertz spectroscopy," *J. Text. Inst.*, vol. 105, no. 8, pp. 794–798, Jan. 2014.

[175] T. Kurabayashi, F. Saitoh, N. Watanabe, and T. Tanno, "Identification of textile fiber by terahertz spectroscopy," in *35th International Conference on Infrared, Millimeter, and Terahertz Waves*, 2010, pp. 1–2.

[176] I. Dunayevskiy, B. Bortnik, K. Geary, R. Lombardo, M. Jack, and H. Fetterman, "Millimeter- and submillimeter-wave characterization of various fabrics.," *Appl. Opt.*, vol. 46, no. 24, pp. 6161–6165, 2007.

[177] D. S. Citrin, A. V. Citrin, D. Denison, S. E. Ralph, and R. Mary Lynn, "Terahertz properties od textiles: metamaterials, sensors and security," *National Textile Center Research Briefs – Materials Competency*, 2005. [Online]. Available: http://www.ntcresearch.org/pdf-rpts/Bref0605/M04-GT19s-05e.pdf. [Accessed: 25-Oct-2015].

[178] M. Webb, *Lacquer: Technology and Conservation : a Comprehensive Guide to the Technology and Conservation of Asian and European Lacquer*. 2000.

[179] Gonzalez, Woods, and Eddins, *Digital image processing using MATLAB*. Gatesmark Publishing, 2009.

[180] W. L. Chan, J. Deibel, and D. M. Mittleman, "Imaging with terahertz radiation," *Reports Prog. Phys.*, vol. 70, no. 8, pp. 1325–1379, Aug. 2007.

[181] C. L. Koch Dandolo, V. Cattersel, and P. Uhd Jepsen, "Terahertz Time-domain Imaging of a 17th Century Lacquered Cabinet: a Contribution to European Lacquerwares Characterization," in *IRMMW-THz 2015 - 40th International Conference on*, 2015.

Appendix A
Publications, lectures and oral contributions

The author of this PhD thesis has contributed to the following journal publications, conference/events contributions and lectures during her PhD project:

Peer-reviewed journal articles

Corinna L. Koch Dandolo, Troels Filtenborg, Jacob Skou-Hansen, Peter Uhd Jepsen, *Analysis of a seventeenth-century panel painting by reflection terahertz time-domain imaging (THz-TDI): contribution of ultrafast optics to museum collections inspection,* Applied Physics A, Vol. 121, No. 3, 2015, p. 981-986. Invited paper

Corinna L. Koch Dandolo, Kaori Fukunaga, Troels Filtenborg, Jacob Skou-Hansen, Peter Uhd Jepsen, *Reflection terahertz time-domain imaging for analysis of an 18th century neoclassical easel painting*, Applied Optics, Vol. 54, No. 16, 2015, p. 5123-5129.

Corinna L. Koch Dandolo, Antonino Cosentino, Angelo Cristaudo, Peter Uhd Jepsen, *Diagnostics pre and post Conservation on a 14th Century Gilded Icon from Taormina, Sicily*, e-conservation Journal, Vol. 3, 2015.

Corinna L. Koch Dandolo, Peter Uhd Jepsen, *Wall Painting Investigation by Means of Non-invasive Terahertz Time-Domain Imaging (THz-TDI): Inspection of Subsurface Structures Buried in Historical Plasters*, Journal of Infrared, Millimeter, and Terahertz Waves, 2015, DOI:10.1007/s10762-015-0218-9, pp 1-11

Peer-reviewed conference articles

Corinna L. Koch Dandolo; Vincent Cattersel, Peter Uhd Jepsen, *Terahertz Time-domain Imaging Of A 17th Century Lacquered Cabinet: A Contribution To European Lacquerwares Characterization,* Infrared, Millimeter, and Terahertz Waves IRMMW-THz, 40th International Conference on, IEEE conference publications, 2015, p.1-2. DOI: 10.1109/IRMMW-THz.2015.7327534

Corinna L. Koch Dandolo; Antonino Cosentino, Peter Uhd Jepsen, *Inspection of panel paintings beneath gilded finishes using terahertz time-domain imaging*, Studies in Conservation, Vol. 60, supplement 1, 2014, p. S159-S166.

Corinna Ludovica Koch Dandolo, Mads C. Christensen, Peter Uhd Jepsen, *Characterization of European Lacquers by Terahertz (THz) Reflectometric Imaging,* Digital Heritage, 1st international Congress on, IEEE conference publications, Vol. 1, 2013. p. 89-94. DOI: 10.1109/DigitalHeritage.2013.6743717

Corinna Ludovica Koch Dandolo, Peter Uhd Jepsen, *THz reflectometric imaging of medieval wall paintings*, Infrared, Millimeter and Terahertz Waves IRMMW-THz, 38th International Conference on, IEEE conference publications, 2013, p. 1-2. DOI: 10.1109/IRMMW-THz.2013.6665839

Corinna Ludovica Koch Dandolo, Peter Uhd Jepsen, *THz reflectometric imaging of contemporary panel artwork*, Infrared, Millimeter and Terahertz Waves IRMMW-THz, 38th International Conference on, IEEE conference publications, 2013, p. 1-2. DOI: 10.1109/IRMMW-THz.2013.6665838

Conference and event contributions

Corinna L. Koch Dandolo (invited speaker), Peter Uhd Jepsen, *Contribution of THz Time-Domain Imaging (THz-TDI) to Multi-layered Artifact Inspection*, Eastern Analytical Symposium & Exposition - Analytical Innovation from Benchtop to Business, Somerset, NJ, United States (16-18 November 2015). Invited talk

Vincent Cattersel (presenter), Louise Decq, Wim Fremout, Stijn Legrand, Koen Janssens, Corinna L. Koch Dandolo, Peter Uhd Jepsen, Emile van binnebeke, Delphine Steyaert, Steven Saverwyns, *White European lacquer: a case study*, VDR-Fachgruppe Möbel und Holzobjekte Tagung, Würzburg, Germany (6-7 November, 2015). Poster

Corinna L. Koch Dandolo, Vincent Cattersel, Peter Uhd Jepsen (speaker), *Terahertz Time-domain Imaging Of A 17th Century Lacquered Cabinet: A Contribution To European Lacquerwares Characterization,* Infrared, Millimeter, and Terahertz Waves IRMMW-THz, 40th International Conference on, Hong-Kong, China (23-28 August, 2015). Talk

Corinna L. Koch Dandolo, Peter Uhd Jepsen (invited speaker), *3-dimensional terahertz imaging and analysis of historical art pieces*, MTSA - 3rd International Symposium on Microwave/Terahertz Science and Applications, Okinawa, Japan (June 30 - July 4, 2015). Invited talk

M. Picollo, A. Casini, C. Cucci, L. Stefani, C. L. Koch Dandolo (speaker) and P. Uhd Jepsen, *Non-invasive investigation of panel paintings by Vis-NIR and THz imaging devices: a few considerations*, Non-destructive and microanalytical techniques in art and cultural heritage TECHNART, International conference on, Catania, Sicily (27-30 April 2015). Talk

Peter Uhd Jepsen (presenter), Corinna L. Koch Dandolo, Presentation of the applications of THz-TDI for artefacts inspection to Mary Elizabeth, Kronprinsesse til Danmark, and Sofie Carsten Nielsen, Minister for Higher Education and Science, during the Research day (Forskningens Døgn) exhibition at DTU, Kgs- Lyngby, Denmark (22 April 2015). Exhibition and presentation

Corinna L. Koch Dandolo (invited speaker), Peter Uhd Jepsen, *Application of terahertz time-domain imaging (THz-TDI) for cultural heritage inspection*, Impact of processing chains on data quality, usability and information content, COST Action TD1201, Saint Etienne, France (26-28 March, 2015). Invited talk

Koch Dandolo, Corinna L. (speaker), Fukunaga K., Kohzuma, Y., Matsuda, K., Kiriyama, K., Filtenborg, T., Skou-Hansen, J.; Cosentino, A., Uhd Jepsen, P., *Contribution of Reflection Terahertz Time Domain-Imaging (THz-TDI) to Imaging Analysis of Artworks,* THz-ARTE International Workshop, ENEA-Frascati, Rome, Italy (2-3 December 2014). Talk

Corinna L. Koch Dandolo (lecturer), Peter Uhd Jepsen *Terahertz applied to artifacts inspection,* Statens Museum for Kunst, Copenhagen, Denmark (1 July 2014). Lecture

Corinna L. Koch Dandolo (presenter), Mads C. Christensen, Peter Uhd Jepsen, *Panels inspection behind the gilded finishes through Terahertz Time-Domain Imaging (THz-TDI),* Lasers in the Conservation of Artworks - LACONA X, Tenth International conference on, Sharjah, United Arab Emirates (9-13 June 2014). Poster

Corinna Ludovica Koch Dandolo (speaker), Mads C. Christensen, Peter Uhd Jepsen, *Characterization of European Lacquers by Terahertz (THz) Reflectometric Imaging,* Digital Heritage, 1st international Congress on, Marseille, France (28 October – 1 November, 2013). Talk

Corinna Ludovica Koch Dandolo (presenter), Peter Uhd Jepsen, *THz reflectometric imaging of contemporary panel artwork* and *THz reflectometric imaging of medieval wall paintings*, Infrared, Millimeter and Terahertz Waves IRMMW-THz, 38th International Conference on, Mainz, Germany, (1-6 September 2013). 2 posters presentation

Journal articles to be submitted:

Corinna L. Koch Dandolo, Marcello Picollo, Costanza Cucci, Peter Uhd Jepsen, *Florentine Renaissance Panel Painting structures revealed by using non-invasive Terahertz Time-Domain Imaging (THz-TDI) technique*

Corinna L. Koch Dandolo, Marcello Picollo, Costanza Cucci, Peter Uhd Jepsen, *Florentine Renaissance Panel Painting structures revealed by using non-invasive Terahertz Time-Domain Imaging (THz-TDI) technique*

Corinna L. Koch Dandolo, Marcello Picollo, Costanza Cucci, A. Casini, L. Stefani, M. Scudieri, E. Prandi, M. Ginanni and Peter Uhd Jepsen, *Insights on the side panels of the Franciscan Triptych by means of Terahertz time-domain imaging (THz-TDI) and VNIR-SWIR hyperspectral imaging*

C.L. Koch-Dandolo, K. Fukunaga, Y. Kohzuma, K. Matsuda, K. Kiriyama, P. Uhd Jepsen, *Analysis of Asian lacquer Substructures by Terahertz Time-Domain Imaging (THz-TDI)*

C.L. Koch-Dandolo, J. Bornemann Mogensen, M. C. Christensen, P. Uhd Jepsen, *Investigation of a XVIII century Chineese lacquer cabinet by Terahertz Time-Domain Imaging (THz-TDI)*